Fabry disease model in Zebrafish

Studying molecular mechanisms of Fabry nephropathy in a Gb3-free environment

Hassan Osman Alhassan Elsaid

Thesis for the degree of Philosophiae Doctor (PhD)
University of Bergen, Norway
2023

UNIVERSITY OF BERGEN

Fabry disease model in Zebrafish

Studying molecular mechanisms of Fabry nephropathy in a Gb3-free environment

Hassan Osman Alhassan Elsaid

Thesis for the degree of Philosophiae Doctor (PhD)
at the University of Bergen

Date of defense: 21.03.2023

Year: 2023

Title: Fabry disease model in Zebrafish

Name: Hassan Osman Alhassan Elsaid

Print: Skipnes Kommunikasjon / University of Bergen

Contents

List of some abbreviations

AKI	Acute Kidney Injury
AVV	Adeno Associated Virus
BP	Biological Process
BSA	Bovine Serum Albumin
CC	Cellular Component
CDK	Cyclin Dependent Kinase
CKD	Chronic Kidney Disease
CRISPR	Clustered Regularly Interspaced Short Palindromic Repeats
DEGs	Differentially Expressed Genes
EC	Enzyme Commission
ECM	Extra Cellular Matrix
EMT	Epithelial-Mesenchymal Transition
ERT	Enzyme Replacement Therapy
ESI	Electrospray Ionization
ESRD	End Stage Renal Disease
FC	Fold Change
FD	Fabry Disease
FDR	False Discovery Rate
FGF-2	Fibroblast Growth Factor 2
FN	Fabry Nephropathy
FPW	Foot Process Width
Gb3	Globotriaosylceramide
GCD	Glycogen Storage Disease
GCS	Glucosylceramide Synthase
GFB	Glomerular Filtration Barrier
GFR	Glomerular Filtration Rate
GLA	Galactosidase Alpha Gene
GT	Gene Therapy
GWAS	Genome-Wide Association Studies
HDFs	Human Dermal Fibroblast
HES1	Hairy Enhancer of Split 1
KEGG	Kyoto Encyclopedia of Genes and Genomes
LSDs	Lysosomal Storage Disorders
lyso-Gb3	Globotriaosylsphingosine
MD	Macula Densa
MF	Molecular Function
MIC	Molecular Imaging Center
MS	Multiple Sclerosis
MSD	Metabolic Storage Disorder
NCBI	National Center for Biotechnology Information
NCM	Nitrocellulose Membrane
NKBR	Norwegian Kidney Biopsy Registry
PD	Parkinson's Disease
PO	Propylene Oxide
ROS	Reactive Oxygen Species
Sod2	Superoxide Dismutase 2
SRT	Substrate Reduction Therapy
TAC	Total Antioxidant Capacity
TEM	Transmission Electron Microscopy
TGF-β1	Tumor Growth Factor Beta 1
TLR4	Toll Like Receptor Type 4
UiB	University Of Bergen
UTI	Urinary Trypsin Inhibitor
VCAM	Vascular Cell Adhesion Molecule
VCAM-1	Vascular Cell Adhesion Molecule 1
VEGF	Vascular Endothelial Growth Factor
VRAC	Volume Regulated Anion Channels
WB	Wild Type
ZFIN	Zebrafish Information Network
α-GAL	A-Galactosidase A Enzyme

Scientific environment

This work was carried out within the Renal Research Group, Department of Clinical Medicine, Faculty of Medicine, at the University of Bergen (UiB), Norway, from 2017 to 2022 under the supervision of Professor Hans Peter Marti, Dr. Janka Babikova, Dr. Jessica Furriol, and Dr. Maximilian Krause.

Collaborating partners were the Departments of Nephrology, Pathology and Urology of Haukeland University Hospital, Bergen; the Molecular Imaging Centre (MIC) Department of Biomedicine, UiB; the sequencing facility, Department of Biological Sciences, UiB; Norwegian Research Centre AS (NORCE) Bergen/Oslo, Norway; and Sahlgrenska University Hospital, Sweden.

Animal experiments were performed at the Zebrafish facility of the Department of Biological Sciences, UiB.

This work was funded by a Helse Vest project to Hans-Peter Marti, Bergen. Project number 912167.

Acknowledgments

I would like to express my ultimate gratitude to Hans-Peter Marti for giving me the chance to work among the amazing people of the Renal Research Group. For his patience, guidance, and unlimited support through the unforeseen tough time I had to experience after the sudden death of my mother. With his wisdom, he tuned me up when I was low, and through him, I learned to keep my high expectations alive regarding science. My words are limited to expressing how much I am grateful to him.

My thanks extend to Janka Babickova, my main supervisor, for crafting this project's idea and making me part of the project. For her assistance with reviewing and guiding me through the thesis writing process.

My special gratitude goes to Jessica Furriol, a supervisor, mentor, friend, and sister. For always allocate time for short and long discussions and chats, even when she is unlimitedly busy. I will always be grateful.

My gratitude extends to Maximilian Krause, who patiently enlightened my path during my early steps in this Ph.D. course.

My thanks and appreciation go to Einar Svarstad, Camilla Tøndel, and Sabine Leh. For showing me and incorporating me into the Fabry Disease scientific community. Also, for their assistance in reviewing the papers and manuscripts produced from this Ph.D. project.

My gratitude extends to Naouel Gharbi for helping me to settle at the Department of Biological Sciences. For her assistance in the brainstorming sessions prior to experiments.

A special Thanks to Mariell Rivedal, who participated in the lab work and revised the paper drafts.

Special thanks to Tarig Osman for establishing my first connection with the Renal Research Group. I am pleased and humbled to have the opportunity to work with you all, and learn from you as well, Lea, Øystein, Dagny Ann, Philipp, August, Ole Petter, Tony Chen, Håvard, Sigrid, Bjørnar Even, Thomas, Rannveig.

My gratitude extended to the Department of biological science, Jon Vidar, Mariann, Sigurd, Rita, Elsa, Valentina, Patrik, and sure Sian, for providing the facility for the experiments and the friendly yet professional environment for the lab work.

I want to extend my thanks to Maria and Mette from Sahlgrenska University Hospital, Sweden, and Jan from Norwegian Research Centre AS (NORCE) Bergen/Oslo, Norway, for their valuable collaboration.

I would like to express my appreciation to Håkon for providing his ultimate assistance in producing the third manuscript generated from this work.

I thank Jutta from the Clinical Nutrition Group for lending us the black 96-well plate for creatinine measurement.

My thanks extend to Randi and Bendik from the Department of Clinical Medicine; and Endy, Linda, and Hege from Molecular Imaging Center for their assistance in microscopy preparations, digital scanning of the slides, and imaging.

I want to express my sincere gratitude to the administration of the Department of Clinical Medicine (K1) for their valuable professional support, in particular, Kjetil, Jorunn, Solveig and Liv Rebecca, who facilitated my settlement at the Department and provided professional guidance throughout my work at the Renal Research Group and for their help during the thesis submission process.

My warm thanks go to Nazar, my friend and big brother, for tolerating my nagging during the thesis writing and cheering me up when I needed it the most. And to my friends in Bergen, Italy, Belgium, Greece, and Sudan for their care.

My ultimate and certainly main gratitude goes to my family, my dearly departed mother to whom I am eternally in debt, my father, and my two brothers for believing and caring; you are the reason I am what I am now. This work would have never been completed without you, my son, Barra; your smile makes me dare.

Abstrakt (Norsk)

Bakgrunn: Fabry sykdom (FS) er en X-bundet lysosomal avleiringssykdom betinget i mutasjon i alfa-galactosidase genet (GLA). Enzymet alfa-galactosidase A (α-GAL) er ansvarlig for nedbryting av fettstoffet globotriaocylceramid (Gb3). Redusert enzymaktivitet fører til Gb3-avleiring i ulike celletyper med organpåvirkning spesielt av nervesystem, hjerte og nyrer. Enzymerstatningsterapi er vist å kunne redusere Gb3-avleiringer, mens det på tross av fjerning av Gb3 synes å være metabolske forstyrrelser som en ikke får bukt med. For å avklare hvilke mekanismer som er direkte knyttet til Gb3 og hvilke ikke, har vi etablert en Fabry modell i zebrafisk (ZF). ZF mangler fra naturens side Gb3 og gir oss mulighet til å utforske Gb3-uavhengige mekanismer og nye potensielle medikamentelle angrepspunkt ved FS.

Metode: Basert i tilgjengelige online data på GLA og α-GAL i ZF, lagde vi ved hjelp av CRISPR/Cas9 gen-editering en GLA-mutert ZF. α-GAL ble målt med standard enzymaktivitet metodologi og fordelingen av enzym i nyrevev ble evaluert ved hjelp av immunhistokjemi. Proteinuri ble målt hos voksne ZF som mål på nyrefunksjon. Vi gjennomførte transcriptomics via RNA sekvensering, proteomics via massespektrometri (MS), oxidativ stress kolometri, immunhistokjemi og elektromikroskopi på nyrevev fra både mutert og ikke-mutert ZF. Vi gjennomførte også plasma metabolom analyse ved hjelp av liquid chromatography mass spectrometry (LC-MS).

Resulter og konklusjon: Forsøkene våre indikerte at reduksjon av α-GAL-aktiviteten til omtrent to tredeler i ZF ga en FD renal fenotype på funksjonelt nivå uavhengig av Gb3-avleiring. Funnene hos mutert ZF taler for lysosomal og mitokondriell dysfunksjon samt morfologiske forandringer i nyrevev. Metabolitt analyser viste potensielle Gb3-uavhengige nyreskade biomarkører. Disse innovative resultatene gir støtte til at det er Gb3-uavhengige mekanismer ved FS og legger grunnlag for videre forskning for bedre å forstå de patofysiologiske mekanismene samt for utforskning av nye medikamentelle muligheter ved denne sykdommen.

Abstract (English)

Background: Fabry Disease (FD) is an X-linked lysosomal storage disorder caused by different galactosidase alpha gene (*GLA*) gene mutations. *GLA* produces the alpha-galactosidase A (α-GAL) enzyme, which is responsible for the degradation of Globotriaosylceramide (Gb3). Inactive or partially active enzyme results in systemic accumulation of Gb3 throughout the body, the main affected organs being the brain, heart, and kidney. Enzyme replacement therapy can lower the Gb3 load from the cells yet cannot reverse the molecular cell alterations. These alterations are believed to be Gb3-dependent or independent. A main issue currently is to find a clear distinction between these two types of alteration. To address this issue, we have established an FD model in ZF that naturally lacks Gb3 enabling us to trace the Gb3-independent alterations and possibly assist in better disease management by identifying potential drug targets.

Methodology: We investigated the *gla* gene and the α-Gal enzyme in ZF using the available online databases, and accordingly, we used a CRISPR/Cas9 gene editing approach to produce *gla* mutant ZF. We measured α-Gal enzyme activity using a standard enzyme activity assay and documented the enzyme kidney tissue distribution in the mutant and wild type fish using immunohistochemistry. We measured proteinuria of adult ZF to evaluate renal function. We conducted transcriptomics via RNA sequencing, proteomics analysis via mass spectrometry (MS), oxidative stress colorimetric assay, immunohistochemistry, and electron microscopy image analysis on the kidney tissue from the mutant and the wild type fish. We also conducted plasma metabolome analysis using Liquid chromatography–mass spectrometry (LC-MS).

Results and conclusion: Our results indicated that lowering the α-Gal enzyme activity by approximately 2/3 in our ZF mutant line results in FD renal phenotype highlighted by alterations at the molecular, subcellular, functional levels independent of Gb3 accumulation. Our results indicated lysosomal dysfunction resulting in evidently mitochondrial functional and morphological alteration in the kidney tissue of the mutant fish. Additionally, metabolite analysis results found potential Gb3-independent renal impairment biomarkers. These innovative results strongly support

the Gb3-independent alterations previously reported in FD and lay the ground for further investigation to better understand the FD pathophysiology. Our results also pave the way to better-tailored disease management by revealing potential drug targets.

List of Publications

Paper I

Elsaid HOA, Furriol J, Blomqvist M, Diswall M, Leh S, Gharbi N, Anonsen JH, Babickova J, Tøndel C, Svarstad E, Marti HP, Krause M. Reduced α-galactosidase A activity in zebrafish (*Danio rerio*) mirrors distinct features of Fabry nephropathy phenotype. Mol Genet Metab Reports, (2022) 31: 100851

Paper II

Elsaid HOA, Rivedal M, Skandalou E, Svarstad E, Tøndel C, Leh S, Birkeland E, Eikrem Ø, Babickova J, Marti HP, Furriol J. Mitochondrial stress in *gla*-mutant Zebrafish despite the absence of globotriaosylceramide accumulation. Manuscript in review: Life Science Alliance.

Paper III

Elsaid HOA, Tjeldnes H, Rivedal M, Serre C, Eikrem Ø, Einar Svarstad E, Tøndel C, Marti H-P, Furriol J, Babickova J. Gene expression analysis in *gla*-mutant zebrafish reveals enhanced Ca^{2+} signaling similar to Fabry disease. Manuscript in review: International Journal of Molecular Sciences.

Other published papers (not included in the thesis)

- Rossi F, Svarstad E, Elsaid H, Binaggia A, Roggero L, Auricchio S, Marti H-P & Pieruzzi F (2021) Elevated Ambulatory Blood Pressure Measurements are Associated with a Progressive Form of Fabry Disease. High Blood Press Cardiovasc Prev 28: 309–319
- Hoel A, Osman T, Hoel F, Elsaid H, Chen T, Landolt L, Babickova J, Tronstad KJ, Lorens JB, Gausdal G, Marti HP, Furriol J (2021) Axl-inhibitor bemcentinib alleviates mitochondrial dysfunction in the unilateral ureter obstruction murine model. J Cell Mol Med 25: 7407–7417

1 Introduction

1.1 Fabry disease overview

Fabry disease FD (OMIM#301500) is a pan-ethnic X-linked lysosomal storage disorder (LSD) (Desnick, Wasserstein et al. 2001) accounted for reduced quality of life, progressive solid organ failure, and premature death (Xiao, Lu et al. 2019). Globally, FD is ranked as the second most common metabolic storage disorder (MSD) (Klingelhofer, Braun et al. 2020). In Norway, the prevalence of FD is the highest of all compared to the other lysosomal storage disorders (LSDs), affecting one person in each 17000 (Guest, Jenssen et al. 2010).

The reported prevalence of the disease varies between studies from 1:40,000–170,000 to 1:1250 in newborn screening studies (Miller, Kanack et al. 2020). This prevalence discrepancy is an indicator of a delayed diagnosis (Germain 2010). The delayed diagnosis is attributed to several FD-specific factors, i.e., the disease's nature, the phenotypes' heterogeneity, the lack of reliable biomarkers, and poor genetic screening approaches (Reisin, Perrin et al. 2017, Carnicer-Caceres, Arranz-Amo et al. 2021). Early diagnosis and timely treatment using enzyme replacement therapy (ERT) have shown improved disease prognosis and increased life expectancy of the patients (Tondel, Bostad et al. 2013). On the contrary, delayed treatment has proven insufficient to restore normal organ functions.

In terms of genotype-phenotype interpretation, the clinical presentation of FD is very variable (Germain 2010). Variability is found in both genders, within the same family, or in unrelated patients with identical mutations. The disease symptoms appear in classical cases very early in life, and if untreated, life-threatening complications such as end-stage renal disease (ESRD) or heart failure are expected to occur by middle age. Common symptoms include chronic neuropathic pain, gastrointestinal problems, angiokeratoma, renal failure, cardiomyopathy, and stroke (Germain 2010).

1.1.1 Genetic basis of FD

Genetically, FD is an X-linked recessive disorder caused by *GLA* gene mutations. *GLA*, which encodes the α-galactosidase enzyme (α-GAL; EC 3.2.1.22), is comprised of 12000 base pairs (bp) organized in seven exons. Pathogenic mutations in this gene

result in decreased or diminished enzyme activity. Over 1000 different mutations have been linked to the disease etiology (Branton, Schiffmann et al. 2002). The first description of the human α-GAL structure was published in 2004 (Garman and Garboczi 2004). Alpha-galactosidase A was shown to be a homodimeric glycoprotein by X-ray crystallography. The monomeric unit consists of two domains: i) (β/α)8 domain containing the active site, and ii) C-terminal domain with eight antiparallel β strands on two sheets in a β sandwich. The first domain extends from amino acids 32 to 330 and contains the active site formed by the C-terminal ends of the strands at the core of the barrel, which is a common position for the active site in (β/α)8 domains. The second domain, composed of amino acid residues 331–428, packs tightly against the first, burying 2500 $Å^2$ of surface area within a single monomer. The dimer has around 75 Å x 75 Å x 50 Å dimensions. In the third dimension, the molecule is concave and ranges in thickness from around 20 Å to 50 Å (Figure 1). Two aspartic acid residues at positions 170 and 231 govern the catalytic process. They play the roles of a nucleophile and an acid/base, respectively. Six N-linked carbohydrate sites on the glycoprotein dimer indicate the basis for lysosomal trafficking via the mannose-6-phosphate receptor (Garman and Garboczi 2004).

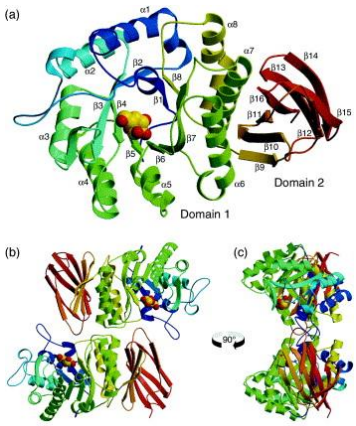

Figure 1. α-GAL X-ray crystallographic structure. (a) The α-GAL monomer unit is colored from the N (blue) terminus to the C terminus (red). The first domain has the active site in the core of the (β/α)8 barrel structure, whereas the second domain comprises antiparallel β strands. Yellow and red CPK atoms represent the galactose/substrate ligand. Two perspectives of the α-GAL dimer are shown in (b) and (c). The active sites in the dimer are 50 Å apart on the concave surface of the molecule, as seen from the side in (c) derived from (Garman and Garboczi 2004) with permission.

Alpha-galactosidase A, α-GAL, is a lysosomal enzyme composed of 429 amino acids which catalyzes the removal of galactose from oligosaccharides, glycoproteins, and glycolipids during the catabolism of macromolecules. The main in vivo substrate for α-GAL is the globotriaosylceramide/ceramidetrihexoside (Gb3/CTH), and to a lesser extent, globotriaosylsphingosine (lysoGb3), galabiosylceramide (Gb2), isoglobotriaosylceramide (iGb3), and blood group B, B1 and P1 antigens (Desnick and Wasserstein 2001, Speak, Salio et al. 2007, Aerts, Groener et al. 2008, Boutin, Menkovic et al. 2017). In FD, α-GAL deficiency results in lysosomal accumulation of Gb3 throughout the body but mainly in the brain, heart, and kidney (Germain 2010).

As a lysosomal enzyme, native α-GAL uptake is mainly via mannose-6-phosphate receptor (M6PR) (Prabakaran, Nielsen et al. 2012). M6PR is involved in the uptake of more than 60 lysosomal enzyme (Johannes and Wunder 2016). Furthermore, due to the localization of M6PR in the plasma membrane, it can retrieve the escaped lysosomal enzyme back to the lysosome (Bajaj, Lotfi et al. 2019, Zhang, Yue et al. 2021). This latter feature is the established basis of ERT in which the infused engineered enzyme can be taken by the cell via the plasma membrane located M6PR (Prabakaran, Nielsen et al. 2012, Shen, Busch et al. 2016). In other LSDs, i.e., Niemann-Pick disease, the ERT was found to be influenced by a lower M6PR presence due to lipid load (Dhami and Schuchman 2004). Only recently similar finding was reported in FD, nevertheless, the lower M6PR expression was not attributed to the Gb3 load in the cardiomyocytes (Frustaci, Verardo et al. 2022). The imbalance in this receptor can therefore disturb the lysosomal integrity regardless of the nature of the loading material.

1.2 Mutations and their effect

Before the discovery of the α-GAL's three-dimensional structure using X-ray crystallography, it was assumed that disease-causing missense mutations would result in modifications to the enzyme's active site. However, Garman has demonstrated that mutations in the residues near the enzyme's active region account for only 10% of all disease-causing mutations. Since most disease-causing mutations occur in the hydrophobic center of the protein, FD is now understood as a protein-folding disorder (Garman 2007).

The pathogenic effect of *GLA* mutations varies considerably (Modrego, Amaranto et al. 2021). While some mutations lead to complete enzymatic deficiency, other mutations still result in residual enzymatic activity. In the latter, the cutoff for clinical diagnosis of g FD is 30–35% of mean regular α-GAL activity (Schiffmann, Fuller et al. 2016). The enzyme activity is typically measured from peripheral white blood cells or dry blood spots; nevertheless, this measured activity does not reflect the enzyme activity in the tissue. Multiple mutations that have been found to be disease-causing in some individuals were shown to cause mild FD or are fully nonpathogenic in others (Schiffmann, Fuller et al. 2016). Therefore, the exact enzyme activity threshold of FD pathogenicity remains to be determined (Varela, Mastroianni Kirsztajn et al. 2020).

1.2.1 Classical Fabry phenotype

The most severe phenotype primarily occurs in hemizygous males and homozygous females (also to a lesser extent in heterozygous females), a consequent of absent or severe deficiency in α-GAL activity (Germain 2010). Heterozygous females can present with various manifestations ranging from severe classical (similar to men) to mild or asymptomatic (Germain 2010). This variation in heterozygous females is attributed to the X-chromosome inactivation (Echevarria, Benistan et al. 2016, Rossanti, Nozu et al. 2021, Reboun, Sikora et al. 2022). Symptoms can be observed during childhood or adolescence, while functional renal or cardiac impairment appears during the patient's life's third and fourth decades (Germain 2010).

Additionally, due to Gb3 accumulation in dermal endothelial cells, angiokeratomas occur in pelvic and thigh regions and spread with disease progression to reach genitalia, mouth, and limb ends (Desnick, Wasserstein et al. 2001). The nervous system is affected by acroparesthesia, hypohidrosis and cerebrovascular accidents. Sight opacity (cornea verticillate) results from Gb3 deposition in the cornea (Bernardes, Foresto et al. 2020). Postprandial belly discomfort and bloating, followed by repeated bowel motions and diarrhea are gastrointestinal complications (Desnick, Wasserstein et al. 2001).

1.2.2 Nonclassical Fabry phenotype

The nonclassical form of FD results from the residual activity of the α-GAL enzyme. This FD form is typical in women and is highly mosaic in manifestation, ranging from asymptomatic to nearly classical phenotype (Germain 2010). Cardiac involvement is

predominant in this phenotype (Monserrat, Gimeno-Blanes et al. 2007, Arends, Wanner et al. 2017). In men, this nonclassical phenotype is less severe than the classical, with all of the classical phenotype's characteristic symptoms postponed until the fourth decade of life (Desnick, Wasserstein et al. 2001). When untreated, 80% of men show proteinuria by their fourth decade of life and develop ESRD. Generally, renal symptoms start with microalbuminuria and advance to proteinuria. The severity of the renal involvement correlates with the residual enzyme activity and depends on the time/age of diagnosis (Branton, Schiffmann et al. 2002).

1.3 Treatment

Current FD treatment involves four therapeutic groups: enzyme replacement therapy (ERT), chaperone therapy (CP), substrate reduction therapy (SRT), and gene therapy (GT). While ERT and CP are currently used in the treatment, SRT and GT are in the trial phases. ERT and chaperon therapy have shown promising results in FD management. However, many issues or adverse effects were reported, which will be addressed in the following two sections.

1.3.1 Therapy in clinical use

ERT is based on enzyme supplementation (Eng, Guffon et al. 2001). Currently, two enzymes are used for FD treatment. Agalsidase alfa Replagal®, Shire HGT produced in fibroblast and agalsidase beta Fabrazyme®, Sanofi Genzyme produced from Chinese hamster ovary (CHO) cells. By 2001, both ERT enzymes were approved in Europe (Eng, Guffon et al. 2001); however, agalsidase alfa is not approved in the United States yet despite the proven efficacy in the long-term assessment (Tondel, Bostad et al. 2013, Skrunes, Tondel et al. 2017). While the infusion of both enzymes is bi-weekly, the dose of agalsidase alfa is lower than that of agalsidase beta, 0.2 mg/kg, and 1 mg/kg, respectively. The uptake and activity of both enzymes test in fibroblast have shown a similar pattern (Sakuraba, Murata-Ohsawa et al. 2006). However, the uptake of enzymes was recently shown to be cell-type dependent based on endogenous activity, with more uptake correlated to cells with lower enzyme activity (Ivanova, Dao et al. 2020).

ERT is the primary treatment for FD; however, several issues were addressed in previous studies regarding the long-term impact of ERT. One of the main issues encountering ERT is the neutralizing antibodies that develop upon chronic exposure

to infusion. This issue is reported in 70% of men with classical FD phenotype (Sakuraba, Tsukimura et al. 2018, Bichet, Aerts et al. 2021). In addition, ERT does not reach all cells with the same efficiency, i.e., podocytes (Vedder, Strijland et al. 2006) and they cannot overcome the blood–brain barrier rendering central nervous system incurable (Concolino, Deodato et al. 2018). Furthermore, recurrent cerebrovascular complications were recently highlighted (Muto, Suzuki et al. 2022). The current research aims to decrease the unfavorable effects of ERT (Azevedo, Gago et al. 2020). For example, an integrated treatment approach accompanied by a comprehensive follow-up of Fabry nephropathy (FN) seems necessary (Ortiz, Germain et al. 2018, Svarstad and Marti 2020). Guidelines for initiation and cessation of ERT were updated in 2015 by the European Fabry Working Group consensus (Biegstraaten, Arngrimsson et al. 2015).

Another approach for FD treatment is chaperone therapy. Chaperone therapy was developed because enzyme substrates/inhibitors (galactose and 1-deoxygalactonojirimycin) can correct enzyme misfolding and enhance its endoplasmic reticulum-lysosome transport (Ishii, Kase et al. 1993, Fan, Ishii et al. 1999). Currently, 1-deoxygalactonojirimycin (DGJ), a pharmacological chaperone, is used under the commercial name Migalastat (Galafold®, Amicus Therapeutics). This orally administrated drug was approved for use in FD in 2016. Studies have shown that joint administration of ERT and a chaperone therapy improves the FD treatment outcome (Benjamin, Khanna et al. 2012, Warnock, Bichet et al. 2015).

1.3.2 Emerging therapeutic options

Additional modified ERT versions are under development in response to current issues elicited by the current two ERTs. Pegunigalsidase-alfa, a plant-based α-GAL produced in tobacco cells, is an enzyme chemically modified by polyethylene glycol (PEG) (Kizhner, Azulay et al. 2015), currently under clinical trials. The stability of the modified enzyme is confirmed both in vitro and in vivo (Ruderfer, Shulman et al. 2018, Schiffmann, Goker-Alpan et al. 2019). Concerns about the prolonged plasma half-life and eliciting immune response (due to its plant-based nature) still need to be addressed (van der Veen, Hollak et al. 2020).

Another potential recombinant enzyme is moss-α-GAL. Moss-α-Gal is a plant-based engineered enzyme produced in the seedless plant moss *Physcomitrella patens*

*(*Shen, Busch et al. 2016*)*. The potentially immunogenic xylose and fucose residues were eliminated for convenient usage of this plant-based enzyme in the mammalian system (Koprivova, Stemmer et al. 2004). The uptake mechanism of this enzyme is via the mannose receptor, as a typical lysosomal enzyme in plants are voided from the mannose 6-phosphate (M6P) modification on terminal mannose residues (Gomord and Faye 2004). Nevertheless, testing this enzyme in mice and clinical trials in humans has shown similar Gb3 clearance and short half-life to Agalsidase alfa (Shen, Busch et al. 2016, Hennermann, Arash-Kaps et al. 2019). While short half-life of the Moss-α-Gal in the plasma can reduce immune system encounter with the enzyme in each single infusion, it necessitates more frequent infusion compared to the currently available ERTs (Alliegro, Ferla et al. 2016).

Clinically approved chaperone therapy is limited to amenable mutations; therefore, only 35-50% of FD patients are eligible for such therapy (Hughes, Nicholls et al. 2017, McCafferty and Scott 2019). Other protein-folding agents need to be developed to increase the range of eligible mutations. New enzyme stabilizers such as cyclophellitol cyclosulfamidates are currently under development (Artola, Hedberg et al. 2019). Additionally, potential allosteric molecules that avoid active site binding are currently being investigated (typical for 1-deoxygalactonojirimycin). A recently suggested candidate molecule, 2,6-dithiopurine (DTP) was found to stabilize the enzyme and rescues the DGJ -non-amenable mutant form (Citro, Pena-Garcia et al. 2016).

Another approach for FD treatment is SRT. This approach aims to eliminate/reduce the enzyme's substrate, which is Gb3 in the case of FD. SRT for FD is currently under investigation. Venglustat/Ibiglustat (Sanofi Genzyme) and Lucerastat (Idorsia Pharmaceuticals, Switzerland) are both orally administered glucosylceramide synthase (GCS) inhibitors under clinical trials (Guerard, Morand et al. 2017, Peterschmitt, Crawford et al. 2021). Both SRT agents effectively reduced Gb3 and lysoGb3 (van der Veen, Hollak et al. 2020). One of the main challenges to be addressed is that while SRT can reduce the direct effect of Gb3 and lysoGb3, they are unable to treat the evident Gb3 and lysoGb3 independent effects that can proceed after or perhaps before tissue accumulation or exposure.

Gene therapy is based on correcting the mutated gene by inserting the correct sequence version into an adeno-associated virus (AAV), lentivirus, retrovirus or a non-viral-based system that can alter the DNA. The first human gene therapy trial for FD was conducted in 2016 in Canada (NCT02800070) (Kok, Zwiers et al. 2021). Another running phase II trial to assess the potential use of gene therapy for classic FD is ongoing (NCT03454893) (Kok, Zwiers et al. 2021).

Experimental results have shown that gene therapy using FLT190 (Freeline therapeutics, UK) and ST-920 (Sangamo Therapeutics) resulted in increased enzyme activity in the plasma of the FD mouse model (Kia, McIntosh et al. 2018, Huston, Yasuda et al. 2019, Yasuda, Huston et al. 2020). The fundamental disadvantage of gene therapy is that symptoms are still observed in certain heterozygous females (who supposedly have 50% normal enzyme production), which suggests that endogenous translated genes, let alone exogenous expression, cannot guard against FD (van der Veen, Hollak et al. 2020).

While FD treatment by the currently available therapies and perhaps soon with the new prospective therapies is improving, the limited treatment efficacy to reverse the molecular and cellular alterations reported in FD needs to be further addressed (Braun, Blomberg et al. 2019). For example, it is still unclear if the unreversed cellular alteration in FD is Gb3-dependent or independent.

1.4 The mechanisms of Fabry Nephropathy development

Nephropathy is among the most significant consequences of FD (Jaurretche, Antogiovanni et al. 2017). It is reported in 59% and 38% of men and women, respectively (Mehta, Beck et al. 2009). The reported incidence rate differs, which can be explained by the well-known heterogeneous nature of the FD (Del Pino, Andres et al. 2018). By age 38, progression to ESRD is observed regardless of gender (Ortiz, Oliveira et al. 2008, Wilcox, Oliveira et al. 2008). In FD, renal involvement contributes to patients' burden and low life quality, including high mortality rates (Germain 2010). The progression rate of FN is comparable to that of diabetic nephropathy, and although FN can start at the early stages of life, the severity of the FN varies considerably between sexes (Sessa, Meroni et al. 2003). The various degree of renal

injury indicates the uniqueness of the renal tissue combined with the heterogenicity of the FD.

Histologically, renal involvement manifests as glycolipid deposits in glomerular cells (especially podocytes, but also mesangial cells and endothelial cells), tubular epithelial cells (particularly in the distal nephron), arterial and arteriolar endothelium and smooth muscle cells, and interstitial cells (Alroy, Sabnis et al. 2002). Renal biopsies show that the disease progression is highlighted by hypertrophic foamy vacuolated mesenchymal cells, endothelial cells, and podocytes (Alroy, Sabnis et al. 2002). In each of the aforementioned renal compartments, the deposition or exposure to the enzyme's substrate (Gb3/lysoGb3) can trigger and maintain specific reactions/pathways, eventually resulting in renal tissue damage (Shen, Meng et al. 2008, Braun, Blomberg et al. 2019).

Current studies suggest that these complications are solely due to Gb3 accumulation and lysoGb3 circulation. However, discrepancies in indicating the tissue involvement indicates that FD is more than a deposit accumulation disease (Levstek, Vujkovac et al. 2020). In FD, the pathophysiological mechanisms of CKD and ESRD need to be elucidated.

1.5 Pathophysiology of Fabry Disease and Fabry Nephropathy

Although it is considered that Gb3 accumulation is the primary event that leads to the sequential clinical course (Kok, Zwiers et al. 2021), it is well documented that Gb3 accumulation is not alone responsible for the whole disease presentation (Braun, Blomberg et al. 2019). There are numerous unsolved questions regarding the role of Gb3 and its soluble form, lysoGb3, in FD (Shen, Meng et al. 2008, Braun, Blomberg et al. 2019). Therefore, the pathophysiology of FD and the progression of FN are not entirely understood (Germain 2010, Miller, Kanack et al. 2020), and attempts to interpret the consequences of Gb3 accumulation/circulation and lysoGb3 circulation is an ongoing research field.

In light of the current knowledge, the pathophysiology depends on the tissue exposed to Gb3 and lysoGb3 (Germain 2010). Identified consequences involving Gb3/lysoGb3 include sclerosis (Weidemann, Sanchez-Nino et al. 2013), inflammation (Meng, Nikolic-Paterson et al. 2014, Mauhin, Lidove et al. 2015), fibrosis (Fogo, Bostad et al.

2010), and immune response (Mauhin, Lidove et al. 2015). These manifestations are mainly present in the glomeruli and include focal segmental sclerosis and ischemic injuries. The severe glomerular injuries result from the podocytes' low regeneration abilities and glomerular hyperfiltration (Rozenfeld, de Los Angeles Bolla et al. 2020). In tubules, the damage is less severe. Pathological changes are mainly present in distal tubules (acidosis, isosthenuria) and, to a lesser extent, in proximal tubules most likely due to their high regeneration capacity.

1.5.1 Glomerular injury

In the renal phenotype of FD, the kidney's glomerular part is the most affected due to the Gb3 accumulation in all its compartments. Due to their limited regeneration capacity, the podocytes are ranked first considering the severity of the Gb3 accumulation among the rest of the cells composing the glomerulus; they are also the least to be reached by ERT; therefore, limited to no Gb3 clearance can be achieved. Other cells with Gb3 deposits are mesangial, endothelial, and parietal epithelial cells (Alroy, Sabnis et al. 2002).

In FD, podocytes were intensively studied in vitro and in vivo, and it is known that they are the first cell type to be influenced by and overloaded with Gb3. Overburdened podocytes undergo cell death early in the disease progression, even before proteinuria develops (Najafian, Tondel et al. 2020). The cytoplasmic area filled with Gb3 increases with age; therefore, monitoring the podocyte during the evolution of the disease and treatment is essential for proper patient care (Eikrem, Skrunes et al. 2017).

1.5.1.1 Podocyte loss

Several factors lead to podocyte loss, with Gb3 loading being the first. The podocyte loss is directly related to Gb3 build-up (Najafian, Tondel et al. 2020). Gb3 is directly engaged in cell contraction, slit diaphragm widening and binding to integrins through its interaction with actin. The podocyte cytoskeleton disruption in FD was already studied 20 years ago (Utsumi, Itoh et al. 1999). FD patients have higher levels of vitronectin and vitronectin receptor in podocytes (VNR, also known as integrin v3) compared to healthy individuals. VNR is necessary for podocyte-basement membrane anchoring, and when it is activated, it induces contraction and migration of the podocyte, resulting in their dissociation (Fornoni, Merscher et al. 2014).

LysoGb3, on the other hand, induces podocyte detachment by increasing the gene expression of the urokinase-type plasminogen activator receptor (uPAR)/αvβ3 integrin system, which plays an essential role in podocyte detachment. In these two studies, urinary podocytes and cultured podocytes revealed higher gene expression patterns of *ITGAV*, *ITGB3*, and *PLAUR* genes encoding integrins αv and β3 and uPAR, respectively (Trimarchi, Canzonieri et al. 2017, Trimarchi, Ortiz et al. 2020).

Additionally, Gb3 promotes angiotensin II (Ang II) overexpression in podocytes. Ang II-induced oxidative stress can itself activate latent tumor growth factor beta 1 (TGF-β1) (Muller-Deile and Schiffer 2016), which then activates the SMADs and Ras/extracellular signal-regulated kinase (SRK) pathways (Pollman, Naumovski et al. 1999). These intercalated interactions are responsible for the progressive loss of the podocytes and eventually result in glomerulosclerosis development (Weidemann, Sanchez-Nino et al. 2013). The renin-angiotensin-aldosterone system (RAAS) plays multiple crucial roles in Fabry nephropathy due to the presence of Ang II receptors on podocytes. Podocyte hypertrophy is closely related to Ang II and causes actin depolymerization and cytoskeleton remodeling. Ang II infusion has been proven to induce proteinuria (Lapinski, Perico et al. 1996). In contrast, supplementation with angiotensin receptor blockers or angiotensin-converting enzyme (ACE) inhibitors decreased both podocyturia and proteinuria in FD (Warnock, Thomas et al. 2015). However, this might not be beneficial in the late stages of CKD as ACE inhibition has no effect (Trimarchi, Forrester et al. 2014).

In an FD podocyte model, a decrease in AKT kinase activity was also demonstrated, suggesting its role in the potential cell damage in FD (Liebau, Braun et al. 2013). Akt proteins suppress podocyte apoptosis, and loss of Akt2 or a decrease in its activity can exacerbate podocyte loss, accelerate the onset of proteinuria, and increase tubular inflammation in CKD (Canaud, Bienaime et al. 2013).

Despite intensive investigation, the exact molecular pathological process leading to podocyte loss remains unknown.

1.5.1.2 Foot process effacement

LysoGb3 was also found to increase the mRNA and protein expression of uPAR in cultured human podocytes (Trimarchi, Canzonieri et al. 2017). uPAR is a

glycosylphosphatidylinositol (GPI)-anchored proteinase receptor for urokinase. It is involved in nonproteolytic pathways by forming signaling complexes with other transmembrane proteins like integrins, caveolin, and G-protein-coupled receptors (Blasi and Carmeliet 2002). It also interacts with extracellular matrix (ECM) proteins like vitronectin (Wei, Waltz et al. 1994). The induction of urokinase receptor (uPAR) signaling in podocytes using lipopolysaccharide (LPS) resulted in foot process effacement and proteinuria via lipid-dependent activation of αvβ3 integrin (Wei, Moller et al. 2008). uPAR-mediated signal transduction in podocytes is facilitated preferentially by the 31 integrin (Utsumi, Itoh et al. 1999, Chapman and Wei 2001), which interacts with actin to induce podocyte contraction (Sachs and Sonnenberg 2013). Indeed, Amiloride, a known inhibitor of uPAR, has proven efficient in decreasing proteinuria in FD (Trimarchi, Forrester et al. 2014).

1.5.1.3 Immune response

Immunological responses, such as inflammation and fibrosis, contribute to the worsening of kidney function in FD. LysoGb3 is the initiating element for Notch1 activation, which leads to hairy enhancer of spilt-1 (HES1) overexpression. Moreover, lysoGb3 increases nuclear factor kappa B (NFκB) DNA binding activity and inflammation (Sanchez-Nino, Carpio et al. 2015). The suppression of Notch1 by Notch1-siRNA or γ-secretase results in the downregulation of HES1 (a canonical Notch transcriptional target), the inactivation of NFκB, and the overexpression of LysoGb3-mediated fibronectin (Sanchez-Nino, Carpio et al. 2015).

Also, Gb3 and lysoGb3 stress/exposure are sufficient to induce the overexpression of fibronectin and transforming growth factor beta (TGF-β1), which results in ECM synthesis upregulation (Sanchez-Nino, Sanz et al. 2011, Weidemann, Sanchez-Nino et al. 2013). The release of such inflammatory cytokines is mediated through the macrophage inhibitory factor receptor (CD74) pathway (Sanchez-Nino, Sanz et al. 2011). The exact impact of lysoGb3 on TGF-β1 was seen in the FD mice model (Lee, Choi et al. 2012). TGF-β1 contributes to chronic inflammation-mediated fibrosis by promoting ECM synthesis via epithelial-to-mesenchymal transition (EMT) (Pohlers, Brenmoehl et al. 2009, Weidemann, Sanchez-Nino et al. 2013, Sutariya, Jhonsa et al. 2016). Inactivation of the Notch receptor inhibited TGF-β1 from promoting epithelial-to-mesenchymal transition (Sanchez-Nino, Sanz et al. 2011). In cultured

podocytes, TGF-β1 inhibition decreased the production of EMT markers (Jeon, Jung et al. 2015).

Also, it was discovered that lymphocyte activation antigen 7-1 (CD80), typically found on antigen-presenting cells, was expressed in renal biopsies from FD patients but not controls. In cultivated podocytes, the role of LysoGb3-induced CD80 expression was verified. This protein expression did not correlate to proteinuria (Trimarchi, Canzonieri et al. 2016).

While podocytes are heavily investigated in FD, other glomerular cells can also be affected by Gb3 accumulation. Gb3 accumulates in the mesangial cells; however, its role in FN is yet to be revealed. Elevated TGF-β1 activity consequent to Gb3 accumulation in the podocytes induces proliferation and thickening of the glomerular basement membrane (GBM) (Lee, Choi et al. 2012), which might indirectly affect mesangial cells through TGF-β1-dependent factors that trigger the expression of vascular endothelial growth factor (VEGF) and connective tissue growth factor (CTGF). Eventually, this induces mesangial matrix synthesis via the paracrine influence on the mesangial cells (Eikrem, Skrunes et al. 2017).

A recent study has shown that in biopsies from Fabry patients, apoptosis marker caspase 3 was detected in the renal tubules, the mesangial glomerular cells, and to a lesser extent, in the peri-glomerular zone. Additionally, a marker of myofibroblasts, the α-smooth muscle actin (αSMA), was detected in pericytes surrounding peritubular capillaries, mesangial cells and the peri-glomerular zone (Rozenfeld, de Los Angeles Bolla et al. 2020). Nevertheless, more investigation is needed on the role of Gb3/lysoGb3 in the pathogenicity of FN via mesangial cells and parietal epithelial cells.

1.5.2 Tubulointerstitial alterations

Gb3 accumulates in distal tubules, the collecting duct, and to a lesser extent, in the proximal tubule. The regenerative potential of the proximal tubule cells may be the reason for a reduced amount of Gb3 accumulation or lower pathogenicity compared to other kidney parts (Warnock, Ortiz et al. 2012, Rozenfeld, de Los Angeles Bolla et al. 2020). Alternatively, binding protein lectin with an affinity toward α-GAL is present on the surface of endothelial and distal tubular epithelial cells, while proximal tubule

epithelium lacks such lectin (Faraggiana, Crescenzi et al. 1989). In kidney biopsies, the renal tubule involvement in Fabry nephropathy is heterogeneous/mosaic due to the variable Gb3 load (Eikrem, Skrunes et al. 2017). Gb3 buildup can cause localized tubular atrophy and interstitial fibrosis on its own (Alroy, Sabnis et al. 2002).

Like the podocytes, both Gb3 and lysoGb3 were found to enhance the expression of TGF-β1 and EMT markers (N-cadherin and α-SMA) and phosphorylation of PI3K/AKT in renal tubular cells. They were also responsible for the decreased expression of the E-cadherin. This presence in the renal epithelial cells triggered tubulointerstitial fibrosis (Jeon, Jung et al. 2015).

In FD patient biopsies, high expression of TGF-β1 accompanied by α-SMA-positive cells (myofibroblasts) on pericytes surrounding the peritubular capillaries was found, strengthening the previous notion of the significant role of development tubulointerstitial fibrosis in FN (Rozenfeld, de Los Angeles Bolla et al. 2020).

Ischemic abnormalities, secondary to vascular accumulation of Gb3, result in tubular injury. In addition, proteinuria and glomerulosclerosis contribute to tubular degeneration (Najafian, Svarstad et al. 2011, Meng, Nikolic-Paterson et al. 2014, Zhou and Liu 2016). Proteinuria causes tubular cells to undergo EMT, cell-cycle arrest, and release of profibrotic cytokines (Meng, Nikolic-Paterson et al. 2014, Zhou and Liu 2016).

Tubular epithelial cells, mainly proximal tubules, contain VEGF (Nakagawa, Lan et al. 2004). VEGF was found elevated in kidney tissue of Fabry mice compared to the normal mice (Lee, Choi et al. 2012), which was also confirmed in the serum of FD patients compared to healthy humans (Zampetti, Gnarra et al. 2013). Furthermore, in cultured rat proximal tubule cells, VEGF was elevated by TGF-β1 induction (Nakagawa, Lan et al. 2004). Additionally, hypoxia, cytokines, and growth hormones can stimulate and modulate VEGF expression (Ferrara 2004). Presumably, VEGF contributes to the fibrogenic effect that results from local tubular ischemia (Lee, Choi et al. 2012), enhancing the upregulation of VEGF in tubular cells. Nevertheless, no study has shown a direct influence of Gb3 and/or lysoGb3 on plasma levels of VEGF.

Moreover, the disease progression is further complicated by interaction between the tubular and glomerular compartments. As the glomerular compartment affects the

tubular part via proteinuria, the tubular part, in turn, can affect the glomerular compartment. The damaged tubules result in poor function of their preceding glomeruli, resulting in hypertrophy of neighboring glomeruli. Hyperfiltration in these glomeruli may develop after localized and segmental glomerulosclerosis (Fogo, Bostad et al. 2010).

1.5.3 Vascular changes.

The role of vasculopathy in FD is due to prolonged exposure to the lysoGb3 and Gb3 circulating in the plasma.

In the blood vessels, two cells are mainly affected by the Gb3 and lysoGb3 exposure, the endothelial cells and smooth muscle cells. In endothelial cells, upon exposure, the expression of adhesion molecules and integrin Mac-1 is increased, resulting in increased interaction between leukocytes and the endothelial cells. This interaction, in turn, promotes the release of other pro-inflammatory molecules, i.e., interleukin 1 beta (IL-1β) and tumor necrosis factor alpha (TNF-α) (Mauhin, Lidove et al. 2015).

Gb3 can also influence the overexpression of the cell adhesion molecules, such as intercellular adhesion molecule 1 (ICAM-1), vascular cell adhesion molecule 1 (VCAM-1), and E-selectin (Shen, Meng et al. 2008). VCAM-1, which is involved in endothelial wall adhesion, is increased in FD patients and regulates the activation of the nicotinamide adenine dinucleotide phosphate (NADPH)-oxidase in the endothelial cell membrane. In addition, VCAM-1 enhances endothelial activation by activating matrix metalloproteinases, which break down the ECM, permit endothelial cell mobility, and enhance capillary permeability (Shen, Meng et al. 2008).

NADPH-oxidase activation induces the production of reactive oxygen species (ROS), which maintains the connection between lymphocytes and endothelial cells (Deem and Cook-Mills 2004). Similarly, Gb3 accumulation reduces SOD2 synthesis, inducing an increase in ROS and activation of cAMP-dependent protein kinase (AMPK), resulting in mitochondrial damage and endothelial dysfunction (Tseng, Chou et al. 2017).

Two studies showed that the nitric oxide (NO) pathway was also implicated in endothelial activation/dysfunction. The first lysoGb3 deposition in the medial artery wall stimulates smooth muscle cell proliferation and may contribute to arterial wall

stiffness via subendothelial compartment remodeling. Alterations to the arterial wall enhance shear stress and stimulate the overexpression of angiotensin 1 and 2 receptors. Consequently, this increases the levels of ROS, NFκβ, β-integrin, and cyclooxygenase 1 and 2 activity while lowering NO synthesis via endothelial NO synthase (eNOS) (Rombach, Twickler et al. 2010). Another study suggested that the buildup of endothelial-lysoGb3 is entirely responsible for eNOS dysfunction (Aerts, Groener et al. 2008). Indeed, plasma levels of 3-nitrotyrosine (3NT), a specific marker for reactive nitrogen species, was significantly elevated in classic FD patients (Shu, Vivekanandan-Giri et al. 2014).

Additionally, intima-media thickening, a well-known feature of FD vasculopathy, was explained by the exposure of smooth muscle cells to lysoGb3, which induced proliferation (Aerts, Groener et al. 2008).

Gb3 accumulation was found to increase the expression of TGF-β1 and VEGF in the bovine aortic endothelial cells, Fabry mouse, and FD patients (Lee, Choi et al. 2012, Zampetti, Gnarra et al. 2013). This combined overexpression resulted in the elevation of Vascular endothelial growth factor receptor 2 (VEGFR2), Fibroblast Growth Factor 2 (FGF-2) and phospho-p38 (P-p38) and induced apoptosis (Lee, Choi et al. 2012).

A recent study using FD patient-derived cells, particularly endothelial cells, found higher expression of thrombospondin-1 (TSP1), an essential component of extracellular matrix (ECM) proteins that govern blood vessel dynamics in their microenvironment. TSP-1 functions as an endogenous angiogenesis inhibitor due to its capacity to bind VEGF or FGF-2. Therefore, its increase may contribute to FN by inhibiting the development of new blood vessels. In the peritubular capillaries of FD patients' renal biopsies, TSP-1, FGF-2, and VEGF showed increased expression, whereas angiogenic factors such as eNOS, kinase domain-containing receptor, and angiopoietin 2 showed decreased expression (Do, Park et al. 2020, Rozenfeld, de Los Angeles Bolla et al. 2020).

Regardless of much evidence of Gb3 and lysoGb3 involvement in the FD pathogenicity, their full role in the deteriorating kidney function and disease development remains unclear. For example, despite early Gb3 accumulation no major early Fabry disease symptoms have been identified, particularly in the nonclassical

phenotype of the disease (Tsutsumi, Sato et al. 1985, Popli, Leehey et al. 1990, Elleder, Poupetova et al. 1998, Chien, Olivova et al. 2011). A greater effort should be devoted to elucidating the ultramicroscopic/subcellular features and the effect of the α-GAL shortage independent of the presence of Gb3, which may aid in understanding, diagnosing, and treating the disease at an earlier stage and improve our capacity to identify asymptomatic patients with residual enzymatic activity, particularly those without a family history of the condition (El Dib, Gomaa et al. 2017).

To sum up, the pathophysiology of FD in the renal tissue is complicated due to the intercalation of many pathways activated by Gb3 and lysoGb3 and the downstream cascades that run independently of their involvement (Shen, Meng et al. 2008, Braun, Blomberg et al. 2019). In the kidney, the damage mainly occurs in the glomerular cells (podocytes), vascular cells (smooth muscle cells and endothelial cells), and tubular cells (distal tubule epithelia) (Eikrem, Skrunes et al. 2017, Carnicer-Caceres, Arranz-Amo et al. 2021, Feriozzi and Rozenfeld 2021).

1.6 The current state of Fabry Nephropathy diagnosis

Diagnosis of FD is well established regardless of its complexity, however, FN diagnosis requires special attention (Ortiz, Oliveira et al. 2008). The available renal function tests and renal injury biomarkers are not sensitive enough to identify the onset of renal involvement in FD (Silva, Moura-Neto et al. 2021). Generally, the diagnosis is based on the integrated application of several tests and markers and in patients with unknown family history, this might lead to delayed diagnosis and hence late ERT intervention (Reisin, Perrin et al. 2017).

1.6.1 Clinical and laboratory findings

One of the leading causes of death in FD is cardiac arrhythmias following ESRD (Ortiz, Oliveira et al. 2008, Germain 2010, Samanta, Chan et al. 2019); therefore, the early detection of renal involvement is crucial in treatment initiation, mainly because the early treatment has shown more efficiency (Germain, Charrow et al. 2015, van der Veen, Korver et al. 2022). Enrolling FD patient in the ERT treatment requires renal function assessment. Currently, evaluation of renal involvement is based on well-established renal function tests, like proteinuria, serum creatinine, and eGFR or kidney biopsy. Unfortunately, these gold standard tests have limited sensitivity to monitor renal disease progression, and FN is no exception. For example, proteinuria

may only appear after the renal tissue is already overloaded with Gb3 (Tondel, Bostad et al. 2008).

1.6.1.1 Assessment of kidney function

Measured and estimated glomerular filtration rates (eGFR) are used to measure Fabry patients' renal function regularly. Because creatinine-based GFR estimations are inaccurate, measured GFR is advised at least once a year (Ortiz and Sanchez-Nino 2018). Because measured GFR is more complex and time-consuming, estimated GFR measurements using an appropriate formula are more commonly employed.

In clinical practice, the Chronic Kidney Disease Epidemiology Collaboration (CKD-EPI) equation for adults and the Schwartz formula for children are currently utilized in serum creatinine-based formulae (Levey, Stevens et al. 2009, Schwartz, Munoz et al. 2009). Nonclassical FD has no clear cutoff for when ERT should be started. However, starting ERT as soon as the symptoms are noticed is generally recommended to prevent irreversible tissue damage (Tondel, Bostad et al. 2013, Waldek and Feriozzi 2014). In untreated FD patients, when eGFR is below 60 ml/min/1.73 m^2 renal function deterioration is fast (Waldek and Feriozzi 2014). The updated guidelines for treatment initiation indicated that ERT should be initiated at 45–60 or 60–90 ml/min/1.73 m^2 based on the targeted class of FD patients according to the European Fabry Working Group consensus and the Fabry Expert Panel of the United States (Biegstraaten, Arngrimsson et al. 2015, Hopkin, Jefferies et al. 2016).

In certain Fabry patients, GFR reduction occurs before developing proteinuria (Wilcox, Oliveira et al. 2008). Additionally, in young FD patients, glomerular hyperfiltration may indicate early renal involvement (Riccio, Sabbatini et al. 2019). Although rare, a reduction in GFR can also be evidence of deteriorating renal function in adolescence in FD (Ramaswami, Najafian et al. 2010). In adult FD patients, the slope of progression of renal insufficiency was associated with the level of proteinuria, and it was not linear (Schiffmann, Warnock et al. 2009). However, like proteinuria, intensive tissue damage was reported in children prior to the eGFR decline (Tondel, Kanai et al. 2015). Furthermore, a recent study reported low FD diagnosis rate using eGFR (Reynolds, Tylee et al. 2021).

1.6.1.2 Cystatin-C

Cystatin-C (CsC), a protease inhibitor, was suggested as a nephropathy marker because it is filtrated freely by the glomerulus. Under normal circumstances, the CsC is reabsorbed and catabolized by tubular epithelial cells (Torralba-Cabeza, Olivera et al. 2011). CsC was reported as an accurate and sensitive indicator of renal function during renal replacement therapy (RRT) and in the determination of renal impairment (Feriozzi, Germain et al. 2007, Braga, Fonseca et al. 2019). However, its widespread clinical application is limited due to its high cost, time-consuming measurement, and limited testing availability than creatinine tests (Torralba-Cabeza, Olivera et al. 2011).

1.6.1.3 Urine microscopy

Urine microscopy can be practical for diagnosing and assessing FD development because it is a non-invasive, low-cost, and quick diagnostic method (Del Pino, Andres et al. 2018). Most abundant cells in Fabry patients' urine are tubular epithelial cells (Chatterjee, Gupta et al. 1984). Under a polarized microscope, mulberry cells/bodies (MB) with characteristic "Maltese cross bodies" (oval fat bodies) can be found in the urine sediments (Desnick, Dawson et al. 1971, Nagao, Satoh et al. 1985, Aoyama, Ushio et al. 2020). Figure 2 depicts a Maltese cross in the urine sediment of FD patients. Furthermore, there is a distinct morphological population of Maltese cross bodies with a lamellarized appearance and protrusions resembling "mosquito coils," which indicates fragmentation of Gb3-loaded epithelial cells (Selvarajah, Nicholls et al. 2011).

In addition, their excretion is linked with albumin concentration in urine, suggesting that MB may be used to assess the burden of Fabry nephropathy (Selvarajah, Nicholls et al. 2011). Recently, this method in 51 FD patients (Yonishi, Namba-Hamano et al. 2021) showed that urinary MB excretion precedes proteinuria and is adversely correlated with the duration of ERT. As such, the method has the potential for early diagnostics, however, it needs to be validated and standardized. A disadvantage is the necessity of specialized equipment (phase contrast microscopy) and well-trained personnel (Levstek, Vujkovac et al. 2020).

Figure 2. Birefringent Maltese cross in the urine sediment of Fabry patient when viewed under a polarized microscope (magnification 400×) (Levstek, Vujkovac et al. 2020). Licensed under Creative Commons Attribution License.

1.6.1.4 Podocyturia

Because podocytes are terminally differentiated cells, they have little regenerative potential (Wanner, Hartleben et al. 2014). There is evidence that Gb3 accumulates in podocytes very early in intrauterine development and infancy (Popli, Leehey et al. 1990, Chien, Olivova et al. 2011). Progressive Gb3 accumulation increases podocyte volume and a concurrent enlargement of the foot process, which eventually causes their separation from the GBM (Najafian, Tondel et al. 2020) and release in urine-podocyturia. This occurrence was documented even before the development of proteinuria in FD patients compared to healthy people (Tondel, Kanai et al. 2015, Fall, Scott et al. 2016, Trimarchi, Canzonieri et al. 2016, Trimarchi, Canzonieri et al. 2016, Vujkovac, Srebotnik Kirbis et al. 2022). Therefore, it could be utilized as an early marker for FN. However, present procedures for assessing podocyturia are not suited for widespread use in clinical settings since they are time-consuming, costly, complex, and non-standardized. Furthermore, the best urine podocyte-specific indicators have yet to be identified (Vujkovac, Srebotnik Kirbis et al. 2022).

1.6.2 Kidney biopsy

A recommended yet invasive diagnostic and treatment monitoring method is kidney biopsy (Svarstad, Iversen et al. 2004, Tondel, Bostad et al. 2008, Skrunes, Tondel et al. 2017). It is currently used for individuals diagnosed with CKD when *GLA* mutation is of unknown significance and when the diagnosis is uncertain (van der Tol, Svarstad

et al. 2015). It is powerful in identifying the hallmark of FD, the Gb3 tissue deposition (van der Tol, Svarstad et al. 2015). Additionally, the usefulness of this method is underlined by the fact that proteinuria and eGFR can be within normal range while tissue damage has already occurred (Najafian, Svarstad et al. 2011). Recently, bedside stereomicroscopy was suggested for easier assessment of Gb3 deposits (Svarstad, Leh et al. 2018). The use of kidney biopsy however is still controversial, particularly when it can be used in FD. For example, in Bergen, Norway, it is routinely being performed, especially prior to therapy initiation and again to monitor its effect e.g. after 5, 10 and 15 years (Svarstad, Iversen et al. 2004, Tondel, Bostad et al. 2008, Tondel, Bostad et al. 2008, Tondel, Ramaswami et al. 2010, Tondel, Bostad et al. 2013, Tondel, Kanai et al. 2015, Skrunes, Tondel et al. 2017, Svarstad, Leh et al. 2018).

1.6.3 Glycosphingolipids in tissue, circulation and urine

Gb3 and its deacylated form, lysoGb3, are used as FD biomarkers in classical and nonclassical phenotypes, respectively (Del Pino, Andres et al. 2018, Shiga, Tsukimura et al. 2021). Gb3 is the main hallmark of FD when using kidney biopsies due to its persistent accumulation in the podocytes (Svarstad, Leh et al. 2018). Additionally, it is elevated in the urine and plasma of classic FD patients. However, in nonclassical and heterozygous females, normal urinary and plasma levels of Gb3 were reported (Vedder, Linthorst et al. 2007). Furthermore, it does not reflect on kidney function deterioration (Tondel, Bostad et al. 2008, Moura, Hammerschmidt et al. 2018). A recent study has shown Gb3 in the peripheral blood mononuclear cells (PBMCs) and its usefulness in diagnosis and treatment monitoring (Uceyler, Bottger et al. 2018). However, this method needs to be clinically validated for routine use.

On the other hand, its soluble form, lysoGb3, in plasma and urine, has shown reasonable prediction of the disease progression and ERT treatment monitoring (Auray-Blais, Ntwari et al. 2010, Togawa, Kawashima et al. 2010, Togawa, Kodama et al. 2010, Paschke, Fauler et al. 2011, Nowak, Mechtler et al. 2017, Sakuraba, Togawa et al. 2018, Nowak, Beuschlein et al. 2022). Recently, lysoGb3 has been argued as not a suitable biomarker for chaperone treatment monitoring (Liu, Lin et al. 2014, Schiffmann, Bichet et al. 2020, Bichet, Aerts et al. 2021). Galabiosylceramide (Ga2) in plasma and urine was recently suggested as an alternative to lysoGb3 in FD

females as it shows a 5-fold increase compared to lysoGb3 in these patients (Heywood, Doykov et al. 2019).

Therefore, the FD community (practitioners and patients) desperately needs a biomarker that can mark the initiation of renal involvement, timely treatment enrollment, and monitor the treatment efficiency.

1.6.4 Novel biomarkers of Fabry nephropathy

Due to the several discrepancies and invasiveness of the current diagnosis and treatment monitoring biomarkers, studies have suggested novel biomarkers for FD and FN. These suggested biomarkers reflect glomerular and/or tubular damage. (Table 1).

Table 1: Suggested novel biomarkers for FN. P plasma; U urine; NI not investigated; NC, not correlated; Y, yes; N, no, T, tubular; G, glomerular, TR, treatment response; RFC, renal function correlation.

Biomarker	Assessed in	RFC	Injury	TR	Reference/s
β2-microglobulin	P	NI	T/G	Y/N	(Tsuboi and Yamamoto 2017, Braga, Fonseca et al. 2019)
α1-microglobulin	U	eGFR	T	NI	(Prabakaran, Birn et al. 2014, Aguiar, Azevedo et al. 2017)
N-acetyl-β-D-glucosaminidase	U	eGFR	T	Y	(Aguiar, Azevedo et al. 2017)
Transferrin	U	eGFR	G	NI	(Aguiar, Azevedo et al. 2017)
Type IV collagen	U	eGFR	G	NI	(Aguiar, Azevedo et al. 2017)
Alanine aminopeptidase	U	NC	T	NI	(Aguiar, Azevedo et al. 2017)
IgG	U	NI	G	Y	(Prabakaran, Birn et al. 2014)
Uromodulin	U	NI	T	NI	(Matafora, Cuccurullo et al. 2015, Doykov, Heywood et al. 2020)
Bikunin	U	NC	T	NI	(Lepedda, Fancellu et al. 2013)

Neutrophil gelatinase-associated lipocalin (NGAL/Lipocalin-2), Netrin-1, and kidney injury molecule (KIM-1) are acute kidney injury (AKI) biomarkers for tubular damage (Adiyanti and Loho 2012). Though they have not been investigated in FD or FN, they can also be of potential benefit considering their high sensitivity, but more studies are needed.

The aberrant urine excretion of tubular and glomerular proteins in Fabry patients reflects their compromised glomerular and tubular function. Consequently, these indicators may help evaluate kidney involvement and predict the course of FN. The sensitivity and their relationships with the course of FN, the currently used biomarkers,

and the changes in response to ERT must be thoroughly investigated in larger-scale studies (Levstek, Vujkovac et al. 2020).

1.6.5 Prospective biomarkers

The progress in genomics, transcriptomics, proteomics and metabolomics can be incredibly beneficial for investigating new FN biomarkers. Indeed, several studies have already highlighted potential biomarkers.

Apart from identifying gene variants, no genomics studies, i.e., genome-wide association studies (GWAS), were reported on FD and the consequent renal involvement. With the current era of omics approaches, it might be of good value to adapt such approaches to investigate novel biomarkers of FN. The nature of FD heterogeneity likely hindered such studies due to the possible high cost and processing time.

Urinary and plasma miRNAs were investigated in a few FD studies. miR-29 and miR-200, associated with renal fibrosis, were decreased in FD patients prior to the onset of proteinuria (Jaurretche, Perez et al. 2019). Additionally, specific serum miRNAs were downregulated upon ERT treatment, and some were gender-specific (Xiao, Lu et al. 2019). A recent study investigated the urinary extracellular vesicles for their molecular load (Levstek, Mlinsek et al. 2021), and they reported elevated expression of miR-29a-3p, miR-200a-3p, and miR-30b-5p. Interestingly, miR-30b-5p has a protective role in podocyte injury. Although not used routinely, miRNA studies can help reveal potential biomarkers due to their high sensitivity and specificity (Condrat, Thompson et al. 2020). Gene expression of kidney biopsies performed by renal research group at UiB indicated variations between FD patients at three-time intervals (baseline, five years post-ERT, and eight to ten years post-ERT) and healthy controls. Extracellular matrix, EMT, fibrosis, and immune response pathway gene set enrichment has been observed. Similar to the control samples, the early ERT intervention appeared to revert the elevated pathways to normal. Long-term, such as after ten years of ERT, these enriched pathways remained elevated (Eikrem, Strauss et al. 2018, Strauss, Eikrem et al. 2019, Eikrem, Delaleu et al. 2020).

Epigenetics (external factors) affecting FD progression and organ involvement are suggested due to the mosaic phenotypes in FD (Schiffmann, Fuller et al. 2016).

Epigenetic changes are reversible, hence can help monitor disease treatment. Although a couple of studies have highlighted the epigenetics changes in FD (Hubner, Metz et al. 2015, Hossain, Wu et al. 2019), none have proved helpful for monitoring FN.

Proteomics studies to detect novel biomarkers should focus on kidney function because their dysfunction correlates with excreting urine. Additionally, the urinary protein content excretion is low; therefore, it might be relatively simple to detect the dysregulation of a specific protein. Therefore, urine-derived proteomics studies are greatly valued (Cuccurullo, Beneduci et al. 2010). This approach identified several potential urinary proteins i.e., uromodulin also known as Tamm–Horsfall protein (THP), prostaglandin H2 d-isomerase (PGD2) and prosaposin (PSAP) (all are involved in renal tubular damage) in FD patients compared to healthy controls (Schiffmann, Waldek et al. 2010, Hollander, Dai et al. 2015, Matafora, Cuccurullo et al. 2015, Tebani, Mauhin et al. 2020).

In a recent study, genetically diagnosed FD patients were classified into three groups based on organ involvement (cardiac, cerebral, or renal involvement) according to the standard diagnostic criteria for each organ, (i.e., proteinuria and eGFR in the renal involvement group). LysoGb3 measured in plasma could not detect all asymptomatic FD patients (Doykov, Heywood et al. 2020). Proteomics analysis of the patients' urine samples revealed an elevation of six proteins before the development of glomerular filtration barrier impairment and albuminuria: albumin (Alb), THP, α1-antitrypsin (AAT), glycogen phosphorylase brain form (PYGB), endothelial protein receptor c (EPCR), and ICAM-1. Only one protein, PYGB, was elevated in the asymptomatic disease and correlated with progressive multiorgan involvement. Podocalyxin (PODXL), fibroblast growth factor 23 (FGF23), cubulin (CUBN), and α1M/Bikunin Precursor (αMBP) were higher in renal phenotype groups. Nephrin, a protein unique to podocytes, was higher in all symptomatic groups. PSAP, a lysosomal sphingolipid hydrolase activator, was higher in all symptomatic groups and exhibited increasing specificity with increased disease severity (Doykov, Heywood et al. 2020) .

GLA-knockout podocytes and FD patient urine-derived cells revealed increased proteins, including lysosomal proteins Glucosylceramidase (GBA), lysosomal integral

membrane protein 2 (LIMP-2/SCARB2), the ECM protein fibrillin (FBN1) and α-internexin (INA) (Slaats, Braun et al. 2018).

Taken together, the proteomics approach has identified several potential target molecules that will likely improve FN's early diagnosis and disease progression. However, further studies must confirm their future potential use in clinical practice.

The state of metabolites in the body changes swiftly with the physiological and pathophysiological changes (Schiffmann, Waldek et al. 2010). Additionally, they can change regardless of protein and mRNA levels. Most metabolite studies have focused on the Gb3 and lysoGb3 (Auray-Blais, Blais et al. 2015, Boutin and Auray-Blais 2015, Tebani, Mauhin et al. 2020). However, to this date, no metabolite study has specifically addressed renal involvement in FD.

1.7 Models of Fabry Disease

Animal and cell culture models proved inevitable for studying human disease pathophysiology. In FD, discrimination of specific FN subcellular processes and molecular pathways can be challenging due to their similarities with other chronic kidney diseases. Therefore, animal or cell models provide an opportunity for a detailed examination to distinguish better the FD-specific alterations, particularly the FN (Eikrem, Skrunes et al. 2017).

1.7.1 Cultured cell lines

The consequences of Gb3 accumulation on FN pathogenicity were studied using various cell lines. In peripheral blood mononuclear cells (PBMC) cultured from a Fabry patient, the Gb3 buildup increased the secretion of proinflammatory cytokines (De Francesco, Mucci et al. 2013). MDCK cells from the kidneys of Madin-Darby canines were used to establish a renal epithelial cell model of Fabry disease using short interfering RNA (siRNA) (Labilloy, Youker et al. 2014). In this model, Gb3 accumulation disrupted raft-mediated cell activities, such as raft-mediated signal transduction through TGF-β.

Jeon et al. produced human proximal renal tubular epithelial cells (HK2) and mouse glomerular mesangial cells (SV40 MES 13) by silencing α-GAL using siRNA (Jeon,

Jung et al. 2015). This model verifies prior findings about the effects of exogenous Gb3 and lysoGb3 on cell lines; EMT is more commonly related to lysoGb3.

In microvascular endothelial cells cultured from FD patients and obtained using skin biopsy from the forearm, it was demonstrated that Gb3 accumulation induces intracellular ROS generation in a dose-dependent manner (Shen, Meng et al. 2008).

A human podocyte model was used to explore FD-dysregulated autophagy. This model, developed by lentiviral transfer of small hairpin RNAs (shRNA) against *GLA*, demonstrates that the increase of Gb3 disrupts mTOR signaling, resulting in dysregulated autophagy and podocyte death (Liebau, Braun et al. 2013).

Using the CRISPR/Cas9 gene-editing tool, another FD model was produced in a human immortalized podocyte cell line (Pereira, Labilloy et al. 2016). This model identified 65 distinct disease-related signaling pathways, among which the MAPK and VEGF pathways were considerably enriched.

The involvement of Gb3 and its soluble form lysoGb3 was examined by exposing normal cell lines to these two molecules (Sanchez-Nino, Sanz et al. 2011, Jeon, Jung et al. 2015, Shin, Jeon et al. 2015). The exposure of the immortalized podocytes cell line to lyso-Gb3 revealed significant increases in TGFβ-1, type IV collagen (ColIV), and CD74 expression (Sanchez-Nino, Sanz et al. 2011). Also, treating human proximal renal tubular epithelial cells (HK2) and mouse renal mesangial cell line (SV40 MES 13) with Gb3 and lysoGb3 results in elevated expression of TGF-β1, EMT markers (N-cadherin and α-SMA) and phosphorylation of PI3K/AKT, and decreased the expression of E-cadherin (Jeon, Jung et al. 2015). The gene expression profiles in the same kidney cells exposed to Gb3 or lyso-Gb3 were substrate- and cell-dependent, suggesting that Gb3 and lyso-Gb3 modulate renal fibrosis through separate biochemical pathways (Shin, Jeon et al. 2015).

1.7.2 Kidney organoids

Recently, kidney organoids (based on human inducible pluripotent stem cells, iPSC) were used to investigate the FN. This FD model revealed disturbed podocytes and tubular cell shape accompanied by the accumulation of globotriaosylceramide (Gb3). Additionally, elevated levels of oxidative stress were observed in the mutant organoid (Kim, Kim et al. 2021).

1.7.3 Rodent models of FD

FD models in mice have been predominantly used to investigate treatment outcomes. Only a few models were used to investigate the role of Gb3 in FD. In 1997, the first FD mouse model with null α-GAL activity was created (Ohshima, Murray et al. 1997). Similar to human FD patients, Gb3 was detected in various tissue types (Christensen, Zhou et al. 2007, Bangari, Ashe et al. 2015); however, this model lacks organ damage features similar to FD. Another mouse model in which human Gb3 synthase is expressed was established (Shiozuka, Taguchi et al. 2011, Taguchi, Maruyama et al. 2013). In contrast to other mouse models, this mouse resembles the human phenotype more closely by showing elevated serum Gb3 concentrations, tissue Gb3 accumulation, renal impairment, and a shorter lifespan. However, in their model, ocular manifestations related to FD classical phenotype were nonconclusive (Miller, Aoki et al. 2019).

1.7.4 Limitations

Despite the enormous contribution of cell lines, cell culture research on podocytes is limited, because podocytes lose their defining characteristics *in vitro*. For example, intercellular connections are neither physically nor functionally like the slit-diaphragm found *in vivo* (Hagmann and Brinkkoetter 2018). Additionally, the FD patient-derived cell lines carry different *GLA* gene mutations that are influenced by variable genetic backgrounds which is an important issue even for monogenic, dominant, and highly penetrant diseases in FD. Therefore, it can be considered a significant limitation of this approach (Kajiwara, Aoi et al. 2012, Pan, Ouyang et al. 2016, Song, Chien et al. 2019).

The significance of the FD models to our understanding of the pathophysiology and histology of Fabry disorders is indisputable. However, neither cell lines nor mice could adequately characterize the physio-histopathology of FN, let alone optimize ERT for individualized treatment.

Another critical issue is that Gb3-dependent and independent disease manifestations have never been addressed clearly in the course of FD. These models can't distinguish between Gb3-dependent and independent injury. Furthermore, investigations on mice or kidney organoids can be laborious and expensive. In addition, studying intra-uterine gestation in mice is complicated by the potential

absence or reduced α-GAL enzymatic activity throughout the early developing stage (Haskins, Giger et al. 2006, Hagmann and Brinkkoetter 2018). Moreover, species variations in metabolic pathways must always be kept in mind (Germain 2010). Thus, there is an urgent need for a new FD model capable of bridging the previously addressed issues and shedding light on the Gb3-independent manifestations of FD to describe the decline of renal function and to aid the screening for prospective medicines.

1.8 Zebrafish: General background and similarity to humans

The zebrafish (ZF) is a widely used animal to study human diseases and new drug screening. The favorable characteristics include anatomical and genetic similarity to humans, short life cycles, transparency of embryonic phases, ex-utero egg development, low maintenance costs, and simple handling (Gut, Reischauer et al. 2017). On top of that, the small size and large offspring numbers allow for time-efficient drug screening in a 96-well plate format (Zon and Peterson 2005, Gehrig, Pandey et al. 2018).

In the laboratory, zebrafish are kept according to defined parameters. Examples include a narrow temperature range, circadian rhythm, water quality, and feeding habits. Adopting such conditions, four stages of a typical life cycle develop the embryo, larva, juvenile, and adult (Kimmel, Ballard et al. 1995). By five days post-fertilization, embryos have hatched, and larvae can feed on external food particles, i.e., fish food. ZF reaches sexual maturity at around three months, depending on the temperature and population density (Meyers 2018). The kidney, heart, liver, and brain of vertebrate fish are functionally equivalent to humans (Lieschke and Currie 2007), and zebrafish are no exception to this rule. Therefore, investigating organ participation in health and disease in ZF is highly reliable.

1.8.1 Genetic similarity

Due to the intensive use of ZF in developmental and neurological studies, the DNA sequence of the ZF genome was published in 2013 (Howe, Clark et al. 2013). When the zebrafish and human reference genomes were compared, it was shown that 71% of human genes had at least one zebrafish orthologue, while 69% of zebrafish genes have at least one human orthologue (Howe, Clark et al. 2013). Importantly, zebrafish orthologues exist for 82 percent of all human illness-associated genes (Howe, Clark

et al. 2013). The zebrafish system was first shown to be genetically amenable in the mid-1980s (Driever, Solnica-Krezel et al. 1996, Haffter, Granato et al. 1996), and it has subsequently proven to be very responsive to genetic manipulation. The feasibility of using variable forward and reverse genetic manipulation approaches have been documented in many diseases (Phillips and Westerfield 2020). More recently, advances in targeted gene editing technologies like Clustered Regularly Interspaced Short Palindromic Repeat- CRISPR Associated Protein 9 (CRISPR-Cas9) with 99% accuracy (Varshney, Pei et al. 2015) have accelerated the growth of stable zebrafish models (Hwang, Fu et al. 2013, Gagnon, Valen et al. 2014).

1.8.2 CRISPR-Cas9 gene editing

CRISPR-Cas9 gene editing technology enables genetic modification that is mainly permanent and highly specific. Cas9 is one of several RNA-guided endonuclease enzymes generated from the immune systems of bacteria and archaea as a natural defense mechanism against invading viruses (Marraffini 2015).

Recently, the CRISPR-Cas9 technology has been effectively developed for editing the genomes of numerous multicellular and complex species, such as zebrafish, mice, and humans (Elmonem, Berlingerio et al. 2018). Cas9 is coupled to two RNA guide molecules, the trans-activating CRISPR RNA (tracrRNA) and the CRISPR RNA (crRNA), to create the Cas9 holoendonuclease system, a trimeric complex in bacteria. Typically, a specially designed single guide RNA (sgRNA) replaces the tracrRNA-crRNA complex in an experimental setting (Wright, Nunez et al. 2016).

Short CRISPR RNAs (crRNA) created from non-repeating spacer DNA sequences acquired from viruses and other mobile genetic elements guide Cas enzymes in prokaryotes (Brouns, Jore et al. 2008). The spacer sequences of prokaryotes are highly similar in areas called protospacer-adjacent motifs (PAMs), which are essential for the CRISPR system (Deveau, Barrangou et al. 2008). These two RNAs are combined into one single guide RNA sgRNA as follows: a 20-nucleotide sequence at the 5' end of the sgRNA binds specifically to the DNA target site. The 3' end is followed by an RNA sequence that, via RNA hairpins, forms a complex with the Cas9 endonuclease. Cas9 protein–sgRNA complex attaches to the DNA when the 20 bp gRNA integrates with its corresponding sequence in the target region of the DNA; the activity of Cas protein is dependent on this 20 bp gRNA's proximity to its particular

PAM sequence. The cut is then created few bases following the PAM triplet sequence (Jinek, East et al. 2013). One of the significant drawbacks of this technology is the off-target binding, which is influenced by sgRNA sequence, cell type, Cas9 enzyme concentration, and delivery methods (Pattanayak, Lin et al. 2013, Lino, Harper et al. 2018). Many disease models were produced in ZF using this technology, and more recently, intensive use of ZF in LSDs has been documented with promising results (Zhang and Peterson 2020).

1.8.3 Zebrafish kidney

The kidney of the zebrafish has two forms: pronephros (embryo and larva) and mesonephros (juvenile and adult). In its simplest form, the pronephros, two nephric units stretch down the mid-dorsal line and are pre-headed by a single fused glomerulus behind the embryo or larva head (Drummond, Majumdar et al. 1998). Hundreds of nephrons are created within the mesonephros at the juvenile stage (about 14 dpf) (Diep, Ma et al. 2011). The mesonephros is typically separated into the head, neck, body, and tail (Figure 3). A fascinating characteristic of ZF mesonephros is its continued regeneration in the event of renal injury (Gerlach and Wingert 2013).

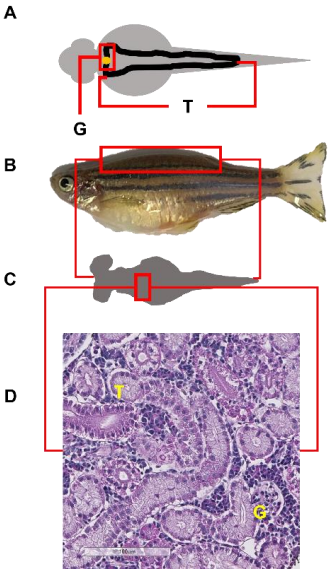

Figure 3. Zebrafish kidney development. (A) The pronephric kidney in the 3-day larva. One fused glomerulus at the midline connects to the pronephric tubules that run backward laterally and are joined at the cloaca (external opening). (B) The adult zebrafish 90 dpf. (C) adult zebrafish mesonephros, a few hundreds of glomeruli

connected to their proximal and distal tubules. (D) hematoxylin stain of the adult kidney. G, glomerulus, T, tubule. (Original figure).

Zebrafish kidneys contain all functional structures present in the human kidney (glomerular corpuscle, proximal and distal tubules, collecting duct) except for the loop of Henle, which can be attributed to their freshwater habitat. In contrast to humans, ZF lacks bone marrow; therefore, blood production occurs in the kidney interstitium (Lieschke and Currie 2007, Jagannathan-Bogdan and Zon 2013).

The glomerular filtration barrier (GFB) partially functions as early as two days post-fertilization and is entirely operational by day four (Kramer-Zucker, Wiessner et al. 2005, Drummond and Davidson 2010). This early kidney development when embryos/larvae are still transparent makes zebrafish an effective model for studying kidney disease since the kidney may be analyzed with minimum intervention.

1.8.4 Zebrafish in Lysosomal storage diseases research

Currently, around 60 genetically engineered zebrafish recapitulate phenotypes of various LSDs (Zhang and Peterson 2020). Sphingolipidoses, mucolipidoses (MLs), neuronal ceroid lipofuscinoses, integral membrane protein disorders, glycogen storage diseases (GSD), glycoproteinoses, mucopolysaccharidoses (MPS), and lysosome-related organelle disorders are among the eight types described (Platt, d'Azzo et al. 2018). Illustrated in Table 2 are the current LSDs models in ZF.

Table 2. Lists of the current available lysosomal storage disease models utilizing zebrafish.

Gene	LSD	References
ASAH1	Farber lipogranulomatosis	(Zhou, Tawk et al. 2012, Zhang, Trauger et al. 2019)
ARSA	Metachromatic leukodystrophy	(Berg, Levitte et al. 2016)
GALC	Globoid cell leukodystrophy/Krabbe disease	(Zizioli, Guarienti et al. 2014)
GBA	Gaucher disease	(Busch-Nentwich 2012, Keatinge, Bui et al. 2015, Zancan, Bellesso et al. 2015, Berg, Levitte et al. 2016, Lelieveld, Mirzaian et al. 2019, Watson, Keatinge et al. 2019)
HEXA	Tay-Sachs disease	(Berg, Levitte et al. 2016)
HEXB	Sandhoff disease	(Kalen, Wallgard et al. 2009, Kuil, Lopez Marti et al. 2019)
GNPTAB	Mucolipidosis II α/β (I-cell disease); Mucolipidosis III α/β (pseudo-Hurler polydystrophy)	(Flanagan-Steet, Sias et al. 2009, Petrey, Flanagan-Steet et al. 2012, Qian, van Meel et al. 2015, Flanagan-Steet, Matheny et al. 2016, Flanagan-Steet, Christian et al. 2018)
GNPTG	Mucolipidosis III γ, variant pseudo-Hurler polydystrophy	(Flanagan-Steet, Matheny et al. 2016)
MCOLN1	Mucolipidosis IV	(Li, Pei et al. 2017, Jin, Dai et al. 2019)
ATP13A2	CLN12/Kufor-Rakeb syndrome	(Lopes da Fonseca, Correia et al. 2013, Spataro, Kousi et al. 2019)
CLN3	CLN3/Batten-Spielmeyer-Sjogren disease	(Wager, Zdebik et al. 2016)
CTSD	CLN10	(Follo, Ozzano et al. 2011, Follo, Ozzano et al. 2013)

GRN	CLN11	(Chitramuthu, Baranowski et al. 2010, Laird, Van Hoecke et al. 2010, Li, Chen et al. 2010, De Muynck, Herdewyn et al. 2013, Li, Chen et al. 2013, Chitramuthu, Kay et al. 2017)
TPP1	CLN2	(Busch-Nentwich 2010, Busch-Nentwich 2010, Busch-Nentwich 2013, Mahmood, Fu et al. 2013)
CTNS	Cystinosis	(Busch-Nentwich 2013, Elmonem, Khalil et al. 2017, Festa, Chen et al. 2018)
NPC1	Niemann-Pick disease type C1; type D	(Schwend, Loucks et al. 2011, Louwette, Regal et al. 2013, Chu, Liao et al. 2015, Lin, Cai et al. 2018, Tseng, Loeb et al. 2018)
SCARB2	Action myoclonus-renal syndrome	(Golling, Amsterdam et al. 2002, Amsterdam, Nissen et al. 2004, Diaz-Tellez, Zampedri et al. 2016)
GAA	Pompe disease	(Wu, Yang et al. 2017)
MANBA	β-mannosidosis	(Ko, Yi et al. 2017)
IDS	Mucopolysaccharidosis II/Hunter syndrome	(Moro, Tomanin et al. 2010, Costa, Urbani et al. 2017, Bellesso, Salvalaio et al. 2018)
HSP5	Hermansky-Pudlak disease type 5	(Driever, Solnica-Krezel et al. 1996, Stemple, Solnica-Krezel et al. 1996, Daly, Willer et al. 2013)
HSP7	Hermansky-Pudlak disease type 7	(Chen, Song et al. 2018)
LYST	Chédiak-Higashi disease	(Kim, Wu et al. 2015)

Regardless of the extensive use of ZF in LSDs research, our search revealed no published research in FD. An interesting fact about ZF is the lack of Gb3 synthase enzyme, the enzyme responsible for Gb3 production; therefore, it could be a useful tool to investigate the possible Gb3-independent renal injury.

1.9 Research question

How can we induce the Gb3-independent findings of Fabry disease (especially nephropathy) in zebrafish?

1.10 Hypothesis

We can lower the activity of α-Gal in zebrafish by introducing a selective mutation, which will be reflected by functional (elevated serum creatinine levels, proteinuria) and histological kidney damage independently of Gb3 accumulation.

1.10.1 Rationale

FD is known for the high heterogeneity between individual FD patents. Additionally, until now, it is not possible to dissect Gb3/lysGb3 tissue injury from an injury unrelated to their accumulations. Such differentiation can help in the early diagnosis of tissue involvement and design of perspective medical therapy, particularly in the kidney, as early ERT intervention indicates better treatment outcomes. Zebrafish is a good tool because it is a naturally Gb3 synthase-free organism. Therefore, by generating an FD

model in ZF, we can study the Gb3 independent tissue injury and identify new potential biomarkers for early tissue involvement.

1.10.2 Aim

To establish an FD model in zebrafish that allows studying the renal pathogenic effects of Fabry disease independent of Gb3.

1.10.3 Objectives

1.10.3.1 General objective

To establish the FD model in zebrafish and investigate the Gb3 independent biomarkers for early tissue injury diagnosis.

1.10.3.2 Specific objectives

- To characterize the *GLA* gene and α-GAL enzyme in zebrafish and compare the similarity to their human counterparts.
- To generate *GLA*-mutant ZF.
- To characterize the impact of the *GLA* mutation on the α-GAL activity, renal function (creatinine levels and proteinuria) and other FD-related phenotypes.
- To study the molecular mechanisms of the FD progression in a Gb3-free environment on the transcriptome, proteome, and metabolome level in a Gb3-free environment.

2 Methods

2.1 Ethical approval (Paper I, II, and III)

The Norwegian Food Safety Authority (Mattilsynet) approved this study as ethical (FOTS ID 15256). All operations were carried out under the approved guidelines of the Zebrafish Facility at the UiB. We used the AB/Tübingen (AB/TU) zebrafish strain for our research.

2.2 Study design (Paper I, II, and III)

The design of this study is illustrated in Figure 4.

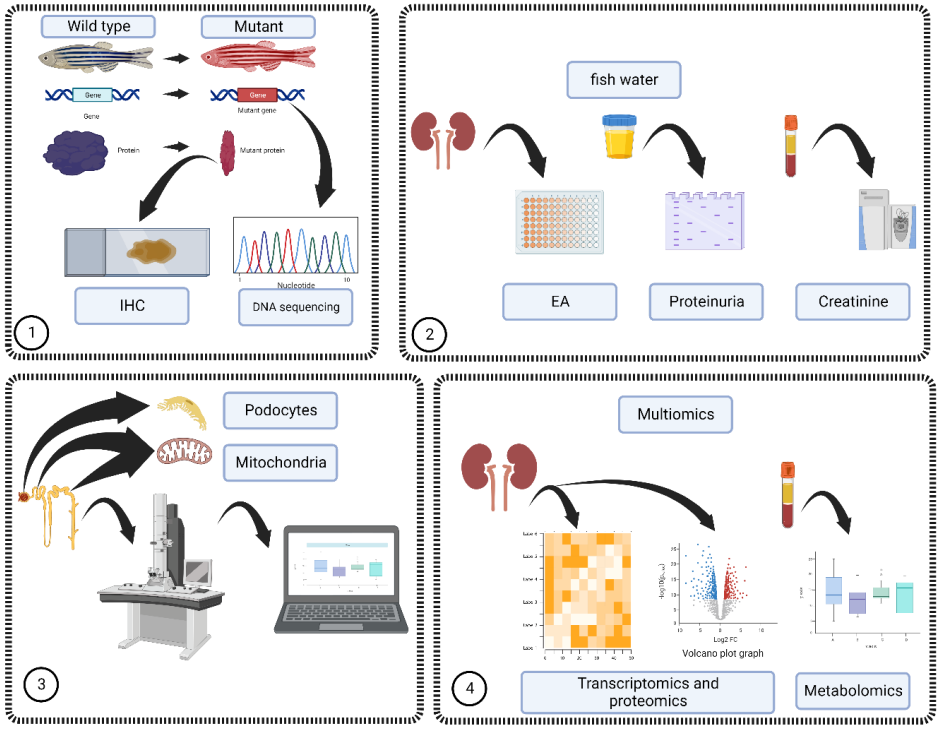

Figure 4. Study design chart. 1: wild type gene and protein compared to their human counterpart, mutant line created and verified using DNA sequencing and by detecting the enzyme abundance in the renal tissue. 2: enzyme activity used to validate the mutant, and renal function was evaluated using plasma creatinine and proteinuria assay. 3: renal tissue was histologically investigated using transmission electron microscopy. 4: multi-omics approach used to identify Gb3-independent markers in the renal tissue. IHC: immunohistochemistry, EA: enzyme activity.

2.3 Zebrafish maintenance and housing (Paper I, II, and III)

Rearing of the early developmental stages (eggs, embryos 1-2 days post-fertilization (dpf), and larva 3-5 dpf), juvenile stage 30+ dpf, and adult stage 90+ dpf was performed according to the universal protocol adopted by the zebrafish facility, UiB.

Under standard laboratory conditions, adults were kept at 28°C with a 14 h light/10 h dark cycle. According to the standard/routine protocol of the zebrafish facility, male and female adults were crossed to produce new fish (www.zfin.org).

Eggs were obtained from the fish tank using a fine mesh strainer, then washed and incubated at 28°C for five days in a petri dish while submerged in E3 medium (5 mM NaCl, 0.17 mM KCl and 0.33 mM $MgSO_4$) with 0.01 percent methylene blue. Egg development into embryo and larva was monitored daily during the first five days. E3 medium with 0.01 percent methylene blue was used on days 1 and 2, and methylene blue was removed from day three. During this period, developing stages are not free feeders. From day six, the free feeder larva was transferred from the incubator into larger fish tanks and installed in the fish tank system. Water circulation was only introduced gradually (low-speed water dripping) by day 14. By day 30, juvenile fish were fully integrated into the circulation system in the zebrafish facility.

2.4 Sample collection (papers I, II, and III)

Different samples were collected: embryo, larva, and juvenile stages, kidney, blood, and fins from adult zebrafish. The collection of samples depended on the stage/tissue and the analysis application needed. The dissection of the adult fish and extraction of their kidneys were similar for all downstream applications unless otherwise stated. According to the standard protocols, all invasive pain-causing treatments on stages older than five dpf were conducted under anesthesia in 100 mg/L tricaine methane sulfonate MS222 (Sigma, Cat. No. A-5040).

2.4.1 Whole animal collection: embryo and larva (papers I and II)

The collection of embryos and/or larvae was performed for DNA extraction, enzyme activity, and oxidative stress assay. Samples were collected using snap-freezing liquid nitrogen for enzyme activity and oxidative stress assays.

2.4.2 Kidney collection from adult fish (paper I, II, and III)

The kidney was collected as follows: after the fish were euthanized in 300 mg/L tricaine methane sulfonate MS222 (Sigma, Cat. No. A-5040), the abdominal cavity was opened, and the viscera were removed, exposing the kidney. The kidney was flushed with cold 1X PBS (ThermoFisher, Cat. No. AM9625) while in the body. Then, the kidney was removed and snap-frozen in liquid nitrogen for protein extraction, lipid extraction, and oxidative stress assays. Alternatively, the head and tail were removed, and the dissected-open fish was placed in paraformaldehyde (Sigma-Aldrich, Cat. No. 16005) for 24 hours. This step was introduced due to the soft nature of the zebrafish kidney, as the immediate extraction will distort the kidney shape for tissue embedding and result in poor tissue sections and tissue consistency on a glass slide. The next day, the fish was flushed with 1X PBS, and the kidney was removed for downstream tissue processing. For electron microscopy, the kidney was removed after dissection and placed in 2.5% glutaraldehyde (in 0.1 M cacodylate buffer) for 24 hours. Then the kidney was flushed with 0.1 M cacodylate buffer and delivered to the molecular imaging center (MIC), UiB for embedding, sectioning, staining, and imaging.

2.4.3 Blood collection (papers I and II)

Blood was collected from adult fish according to the previously described protocol (Jagadeeswaran, Sheehan et al. 1999). After fish were euthanized, a transverse cut was made just caudal to the dorsal fin, leading the blood to pool on the surface. The pooled blood was collected using a heparin-coated micropipette tip (Heparin 5000 IE/ml, LEO Pharma Cat. No. 464327). The plasma was then separated from the blood by centrifugation (Eppendorf, 5415R) for 10 minutes at 1000 g at 4°C. Then the plasma was frozen in liquid nitrogen and stored at -80°C.

2.5 Generation of antibody against zebrafish α-GAL (Paper I)

Due to the lack of good quality antibodies that can work in zebrafish, we evaluated four anti-human α-GAL Abs (Table 3) based on their published antigenic sequences and their predicted cross-reactivity with ZF. After being evaluated for western blot and immunohistochemistry, none could specifically detect ZF α-GAL of 46 kDa.

Zebrafish-specific antibody against the α-GAL protein was produced using GenScript® services. α-GAL protein sequence was retrieved using Geneious prime software. The screen for putative antigenic regions via the EMBOSS6.5.7 plugin

embedded in the Geneious prime software. The potential sequences were then shared with GenScript®, where they conducted another level of assurance by testing the predicted reactivity, sequence similarity, and antigenicity. In the end, five sequences were chosen to produce polyclonal antibodies against zebrafish α-GAL (Table 3). Antibodies were then generated by GenScript® in New Zealand rabbits using GenScript's standard process.

Table 3: The list of all primary antibodies used in this study. WB: western blot, IHC: immunohistochemistry, Cat. No.: catalog number, NC: nonconclusive, N/A: not available, AR: antigen retrieval, HIER: heat-induced epitope retrieval, H: human, M: mouse, Z: zebrafish. N/A: not applicable.

Code/Cat. No.	Conc.	Peptide sequence/ target protein	WB conc.	IHC conc.	Company	AR HIER
ab24170	1 mg/ml	LAMP1 (H)	N/A	1:400	Abcam	pH9
ab134045	0.36 mg/ml	CD63 (H)	N/A	1:800	Abcam	pH9
ARP54296	0.5 mg/ml	HU α-GAL	1:1000	NC	Aviva	NC
GTX124431	0.84 mg/ml	Idh3a (Z)	N/A	1:200	GeneTex	pH9
GTX124294	1 mg/ml	Sod2 (Z)	N/A	1:50	GeneTex	Skipped
GTX125890	1.27 mg/ml	Cdh1 (Z)	N/A	1:200	GeneTex	pH6
GTX129952	1 mg/ml	OPA1 (H)	N/A	1:1000	GeneTex	pH6
gla pAb1	1.683 mg/ml	MVKEGWKDAGYEFVC (Z)	NC	NC	GenScript	NC
gla pAb2	0.803 mg/ml	CVMNRQEIGGPRRFT (Z)	NC	NC	GenScript	NC
gla pAb3	0.482 mg/ml	QHQQPDYEAIRKTC (Z)	NC	NC	GenScript	NC
gla pAb4	0.462 mg/ml	CVVNRQEIGGPRRFT (Z)	NC	NC	GenScript	NC
ZF-gla pAb5*	1.107 mg/ml	CKADSFELWERPLSG (Z)	1:1000	1:600	GenScript	Skipped
M1506-1	2μg/μl	CTSB (M)	N/A	1:1000	HUABIO	pH6
LS-C166494	N/A	HU α-GAL	1:1000	NC	LSBio	NC
LS-C80577	1 mg/ml	GOT2 (H)	N/A	NC	LSBio	NC
15428-1-AP	450μg/ml	HU α-GAL	1:1000	NC	Proteintech	NC
20384-1-AP	0.5 mg/ml	NPHS2 (M)	N/A	NC	Proteintech	NC
AV54296	1 mg/mL	HU α-GAL	1:1000	NC	Sigma-Aldrich	NC
V9131	N/A	VCL (H)	N/A	NC	Sigma-Aldrich	NC

2.6 Computation analysis, protein modeling of *GLA*, and generation of the mutant (Paper I)

Our study strategy was aimed at generating *GLA* mutant zebrafish. ZF *GLA* gene and protein sequences were compared to their human counterparts using several databases, including the National Centre for Biotechnology Information GenBank database (NCBI), Ensembl database, Universal Protein Resource (UniProt), Zebrafish Information Network (ZFIN), Swiss Institute of Bioinformatics (Expasy) and Iterative Threading Assembly Refinement (I-TASSER).

In detail, we compared nucleotide and amino acid sequences to non-redundant gene databases accessible through NCBI http://blast.ncbi.nlm.nih.gov using the BLAST method under the default online tool settings. The NCBI BLAST online tool (https://blast.ncbi.nlm.nih.gov/Blast.cgi) was used to assess sequence similarity to the most updated (at the time of search, 2018) genome assembly of zebrafish (GRCz11/danRer11). ClustalW plugin was used to produce the multiple sequence alignment, which was then executed using the Geneious program. The Ensembl database (http://www.ensembl.org) was used for comparative genomics analysis of zebrafish and human *GLA* sequences. The homology modeling study was conducted using the ITASSER online modeling program (Roy, Xu et al. 2011). The final model was selected based on the confidence score (C-score), which assesses a model's prediction and is computed using the relevance of threading template alignments and convergence parameters in structure assembly simulations. The usual range for the C-score is -5 to 2, with a higher C-score suggesting a model with greater confidence. The predicted 3D model with the greatest C-score was used to pick the potential protein structure.

2.6.1 CRISPR target design and Generation of short guide RNA

CHOPCHOP online tool (https://chopchop.cbu.uib.no) was used to select the target sequence following previously published protocols (Labun, Montague et al. 2019, Labun, Krause et al. 2021). Three target sequences were selected, covering exons 2, 3, and 5 based on the following criteria: high efficiency, low number of off-targets, proximity, location in the exons shared by all known splice variants, and a preference for the center of the exon. Eventually, our target sequences, PCR primers for genotyping and sequencing, and the Cas9 enzyme were acquired from Integrated DNA Technologies BVBA (IDT, Leuven, Belgium). Ribonucleoprotein (RNP) combinations were assembled according to manufacturer instructions. Sequences are shown in Table 4.

Table 4: gRNA sequences

Exon target	gRNA	sequence
Exon 2	GLA2	GACCCCAAAAGGTTTCCCAGTGG
	GLA3	TGTGCGTCCCTTTGTTGCGAAGG
	GLA5	TGCCAGTTTTTTGATGCCACTGG
Exon 3	GLA1	GTGGGCACAAAAACTTGCGCAGG
	GLA4	GCTGGGAATATATGCAGATGTGG

Exon 5	GLA6	GCAGAAGATCGTCGTCCCAGTGG
Exon 6	GLA7	CTTTGGGACAGATGTCTCGCAGG

2.6.2 CRISPR/Cas9 injection and rearing the mutants

We used the untargeted approach for generating the mutant line. In this approach, we injected a single or combination of the selected gRNAs (see sgRNA combinations in Table 5). At the 1-cell stage, a wild type zebrafish egg was injected with the ribonucleoprotein (RNP: sgRNA 200ng/µl and cas9 protein 250ng/µl). Two nL of the injection mix was delivered into the yolk neighboring the cell membrane. PCR fragment analysis was performed as detailed in the next section for genotyping. The detailed methodology for detecting and rearing mutant fish was as follows: five dpf embryos injected with sgRNA (Founder 0/F_0) were genotyped to validate effective mutant creation. After verifying the success of the F_0 mosaic mutant, mature larvae were raised to adulthood. Individual adult fish were screened, and positive mutants were outcrossed to wild type to produce F_1 embryos with a heterozygous genotype $GLA^{+/-}$. F_1 adults were inbred to produce the F_2 generation ($GLA^{+/+}$, $GLA^{+/-}$, and $GLA^{-/-}$ offspring). To obtain a pure $GLA^{-/-}$ mutant line, F_2 mutants were genotyped, sequenced, and mutants with potential premature stop codon were bred to generate F_3 homozygous $GLA^{-/-}$ mutants. All studies have been undertaken on the F_3 generation or its inbred offspring compared to their similar generation wildtype. Based on the enzyme activity evaluation, the mutant line was validated further. The mutant with predicted low or null enzyme activity was chosen for further examination in this work. The general workflow for generating the mutant line is illustrated in Figure 5.

Table 5: gRNAs combination for microinjection X2: exon 2, X3: exon 3, X5.6: exon 5 and 6, X2,3,5,6: exon 2, 3, 5, and 6, GLA 1-7: gRNAs for the target sequence.

			EXON/S			
			X2	X2.3	X5.6	X2.3.5.6
Cas9 protein 0.5 µg/µL			2.5µL	2.5µL	2.5µL	2.5µL
gRNA 3 µM	GLA2	2	0.67µL	0.5µL		0.5µL
	GLA3		0.67µL	0.5µL		
	GLA5		0.67µL			
	GLA1	3		0.5µL		0.5µL
	GLA4			0.5µL		
	GLA6	5			1µL	0.5µL
	GLA7	6			1µL	0.5µL
Phenol Red2.5%			0.5µL	0.5µL	0.5µL	0.5µL

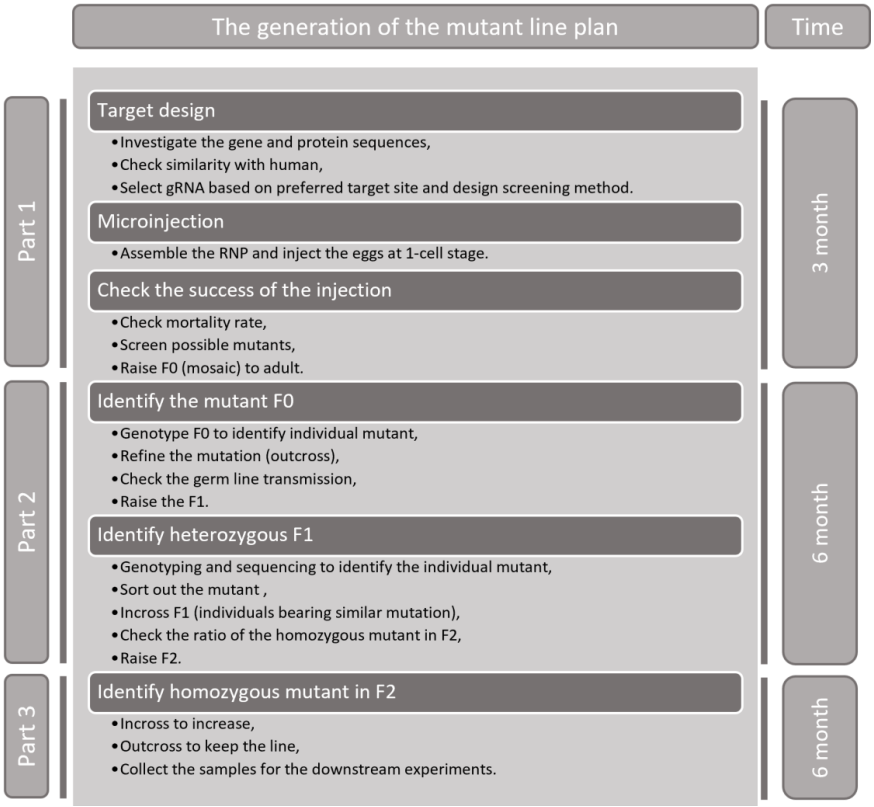

Figure 5. The workflow of generating the mutant line using the CRISPR/Cas9 gene editing tool. F0 is the founder generation, F1 is the first generation, and F2 is the second generation.

2.6.3 DNA extraction, genotyping, and sequencing

DNA was extracted from the whole larva or adult tail fin. For larval DNA extraction, a pooled sample of five larvae per sample or a single larva per sample was utilized based on the purpose. Larval sample treatment followed the adult sample treatment described below. For adult fish screening, one-third of the tip of the adult's tail fin was cut and placed in 50mM NaOH and heated for 25 minutes at 95°C using a thermocycler (Bio-Rad: C1000 Touch™ Thermal Cycler). The samples were then stored at -20°C until further analysis. PCR reaction was prepared as described in (Table 6). PCR conditions were modified for each primer set (Table 7). The digestion was performed using NEB enzymes (Table 8) per NEB's instructions. The selection of the digestive enzyme is based on their recognition motif in proximity to the potential

mutation site and their single or double cutting sites. The planned mutation/s interrupt the sequence of the restriction enzyme cutting site, preventing the enzyme from recognizing the region to cut and, therefore, retaining the enzyme passive. The digestive reaction was carried out on a thermocycler.

Table 6: PCR reaction

Cat. No.				Notes
		Initial conc.	Final conc.	
Taq buffer	ThermoFisher, EP0703	10X	1X	
dNTP mix	ThermoFisher, R0193	10mM	0.2 mM	
FW primer		100 µM	0.5 µM	Electrophoresis: Run at 80 Am for 40-50 min.
RV primer		100 µM	0.5 µM	
DNA template		varies	5 ng/µL	
DreamTaq polymerase	ThermoFisher, EP0703	5 U/µL	1.25 U	
HiFi Taq polymerase	ThermoFisher, F530S	2 U/µL	0.02 U/µL	
Nuclease free water		top up	top up	

Table 7: Primer sequences for genotyping and sequencing.

Region	primer direction	Adjusted Tm	PCR length (mutant) bp	Extension time (sec.)	Sequence
exon 5 to 6	forward	59.1	562 (+11)	30	TGCATCCCATTCCTTTTGCC
	reverse	58.6			TCTCTTGCATTTCAGCCTGAC
exon 3	forward	58.3	288	20	AATATCCACTCACCTTCTCCCA
	reverse	58.8			CCCCTAGTGTTGTTTTGCTGAT
exon 2	forward	60.3	272 (+18)	20	ACCTCTTCCAGCCTCATACTCA
	reverse	58.3			AGAGCAGATGCAGATTTGAACA
exon 2 to 6	forward	59.1	6915	180	TGCATCCCATTCCTTTTGCC
	reverse	58.3			AGAGCAGATGCAGATTTGAACA
exon 2 to 3	forward	58.3	2405	60	AATATCCACTCACCTTCTCCCA
	reverse	58.3			AGAGCAGATGCAGATTTGAACA

Table 8: restriction enzymes

Enzymatic digestion	Initial conc.	Final conc.	Incubation
Enzyme buffer	10X	1X	
BmrI NEB, R0600S	5000 U/mL	0.05	37 C
BsmFI NEB, R0572S	2000 U/mL	0.02	65 C

According to the anticipated product size, PCR or digestion products were run on agarose gels of 1, 1.5, or 2.5 percent. The gel was imaged using the gel

documentation system (Synoptics, GBox HR) with embedded image processing software (GeneSnap). The retrieval and labeling of images were performed using the PowerPoint package.

ExoSAP-IT™ (Applied Biosystems™ Cat. No. 78201.1.ML) was used to clean PCR products for sequencing according to manufacturer's instructions. Sequencing reactions were prepared following the BigDye v.3.1 Protocol (https://assets.thermofisher.com/TFS-Assets/LSG/manuals/cms_081527.pdf) adapted by Sequencing Facility, High Technology Center, UiB, using the following sequencing cycle: 96°C for 5 minutes; 25 cycles of 96°C for 10 seconds, 58°C for 5 seconds, and 60°C for 4 minutes. Automated Sanger DNA sequencing was performed using the capillary-based Applied Biosystem 3730XL Analyzer.

2.7 RNA extraction and transcriptome analysis (Paper III)

Samples of kidneys were collected as described earlier, washed, and preserved in RNAlater reagent (ThermoFisher, Cat. No. AM7024). The samples were kept at 4°C for one night before being transported to -80°C for further processing. RNA was isolated using RNeasy Plus Mini Kit (Cat. No. 74134) according to the manufacturer's instructions. The extracted RNA was quantified using the nanodrop (ThermoFisher, Cat. No. ND-ONE-W) and Qubit 3 (Thermo Fisher: Cat. No. Q33216). Prior to shipment for RNA sequencing, samples were kept at -80°C. For transportation purposes, dry ice was used. RNA integrity, cDNA library and RNA sequencing were conducted at Novogene, Oxford, UK according to the company's guidelines (https://en.novogene.com).

2.8 Protein extraction for enzyme activity, western blot, and proteomics (Paper I and II)

Adult kidney tissue was used for western blot, enzyme activity, and proteomics analysis. The kidney was collected as described earlier and processed similarly for all the current purposes.

For assessing our customized α-GAL antibodies, and the four human α-GAL antibodies specificity on western blot, samples were homogenized in RIPA lysis buffer (Sigma-Aldrich, Cat. No. R0278) provided with a protease inhibitor cocktail (Roche,

Cat. No. 4693116001) and phosphatase inhibitor (Sigma-Aldrich, Cat. No. P5726) using soft tissue homogenizing kit CK14 (0.5 ml) for precellys (BertinPharma, Cat. No. D34004). After homogenization, samples were centrifuged at 4°C for 20 minutes at 12,000 rpm. The supernatant was transferred into a new tube, and the protein concentration was assessed using the standard BCA assay (ThermoFisher, Cat. No. 23225).

For enzyme activity assay, sample preparation was conducted on ice. The samples were diluted based on the tissue weight in 100-200 µL of deionized water and homogenized at 4°C (glass/Teflon; 10-15 strokes). Protein concentration was determined using the BCA protein assay (ThermoFisher, Cat. No. 23225).

For proteomics, proteins was extracted similarly to the WB. Protein samples were reduced in 100mM DTT for 20 minutes at 60°C. Cysteine alkylation was performed using 200mM iodoacetic acid (IAA) for 1 hour at room temperature. Protein cleanup was performed at 24°C (RT) for 7 min at 1,000 rpm using SP3 beads (Automated Magnetic Separations for Proteomics, ThermoScientific) and 100% ethanol. A magnetic rack was used to collect the beads, which were then washed and rinsed in 80% ethanol SP3. Peptides were digested in trypsin prepared in 100mM AmBic/1mM CaCl2. Samples in trypsin were sonicated for 30 seconds in a water bath to disaggregate the beads fully, then incubated at 37°C for 16 hours at 1,000 rpm. Then they were centrifuged at 13,000 rpm at 24°C for 3 minutes. Beads were then separated from the solution again using the magnetic rack, and the solution was transferred into a new tube and diluted with 0.5M NaCl. Eventually, peptides were desalted using Oasis C18 30µg Elution plates (Waters, Milford, MA) and dried in a vacuum centrifuge. The samples were then resuspended in 200 mM HEPES, pH 8. Proteins were labeled using Tandem Mass Tag (TMT) 16plex label reagent (ThermoFisher, Cat. No. A44520) following the manufacturer's protocol. The samples were desalted and vacuum-dried again.

2.8.1 Western blot

For protein separation, protein samples were loaded into Bolt 4-12% Bis-Tris Plus electrophoresis gels, and then they were transferred to nitrocellulose membranes (NCM) using the iBlot 2 System. Nonspecific binding was blocked with 5% bovine serum albumin (BSA) in PBS containing 0.1% Tween-20 (PBST) for 1 hour at 37°C.

Later, the NCM was incubated overnight with the primary antibodies (Table 5). Protein standard SeeBlue Plus2 Pre-stained (Invitrogen, LC5925) was used to track protein's molecular weight. After washing for three times with a wash buffer (PBST), NCM was incubated with goat anti-rabbit (Abcam, ab205718) HRP-linked antibodies (1:20000) for 1 hour and then washed again with PBST. NCM was developed using Pierce ECL Plus Western blotting substrate (Thermo Fisher, Cat. No. 32132). Chemo-luminescence signals were captured using ChemiDoc Imaging System (Bio-Rad).

2.8.2 α-GAL activity assay (Paper I)

Enzyme activity was assessed using the α-GAL standardized protocol used in clinical diagnostics (Svennerholm, Hakansson et al. 1979, Mayes, Scheerer et al. 1981) at Sahlgrenska university hospital, Sweden. The artificial α-GAL substrate 4-metylumbelliferyl (MU)-alpha-galactopyranoside was used. Due to the cross activity of the alpha-N-acetyl-galactosamidase, N-acetyl-D-galactosamine was used as an inhibitor of alpha-N-acetyl-galactosamidase. The fluorescence of samples, blanks, and the standard solution was measured by spectrofluorometry (Jasco FP-6500, Jasco Inc., Easton, MD, USA) using an excitation wavelength of 360 nm and an emission wavelength of 448 nm.

2.8.3 Protein expression analysis using NanoLC-ESI- Orbitrap Exploris mass spectrometry (Paper II).

Protein expression was conducted at PROBE, UiB. Trypsin-digested peptide sample (0.5ug) was reconstituted in 2% acetonitrile (ACN), and 0.5% formic acid (FA) for injection. The sample was injected into the Ultimate 3000 RSLC system (Thermo Scientific, Sunnyvale, California, USA), which is connected online to an Orbitrap Exploris mass spectrometer (Thermo Scientific, San Jose, CA, USA) equipped with EASY-spray nano-electrospray ion source (Thermo Scientific). The sample was loaded and desalted at a flow rate of 5 l/min for 5 min with 0.1% TFA on a pre-column (Acclaim PepMap 100, 2cm x 75µm ID nanoViper column, filled with 3µm C18 beads).

Peptide separation was performed using a 25 cm analytical column (PepMap RSLC, 50 cm x 75 µm ID EASY-spray column, filled with 2 µm C18 beads) with solvent gradients (ACN) at a flow rate of (flow rate of 250 nl/min). The two solvents were A (100% ACN) and B (0.1% FA (vol/vol) in water). The gradient's composition was 5%B for the first five minutes of trapping, followed by 5-7%B over 0.5min, 8-22%B for

80min, 22-28%B over 10 min, and 35-80%B over 10min. Elution of highly hydrophobic peptides and column conditioning was performed for 15 minutes with 90%B isocratic elution and 20 minutes with 5%B isocratic conditioning. The LC-column-eluted peptides were ionized by electrospray and analyzed by the Orbitrap Eclipse. The mass spectrometer (operated through Tune 2.7.0 and Xcalibur 4.4.16.14 software) was operated in DDA mode (data-dependent acquisition) to automatically transition between full scan MS and MS/MS acquisition. With ion accumulation time set to auto after accumulation to a target value of 4e5 in the C-trap, full survey scan MS spectra (from m/z 375 to 1500) were acquired in the Orbitrap with resolution R = 120.000 at m/z 200.

At compensation voltages (CVs) of -45V and -65V, FAIMS was enabled, and the mass spectrometer (in the DDA mode) operated to automatically transition between full scan MS and MS/MS acquisition, while the cycle duration remained constant at 0.9s/CV. Prior to fragmentation in the HCD (Higher-Energy Collision Dissociation) cell during the 1.5s cycle time, the most intensely eluting peptides with charge states 2 to 6 were sequentially isolated to a target value (AGC) of 2e5 and a maximum IT of 120 ms in the C-trap, while maintaining an isolation width of 0.7 m/z. Fragmentation was carried out using normalized collision energy (NCE) of 30%, and fragments were detected in the Orbitrap with a resolution of 300,000 at m/z 200, with the initial mass fixed at m/z 110. Spray and ion-source parameters were as follow: Ion spray voltage = 1900V, no sheath or auxiliary gas flow, and capillary temperature = 275°C.

2.9 Lipid extraction (Paper I)

Lipid analysis was conducted at Sahlgrenska university hospital, Sweden. Lipid extraction was performed following (Polo, Burlina et al. 2017). Lipids were measured using reverse-phase liquid chromatography. The mass spectrometry was detected using a Xevo TQ MS detector (Waters, USA) in positive mode using electrospray ionization (ESI) source following (Polo, Burlina et al. 2017).

2.10 Proteinuria assay and protein identification (Paper I)

2.10.1 Proteinuria assay

The assay was performed in larva and adult stages. For proteinuria evaluation, larvae or adults were kept overnight in 1mL and 200ml of water, respectively. The larva and

the adult fish were removed from the 24-well plate and the fish tank, respectively, on the following day. For the adult, 50 ml of water was used for protein precipitation, whereas the entire amount (1 mL) was utilized for the larva.

2.10.2 Urine protein precipitation

Protein was precipitated from the fish water using Trichloroacetic acid (TCA) (Sigma-Aldrich, Cat. No. T0699) and chloroform. Upon mixing the water samples with TCA/Chloroform, samples were incubated for 30 minutes at 4 °C, then centrifuged for 5 minutes at 13,000 rpm at 4°C. The supernatants were discarded. Then the pellets were washed in cold acetone and dried on a hot plate for 5 minutes. Dried pellets were resuspended in 20 ul of sample buffer, and the mixture was incubated for 10 minutes at 70°C. Then the samples were run in Gels for SDS-PAGE (ThermoFisher, Cat. No. NP0321BOX). The gel was stained and destained upon run completion using the Coomassie Brilliant Blue R-250 Staining Solution kit (Bio-Rad Cat. No.1610436). The gel was imaged using the ChemiDoc XRS+ imaging system (Bio-Rad). Gel bands were excised, suspended in deionized water, and stored at -20°C before being shipped to the Department of Biosciences at the University of Oslo for protein identification using LC-MS/MS where the analysis was conducted. Sample preparation for LC-MS/MS was performed according to a previously published protocol (Anonsen, Vik et al. 2012).

2.10.3 LC-MS/MS analysis of protein fractions

Using an Ultimate 3000 nano-UHPLC system (Dionex, Sunnyvale, CA, USA) coupled to a QExactive mass spectrometer (ThermoElectron, Bremen, Germany) equipped with a nano electrospray ion source, peptide samples were examined. Acclaim PepMap 100 column (C18, 3 µm beads, 100 Å, 75 µm inner diameter, 50 cm) (Dionex, Sunnyvale, CA, United States) was utilized for liquid chromatographic separation.

The mass spectrometer automatically switched between MS and MS/MS collection in data-dependent mode. After accumulating to a target of 1e6, survey full scan MS spectra (from m/z 200 to 2000) were obtained with the resolution R = 70,000 at m/z 200. The maximum allowable time for ion buildup was 100ms. The used approach permitted the sequential separation of up to ten most intense ions (intensity threshold 1.7e4) for fragmentation utilizing higher-energy collision-induced dissociation (HCD) with a target value of 10,000 charges and a resolution R = 17,500 with NCE 28. The

isolation window has an m/z value of 2 without any offset. The maximum ion accumulation time for the MS/MS spectrum was 60ms. For precise mass measurements, the lock mass option for internal recalibration during the analysis was activated in MS mode.

2.10.4 Database search and label-free quantitation

Data were acquired using Xcalibur v2.5.5. After raw data processing, the database search was conducted on the Zebrafish (Danio rerio) (NCBI; taxon ID7955; 55761) and the common contaminant list using Proteome Discoverer v2.4 software (ThermoScientific, Whaltham, Massachusetts, USA).

Percolator was used to evaluate peptide-spectrum matches with FDR targets of 0.01 (strict) and 0.05 (relaxed). Low FDR proteins, proteins with a single (low-scoring) peptide, and contaminants were deleted from generated protein lists by hand curation. Proteins were functionally annotated using the PD protein knowledge database connected to GO: annotations.

2.11 Metabolite analysis (Paper I and II)

Adult zebrafish samples were used for the analysis. The plasma metabolites were measured using high-performance liquid chromatography/tandem mass spectrometry in collaboration with Bevital AS, Bergen, Norway (Midttun, Kvalheim et al. 2013).

2.12 Tissue preparation for oxidative stress assessment (Paper II)

Adult zebrafish kidneys and whole larva were used for oxidative stress assessment. Tissue homogenization was performed using precellys beads. Total antioxidant capacity (TAC), lipid peroxidation assay (MDA), and total/reduced glutathione GSH+GSSG / GSH were measured using abcam kits (ab65329), (ab118970), and (ab239709), respectively. All tests were performed following the manufacturer's guidelines on a 96-well plate. The SpectraMax Spectrophotometer from Molecular Devices was used to measure the optical density of TAC, MDA, and total GSH+GSSG/GSH at 570 nm, 532 nm, and 412 nm, respectively. The tissue/larvae weights were used for data normalization.

2.13 Tissue processing for IHC and TEM and image acquisition (Papers I, II, and III)

Adult zebrafish kidney was used for immunohistochemical and transmission electron microscopy analysis. For standard histology processing, kidney samples were processed according to the standard protocol of tissue dehydration and embedding at the histology laboratory, Department of Pathology, UiB. Sections of 5 µM were acquired for histology and immunohistochemical staining.

Immunohistochemistry was performed as previously described (Zhang, Wen et al. 2017) with slight modifications. The antigen retrieval step was abandoned for some antibodies (Table 5). After tissue rehydration, nonspecific binding was blocked using normal goat serum (5%) in 1X PBST, and tissue was incubated with the primary antibodies for 1 hour at room temperature. Later, tissue was washed in 1X PBST (3X) and incubated with EnVision+ HRP rabbit or mouse (Agilent Technologies, Cat. No. K4003 or K4001) secondary antibodies. Signal was developed using EnVision FLEX DAB+ Substrate Chromogen System (Agilent Technologies, Cat. No. K3468). For negative controls, the primary antibody was omitted. Slides were scanned with ScanScope XT® (Aperio) at x40 resulting in a resolution of 0.25 micrometer per Pixel. Digital slides were viewed in ImageScope 12.

For transmission electron microscopy preparation, samples were processed at Molecular Imaging Center (MIC), UiB. Samples were washed in cacodylate buffer and incubated for 1 hour in 1% osmium tetraoxide and then washed again in cacodylate buffer. Dehydration was done in ascending ethanol concentrations. After dehydration, samples were incubated in a mixture of ethanol and propylene oxide (PO), and the infiltration was performed overnight by gradually the PO with the embedding medium (Epon 812 resin). Epon 812 resin (100%) was polymerized at 60°C for 48 h. Sections (70–80 nm) were collected using a Leica ULTRACUT microtome, stained with 2% uranyl acetate (aqueous) for 16 min and then with lead citrate for 12 min. Jeol JEM-1230 electron microscope was used for image acquisition.

2.14 Image processing and quantification for IHC and TEM (Paper I, II, and III)

2.14.1 Immunohistochemistry (IHC)

IHC quantification was done using the color deconvolution algorithm version 9.1 (Aperio, CA, USA) after adjusting the default parameters to DAB staining. The signal for each antibody was corrected at three levels: low, medium, and high, as per quantification algorithm parameters. The percentage of positive pixels was used as a visualization parameter.

2.14.2 Transmission electron microscopy (TEM)

Foot process effacement was quantified as foot process width (FPW), mitochondrial morphology, and cristae structure were analyzed to assess mitochondrial alterations using transmission electron microscopy (TEM). Images retrieved were at different magnifications (×12,000 for mitochondria, x50,000 for cristae, and x20,000-25,000 for the podocyte). FPW was analyzed following previously published protocols (Gundersen, Seefeldt et al. 1980, van den Berg, van den Bergh Weerman et al. 2004, Khalil, Lalai et al. 2019). Mitochondrial morphology was performed following previously published protocols (Koopman, Visch et al. 2006, Picard, White et al. 2013, Lam, Katti et al. 2021). Cristae morphology was assessed following previously published protocols (Eisner, Cupo et al. 2017). All images were processed manually using image processing package Fiji in Image J (Schindelin, Arganda-Carreras et al. 2012, Schneider, Rasband et al. 2012). Manual tracing of images to produce raw data is illustrated in Figure 6.

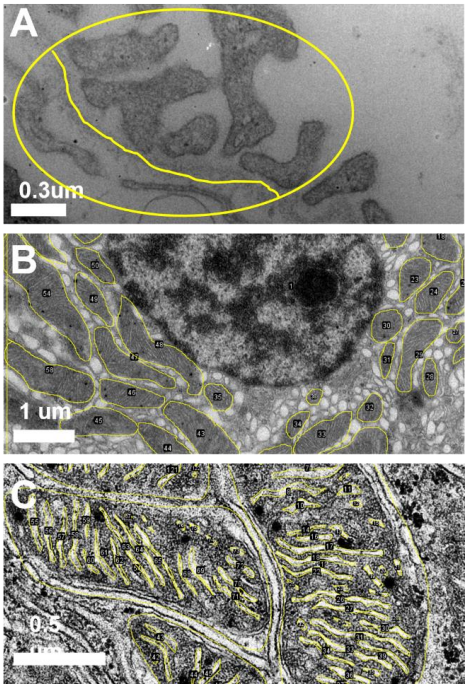

Figure 6. Demonstration of manual tracing of A: PFW yellow circle, including the region of the count, spread over the highlighted line of the glomerular basement membrane, B: mitochondria morphology, and C: cristae organization using ImageJ software.

2.15 Statistical and multiomics analysis (Papers I, II, and III)

For the assessment of the enzyme activity, Glutathione assay, FPW, mitochondria, cristae, and IHC, statistical analysis was performed using GraphPad Prism V 9.2.0. Values were presented as median/interquartile ranges or as mean ±SD. The Kruskal–Wallis test with Dunn test for post hoc comparison (more than two groups) or Mann-Whitney test (two groups) was used to assess statistical significance. Differences were considered significant with p-values <0.05.

Proteome analysis was performed using Perseus v. 1.5.5.3 (Tyanova, Temu et al. 2016). General statistics was performed using SPSS (IBM SPSS Statistics v.29). Relevant GO terms and Kyoto Encyclopedia of Genes and Genomes (KEGG) enrichment analysis were retrieved from ShinyGO (http://bioinformatics.sdstate.edu/go/). GO terms with FDR < 0.05 were considered significantly enriched. KEGG figures were generated using FASTA sequences in

GhostKOALA (Kanehisa, Sato et al. 2016). Data available in the ProteomeXchange Consortium (http://proteomecentral.proteomexchange.org/cgi/GetDataset) via the PRIDE partner repository (Vizcaino, Deutsch et al. 2014) with the project accession number: PXD035409.

For the transcriptomic analysis, the sequencing reads were aligned to the zebrafish reference genome (GRCz11). Data were processed with R/Bioconductor packages (R version 4.2). DEGs were identified by using the DESeq2 R package (version 1.36.0) and selected using a Wald's test with filter criterion of FDR <0.05 and FC >0.5 (Love, Huber et al. 2014). FC values were shrunk using a Normal prior, with the remaining options for DESeq2 set to default values. Processing script found at: https://github.com/Roleren/fabry_article_code. Data is available at ENA project id number: PRJEB55250.

Gene ontology (GO) and KEGG pathway analyses were performed using ShinyGO 0.76. Genes/pathways with adjusted p-value < 0.05 were considered significantly differentially enriched.

3 Summary of the main results

ERT can lower the Gb3 accumulation in FD if a timely ERT is applied. Nevertheless, it has long been shown that ERT can not reverse cellular alterations caused by Gb3 accumulation. Cellular alterations in FD are not limited to Gb3 accumulation, indicating Gb3-independent alterations. The distinction between Gb3-dependent and independent alteration is still unclear. We aim to study the potential Gb3-independent alteration *in vivo* using ZF. ZF can efficiently reflect the Gb3 independent alterations as they cannot produce Gb3 due to natural lack of Gb3 synthase enzyme produced via the *A4GALT* gene. This feature, accompanied by the other advantageous features of ZF, enables us to investigate the Gb3-independent alterations.

In this regard, our in-silico search revealed only one ortholog to the human *GLA* gene, in ZF identified as *gla*, which is predicted to produce the α-Gal enzyme. We have also shown that the predicted enzyme sequence is similar to its human counterpart. Our *in silico* 3D protein structure modeling prediction is also similar to humans. Additionally, we have proved similar *in vitro* functionality of zebrafish α-Gal to its human counterpart using conventional human α-Gal enzyme activity assay during different life stages of the fish and in the renal tissue of adult fish. Similar to humans, kidney tissue distribution of ZF-α-Gal was observed using the ZF-α-Gal antibody produced via GenScript. Furthermore, the knockdown of this ZF's *gla* resulted in lower enzyme activity. We have observed renal alterations, such as podocyte foot process effacement, and we have documented renal malfunction as indicated by higher plasma creatinine and proteinuria in the mutant fish compared to the wild type.

We expanded our investigation at transcriptome, proteome, and metabolome levels. Transcriptomic analysis revealed DEG in the mutant compared to the wild type and GO term analysis indicated that the immune response gene set was overrepresented among the upregulated genes. In contrast, the energy production and consumption, aerobic respiration and oxidative phosphorylation gene sets were overrepresented among the downregulated genes. The KEGG pathway analysis also further indicated where glutathione and Ca^{2+} pathways were upregulated while oxidative phosphorylation and fatty acid metabolism were downregulated. Proteomic analysis strengthened this finding and has shown an overrepresentation of downregulated

carbon metabolism. Also, the involvement of the subcellular organelles was indicated, i.e., lysosome, mitochondria, and cytoskeleton.

Additionally, interrupted glutathione activity, isocitrate dehydrogenase, superoxidase mutase, and oxidoreductase were observed in the mutant fish. FD is an LSD in which the lysosome is the prominently affected organelle in the cell due to the Gb3 accumulation. The disruption of lysosomal protein trafficking/sorting and the autophagy process is influenced by Gb3 accumulation. In our study, however, we have seen interrupted lysosomal proteins as indicated by KEGG analysis of both transcriptomic and proteomic analysis. Besides the internal controls *gla or* α-Gal, our results revealed disrupted lysosomal hydrolyses (Cathepsins), lysosomal membrane proteins, e.g., Tetraspanin (Cd63/Limp1), and proteins and receptors associated with the transport of synthesized lysosomal enzymes (M6pr). These results were validated using IHC for Cd63/Limp and Ctsba.

In FD, disrupted mitochondrial function resulted from Gb3-dependent impaired lysosomal function (Biancini et al, 2012; Schumann et al, 2021). Our proteomics results aligned with this, showing affected mitochondrial-related pathways. We validated these observations by measuring the oxidative stress (via glutathione assay), semiquantitative IHC, and semiquantitative image analysis of electron microscopy of the renal tubules.

Our results indicated a significantly higher state of oxidative stress in the renal tissue from the adult mutant fish and the larval stage, consistent with transcriptomics and proteomics analysis.

The affected mitochondrial function was further evaluated by immunohistochemistry. IHC analysis confirmed the mitochondria malfunction showing reduced expression of two proteins highlighted in our omics analysis; these are Sod2 and Idh3a. Furthermore, the assessment of mitochondria and cristae using TEM indicated distorted mitochondrial morphology, particularly in the proximal tubules. Additionally, in both tubules, cristae morphology was affected (less healthy mitochondria in mutant compared to wild type), consistent with the impaired mitochondrial function proven earlier in our study.

Our Omics analysis indicated dysregulation in the cytoskeleton and cell-to-cell adhesion. Therefore, Cadherin (Cdh1) was assessed by IHC and was lower in the mutant compared to the wild type, consistent with our omics analysis.

Further plasma metabolome investigation revealed (not statistically analyzed due to low sample number) differences in Trimethylamine N-oxide (TMAO), carnitine, methionine sulfoxide (MetSO), trimethyl-lysine, creatine, histidine citrulline, betaine and asymmetric dimethylarginine (ADMA). Figure 7 illustrate our main findings in this study.

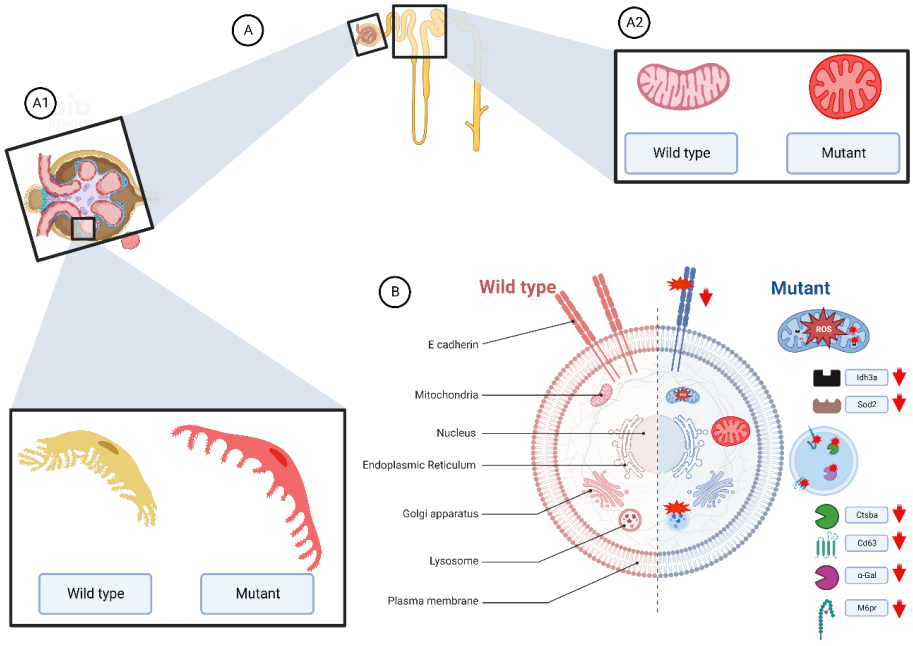

Figure 7. Graphical summary of the main results. Histological observations (A1 and A2) on the podocyte and renal tubule's mitochondria revealed PFPE and mitochondrial shape and cristae alterations which was further validated using multi-omics approach revealing stressed mitochondria and disturbed lysosomal contents (B) and IHC.

4 Discussion

4.1 Discussion of the main results

4.1.1 Zebrafish's *gla* and α-Gal are similar to their human counterparts

For the first time, this study documented that in ZF, *gla* mutation resulting in reduced enzyme activity can lead to FD renal phenotype accompanied by molecular, cellular, functional, and histological alterations in the renal tissue independent of Gb3 accumulation. This innovative finding adds the first non-human *in vivo* evidence of Gb3-independent alterations in FD.

In the current study, we did not just document the presence of *gla* in ZF as one ortholog to its human counterpart, but we have also shown that its product, α-Gal, resembles the human version of the enzyme at the structural, functional, and histological distribution levels. Interestingly, using the CRISPR/Cas9 gene editing tool, we successfully generated mutant ZF characterized by low enzyme activity resembling the nonclassical FD phenotype in humans (Arends, Wanner et al. 2017).

4.1.2 Gb3-independent renal impairment

Contrary to previous understanding of the Fabry disease progress in light of Gb3 (Germain 2010), we have observed leaky kidneys in the mutant fish reflected by the high molecular weight proteins detected in fish's urine. Furthermore, high plasma creatinine was observed in the mutant, indicating impaired kidney function.

We were interested in investigating whether this renal impairment is of glomerular or tubular origin. Therefore, we histologically investigated the glomerulus and renal tubules in the kidney tissue of mutant and wild type fish. Surprisingly, we have observed a widening of the podocyte foot process (also known as foot process effacement) in the mutant fish without Gb3. Although podocyte foot effacement, which leads to podocyturia, can also occur in normal individuals (Maestroni, Maestroni et al. 2014), in FD, it has been shown that it follows Gb3 load in the podocytes or the lysoGb3 interactions that can elicit the podocytes detachment (Trimarchi, Ortiz et al. 2020). Nevertheless, we have shown a similar effect on the ZF podocytes without Gb3. This finding indicates that either another α-Gal substrate is involved in triggering this effect or the molecular unbalance resulting from mutant α-Gal. Another reason

could be that the trafficking of the malformed enzyme to the lysosome affects the cell and leads to apoptosis, reflecting the podocytes' cellular morphological alteration and resulting in an impaired glomerular filtration barrier.

4.1.3 Molecular evidence for renal impairment

Our omics approach (transcriptomics and proteomics) revealed subcellular organelle involvement in addition to dysregulated pathways that are well-known in human FD. Lysosomes, mitochondria, and cell junctions were highlighted in the GO term of cellular components. Furthermore, genes involved in Cellular respiration, Aerobic respiration, Oxidative phosphorylation, glutathione metabolism, Ca2+ cell signaling, and immune response were markedly affected in the mutant fish renal tissue.

4.1.3.1 Gb3-independent lysosomal disturbance

Our omics data analysis revealed the downregulation of the lysosomal enzymes (i.e., Ctsba), lysosomal membrane proteins (i.e., Cd63), and transport proteins (i.e., Ap-1, Ap-3, and M6pr) in MU fish.

While our study highlighted the downregulation in Cd63, in a stable α-GAL-deficient podocyte cell line model for FD, CD63 protein expression remains unaffected (Jehn, Bayraktar et al. 2021). One possible explanation for the disparity between the latter study and ours is that in the absence of Gb3 accumulation, additional pathways leading to an FD-related phenotype may be activated. Docking of Limp-1/Cd63 from the trans-Golgi network to lysosomes requires the AP-3 adaptor complex (Eskelinen, Tanaka et al. 2003), which was shown to be downregulated in our data. It has been shown that the inactivation of CD63 in mice results in polyuria and decreased urine osmolality, indicating that lysosomes contribute to renal homeostasis (Schroder, Lullmann-Rauch et al. 2009), consistent with our finding. Additionally, lysosome membrane proteins play crucial roles in lysosomal-related diseases (Gonzalez, Valeiras et al. 2014). CD63 can be detected in the urine of chronic kidney disease (CKD) model rats (Adam, Paterson et al. 2020) and human urine (Bryzgunova, Zaripov et al. 2016, Campos-Silva, Suarez et al. 2019, Salvi, Bandini et al. 2021). In line with our results, CD63 might be considered a novel, noninvasive potential biomarker for Gb3-independent FD disease progression.

Another lysosomal-related protein observed in our study is the lysosomal/cytoplasmic vessel cysteine protease cathepsin Ba (Ctsba). This enzyme is a critical player in lysosomal homeostasis, and its dysregulation is attributed to variable lysosomal abnormalities (Man and Kanneganti 2016, De Pasquale, Moles et al. 2020, Yadati, Houben et al. 2020). For example, CTSB downregulation results in autophagosome accumulation due to compromised lysosomal clearance (Mizunoe, Kobayashi et al. 2019). Generally, dysregulation of cathepsins (CTSs) leads to a variety of human diseases, including, cardiovascular diseases, neurodegenerative disorders, and kidney diseases (De Pasquale, Moles et al. 2020). However, in FD, CTSB expression has not been analyzed. In Niemann-Pick type C (NPC) disease (another LSD), inhibition of this protease results in lysosomal dysfunction (Cermak, Kosicek et al. 2016). The role of CTSB is not restricted to the lysosomal as its presence is also reported in the extracellular space, where it participates in many functions, e.g., inflammasome triggering, apoptosis, and extracellular matrix degradation (Yadati, Houben et al. 2020). CTSB can be measured in the urine and plasma (Aisa, Cappuccini et al. 2016, Wang, Bai et al. 2016). Downregulation of CTSB is associated with renal tubular injury (Svara, Pogacnik et al. 2010, Herzog, Yang et al. 2012, Liu, Shen et al. 2015, Goncalves, Hultman et al. 2016, Wang, Bai et al. 2016), even at an early stage in life (Aisa, Cappuccini et al. 2016); we, therefore, suggest it as a possible Gb3-independent noninvasive biomarker that can report the lysosomal homeostasis and early tubular injury in FD.

Our results have also highlighted the upregulation of Mannose-6-Phosphate Receptors (m6pr) at the gene expression level and its downregulation at the protein level in the mutant fish kidney. A similar result was recently published by Frustaci et al. in endomyocardial biopsies (Frustaci, Verardo et al. 2022). The contrasted upregulation and downregulation at gene and protein levels can be attributed to post-translation degradation. It is well established that M6PR is the lysosomal receptor for α-GAL (Sands and Davidson 2006, Prabakaran, Nielsen et al. 2012); hence downregulation of this receptor can negatively impact the efficacy of the ERT.

Lysosomal and mitochondrial interactions/functions are inseparable for sustaining cellular homeostasis. In FD, autophagy-mitophagy processes are affected (Todkar, Ilamathi et al. 2017, Deus, Yambire et al. 2020). A reasonable explanation for such disruption is the inability of the lysosome to integrate into the mitophagosome

resulting in an impaired downstream mitophagy process and might explain the elevated oxidative stress and the altered mitochondrial morphology we have observed in the mutant kidney tissue (Das and Naim 2009, Platt, Boland et al. 2012, Ivanova, Changsila et al. 2019, Parenti, Medina et al. 2021, Schumann, Schaller et al. 2021).

4.1.3.2 Oxidative stress and mitochondria morphology

Consistent with the assumption on the lysosomal-dependent mitochondrial alterations in FD (Biancini, Vanzin et al. 2012, Todkar, Ilamathi et al. 2017, Deus, Yambire et al. 2020, Schumann, Schaller et al. 2021), and other metabolic disorders (Platt, Boland et al. 2012, de la Mata, Cotan et al. 2016, Abed Rabbo, Khodour et al. 2021, Parenti, Medina et al. 2021), the unbalanced glutathione metabolism indicated mitochondrial dysfunction in the mutant fish kidney compared to the wild type. This observation was further validated at the morphological level. Observing mitochondria and cristae morphology indicated shape alterations of the mitochondria in the proximal tubules, while the cristae area was affected in both proximal and distal tubules. Recent findings in tubular cells of an FD mouse model and human-derived tubular cells have shown similar results (Maruyama, Taguchi et al. 2018, Schumann, Schaller et al. 2021). While the higher oxidative stress state is suggested to accompany Gb3 buildup in FD (Biancini, Vanzin et al. 2012), it was also observed that oxidative stress could be increased while lysoGb3 is at the expected levels in some FD patients (Simoncini, Torri et al. 2020). Our results align with the assumption that oxidative stress can also be initiated and maintained in a Gb3-free environment.

Consistent with the above, we have found disrupted mitochondrial proteins Sod2 and Idh3a. Reduced Sod2 activity in ZF is associated with increased oxidative stress (Ding, Zhang et al. 2021), consistent with our observation. Similarly, alterations were observed in pluripotent stem cells from the peripheral blood of FD patients (Tseng, Chou et al. 2017). While Sod2 downregulation was attributed to Gb3 accumulation in their study, our data suggest that Sod2 disruption can occur in the absence of Gb3. On the other hand, Sod2 was not altered in the unilateral ureteral obstruction (UUO) FD mice, a combined model of obstructive nephropathy and FN (Chung, Son et al. 2021). Nonetheless, we hypothesize that Gb3 accumulation exacerbates Sod2 downregulation.

Moreover, the Isocitrate dehydrogenase catalytic subunit alpha (Idh3a), a mitochondrial protein, was also downregulated in kidneys from mutant fish. IDH3a promotes ATP production by catalyzing oxidative decarboxylation of isocitrate to 2-oxoglutarate. Downregulation of this enzyme is also known to affect neurotransmission in *Drosophila melanogaster* (Ugur, Bao et al. 2017). In addition, dysregulation of this enzyme interrupts the energy production in the cell, consistent with our observation of the stressed mitochondria. Unluckily, disruption of Idh3a has not been investigated in FD.

4.1.3.3 Cell junctions

Our omics analysis highlights the disruption of cytoskeleton genes, including the Cadherin 1 (Cdh1) in renal tissue from mutant fish. Using IHC, we validated this observation. Previous investigations in FD have also shown downregulation of Cdh1 expression at the RNA and protein levels in urine-derived cells (Jeon, Jung et al. 2015, Slaats, Braun et al. 2018). However, this marker has never been used as a diagnostic or monitoring tool. Interestingly, Cdh1 depletion is associated with EMT, cell death, and ferroptosis (Eikrem, Beisland et al. 2016, Tang, Chen et al. 2021). Our results indicate that these pathways are altered in MU compared to WT ZF and unrelated to the cellular Gb3 load.

4.1.4 Immune response-mediated calcium signaling

The observed oxidative stress reflected by the down-regulation of Cellular respiration, Aerobic respiration, and Oxidative phosphorylation suggests a prevailingly anaerobic, glycolytic metabolism, representing an inefficient, emergency energy production pathway in mutant fish kidney tissue consistent with an ongoing immune system activation (Pearce and Pearce 2013).

KEGG analysis has provided additional support to our findings. Pathways associated with inflammation, such as phagosome activation, endocytosis and ferroptosis, are upregulated in mutant fish. Due to immune stimulation, the calcium signaling pathway is upregulated in mutant fish. Indeed, oxidative stress-dependent calcium influx was previously highlighted using *GLA* mutant human inducible pluripotent stem cells (iPSC) in a kidney organoid template (Kim, Kim et al. 2021). Furthermore, in Fabry knockout murine tissues, expression of S100 calcium-binding proteins A8 and A9 (also known as MRP8 and MRP14) was markedly elevated at the gene and protein

levels (Park, Choi et al. 2009). Significantly, S100A8/A9, Ca^{2+} sensors involved in cytoskeleton remodeling and arachidonic acid metabolism, are expressed constitutively by neutrophils and monocytes and are actively produced during inflammation, promoting leukocyte recruitment and cytokine production (Wang, Song et al. 2018).

In our renal research group at UiB similar finding was observed in the kidney biopsy of FD patients (Eikrem, Strauss et al. 2018, Strauss, Eikrem et al. 2019, Eikrem, Delaleu et al. 2020). Besides the enriched set of genes involved in the extracellular matrix and EMT, fibrosis and immune response were also enriched in the microdissected glomerular compartment. Evident to our Gb3-independent cellular alteration, ERT intervention returned the upregulated pathways to a normal state; however, this was not the case in the long-term, i.e., ten years of ERT (Eikrem, Strauss et al. 2018, Strauss, Eikrem et al. 2019). Furthermore, we have also identified that complement component 1, q subcomponent, C chain gene (*c1qc*) is significantly upregulated in the mutant fish compared to the wild type, which has already been shown in FD (Heo, Kang et al. 2017, Strauss, Eikrem et al. 2019). While the previous observations were reported in humans in the presence of Gb3, our results suggest that activation and maintaining immune response is present in its absence, which is supported by previous research (Braun, Blomberg et al. 2019).

4.1.5 Metabolites analysis supports elevated oxidative stress, and renal dysfunction observation

The profile of plasma metabolites from mutant fish further supported our oxidative stress, and renal impairment.

Generally, elevated levels of TMAO, MetSO, citrulline, and ADMA were observed in mutant fish in contrast to the lower levels of carnitine, trimethyllysine, creatine, histidine, and betaine.

TMAO elevation indicates declining kidney function and an increased risk of significant adverse cardiovascular events (Janeiro, Ramirez et al. 2018). In humans, TMAO is converted from choline, betaine, and carnitine (Velasquez, Ramezani et al. 2016). Increased plasma TMAO levels impact cardiovascular health and correlate with impaired renal function (Tang, Wang et al. 2015, Velasquez, Ramezani et al. 2016, Vallance, Koochin et al. 2018).

Additionally, low carnitine, an essential metabolite for transporting long-chain fatty acids across the inner mitochondrial membrane (Maas, Hintzen et al. 2020), indicates decreased energy output. In our KEGG pathway analysis, we found fatty acid metabolism disturbances. One of the three sites of carnitine production is the kidney, where it is efficiently reabsorbed to reduce urine loss. Our data on low carnitine in the plasma reflects the renal tubular dysfunction in mutant fish. Indeed, previous studies attributed its deficiency to metabolic disorders (Sharma and Black 2009, Virmani and Cirulli 2022).

Another source for TMAO is betaine. In contrast to the high plasma levels of TMAO, betaine was found to be decreased in the mutant fish plasma. Generally, low betaine concentration is associated with an unfavorable cardiovascular risk and metabolic syndrome (Ueland 2011). The other metabolite that yields TMAO is choline, which was inconclusive.

We found low plasma trimethyllysine concentration, which might also explain the low carnitine levels in the plasma. Trimethyllysine is a precursor for carnitine synthesis. A low concentration of trimethyllysine has been described in systemic carnitine deficiency patients, which is similar to our results (Lehman, Olson et al. 1987).

We have also observed elevated plasma levels of methionine sulfoxide (MetSO) in the mutant fish. The elevation of this metabolite is associated with higher oxidative stress in yeast and mice (Stadtman, Van Remmen et al. 2005). In FD, similar results were reported (Ducatez, Mauhin et al. 2021). While the above-mentioned human FD study results are attributed to the Gb3 load, we have shown that such elevation is independent of Gb3 accumulation.

The amino acid histidine, which is known to have anti-inflammatory and antioxidant properties (Hasegawa, Ichiyama et al. 2012), was lower in mutant fish. Consistent with our observation, low plasma histidine concentrations are relevant to the higher mortality rates in CKD patients (Watanabe, Suliman et al. 2008).

The endogenous inhibitor of nitric oxide synthase (NOS), Asymmetric dimethylarginine (ADMA), which catalyzes the synthesis of nitric oxide (NO) from arginine and is a marker of endothelial dysfunction, revealed a higher plasma level in the mutant fish. In Fabry-associated cardiomyopathy, elevated ADMA has been

described to be higher (insignificant) in the FD patient (Loso, Lund et al. 2018). Furthermore, serum ADMA levels inversely correlate with coronary flow reserve in Fabry patients who received *de novo* enzyme replacement therapy (Fujii, Kono et al. 2012). Additionally, elevated plasma ADMA was observed in patients with renal dysfunction and cardiovascular disease (Tousoulis, Georgakis et al. 2015).

Three urea cycle intermediates were detected in our metabolite analysis. Only citrulline presented apparent elevation in the mutant fish, whereas no clear differences were found in ornithine and arginine levels. In children with early CKD, a high plasma citrulline-to-arginine ratio has been described as a marker of cardiovascular involvement (Lin, Hsu et al. 2013). Citrulline can ,therefore, be used as an early marker for renal involvement in FD.

Our results indicated low levels of plasma creatine. Creatine is essential in energy storage and transmission (Boenzi, Pastore et al. 2012) and is also known as an antioxidant (Lawler, Barnes et al. 2002). Creatine supplementation has been proposed as a treatment for different age-related diseases (Smith, Agharkar et al. 2014). Creatine levels in plasma are not generally monitored in FD.

4.2 Methodological consideration

4.2.1 Choice of the animal model

Besides many cited advantages of using ZF as a disease model, particularly in LSDs (Zhang and Peterson 2020), one that was of particular interest to our purpose is that it lacks the Gb3 synthase enzyme, which is responsible for producing Gb3. The absence of this gene in ZF was crucial as we were interested in investigating the Gb3-independent FD characteristics if any.

4.2.2 Why kidney samples only?

Gb3 deposits at the early stages of life in every cell in the renal tissue; however, the renal function assessment cannot reflect the degree of its deposition. Additionally, ERT is limited to reverse molecular and cellular alteration caused by Gb3-dependent and independent injuries that lead to deterioration of the renal function. Therefore, new tools and/or biomarkers are urgently needed to effectively assess renal function (Waldek and Feriozzi 2014, Silva, Moura-Neto et al. 2021). Furthermore, we are a

renal research group and time/resources too limited to study the other involved organs in this thesis.

4.2.3 Why the use of gene and protein expression together?

Compared to the non-differentially expressed gene, the differentially expressed mRNAs correlate with their protein product substantially better, which strengthens the cause for using differential mRNA expression for biological findings, i.e., diagnostic or treatment biomarkers (Koussounadis, Langdon et al. 2015). Furthermore, transcriptome of ZF is well described in contrast to its proteome, although proteome is more informative at the molecular level. Our consistent finding in both transcriptomics and proteomics analysis strengthen our results. It is worth noting that the RNA sequencing and proteomics samples were not from the same kidney tissue.

The issue when working with both tools, the current state-of-art technology is still limited, particularly for protein detection. For example, protein abundance analysis typically yields fewer proteins than genes detected by gene expression, which many factors can explain due to the theory behind protein detection used in the current proteomics platforms. For instance, high abundance proteins tend to mask the low abundance proteins, rendering them invisible to the detection method. This may explain the differences between the number of genes and proteins we found. While the total number of protein-coding genes in ZF is 26206, our gene expression analysis has shown almost all of them at 25592. While the total number of proteins found in our study was 8075, as shown in Figure 8. It is worth mentioning that ZF, like humans, has tissue-specific proteomics patterns (Desgrange and Cereghini 2015, Banu, Srivastava et al. 2021).

Also technically-wise, RNA is amplified in before running transcriptomics analysis while the same is not applied to proteomics analysis. On top of that, not all RNAs are translated into proteins.

Another issue with protein expression analysis in ZF is that not all proteins are curated/validated in the current databases. Therefore, multiple databases must be used concurrently to retrieve the most updated protein information to produce a better interpretation. Several databases can be consulted for such purposes, including:

- ZFIN (Bradford, Van Slyke et al. 2022),

- NCBI (https://www.ncbi.nlm.nih.gov/genome/gdv/?org=danio-rerio),
- GRC (https://www.ncbi.nlm.nih.gov/grc),
- UCSC (http://genome.ucsc.edu/cite.html),
- UNIPROT (UniProt 2021),
- and Ensembl (Cunningham, Allen et al. 2022).

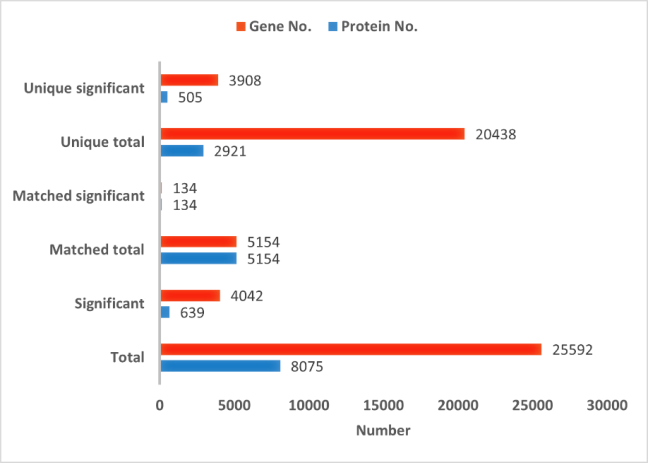

Figure 8. Comparison between the gene expression and protein expression raw numbers. Original figure generated using data from papers II and III.

4.2.4 Choice of quantification methods

4.2.4.1 Quantification of podocyte foot process

Kidney podocytes are the ultimate barrier to urinary protein loss. They are terminally developed epithelial cells with complicated cellular architecture. On electron microscopy, podocyte foot process effacement (FPE) is a typical characteristic in proteinuric renal disorders like focal segmental glomerulosclerosis (FSGS), minimal change disease, immunoglobulin (Ig) A nephropathy, Fabry disease (FD) and diabetic nephropathy (DN). In FSGS, podocyte loss was correlated with the degree of proteinuria. In contrast, this was not the typical case in other diseases like FD, which suggest that the timing of the initiation of proteinuria and the development of podocyte foot process effacement is inconsistent (Deegens, Dijkman et al. 2008). However, reduction of PFPE after treatment with ERT or Chaperone therapy was demonstrated in FD, which makes it a good treatment efficiency detector (Mauer, Sokolovskiy et al. 2017).

Foot process effacement is measured by foot process width (FPW). Accurate podocyte effacement measures need an understanding of the 3-dimensional nature of the glomerulus and glomerular components, often seen as 2-dimensional structures on microscopic imaging. The challenge with direct measurement of foot process width is determining the extent of the foot processes as they curve around the capillary wall (Becherucci and Romagnani 2015, Mauer, Sokolovskiy et al. 2017, Basgen, Wong et al. 2021).

In ZF, fewer glomeruli are found compared to humans, and only one glomerulus can be found during the early developmental stages (less than 16 dpf). In our work, we evaluated the FPW in adult fish. Currently used methods in quantifying FPE in ZF are similar to humans (van den Berg, van den Bergh Weerman et al. 2004, Deegens, Dijkman et al. 2008, Lindahl, Reinholt et al. 2014, Rider, Bruton et al. 2018, Jobst-Schwan, Hoogstraten et al. 2019, Khalil, Lalai et al. 2019).

4.2.4.2 Mitochondria morphology

Mitochondria are dynamic organelles that often change shape and intracellular distribution throughout their lifespan. The appropriate rates of fusion and fission determine the number and form of mitochondria. Many articles have reported substantial mitochondrial network remodeling throughout a range of pathological situations such as differentiation, cell cycle progression, mitochondrial respiratory chain performance, Ca^{2+} transport, and apoptosis. Changes in mitochondrial shape thus play a critical role in regulating both autophagy and mitophagy (Marchi, Bonora et al. 2017).

It has been highlighted recently that mitochondria morphology is altered in renal tubule in FD, which was accompanied by elevated oxidative stress (Schumann, Schaller et al. 2021). We, therefore, used the mitochondrial morphology assessment approach to reproduce the current finding in FD.

4.2.4.3 Cristae morphology

Cristae vary in size, form, and packing density between species, tissues within the same organism, and even different parts of the same cell. For example, in cells with higher energy demands, mitochondria generate more prominent, more densely packed cristae, presumably to maximize ATP generation per volume occupied by

mitochondria in the cell. Evidence of inner mitochondrial membrane morphing has also been observed in response to physiological changes such as energy production, apoptosis, and oxidative stress. A delicate balance of organelle fusion and fission, regulated by specific proteins, determines mitochondria overall size and structure. Likewise, cristae do not appear at random, for example, by simply expanding. Instead, cristae are formed, and their integrity and shape are maintained through complex protein-protein interactions (Afzal, Lederer et al. 2021).

We used the recently suggested approach to assess the cristae morphology in response to the observed oxidative stress in the mutant compared to the wild type fish (Eisner, Cupo et al. 2017, Lam, Katti et al. 2021).

4.2.5 No behavioral or external morphology investigation?

During this work, no abnormal body morphology was observed in the mutant. However, at the F5 generation, high mortality rates were observed in the mutant compared to the wild type. Unfortunately, that was observed late in the study; therefore, the results were not critically investigated.

4.3 Limitations

Notably, residual α-GAL enzyme activity was seen in mutant animals. Because the α-GAL protein in the mutant line is notably undetectable by IHC while still partially functional, we suggest that the produced stop codon may be partially skipped during protein translation, resulting in structural deformation/protein misfolding with residual enzymatic activity.

Additionally, pathophysiological gender disparities represent a challenge (Hollander, Dai et al. 2015) because in humans *GLA* gene is located on the X chromosome, but in ZF, it is located on an autosomal chromosome. Hence, pathophysiological differences between male and female zebrafish cannot be reliably addressed (Babaei, Ramalingam et al. 2013, Zheng, Xu et al. 2013, Li, Tan et al. 2016).

Another limitation is that no eGFR was measured in our model. In FD patients, renal function can be measured using eGFR, proteinuria/albuminuria or even podocyturia. In zebrafish, however, eGFR measurement is currently not feasible, and zebrafish do not produce albumin. Nevertheless, alternatives to evaluate renal function have been

developed, i.e., by injecting fluorescently labeled dextran into the bloodstream and measuring decreasing fluorescent intensity over time. This technique is currently used for the larval stage as they are transparent (Hentschel, Mengel et al. 2007, Tobin and Beales 2008, Christou-Savina, Beales et al. 2015, Hanke, King et al. 2015, Bolten, Pratsinis et al. 2022). In adult fish, one way to evaluate renal function is via the transgenic zebrafish that expresses a fluorescent protein that in healthy fish does not cross the glomerular filtration barrier (GFB), while when the kidney is damaged it filtrates easily through the glomerulus (Elmonem, Berlingerio et al. 2018, Outtandy, Russell et al. 2019). Indeed, several transgenic lines were developed for this purpose (Xie, Farage et al. 2010, Zhou and Hildebrandt 2012, Chen, Luciani et al. 2020). These methods are laborious and time-consuming. In our study, we overcame such limitation by using a simple proteinuria assay which was used in the larval stage (Nishibori, Katayama et al. 2011, Jobst-Schwan, Hoogstraten et al. 2019), and we have adopted this approach for the adult stage, which proved to be easy, cheap, efficient, and time-saving (paper I). Additionally, we were able to measure plasma creatinine by pooling several blood samples as recommended by previous work in zebrafish (Jagadeeswaran, Sheehan et al. 1999, Babaei, Ramalingam et al. 2013). It is worth mentioning that only two pooled samples were used for the plasma metabolite measurements due to the high blood volume needed for this analysis.

Lastly, no histological abnormalities were seen in the mutant fish other than the podocyte foot process effacement and the altered mitochondrial morphology. The lack of histological abnormalities can be attributed to the lack of Gb3 load in the cells.Additionally, ZF is known for its high tissue regeneration capacity, in contrary to human (Kamei and Drummond 2014).

5 Conclusion and future perspectives

5.1 Conclusions

We successfully generated a nonclassical FD model in zebrafish that mirrors some of FN's main features. Our model is valuable in studying the Gb3-independent alterations. Using this model, we have shown that Gb3-independent alteration can lead to evident renal impairment.

Our findings suggest that gla mutation, independent of Gb3 accumulation, is sufficient to alter renal tissue at the molecular and histological levels. This surprising observation indicates that Gb3 and lysoGb3 amplify the cellular alterations initiated by *gla* mutation. Our findings open the way for developing novel diagnostic, monitoring, and perhaps therapeutic approaches, which would be especially useful in the early stages of FD before Gb3 buildup.

5.2 Future perspectives

Our innovative Gb3-free FD disease model in zebrafish is valuable in studying disease progression, potential early diagnosis biomarkers, and treatment efficacy independent of Gb3 accumulation. We are interested in reproducing our main finding in archival human renal biopsies, which we can access through the Norwegian Kidney Biopsy Registry. We have previously shown that these biopsies are viable for gene expression studies. Using such a resource will help us define potential noninvasive FD/FN diagnoses and more efficient and universal treatment monitoring biomarkers. In addition, we hope to study zebrafish with and without the Gb3 synthase gene by inserting the gene into the fish. This way, we can exclusively highlight the Gb3-dependent and independent effects of the FD.

6 References

Abed Rabbo, M., Y. Khodour, L. S. Kaguni and J. Stiban (2021). "Sphingolipid lysosomal storage diseases: from bench to bedside." Lipids Health Dis **20**(1): 44.

Adam, R. J., M. R. Paterson, L. Wardecke, B. R. Hoffmann and A. J. Kriegel (2020). "Functionally Essential Tubular Proteins Are Lost to Urine-Excreted, Large Extracellular Vesicles during Chronic Renal Insufficiency." Kidney360 **1**(10): 1105-1115.

Adiyanti, S. S. and T. Loho (2012). "Acute Kidney Injury (AKI) biomarker." Acta Med Indones **44**(3): 246-255.

Aerts, J. M., J. E. Groener, S. Kuiper, W. E. Donker-Koopman, A. Strijland, R. Ottenhoff, C. van Roomen, M. Mirzaian, F. A. Wijburg, G. E. Linthorst, A. C. Vedder, S. M. Rombach, J. Cox-Brinkman, P. Somerharju, R. G. Boot, C. E. Hollak, R. O. Brady and B. J. Poorthuis (2008). "Elevated globotriaosylsphingosine is a hallmark of Fabry disease." Proc Natl Acad Sci U S A **105**(8): 2812-2817.

Afzal, N., W. J. Lederer, M. S. Jafri and C. A. Mannella (2021). "Effect of crista morphology on mitochondrial ATP output: A computational study." Curr Res Physiol **4**: 163-176.

Aguiar, P., O. Azevedo, R. Pinto, J. Marino, R. Baker, C. Cardoso, J. L. Ducla Soares and D. Hughes (2017). "New biomarkers defining a novel early stage of Fabry nephropathy: A diagnostic test study." Mol Genet Metab **121**(2): 162-169.

Aisa, M. C., B. Cappuccini, A. Barbati, A. Orlacchio, M. Baglioni and G. C. Di Renzo (2016). "Biochemical parameters of renal impairment/injury and surrogate markers of nephron number in intrauterine growth-restricted and preterm neonates at 30-40 days of postnatal corrected age." Pediatr Nephrol **31**(12): 2277-2287.

Alliegro, M., R. Ferla, E. Nusco, C. De Leonibus, C. Settembre and A. Auricchio (2016). "Low-dose Gene Therapy Reduces the Frequency of Enzyme Replacement Therapy in a Mouse Model of Lysosomal Storage Disease." Mol Ther **24**(12): 2054-2063.

Alroy, J., S. Sabnis and J. B. Kopp (2002). "Renal pathology in Fabry disease." J Am Soc Nephrol **13 Suppl 2**: S134-138.

Amsterdam, A., R. M. Nissen, Z. Sun, E. C. Swindell, S. Farrington and N. Hopkins (2004). "Identification of 315 genes essential for early zebrafish development." Proc Natl Acad Sci U S A **101**(35): 12792-12797.

Anonsen, J. H., A. Vik, W. Egge-Jacobsen and M. Koomey (2012). "An extended spectrum of target proteins and modification sites in the general O-linked protein glycosylation system in Neisseria gonorrhoeae." J Proteome Res **11**(12): 5781-5793.

Aoyama, Y., Y. Ushio, T. Yokoyama, S. Taneda, S. Makabe, M. Nishida, S. Manabe, M. Sato, H. Kataoka, K. Tsuchiya, K. Nitta and T. Mochizuki (2020). "Urinary Mulberry Cells as a Biomarker of the Efficacy of Enzyme Replacement Therapy for Fabry Disease." Intern Med **59**(7): 971-976.

Arends, M., C. Wanner, D. Hughes, A. Mehta, D. Oder, O. T. Watkinson, P. M. Elliott, G. E. Linthorst, F. A. Wijburg, M. Biegstraaten and C. E. Hollak (2017). "Characterization of Classical and Nonclassical Fabry Disease: A Multicenter Study." J Am Soc Nephrol **28**(5): 1631-1641.

Artola, M., C. Hedberg, R. J. Rowland, L. Raich, K. Kytidou, L. Wu, A. Schaaf, M. J. Ferraz, G. A. van der Marel, J. D. C. Codée, C. Rovira, J. M. F. G. Aerts, G. J. Davies and H. S. Overkleeft (2019). "α-d-Gal-cyclophellitol cyclosulfamidate is a Michaelis complex analog that stabilizes therapeutic lysosomal α-galactosidase A in Fabry disease." Chemical Science **10**(40): 9233-9243.

Auray-Blais, C., C. M. Blais, U. Ramaswami, M. Boutin, D. P. Germain, S. Dyack, O. Bodamer, G. Pintos-Morell, J. T. Clarke, D. G. Bichet, D. G. Warnock, L. Echevarria, M. L. West and P. Lavoie (2015). "Urinary biomarker investigation in children with Fabry disease using tandem mass spectrometry." Clin Chim Acta **438**: 195-204.

Auray-Blais, C., A. Ntwari, J. T. Clarke, D. G. Warnock, J. P. Oliveira, S. P. Young, D. S. Millington, D. G. Bichet, S. Sirrs, M. L. West, R. Casey, W. L. Hwu, J. M. Keutzer, X. K. Zhang and R. Gagnon (2010). "How well does urinary lyso-Gb3 function as a biomarker in Fabry disease?" Clin Chim Acta **411**(23-24): 1906-1914.

Azevedo, O., M. F. Gago, G. Miltenberger-Miltenyi, N. Sousa and D. Cunha (2020). "Fabry Disease Therapy: State-of-the-Art and Current Challenges." Int J Mol Sci **22**(1).

Babaei, F., R. Ramalingam, A. Tavendale, Y. Liang, L. S. Yan, P. Ajuh, S. H. Cheng and Y. W. Lam (2013). "Novel blood collection method allows plasma proteome analysis from single zebrafish." J Proteome Res **12**(4): 1580-1590.

Bajaj, L., P. Lotfi, R. Pal, A. D. Ronza, J. Sharma and M. Sardiello (2019). "Lysosome biogenesis in health and disease." J Neurochem **148**(5): 573-589.

Bangari, D. S., K. M. Ashe, R. J. Desnick, C. Maloney, J. Lydon, P. Piepenhagen, E. Budman, J. P. Leonard, S. H. Cheng, J. Marshall and B. L. Thurberg (2015). "alpha-Galactosidase A knockout mice: progressive organ pathology resembles the type 2 later-onset phenotype of Fabry disease." Am J Pathol **185**(3): 651-665.

Banu, S., S. Srivastava, A. Mohammed, G. Kushawah, D. T. Sowpati and R. K. Mishra (2021). "Tissue-specific transcriptome recovery on withdrawal from chronic alcohol exposure in zebrafish." Alcohol **91**: 29-38.

Basgen, J. M., J. S. Wong, J. Ray, S. B. Nicholas and K. N. Campbell (2021). "Podocyte Foot Process Effacement Precedes Albuminuria and Glomerular Hypertrophy in CD2-Associated Protein Deficient Mice." Front Med (Lausanne) **8**: 745319.

Becherucci, F. and P. Romagnani (2015). "When foots come first: early signs of podocyte injury in Fabry nephropathy without proteinuria." Nephron **129**(1): 3-5.

Bellesso, S., M. Salvalaio, S. Lualdi, E. Tognon, R. Costa, P. Braghetta, C. Giraudo, R. Stramare, L. Rigon, M. Filocamo, R. Tomanin and E. Moro (2018). "FGF signaling deregulation is associated with early developmental skeletal defects in animal models for mucopolysaccharidosis type II (MPSII)." Hum Mol Genet **27**(13): 2262-2275.

Benjamin, E. R., R. Khanna, A. Schilling, J. J. Flanagan, L. J. Pellegrino, N. Brignol, Y. Lun, D. Guillen, B. E. Ranes, M. Frascella, R. Soska, J. Feng, L. Dungan, B. Young, D. J. Lockhart and K. J. Valenzano (2012). "Co-administration with the pharmacological chaperone AT1001 increases recombinant human alpha-galactosidase A tissue uptake and improves substrate reduction in Fabry mice." Mol Ther **20**(4): 717-726.

Berg, R. D., S. Levitte, M. P. O'Sullivan, S. M. O'Leary, C. J. Cambier, J. Cameron, K. K. Takaki, C. B. Moens, D. M. Tobin, J. Keane and L. Ramakrishnan (2016). "Lysosomal Disorders Drive Susceptibility to Tuberculosis by Compromising Macrophage Migration." Cell **165**(1): 139-152.

Bernardes, T. P., R. D. Foresto and G. M. Kirsztajn (2020). "Fabry disease: genetics, pathology, and treatment." Rev Assoc Med Bras (1992) **66Suppl 1**(Suppl 1): s10-s16.

Biancini, G. B., C. S. Vanzin, D. B. Rodrigues, M. Deon, G. S. Ribas, A. G. Barschak, V. Manfredini, C. B. Netto, L. B. Jardim, R. Giugliani and C. R. Vargas (2012). "Globotriaosylceramide is correlated with oxidative stress and inflammation in Fabry patients treated with enzyme replacement therapy." Biochim Biophys Acta **1822**(2): 226-232.

Bichet, D. G., J. M. Aerts, C. Auray-Blais, H. Maruyama, A. B. Mehta, N. Skuban, E. Krusinska and R. Schiffmann (2021). "Assessment of plasma lyso-Gb3 for clinical monitoring of treatment response in migalastat-treated patients with Fabry disease." Genet Med **23**(1): 192-201.

Biegstraaten, M., R. Arngrimsson, F. Barbey, L. Boks, F. Cecchi, P. B. Deegan, U. Feldt-Rasmussen, T. Geberhiwot, D. P. Germain, C. Hendriksz, D. A. Hughes, I. Kantola, N. Karabul, C. Lavery, G. E. Linthorst, A. Mehta, E. van de Mheen, J. P. Oliveira, R. Parini, U. Ramaswami, M. Rudnicki, A. Serra, C. Sommer, G. Sunder-Plassmann, E. Svarstad, A. Sweeb, W. Terryn, A. Tylki-Szymanska, C. Tondel, B. Vujkovac, F. Weidemann, F. A. Wijburg, P. Woolfson and C. E. Hollak (2015). "Recommendations for initiation and cessation of enzyme replacement therapy in patients with Fabry disease: the European Fabry Working Group consensus document." Orphanet J Rare Dis **10**: 36.

Blasi, F. and P. Carmeliet (2002). "uPAR: a versatile signalling orchestrator." Nat Rev Mol Cell Biol **3**(12): 932-943.

Boenzi, S., A. Pastore, D. Martinelli, B. M. Goffredo, A. Boiani, C. Rizzo and C. Dionisi-Vici (2012). "Creatine metabolism in urea cycle defects." J Inherit Metab Dis **35**(4): 647-653.

Bolten, J. S., A. Pratsinis, C. L. Alter, G. Fricker and J. Huwyler (2022). "Zebrafish (Danio rerio) larva as an in vivo vertebrate model to study renal function." Am J Physiol Renal Physiol **322**(3): F280-F294.

Boutin, M. and C. Auray-Blais (2015). "Metabolomic discovery of novel urinary galabiosylceramide analogs as Fabry disease biomarkers." J Am Soc Mass Spectrom **26**(3): 499-510.

Boutin, M., I. Menkovic, T. Martineau, V. Vaillancourt-Lavigueur, A. Toupin and C. Auray-Blais (2017). "Separation and Analysis of Lactosylceramide, Galabiosylceramide, and Globotriaosylceramide by LC-MS/MS in Urine of Fabry Disease Patients." Anal Chem **89**(24): 13382-13390.

Bradford, Y. M., C. E. Van Slyke, L. Ruzicka, A. Singer, A. Eagle, D. Fashena, D. G. Howe, K. Frazer, R. Martin, H. Paddock, C. Pich, S. Ramachandran and M. Westerfield (2022). "Zebrafish information network, the knowledgebase for Danio rerio research." Genetics **220**(4).

Braga, M. C., F. L. A. Fonseca, M. M. Marins, C. P. Gomes, M. R. Bacci, A. M. Martins and V. D'Almeida (2019). "Evaluation of Beta 2-Microglobulin, Cystatin C, and Lipocalin-2 as Renal Biomarkers for Patients with Fabry Disease." Nephron **143**(4): 217-227.

Branton, M., R. Schiffmann and J. B. Kopp (2002). "Natural history and treatment of renal involvement in Fabry disease." J Am Soc Nephrol **13 Suppl 2**: S139-143.

Braun, F., L. Blomberg, S. Brodesser, M. C. Liebau, B. Schermer, T. Benzing and C. E. Kurschat (2019). "Enzyme Replacement Therapy Clears Gb3 Deposits from a Podocyte Cell Culture Model of Fabry Disease but Fails to Restore Altered Cellular Signaling." Cell Physiol Biochem **52**(5): 1139-1150.

Brouns, S. J., M. M. Jore, M. Lundgren, E. R. Westra, R. J. Slijkhuis, A. P. Snijders, M. J. Dickman, K. S. Makarova, E. V. Koonin and J. van der Oost (2008). "Small CRISPR RNAs guide antiviral defense in prokaryotes." Science **321**(5891): 960-964.

Bryzgunova, O. E., M. M. Zaripov, T. E. Skvortsova, E. A. Lekchnov, A. E. Grigor'eva, I. A. Zaporozhchenko, E. S. Morozkin, E. I. Ryabchikova, Y. B. Yurchenko, V. E. Voitsitskiy and P. P. Laktionov (2016). "Comparative Study of Extracellular Vesicles from the Urine of Healthy Individuals and Prostate Cancer Patients." PLoS One **11**(6): e0157566.

Busch-Nentwich, E., Kettleborough, R., Dooley, C. M., Scahill, C., Sealy, I., White, R., Herd, C., Mehroke, S., Wali, N., Carruthers, S., Hall, A., Collins, J., Gibbons, R., Pusztai, Z., Clark, R., and Stemple, D.L. (2013). Sanger Institute Zebrafish Mutation Project mutant data submission. ZFIN Direct Data Submission.

Busch-Nentwich, E., Kettleborough, R., Fenyes, F., Herd, C., Collins, J., and Stemple, D.L. (2010). Sanger Institute Zebrafish Mutation Resource targeted knock-out mutants phenotype and image data submission. ZFIN Direct Data Submission.

Busch-Nentwich, E., Kettleborough, R., Fenyes, F., Herd, C., Collins, J., de Bruijn, E., van Eeden, F., Cuppen, E., and Stemple, D.L. (2010). Sanger Institute Zebrafish Mutation Resource targeted knock-out mutants phenotype and image data submission, Sanger Institute Zebrafish Mutation Resource and Hubrecht laboratory. ZFIN Direct Data Submission.

Busch-Nentwich, E., Kettleborough, R., Harvey, S., Collins, J., Ding, M., Dooley, C., Fenyes, F., Gibbons, R., Herd, C., Mehroke, S., Scahill, C., Sealy, I., Wali, N., White, R., and Stemple, D.L. (2012). Sanger Institute Zebrafish Mutation Project mutant, phenotype and image data submission. ZFIN Direct Data Submission.

Campos-Silva, C., H. Suarez, R. Jara-Acevedo, E. Linares-Espinos, L. Martinez-Pineiro, M. Yanez-Mo and M. Vales-Gomez (2019). "High sensitivity detection of extracellular vesicles immune-captured from urine by conventional flow cytometry." Sci Rep **9**(1): 2042.

Canaud, G., F. Bienaime, A. Viau, C. Treins, W. Baron, C. Nguyen, M. Burtin, S. Berissi, K. Giannakakis, A. O. Muda, S. Zschiedrich, T. B. Huber, G. Friedlander, C. Legendre, M. Pontoglio, M. Pende and F. Terzi (2013). "AKT2 is essential to maintain podocyte viability and function during chronic kidney disease." Nat Med **19**(10): 1288-1296.

Carnicer-Caceres, C., J. A. Arranz-Amo, C. Cea-Arestin, M. Camprodon-Gomez, D. Moreno-Martinez, S. Lucas-Del-Pozo, M. Molto-Abad, A. Tigri-Santina, I. Agraz-Pamplona, J. F. Rodriguez-Palomares, J. Hernandez-Vara, M. Armengol-Bellapart, M. Del-Toro-Riera and G. Pintos-Morell (2021). "Biomarkers in Fabry Disease. Implications for Clinical Diagnosis and Follow-up." J Clin Med **10**(8).

Cermak, S., M. Kosicek, A. Mladenovic-Djordjevic, K. Smiljanic, S. Kanazir and S. Hecimovic (2016). "Loss of Cathepsin B and L Leads to Lysosomal Dysfunction, NPC-Like Cholesterol Sequestration and Accumulation of the Key Alzheimer's Proteins." PLoS One **11**(11): e0167428.

Chapman, H. A. and Y. Wei (2001). "Protease crosstalk with integrins: the urokinase receptor paradigm." Thromb Haemost **86**(1): 124-129.

Chatterjee, S., P. Gupta, R. E. Pyeritz and P. O. Kwiterovich, Jr. (1984). "Immunohistochemical localization of glycosphingolipid in urinary renal tubular cells in Fabry's disease." Am J Clin Pathol **82**(1): 24-28.

Chen, T., G. Song, H. Yang, L. Mao, Z. Cui and K. Huang (2018). "Development of the Swimbladder Surfactant System and Biogenesis of Lysosome-Related Organelles Is Regulated by BLOS1 in Zebrafish." Genetics **208**(3): 1131-1146.

Chen, Z., A. Luciani, J. M. Mateos, G. Barmettler, R. H. Giles, S. C. F. Neuhauss and O. Devuyst (2020). "Transgenic zebrafish modeling low-molecular-weight proteinuria and lysosomal storage diseases." Kidney Int **97**(6): 1150-1163.

Chien, Y. H., P. Olivova, X. K. Zhang, S. C. Chiang, N. C. Lee, J. Keutzer and W. L. Hwu (2011). "Elevation of urinary globotriaosylceramide (GL3) in infants with Fabry disease." Mol Genet Metab **102**(1): 57-60.

Chitramuthu, B. P., D. C. Baranowski, D. G. Kay, A. Bateman and H. P. Bennett (2010). "Progranulin modulates zebrafish motoneuron development in vivo and rescues truncation defects associated with knockdown of Survival motor neuron 1." Mol Neurodegener **5**: 41.

Chitramuthu, B. P., D. G. Kay, A. Bateman and H. P. Bennett (2017). "Neurotrophic effects of progranulin in vivo in reversing motor neuron defects caused by over or under expression of TDP-43 or FUS." PLoS One **12**(3): e0174784.

Christensen, E. I., Q. Zhou, S. S. Sorensen, A. K. Rasmussen, C. Jacobsen, U. Feldt-Rasmussen and R. Nielsen (2007). "Distribution of alpha-galactosidase A in normal human kidney and renal accumulation and distribution of recombinant alpha-galactosidase A in Fabry mice." J Am Soc Nephrol **18**(3): 698-706.

Christou-Savina, S., P. L. Beales and D. P. Osborn (2015). "Evaluation of zebrafish kidney function using a fluorescent clearance assay." J Vis Exp(96): e52540.

Chu, B. B., Y. C. Liao, W. Qi, C. Xie, X. Du, J. Wang, H. Yang, H. H. Miao, B. L. Li and B. L. Song (2015). "Cholesterol transport through lysosome-peroxisome membrane contacts." Cell **161**(2): 291-306.

Chung, S., M. Son, Y. Chae, S. Oh, E. S. Koh, Y. K. Kim, S. J. Shin, C. W. Park, S. C. Jung and H. S. Kim (2021). "Fabry disease exacerbates renal interstitial fibrosis after unilateral ureteral obstruction via impaired autophagy and enhanced apoptosis." Kidney Res Clin Pract **40**(2): 208-219.

Citro, V., J. Pena-Garcia, H. den-Haan, H. Perez-Sanchez, R. Del Prete, L. Liguori, C. Cimmaruta, J. Lukas, M. V. Cubellis and G. Andreotti (2016). "Identification of an Allosteric Binding Site on Human Lysosomal Alpha-Galactosidase Opens the Way to New Pharmacological Chaperones for Fabry Disease." PLoS One **11**(10): e0165463.

Concolino, D., F. Deodato and R. Parini (2018). "Enzyme replacement therapy: efficacy and limitations." Ital J Pediatr **44**(Suppl 2): 120.

Condrat, C. E., D. C. Thompson, M. G. Barbu, O. L. Bugnar, A. Boboc, D. Cretoiu, N. Suciu, S. M. Cretoiu and S. C. Voinea (2020). "miRNAs as Biomarkers in Disease: Latest Findings Regarding Their Role in Diagnosis and Prognosis." Cells **9**(2).

Costa, R., A. Urbani, M. Salvalaio, S. Bellesso, D. Cieri, I. Zancan, M. Filocamo, P. Bonaldo, I. Szabo, R. Tomanin and E. Moro (2017). "Perturbations in cell signaling elicit early cardiac defects in mucopolysaccharidosis type II." Hum Mol Genet **26**(9): 1643-1655.

Cuccurullo, M., A. Beneduci, S. Anand, R. Mignani, B. Cianciaruso, A. Bachi and G. Capasso (2010). "Fabry disease: perspectives of urinary proteomics." J Nephrol **23 Suppl 16**: S199-212.

Cunningham, F., J. E. Allen, J. Allen, J. Alvarez-Jarreta, M. R. Amode, I. M. Armean, O. Austine-Orimoloye, A. G. Azov, I. Barnes, R. Bennett, A. Berry, J. Bhai, A. Bignell, K. Billis, S. Boddu, L. Brooks, M. Charkhchi, C. Cummins, L. Da Rin Fioretto, C. Davidson, K. Dodiya, S. Donaldson, B. El Houdaigui, T. El Naboulsi, R. Fatima, C. G. Giron, T. Genez, J. G. Martinez, C. Guijarro-Clarke, A. Gymer, M. Hardy, Z. Hollis, T. Hourlier, T. Hunt, T. Juettemann, V. Kaikala, M. Kay, I. Lavidas, T. Le, D. Lemos, J. C. Marugan, S. Mohanan, A. Mushtaq, M. Naven, D. N. Ogeh, A. Parker, A. Parton, M. Perry, I. Pilizota, I. Prosovetskaia, M. P. Sakthivel, A. I. A. Salam, B. M. Schmitt, H. Schuilenburg, D. Sheppard, J. G. Perez-Silva, W. Stark, E. Steed, K. Sutinen, R. Sukumaran, D. Sumathipala, M.

M. Suner, M. Szpak, A. Thormann, F. F. Tricomi, D. Urbina-Gomez, A. Veidenberg, T. A. Walsh, B. Walts, N. Willhoft, A. Winterbottom, E. Wass, M. Chakiachvili, B. Flint, A. Frankish, S. Giorgetti, L. Haggerty, S. E. Hunt, I. I. GR, J. E. Loveland, F. J. Martin, B. Moore, J. M. Mudge, M. Muffato, E. Perry, M. Ruffier, J. Tate, D. Thybert, S. J. Trevanion, S. Dyer, P. W. Harrison, K. L. Howe, A. D. Yates, D. R. Zerbino and P. Flicek (2022). "Ensembl 2022." Nucleic Acids Res **50**(D1): D988-D995.

Daly, C. M., J. Willer, R. Gregg and J. M. Gross (2013). "snow white, a zebrafish model of Hermansky-Pudlak Syndrome type 5." Genetics **195**(2): 481-494.

Das, A. M. and H. Y. Naim (2009). "Biochemical basis of Fabry disease with emphasis on mitochondrial function and protein trafficking." Adv Clin Chem **49**: 57-71.

De Francesco, P. N., J. M. Mucci, R. Ceci, C. A. Fossati and P. A. Rozenfeld (2013). "Fabry disease peripheral blood immune cells release inflammatory cytokines: role of globotriaosylceramide." Mol Genet Metab **109**(1): 93-99.

de la Mata, M., D. Cotan, M. Villanueva-Paz, I. de Lavera, M. Alvarez-Cordoba, R. Luzon-Hidalgo, J. M. Suarez-Rivero, G. Tiscornia and M. Oropesa-Avila (2016). "Mitochondrial Dysfunction in Lysosomal Storage Disorders." Diseases **4**(4).

De Muynck, L., S. Herdewyn, S. Beel, W. Scheveneels, L. Van Den Bosch, W. Robberecht and P. Van Damme (2013). "The neurotrophic properties of progranulin depend on the granulin E domain but do not require sortilin binding." Neurobiol Aging **34**(11): 2541-2547.

De Pasquale, V., A. Moles and L. M. Pavone (2020). "Cathepsins in the Pathophysiology of Mucopolysaccharidoses: New Perspectives for Therapy." Cells **9**(4).

Deegens, J. K., H. B. Dijkman, G. F. Borm, E. J. Steenbergen, J. G. van den Berg, J. J. Weening and J. F. Wetzels (2008). "Podocyte foot process effacement as a diagnostic tool in focal segmental glomerulosclerosis." Kidney Int **74**(12): 1568-1576.

Deem, T. L. and J. M. Cook-Mills (2004). "Vascular cell adhesion molecule 1 (VCAM-1) activation of endothelial cell matrix metalloproteinases: role of reactive oxygen species." Blood **104**(8): 2385-2393.

Del Pino, M., A. Andres, A. A. Bernabeu, J. de Juan-Rivera, E. Fernandez, J. de Dios Garcia Diaz, D. Hernandez, J. Luno, I. M. Fernandez, J. Paniagua, M. Posada de la Paz, J. C. Rodriguez-Perez, R. Santamaria, R. Torra, J. T. Ambros, P. Vidau and J. V. Torregrosa (2018). "Fabry Nephropathy: An Evidence-Based Narrative Review." Kidney Blood Press Res **43**(2): 406-421.

Desgrange, A. and S. Cereghini (2015). "Nephron Patterning: Lessons from Xenopus, Zebrafish, and Mouse Studies." Cells **4**(3): 483-499.

Desnick, R. J., G. Dawson, S. J. Desnick, C. C. Sweeley and W. Krivit (1971). "Diagnosis of glycosphingolipidoses by urinary-sediment analysis." N Engl J Med **284**(14): 739-744.

Desnick, R. J. and M. P. Wasserstein (2001). "Fabry disease: clinical features and recent advances in enzyme replacement therapy." Adv Nephrol Necker Hosp **31**: 317-339.

Desnick, R. J., M. P. Wasserstein and M. Banikazemi (2001). "Fabry disease (alpha-galactosidase A deficiency): renal involvement and enzyme replacement therapy." Contrib Nephrol(136): 174-192.

Deus, C. M., K. F. Yambire, P. J. Oliveira and N. Raimundo (2020). "Mitochondria-Lysosome Crosstalk: From Physiology to Neurodegeneration." Trends Mol Med **26**(1): 71-88.

Deveau, H., R. Barrangou, J. E. Garneau, J. Labonte, C. Fremaux, P. Boyaval, D. A. Romero, P. Horvath and S. Moineau (2008). "Phage response to CRISPR-encoded resistance in Streptococcus thermophilus." J Bacteriol **190**(4): 1390-1400.

Dhami, R. and E. H. Schuchman (2004). "Mannose 6-phosphate receptor-mediated uptake is defective in acid sphingomyelinase-deficient macrophages: implications for Niemann-Pick disease enzyme replacement therapy." J Biol Chem **279**(2): 1526-1532.

Diaz-Tellez, A., C. Zampedri, J. L. Ramos-Balderas, F. Garcia-Hernandez and E. Maldonado (2016). "Zebrafish scarb2a insertional mutant reveals a novel function for the Scarb2/Limp2 receptor in notochord development." Dev Dyn **245**(4): 508-519.

Diep, C. Q., D. Ma, R. C. Deo, T. M. Holm, R. W. Naylor, N. Arora, R. A. Wingert, F. Bollig, G. Djordjevic, B. Lichman, H. Zhu, T. Ikenaga, F. Ono, C. Englert, C. A. Cowan, N. A. Hukriede, R. I. Handin and A. J. Davidson (2011). "Identification of adult nephron progenitors capable of kidney regeneration in zebrafish." Nature **470**(7332): 95-100.

Ding, Q., Z. Zhang, Y. Li, H. Liu, Q. Hao, Y. Yang, E. Ringo, R. E. Olsen, J. L. Clarke, C. Ran and Z. Zhou (2021). "Propionate induces intestinal oxidative stress via Sod2 propionylation in zebrafish." iScience **24**(6): 102515.

Do, H. S., S. W. Park, I. Im, D. Seo, H. W. Yoo, H. Go, Y. H. Kim, G. Y. Koh, B. H. Lee and Y. M. Han (2020). "Enhanced thrombospondin-1 causes dysfunction of vascular endothelial cells derived from Fabry disease-induced pluripotent stem cells." EBioMedicine **52**: 102633.

Doykov, I. D., W. E. Heywood, V. Nikolaenko, J. Spiewak, J. Hallqvist, P. T. Clayton, P. Mills, D. G. Warnock, A. Nowak and K. Mills (2020). "Rapid, proteomic urine assay for monitoring progressive organ disease in Fabry disease." J Med Genet **57**(1): 38-47.

Driever, W., L. Solnica-Krezel, A. F. Schier, S. C. Neuhauss, J. Malicki, D. L. Stemple, D. Y. Stainier, F. Zwartkruis, S. Abdelilah, Z. Rangini, J. Belak and C. Boggs (1996). "A genetic screen for mutations affecting embryogenesis in zebrafish." Development **123**: 37-46.

Drummond, I. A. and A. J. Davidson (2010). "Zebrafish kidney development." Methods Cell Biol **100**: 233-260.

Drummond, I. A., A. Majumdar, H. Hentschel, M. Elger, L. Solnica-Krezel, A. F. Schier, S. C. Neuhauss, D. L. Stemple, F. Zwartkruis, Z. Rangini, W. Driever and M. C. Fishman (1998). "Early development of the zebrafish pronephros and analysis of mutations affecting pronephric function." Development **125**(23): 4655-4667.

Ducatez, F., W. Mauhin, A. Boullier, C. Pilon, T. Pereira, R. Aubert, O. Benveniste, S. Marret, O. Lidove, S. Bekri and A. Tebani (2021). "Parsing Fabry Disease Metabolic Plasticity Using Metabolomics." J Pers Med **11**(9).

Echevarria, L., K. Benistan, A. Toussaint, O. Dubourg, A. A. Hagege, D. Eladari, F. Jabbour, C. Beldjord, P. De Mazancourt and D. P. Germain (2016). "X-chromosome inactivation in female patients with Fabry disease." Clin Genet **89**(1): 44-54.

Eikrem, O., C. Beisland, K. Hjelle, A. Flatberg, A. Scherer, L. Landolt, T. Skogstrand, S. Leh, V. Beisvag and H. P. Marti (2016). "Transcriptome Sequencing (RNAseq) Enables Utilization of Formalin-Fixed, Paraffin-Embedded Biopsies with Clear Cell Renal Cell Carcinoma for Exploration of Disease Biology and Biomarker Development." PLoS One **11**(2): e0149743.

Eikrem, O., N. Delaleu, P. Strauss, M. Sekulic, C. Tøndel, S. Leh, E. Svarstad, R. Skrunes, A. Nowak, E. E. Rusu, T. A. Osman and H. P. Marti (2020). Systems Analyses of Renal Fabry Transcriptome and Response to Enzyme Replacement Therapy (ERT) Identifies a Cross-Validated and Druggable ERT-Resistant Module (Abstract, ASN, Kidney Week). J Am Soc Nephrol 31, 2020: 510.

Eikrem, O., R. Skrunes, C. Tondel, S. Leh, G. Houge, E. Svarstad and H. P. Marti (2017). "Pathomechanisms of renal Fabry disease." Cell Tissue Res **369**(1): 53-62.

Eikrem, O., P. Strauss, M. Sekulic, C. Tøndel, A. Flatberg, R. Skrunes, L. Landolt, J. Babickova, S. Leh, A. Scherer, E. Svarstad and H. P. Marti (2018). Fabry Nephropathy: Transcriptome Sequencing of Microdissected Renal Compartments from Archival Kidney Biopsies at Baseline, and After 5 and 10 Years of Enzyme Replacement Therapy (Abstract, ASN, Kidney Week). J Am Soc Nephrol 29, 2018: 310.

Eisner, V., R. R. Cupo, E. Gao, G. Csordas, W. S. Slovinsky, M. Paillard, L. Cheng, J. Ibetti, S. R. Chen, J. K. Chuprun, J. B. Hoek, W. J. Koch and G. Hajnoczky (2017). "Mitochondrial fusion dynamics is robust in the heart and depends on calcium oscillations and contractile activity." Proc Natl Acad Sci U S A **114**(5): E859-E868.

El Dib, R., H. Gomaa, A. Ortiz, J. Politei, A. Kapoor and F. Barreto (2017). "Enzyme replacement therapy for Anderson-Fabry disease: A complementary overview of a Cochrane publication through a linear regression and a pooled analysis of proportions from cohort studies." PLoS One **12**(3): e0173358.

Elleder, M., H. Poupetova and V. Kozich (1998). "[Fetal pathology in Fabry's disease and mucopolysaccharidosis type I]." Cesk Patol **34**(1): 7-12.

Elmonem, M. A., S. P. Berlingerio, L. P. van den Heuvel, P. A. de Witte, M. Lowe and E. N. Levtchenko (2018). "Genetic Renal Diseases: The Emerging Role of Zebrafish Models." Cells **7**(9).

Elmonem, M. A., R. Khalil, L. Khodaparast, L. Khodaparast, F. O. Arcolino, J. Morgan, A. Pastore, P. Tylzanowski, A. Ny, M. Lowe, P. A. de Witte, H. J. Baelde, L. P. van den Heuvel and E. Levtchenko (2017). "Cystinosis (ctns) zebrafish mutant shows pronephric glomerular and tubular dysfunction." Sci Rep **7**: 42583.

Eng, C. M., N. Guffon, W. R. Wilcox, D. P. Germain, P. Lee, S. Waldek, L. Caplan, G. E. Linthorst, R. J. Desnick and G. International Collaborative Fabry Disease Study (2001). "Safety and efficacy of recombinant human alpha-galactosidase A replacement therapy in Fabry's disease." N Engl J Med **345**(1): 9-16.

Eskelinen, E. L., Y. Tanaka and P. Saftig (2003). "At the acidic edge: emerging functions for lysosomal membrane proteins." Trends Cell Biol **13**(3): 137-145.

Fall, B., C. R. Scott, M. Mauer, S. Shankland, J. Pippin, J. A. Jefferson, E. Wallace, D. Warnock and B. Najafian (2016). "Urinary Podocyte Loss Is Increased in Patients with Fabry Disease and Correlates with Clinical Severity of Fabry Nephropathy." PLoS One **11**(12): e0168346.

Fan, J. Q., S. Ishii, N. Asano and Y. Suzuki (1999). "Accelerated transport and maturation of lysosomal alpha-galactosidase A in Fabry lymphoblasts by an enzyme inhibitor." Nat Med **5**(1): 112-115.

Faraggiana, T., A. Crescenzi and V. Marinozzi (1989). "Presence of an alpha-galactolipid on the cell surfaces of endothelial cells of human kidney." Histochem J **21**(4): 235-240.

Feriozzi, S., D. P. Germain, R. Di Vito, A. Legrand, R. Ricci and F. Barbey (2007). "Cystatin C as a marker of early changes of renal function in Fabry nephropathy." J Nephrol **20**(4): 437-443.

Feriozzi, S. and P. Rozenfeld (2021). "Pathology and pathogenic pathways in fabry nephropathy." Clin Exp Nephrol **25**(9): 925-934.

Ferrara, N. (2004). "Vascular endothelial growth factor: basic science and clinical progress." Endocr Rev **25**(4): 581-611.

Festa, B. P., Z. Chen, M. Berquez, H. Debaix, N. Tokonami, J. A. Prange, G. V. Hoek, C. Alessio, A. Raimondi, N. Nevo, R. H. Giles, O. Devuyst and A. Luciani (2018). "Impaired autophagy bridges lysosomal storage disease and epithelial dysfunction in the kidney." Nat Commun **9**(1): 161.

Flanagan-Steet, H., C. Christian, P. N. Lu, M. Aarnio-Peterson, L. Sanman, S. Archer-Hartmann, P. Azadi, M. Bogyo and R. A. Steet (2018). "TGF-ss Regulates Cathepsin Activation during Normal and Pathogenic Development." Cell Rep **22**(11): 2964-2977.

Flanagan-Steet, H., C. Matheny, A. Petrey, J. Parker and R. Steet (2016). "Enzyme-specific differences in mannose phosphorylation between GlcNAc-1-phosphotransferase alphabeta and gamma subunit deficient zebrafish support cathepsin proteases as early mediators of mucolipidosis pathology." Biochim Biophys Acta **1860**(9): 1845-1853.

Flanagan-Steet, H., C. Sias and R. Steet (2009). "Altered chondrocyte differentiation and extracellular matrix homeostasis in a zebrafish model for mucolipidosis II." Am J Pathol **175**(5): 2063-2075.

Fogo, A. B., L. Bostad, E. Svarstad, W. J. Cook, S. Moll, F. Barbey, L. Geldenhuys, M. West, D. Ferluga, B. Vujkovac, A. J. Howie, A. Burns, R. Reeve, S. Waldek, L. H. Noel, J. P. Grunfeld, C. Valbuena, J. P. Oliveira, J. Muller, F. Breunig, X. Zhang, D. G. Warnock and N. all members of the International Study Group of Fabry (2010). "Scoring system for renal pathology in Fabry disease: report of the International Study Group of Fabry Nephropathy (ISGFN)." Nephrol Dial Transplant **25**(7): 2168-2177.

Follo, C., M. Ozzano, C. Montalenti, M. M. Santoro and C. Isidoro (2013). "Knockdown of cathepsin D in zebrafish fertilized eggs determines congenital myopathy." Biosci Rep **33**(2): e00034.

Follo, C., M. Ozzano, V. Mugoni, R. Castino, M. Santoro and C. Isidoro (2011). "Knock-down of cathepsin D affects the retinal pigment epithelium, impairs swim-bladder ontogenesis and causes premature death in zebrafish." PLoS One **6**(7): e21908.

Fornoni, A., S. Merscher and J. B. Kopp (2014). "Lipid biology of the podocyte--new perspectives offer new opportunities." Nat Rev Nephrol **10**(7): 379-388.

Frustaci, A., R. Verardo, R. Scialla, G. Bagnato, M. Verardo, M. Alfarano and M. A. Russo (2022). "Downregulation of Mannose-6-Phosphate Receptors in Fabry Disease Cardiomyopathy: A Potential Target for Enzyme Therapy Enhancement." J Clin Med **11**(18).

Fujii, H., K. Kono, T. Yamamoto, T. Onishi, S. Goto, K. Nakai, H. Kawai, K. I. Hirata, M. Fukagawa and S. Nishi (2012). "Effect of enzyme replacement therapy on serum asymmetric dimethylarginine levels, coronary flow reserve and left ventricular hypertrophy in patients with Fabry disease." Clin Kidney J **5**(6): 512-518.

Gagnon, J. A., E. Valen, S. B. Thyme, P. Huang, L. Akhmetova, A. Pauli, T. G. Montague, S. Zimmerman, C. Richter and A. F. Schier (2014). "Efficient mutagenesis by Cas9 protein-mediated oligonucleotide insertion and large-scale assessment of single-guide RNAs." PLoS One **9**(5): e98186.

Garman, S. C. (2007). "Structure-function relationships in alpha-galactosidase A." Acta Paediatr **96**(455): 6-16.

Garman, S. C. and D. N. Garboczi (2004). "The molecular defect leading to Fabry disease: structure of human alpha-galactosidase." J Mol Biol **337**(2): 319-335.

Gehrig, J., G. Pandey and J. H. Westhoff (2018). "Zebrafish as a Model for Drug Screening in Genetic Kidney Diseases." Front Pediatr **6**: 183.

Gerlach, G. F. and R. A. Wingert (2013). "Kidney organogenesis in the zebrafish: insights into vertebrate nephrogenesis and regeneration." Wiley Interdiscip Rev Dev Biol **2**(5): 559-585.

Germain, D. P. (2010). "Fabry disease." Orphanet J Rare Dis **5**: 30.

Germain, D. P., J. Charrow, R. J. Desnick, N. Guffon, J. Kempf, R. H. Lachmann, R. Lemay, G. E. Linthorst, S. Packman, C. R. Scott, S. Waldek, D. G. Warnock, N. J. Weinreb and W. R. Wilcox (2015). "Ten-year outcome of enzyme replacement therapy with agalsidase beta in patients with Fabry disease." J Med Genet **52**(5): 353-358.

Golling, G., A. Amsterdam, Z. Sun, M. Antonelli, E. Maldonado, W. Chen, S. Burgess, M. Haldi, K. Artzt, S. Farrington, S. Y. Lin, R. M. Nissen and N. Hopkins (2002). "Insertional mutagenesis in zebrafish rapidly identifies genes essential for early vertebrate development." Nat Genet **31**(2): 135-140.

Gomord, V. and L. Faye (2004). "Posttranslational modification of therapeutic proteins in plants." Curr Opin Plant Biol **7**(2): 171-181.

Goncalves, I., K. Hultman, P. Duner, A. Edsfeldt, B. Hedblad, G. N. Fredrikson, H. Bjorkbacka, J. Nilsson and E. Bengtsson (2016). "High levels of cathepsin D and cystatin B are associated with increased risk of coronary events." Open Heart **3**(1): e000353.

Gonzalez, A., M. Valeiras, E. Sidransky and N. Tayebi (2014). "Lysosomal integral membrane protein-2: a new player in lysosome-related pathology." Mol Genet Metab **111**(2): 84-91.

Guerard, N., O. Morand and J. Dingemanse (2017). "Lucerastat, an iminosugar with potential as substrate reduction therapy for glycolipid storage disorders: safety, tolerability, and pharmacokinetics in healthy subjects." Orphanet J Rare Dis **12**(1): 9.

Guest, J. F., T. Jenssen, G. Houge, W. Aaseboe, C. Tondel and E. Svarstad (2010). "Modelling the resource implications of managing adults with Fabry disease in Norway favours home infusion." Eur J Clin Invest **40**(12): 1104-1112.

Gundersen, H. J., T. Seefeldt and R. Osterby (1980). "Glomerular epithelial foot processes in normal man and rats. Distribution of true width and its intra- and inter-individual variation." Cell Tissue Res **205**(1): 147-155.

Gut, P., S. Reischauer, D. Y. R. Stainier and R. Arnaout (2017). "Little Fish, Big Data: Zebrafish as a Model for Cardiovascular and Metabolic Disease." Physiol Rev **97**(3): 889-938.

Haffter, P., M. Granato, M. Brand, M. C. Mullins, M. Hammerschmidt, D. A. Kane, J. Odenthal, F. J. van Eeden, Y. J. Jiang, C. P. Heisenberg, R. N. Kelsh, M. Furutani-Seiki, E. Vogelsang, D. Beuchle, U. Schach, C. Fabian and C. Nusslein-Volhard (1996). "The identification of genes with unique and essential functions in the development of the zebrafish, Danio rerio." Development **123**: 1-36.

Hagmann, H. and P. T. Brinkkoetter (2018). "Experimental Models to Study Podocyte Biology: Stock-Taking the Toolbox of Glomerular Research." Front Pediatr **6**: 193.

Hanke, N., B. L. King, B. Vaske, H. Haller and M. Schiffer (2015). "A Fluorescence-Based Assay for Proteinuria Screening in Larval Zebrafish (Danio rerio)." Zebrafish **12**(5): 372-376.

Hasegawa, S., T. Ichiyama, I. Sonaka, A. Ohsaki, S. Okada, H. Wakiguchi, K. Kudo, S. Kittaka, M. Hara and S. Furukawa (2012). "Cysteine, histidine and glycine exhibit anti-inflammatory effects in human coronary arterial endothelial cells." Clin Exp Immunol **167**(2): 269-274.

Haskins, M. E., U. Giger and D. F. Patterson (2006). Animal models of lysosomal storage diseases: their development and clinical relevance. Fabry Disease: Perspectives from 5 Years of FOS. A. Mehta, M. Beck and G. Sunder-Plassmann. Oxford.

Hennermann, J. B., L. Arash-Kaps, G. Fekete, A. Schaaf, A. Busch and T. Frischmuth (2019). "Pharmacokinetics, pharmacodynamics, and safety of moss-aGalactosidase A in patients with Fabry disease." J Inherit Metab Dis **42**(3): 527-533.

Hentschel, D. M., M. Mengel, L. Boehme, F. Liebsch, C. Albertin, J. V. Bonventre, H. Haller and M. Schiffer (2007). "Rapid screening of glomerular slit diaphragm integrity in larval zebrafish." Am J Physiol Renal Physiol **293**(5): F1746-1750.

Heo, S. H., E. Kang, Y. M. Kim, H. Go, K. Y. Kim, J. Y. Jung, M. Kang, G. H. Kim, J. M. Kim, I. H. Choi, J. H. Choi, S. C. Jung, R. J. Desnick, H. W. Yoo and B. H. Lee (2017). "Fabry disease: characterisation of the plasma proteome pre- and post-enzyme replacement therapy." J Med Genet **54**(11): 771-780.

Herzog, C., C. Yang, A. Holmes and G. P. Kaushal (2012). "zVAD-fmk prevents cisplatin-induced cleavage of autophagy proteins but impairs autophagic flux and worsens renal function." Am J Physiol Renal Physiol **303**(8): F1239-1250.

Heywood, W. E., I. Doykov, J. Spiewak, J. Hallqvist, K. Mills and A. Nowak (2019). "Global glycosphingolipid analysis in urine and plasma of female Fabry disease patients." Biochim Biophys Acta Mol Basis Dis **1865**(10): 2726-2735.

Hollander, Z., D. L. Dai, B. N. Putko, H. Yogasundaram, J. E. Wilson-McManus, R. B. Thompson, A. Khan, M. L. West, B. M. McManus and G. Y. Oudit (2015). "Gender-specific plasma proteomic biomarkers in patients with Anderson-Fabry disease." Eur J Heart Fail **17**(3): 291-300.

Hopkin, R. J., J. L. Jefferies, D. A. Laney, V. H. Lawson, M. Mauer, M. R. Taylor, W. R. Wilcox and P. Fabry Pediatric Expert (2016). "The management and treatment of children with Fabry disease: A United States-based perspective." Mol Genet Metab **117**(2): 104-113.

Hossain, M. A., C. Wu, H. Yanagisawa, T. Miyajima, K. Akiyama and Y. Eto (2019). "Future clinical and biochemical predictions of Fabry disease in females by methylation studies of the GLA gene." Mol Genet Metab Rep **20**: 100497.

Howe, K., M. D. Clark, C. F. Torroja, J. Torrance, C. Berthelot, M. Muffato, J. E. Collins, S. Humphray, K. McLaren, L. Matthews, S. McLaren, I. Sealy, M. Caccamo, C. Churcher, C. Scott, J. C. Barrett, R. Koch, G. J. Rauch, S. White, W. Chow, B. Kilian, L. T. Quintais, J. A. Guerra-Assuncao, Y. Zhou, Y. Gu, J. Yen, J. H. Vogel, T. Eyre, S. Redmond, R. Banerjee, J. Chi, B. Fu, E. Langley, S. F. Maguire, G. K. Laird, D. Lloyd, E. Kenyon, S. Donaldson, H. Sehra, J. Almeida-King, J. Loveland, S. Trevanion, M. Jones, M. Quail, D. Willey, A. Hunt, J. Burton, S. Sims, K. McLay, B. Plumb, J. Davis, C. Clee, K. Oliver, R. Clark, C. Riddle, D. Elliot, G. Threadgold, G. Harden, D. Ware, S. Begum, B. Mortimore, G. Kerry, P. Heath, B. Phillimore, A. Tracey, N. Corby, M. Dunn, C. Johnson, J. Wood, S. Clark, S. Pelan, G. Griffiths, M. Smith, R. Glithero, P. Howden, N. Barker, C. Lloyd, C. Stevens, J. Harley, K. Holt, G. Panagiotidis, J. Lovell, H. Beasley, C. Henderson, D. Gordon, K. Auger, D. Wright, J. Collins, C. Raisen, L. Dyer, K. Leung, L. Robertson, K. Ambridge, D. Leongamornlert, S. McGuire, R. Gilderthorp, C. Griffiths, D. Manthravadi, S. Nichol, G. Barker, S. Whitehead, M. Kay, J. Brown, C. Murnane, E. Gray, M. Humphries, N. Sycamore, D. Barker, D. Saunders, J. Wallis, A. Babbage, S. Hammond, M. Mashreghi-Mohammadi, L. Barr, S. Martin, P. Wray, A. Ellington, N. Matthews, M. Ellwood, R. Woodmansey, G. Clark, J. Cooper, A. Tromans, D. Grafham, C. Skuce, R. Pandian, R. Andrews, E. Harrison, A. Kimberley, J. Garnett, N. Fosker, R. Hall, P. Garner, D. Kelly, C. Bird, S. Palmer, I. Gehring, A. Berger, C. M. Dooley, Z. Ersan-Urun, C. Eser, H. Geiger, M. Geisler, L. Karotki, A. Kirn, J. Konantz, M. Konantz, M. Oberlander, S. Rudolph-Geiger, M. Teucke, C. Lanz, G. Raddatz, K. Osoegawa, B. Zhu, A. Rapp, S. Widaa, C. Langford, F. Yang, S. C. Schuster, N. P. Carter, J. Harrow, Z. Ning, J. Herrero, S. M. Searle, A. Enright, R. Geisler, R. H. Plasterk, C. Lee, M. Westerfield, P. J. de Jong, L. I. Zon, J. H. Postlethwait, C. Nusslein-Volhard, T. J. Hubbard, H. Roest Crollius, J. Rogers and D. L. Stemple (2013). "The zebrafish reference genome sequence and its relationship to the human genome." Nature **496**(7446): 498-503.

Hubner, A., T. Metz, A. Schanzer, S. Greber-Platzer and C. B. Item (2015). "Aberrant DNA methylation of calcitonin receptor in Fabry patients treated with enzyme replacement therapy." Mol Genet Metab Rep **5**: 1-2.

Hughes, D. A., K. Nicholls, S. P. Shankar, G. Sunder-Plassmann, D. Koeller, K. Nedd, G. Vockley, T. Hamazaki, R. Lachmann, T. Ohashi, I. Olivotto, N. Sakai, P. Deegan, D. Dimmock, F. Eyskens, D. P. Germain, O. Goker-Alpan, E. Hachulla, A. Jovanovic, C. M. Lourenco, I. Narita, M. Thomas, W. R. Wilcox, D. G. Bichet, R. Schiffmann, E. Ludington, C. Viereck, J. Kirk, J. Yu, F. Johnson, P. Boudes, E. R. Benjamin, D. J. Lockhart, C. Barlow, N. Skuban, J. P. Castelli, J. Barth and U. Feldt-Rasmussen (2017). "Oral pharmacological chaperone migalastat compared with enzyme replacement therapy in Fabry disease: 18-month results from the randomised phase III ATTRACT study." J Med Genet **54**(4): 288-296.

Huston, M. W., M. Yasuda, S. Pagant, S. S. Martin, L. Cao, L. Falese, K. Meyer, R. J. Desnick and T. Wechsler (2019). "Liver-targeted AAV gene therapy vectors produced by a clinical scale manufacturing process result in high, continuous therapeutic levels of enzyme activity and effective substrate reduction in mouse model of Fabry disease." Molecular Genetics and Metabolism **126**(2): S77.

Hwang, W. Y., Y. Fu, D. Reyon, M. L. Maeder, S. Q. Tsai, J. D. Sander, R. T. Peterson, J. R. Yeh and J. K. Joung (2013). "Efficient genome editing in zebrafish using a CRISPR-Cas system." Nat Biotechnol **31**(3): 227-229.

Ishii, S., R. Kase, H. Sakuraba and Y. Suzuki (1993). "Characterization of a mutant alpha-galactosidase gene product for the late-onset cardiac form of Fabry disease." Biochem Biophys Res Commun **197**(3): 1585-1589.

Ivanova, M. M., E. Changsila, C. Iaonou and O. Goker-Alpan (2019). "Impaired autophagic and mitochondrial functions are partially restored by ERT in Gaucher and Fabry diseases." PLoS One **14**(1): e0210617.

Ivanova, M. M., J. Dao, N. Kasaci, B. Adewale, J. Fikry and O. Goker-Alpan (2020). "Rapid Clathrin-Mediated Uptake of Recombinant alpha-Gal-A to Lysosome Activates Autophagy." Biomolecules **10**(6).

Jagadeeswaran, P., J. P. Sheehan, F. E. Craig and D. Troyer (1999). "Identification and characterization of zebrafish thrombocytes." Br J Haematol **107**(4): 731-738.

Jagannathan-Bogdan, M. and L. I. Zon (2013). "Hematopoiesis." Development **140**(12): 2463-2467.

Janeiro, M. H., M. J. Ramirez, F. I. Milagro, J. A. Martinez and M. Solas (2018). "Implication of Trimethylamine N-Oxide (TMAO) in Disease: Potential Biomarker or New Therapeutic Target." Nutrients **10**(10).

Jaurretche, S., N. Antogiovanni and F. Perretta (2017). "Prevalence of chronic kidney disease in fabry disease patients: Multicenter cross sectional study in Argentina." Mol Genet Metab Rep **12**: 41-43.

Jaurretche, S., G. R. Perez and G. Venera (2019). "High Lyso-Gb3 Plasma Levels Associated with Decreased miR-29 and miR-200 Urinary Excretion in Young Non-Albuminuric Male Patient with Classic Fabry Disease." Case Rep Nephrol **2019**: 4980942.

Jehn, U., S. Bayraktar, S. Pollmann, V. Van Marck, T. Weide, H. Pavenstadt, E. Brand and M. Lenders (2021). "alpha-Galactosidase a Deficiency in Fabry Disease Leads to Extensive Dysregulated Cellular Signaling Pathways in Human Podocytes." Int J Mol Sci **22**(21).

Jeon, Y. J., N. Jung, J. W. Park, H. Y. Park and S. C. Jung (2015). "Epithelial-Mesenchymal Transition in Kidney Tubular Epithelial Cells Induced by Globotriaosylsphingosine and Globotriaosylceramide." PLoS One **10**(8): e0136442.

Jin, W., Y. Dai, F. Li, L. Zhu, Z. Huang, W. Liu, J. Li, M. Zhang, J. Du, W. Zhang and Z. Wen (2019). "Dysregulation of Microglial Function Contributes to Neuronal Impairment in Mcoln1a-Deficient Zebrafish." iScience **13**: 391-401.

Jinek, M., A. East, A. Cheng, S. Lin, E. Ma and J. Doudna (2013). "RNA-programmed genome editing in human cells." Elife **2**: e00471.

Jobst-Schwan, T., C. A. Hoogstraten, C. M. Kolvenbach, J. M. Schmidt, A. Kolb, K. Eddy, R. Schneider, S. Ashraf, E. Widmeier, A. J. Majmundar and F. Hildebrandt (2019). "Corticosteroid treatment exacerbates nephrotic syndrome in a zebrafish model of magi2a knockout." Kidney Int **95**(5): 1079-1090.

Johannes, L. and C. Wunder (2016). Retrograde Transport. Encyclopedia of Cell Biology. R. A. Bradshaw and P. D. Stahl. Waltham, Academic Press**:** 433-441.

Kajiwara, M., T. Aoi, K. Okita, R. Takahashi, H. Inoue, N. Takayama, H. Endo, K. Eto, J. Toguchida, S. Uemoto and S. Yamanaka (2012). "Donor-dependent variations in hepatic differentiation from human-induced pluripotent stem cells." Proc Natl Acad Sci U S A **109**(31): 12538-12543.

Kalen, M., E. Wallgard, N. Asker, A. Nasevicius, E. Athley, E. Billgren, J. D. Larson, S. A. Wadman, E. Norseng, K. J. Clark, L. He, L. Karlsson-Lindahl, A. K. Hager, H. Weber, H. Augustin, T. Samuelsson, C. K. Kemmet, C. M. Utesch, J. J. Essner, P. B. Hackett and M. Hellstrom (2009). "Combination of reverse and chemical genetic screens reveals angiogenesis inhibitors and targets." Chem Biol **16**(4): 432-441.

Kamei, C. N. and I. A. Drummond (2014). "Zebrafish as a Model for Studying Kidney Regeneration." Current Pathobiology Reports **2**(2): 53-59.

Kanehisa, M., Y. Sato and K. Morishima (2016). "BlastKOALA and GhostKOALA: KEGG Tools for Functional Characterization of Genome and Metagenome Sequences." J Mol Biol **428**(4): 726-731.

Keatinge, M., H. Bui, A. Menke, Y. C. Chen, A. M. Sokol, Q. Bai, F. Ellett, M. Da Costa, D. Burke, M. Gegg, L. Trollope, T. Payne, A. McTighe, H. Mortiboys, S. de Jager, H. Nuthall, M. S. Kuo, A. Fleming, A. H. Schapira, S. A. Renshaw, J. R. Highley, A. Chacinska, P. Panula, E. A. Burton, M. J. O'Neill and O. Bandmann (2015). "Glucocerebrosidase 1 deficient Danio rerio mirror key pathological aspects of human Gaucher disease and provide evidence of early microglial activation preceding alpha-synuclein-independent neuronal cell death." Hum Mol Genet **24**(23): 6640-6652.

Khalil, R., R. A. Lalai, M. I. Wiweger, C. M. Avramut, A. J. Koster, H. P. Spaink, J. A. Bruijn, P. C. W. Hogendoorn and H. J. Baelde (2019). "Glomerular permeability is not affected by heparan sulfate glycosaminoglycan deficiency in zebrafish embryos." Am J Physiol Renal Physiol **317**(5): F1211-F1216.

Kia, A., J. McIntosh, C. Rosales, P. Hosseini, R. Sheridan, J. Spiewak, K. Mills, R. Corbau and A. C. Nathwani (2018). "Efficacy Evaluation of Liver-Directed Gene Therapy in Fabry Mice." Blood **132**(Supplement 1): 2209-2209.

Kim, J. W., H. W. Kim, S. A. Nam, J. Y. Lee, H. J. Cho, T. M. Kim and Y. K. Kim (2021). "Human kidney organoids reveal the role of glutathione in Fabry disease." Exp Mol Med **53**(10): 1580-1591.

Kim, S. H., S. Y. Wu, J. I. Baek, S. Y. Choi, Y. Su, C. R. Flynn, J. T. Gamse, K. C. Ess, G. Hardiman, J. H. Lipschutz, N. N. Abumrad and D. C. Rockey (2015). "A post-developmental genetic screen for zebrafish models of inherited liver disease." PLoS One **10**(5): e0125980.

Kimmel, C. B., W. W. Ballard, S. R. Kimmel, B. Ullmann and T. F. Schilling (1995). "Stages of embryonic development of the zebrafish." Dev Dyn **203**(3): 253-310.

Kizhner, T., Y. Azulay, M. Hainrichson, Y. Tekoah, G. Arvatz, A. Shulman, I. Ruderfer, D. Aviezer and Y. Shaaltiel (2015). "Characterization of a chemically modified plant cell culture expressed human alpha-Galactosidase-A enzyme for treatment of Fabry disease." Mol Genet Metab **114**(2): 259-267.

Klingelhofer, D., M. Braun, R. K. Seeger-Zybok, D. Quarcoo, D. Bruggmann and D. A. Groneberg (2020). "Global research on Fabry's disease: Demands for a rare disease." Mol Genet Genomic Med **8**(9): e1163.

Ko, Y. A., H. Yi, C. Qiu, S. Huang, J. Park, N. Ledo, A. Kottgen, H. Li, D. J. Rader, M. A. Pack, C. D. Brown and K. Susztak (2017). "Genetic-Variation-Driven Gene-Expression Changes Highlight Genes with Important Functions for Kidney Disease." Am J Hum Genet **100**(6): 940-953.

Kok, K., K. C. Zwiers, R. G. Boot, H. S. Overkleeft, J. Aerts and M. Artola (2021). "Fabry Disease: Molecular Basis, Pathophysiology, Diagnostics and Potential Therapeutic Directions." Biomolecules **11**(2).

Koopman, W. J., H. J. Visch, J. A. Smeitink and P. H. Willems (2006). "Simultaneous quantitative measurement and automated analysis of mitochondrial morphology, mass, potential, and motility in living human skin fibroblasts." Cytometry A **69**(1): 1-12.

Koprivova, A., C. Stemmer, F. Altmann, A. Hoffmann, S. Kopriva, G. Gorr, R. Reski and E. L. Decker (2004). "Targeted knockouts of Physcomitrella lacking plant-specific immunogenic N-glycans." Plant Biotechnol J **2**(6): 517-523.

Koussounadis, A., S. P. Langdon, I. H. Um, D. J. Harrison and V. A. Smith (2015). "Relationship between differentially expressed mRNA and mRNA-protein correlations in a xenograft model system." Sci Rep **5**: 10775.

Kramer-Zucker, A. G., S. Wiessner, A. M. Jensen and I. A. Drummond (2005). "Organization of the pronephric filtration apparatus in zebrafish requires Nephrin, Podocin and the FERM domain protein Mosaic eyes." Dev Biol **285**(2): 316-329.

Kuil, L. E., A. Lopez Marti, A. Carreras Mascaro, J. C. van den Bosch, P. van den Berg, H. C. van der Linde, K. Schoonderwoerd, G. J. G. Ruijter and T. J. van Ham (2019). "Hexb enzyme deficiency leads to lysosomal abnormalities in radial glia and microglia in zebrafish brain development." Glia **67**(9): 1705-1718.

Labilloy, A., R. T. Youker, J. R. Bruns, I. Kukic, K. Kiselyov, W. Halfter, D. Finegold, S. J. do Monte and O. A. Weisz (2014). "Altered dynamics of a lipid raft associated protein in a kidney model of Fabry disease." Mol Genet Metab **111**(2): 184-192.

Labun, K., M. Krause, Y. Torres Cleuren and E. Valen (2021). "CRISPR Genome Editing Made Easy Through the CHOPCHOP Website." Curr Protoc **1**(4): e46.

Labun, K., T. G. Montague, M. Krause, Y. N. Torres Cleuren, H. Tjeldnes and E. Valen (2019). "CHOPCHOP v3: expanding the CRISPR web toolbox beyond genome editing." Nucleic Acids Res **47**(W1): W171-W174.

Laird, A. S., A. Van Hoecke, L. De Muynck, M. Timmers, L. Van den Bosch, P. Van Damme and W. Robberecht (2010). "Progranulin is neurotrophic in vivo and protects against a mutant TDP-43 induced axonopathy." PLoS One **5**(10): e13368.

Lam, J., P. Katti, M. Biete, M. Mungai, S. AshShareef, K. Neikirk, E. Garza Lopez, Z. Vue, T. A. Christensen, H. K. Beasley, T. A. Rodman, S. A. Murray, J. L. Salisbury, B. Glancy, J. Shao, R. O. Pereira, E. D. Abel and A. Hinton, Jr. (2021). "A Universal Approach to Analyzing Transmission Electron Microscopy with ImageJ." Cells **10**(9).

Lapinski, R., N. Perico, A. Remuzzi, F. Sangalli, A. Benigni and G. Remuzzi (1996). "Angiotensin II modulates glomerular capillary permselectivity in rat isolated perfused kidney." J Am Soc Nephrol **7**(5): 653-660.

Lawler, J. M., W. S. Barnes, G. Wu, W. Song and S. Demaree (2002). "Direct antioxidant properties of creatine." Biochem Biophys Res Commun **290**(1): 47-52.

Lee, M. H., E. N. Choi, Y. J. Jeon and S. C. Jung (2012). "Possible role of transforming growth factor-beta1 and vascular endothelial growth factor in Fabry disease nephropathy." Int J Mol Med **30**(6): 1275-1280.

Lehman, L. J., A. L. Olson and C. J. Rebouche (1987). "Measurement of Epsilon-N-Trimethyllysine in Human-Blood Plasma and Urine." Analytical Biochemistry **162**(1): 137-142.

Lelieveld, L. T., M. Mirzaian, C. L. Kuo, M. Artola, M. J. Ferraz, R. E. A. Peter, H. Akiyama, P. Greimel, R. van den Berg, H. S. Overkleeft, R. G. Boot, A. H. Meijer and J. Aerts (2019). "Role of beta-glucosidase 2 in aberrant glycosphingolipid metabolism: model of glucocerebrosidase deficiency in zebrafish." J Lipid Res **60**(11): 1851-1867.

Lepedda, A. J., L. Fancellu, E. Zinellu, P. De Muro, G. Nieddu, G. A. Deiana, P. Canu, D. Concolino, S. Sestito, M. Formato and G. Sechi (2013). "Urine bikunin as a marker of renal impairment in Fabry's disease." Biomed Res Int **2013**: 205948.

Levey, A. S., L. A. Stevens, C. H. Schmid, Y. L. Zhang, A. F. Castro, 3rd, H. I. Feldman, J. W. Kusek, P. Eggers, F. Van Lente, T. Greene, J. Coresh and E. P. I. Ckd (2009). "A new equation to estimate glomerular filtration rate." Ann Intern Med **150**(9): 604-612.

Levstek, T., T. Mlinsek, M. Holcar, K. Goricar, M. Lenassi, V. Dolzan, B. Vujkovac and K. Trebusak Podkrajsek (2021). "Urinary Extracellular Vesicles and Their miRNA Cargo in Patients with Fabry Nephropathy." Genes (Basel) **12**(7).

Levstek, T., B. Vujkovac and K. Trebusak Podkrajsek (2020). "Biomarkers of Fabry Nephropathy: Review and Future Perspective." Genes (Basel) **11**(9).

Li, C., X. F. Tan, T. K. Lim, Q. Lin and Z. Gong (2016). "Comprehensive and quantitative proteomic analyses of zebrafish plasma reveals conserved protein profiles between genders and between zebrafish and human." Sci Rep **6**: 24329.

Li, H., W. Pei, S. Vergarajauregui, P. M. Zerfas, N. Raben, S. M. Burgess and R. Puertollano (2017). "Novel degenerative and developmental defects in a zebrafish model of mucolipidosis type IV." Hum Mol Genet **26**(14): 2701-2718.

Li, Y. H., H. Y. Chen, Y. W. Li, S. Y. Wu, L. Wangta, G. H. Lin, S. Y. Hu, Z. K. Chang, H. Y. Gong, C. H. Liao, K. Y. Chiang, C. W. Huang and J. L. Wu (2013). "Progranulin regulates zebrafish muscle growth and regeneration through maintaining the pool of myogenic progenitor cells." Sci Rep **3**: 1176.

Li, Y. H., M. H. Chen, H. Y. Gong, S. Y. Hu, Y. W. Li, G. H. Lin, C. C. Lin, W. Liu and J. L. Wu (2010). "Progranulin A-mediated MET signaling is essential for liver morphogenesis in zebrafish." J Biol Chem **285**(52): 41001-41009.

Liebau, M. C., F. Braun, K. Hopker, C. Weitbrecht, V. Bartels, R. U. Muller, S. Brodesser, M. A. Saleem, T. Benzing, B. Schermer, M. Cybulla and C. E. Kurschat (2013). "Dysregulated autophagy contributes to podocyte damage in Fabry's disease." PLoS One **8**(5): e63506.

Lieschke, G. J. and P. D. Currie (2007). "Animal models of human disease: zebrafish swim into view." Nat Rev Genet **8**(5): 353-367.

Lin, Y., X. Cai, G. Wang, G. Ouyang and H. Cao (2018). "Model construction of Niemann-Pick type C disease in zebrafish." Biol Chem **399**(8): 903-910.

Lin, Y. J., C. N. Hsu, M. H. Lo, C. F. Huang, S. J. Chien and Y. L. Tain (2013). "High citrulline-to-arginine ratio associated with blood pressure abnormalities in children with early chronic kidney disease." Circ J **77**(1): 181-187.

Lindahl, J. P., F. P. Reinholt, I. A. Eide, A. Hartmann, K. Midtvedt, H. Holdaas, L. T. Dorg, T. M. Reine, S. O. Kolset, R. Horneland, O. Oyen, K. Brabrand and T. Jenssen (2014). "In patients with type 1 diabetes simultaneous pancreas and kidney transplantation preserves long-term kidney graft ultrastructure and function better than transplantation of kidney alone." Diabetologia **57**(11): 2357-2365.

Lino, C. A., J. C. Harper, J. P. Carney and J. A. Timlin (2018). "Delivering CRISPR: a review of the challenges and approaches." Drug Deliv **25**(1): 1234-1257.

Liu, H. C., H. Y. Lin, C. F. Yang, H. C. Liao, T. R. Hsu, C. W. Lo, F. P. Chang, C. K. Huang, Y. H. Lu, S. P. Lin, W. C. Yu and D. M. Niu (2014). "Globotriaosylsphingosine (lyso-Gb3) might not be a reliable marker for monitoring the long-term therapeutic outcomes of enzyme replacement therapy for late-onset Fabry patients with the Chinese hotspot mutation (IVS4+919G>A)." Orphanet J Rare Dis **9**: 111.

Liu, W. J., T. T. Shen, R. H. Chen, H. L. Wu, Y. J. Wang, J. K. Deng, Q. H. Chen, Q. Pan, C. M. Huang Fu, J. L. Tao, D. Liang and H. F. Liu (2015). "Autophagy-Lysosome Pathway in Renal Tubular Epithelial Cells Is Disrupted by Advanced Glycation End Products in Diabetic Nephropathy." J Biol Chem **290**(33): 20499-20510.

Lopes da Fonseca, T., A. Correia, W. Hasselaar, H. C. van der Linde, R. Willemsen and T. F. Outeiro (2013). "The zebrafish homologue of Parkinson's disease ATP13A2 is essential for embryonic survival." Brain Res Bull **90**: 118-126.

Loso, J., N. Lund, M. Avanesov, N. Muschol, S. Lezius, K. Cordts, E. Schwedhelm and M. Patten (2018). "Serum Biomarkers of Endothelial Dysfunction in Fabry Associated Cardiomyopathy." Front Cardiovasc Med **5**: 108.

Louwette, S., L. Regal, C. Wittevrongel, C. Thys, G. Vandeweeghde, E. Decuyper, P. Leemans, R. De Vos, C. Van Geet, J. Jaeken and K. Freson (2013). "NPC1 defect results in abnormal platelet formation and function: studies in Niemann-Pick disease type C1 patients and zebrafish." Hum Mol Genet **22**(1): 61-73.

Love, M. I., W. Huber and S. Anders (2014). "Moderated estimation of fold change and dispersion for RNA-seq data with DESeq2." Genome Biol **15**(12): 550.

Maas, M. N., J. C. J. Hintzen, M. R. B. Porzberg and J. Mecinovic (2020). "Trimethyllysine: From Carnitine Biosynthesis to Epigenetics." Int J Mol Sci **21**(24).

Maestroni, S., A. Maestroni, G. Dell'Antonio, D. Gabellini, S. Terzi, A. Spinello, G. Meregalli, G. Castoldi and G. Zerbini (2014). "Viable podocyturia in healthy individuals: implications for podocytopathies." Am J Kidney Dis **64**(6): 1003-1005.

Mahmood, F., S. Fu, J. Cooke, S. W. Wilson, J. D. Cooper and C. Russell (2013). "A zebrafish model of CLN2 disease is deficient in tripeptidyl peptidase 1 and displays progressive neurodegeneration accompanied by a reduction in proliferation." Brain **136**(Pt 5): 1488-1507.

Man, S. M. and T. D. Kanneganti (2016). "Regulation of lysosomal dynamics and autophagy by CTSB/cathepsin B." Autophagy **12**(12): 2504-2505.

Marchi, S., M. Bonora, S. Patergnani, C. Giorgi and P. Pinton (2017). "Methods to Assess Mitochondrial Morphology in Mammalian Cells Mounting Autophagic or Mitophagic Responses." Methods Enzymol **588**: 171-186.

Marraffini, L. A. (2015). "CRISPR-Cas immunity in prokaryotes." Nature **526**(7571): 55-61.

Maruyama, H., A. Taguchi, Y. Nishikawa, C. Guili, M. Mikame, M. Nameta, Y. Yamaguchi, M. Ueno, N. Imai, Y. Ito, T. Nakagawa, I. Narita and S. Ishii (2018). "Medullary thick ascending limb impairment in the Gla(tm)Tg(CAG-A4GALT) Fabry model mice." FASEB J **32**(8): 4544-4559.

Matafora, V., M. Cuccurullo, A. Beneduci, O. Petrazzuolo, A. Simeone, P. Anastasio, R. Mignani, S. Feriozzi, A. Pisani, C. Comotti, A. Bachi and G. Capasso (2015). "Early markers of Fabry disease revealed by proteomics." Mol Biosyst **11**(6): 1543-1551.

Mauer, M., A. Sokolovskiy, J. A. Barth, J. P. Castelli, H. N. Williams, E. R. Benjamin and B. Najafian (2017). "Reduction of podocyte globotriaosylceramide content in adult male patients with Fabry disease with amenable GLA mutations following 6 months of migalastat treatment." J Med Genet **54**(11): 781-786.

Mauhin, W., O. Lidove, E. Masat, F. Mingozzi, K. Mariampillai, J. M. Ziza and O. Benveniste (2015). "Innate and Adaptive Immune Response in Fabry Disease." JIMD Rep **22**: 1-10.

Mayes, J. S., J. B. Scheerer, R. N. Sifers and M. L. Donaldson (1981). "Differential assay for lysosomal alpha-galactosidases in human tissues and its application to Fabry's disease." Clin Chim Acta **112**(2): 247-251.

McCafferty, E. H. and L. J. Scott (2019). "Migalastat: A Review in Fabry Disease." Drugs **79**(5): 543-554.

Mehta, A., M. Beck, P. Elliott, R. Giugliani, A. Linhart, G. Sunder-Plassmann, R. Schiffmann, F. Barbey, M. Ries, J. T. Clarke and i. Fabry Outcome Survey (2009). "Enzyme replacement therapy with agalsidase alfa in patients with Fabry's disease: an analysis of registry data." Lancet **374**(9706): 1986-1996.

Meng, X. M., D. J. Nikolic-Paterson and H. Y. Lan (2014). "Inflammatory processes in renal fibrosis." Nat Rev Nephrol **10**(9): 493-503.

Meyers, J. R. (2018). "Zebrafish: Development of a Vertebrate Model Organism." Current Protocols Essential Laboratory Techniques **16**(1): e19.

Midttun, O., G. Kvalheim and P. M. Ueland (2013). "High-throughput, low-volume, multianalyte quantification of plasma metabolites related to one-carbon metabolism using HPLC-MS/MS." Anal Bioanal Chem **405**(6): 2009-2017.

Miller, J. J., K. Aoki, C. A. Reid, M. Tiemeyer, N. M. Dahms and I. S. Kassem (2019). "Rats deficient in alpha-galactosidase A develop ocular manifestations of Fabry disease." Sci Rep **9**(1): 9392.

Miller, J. J., A. J. Kanack and N. M. Dahms (2020). "Progress in the understanding and treatment of Fabry disease." Biochim Biophys Acta Gen Subj **1864**(1): 129437.

Mizunoe, Y., M. Kobayashi, R. Tagawa, Y. Nakagawa, H. Shimano and Y. Higami (2019). "Association between Lysosomal Dysfunction and Obesity-Related Pathology: A Key Knowledge to Prevent Metabolic Syndrome." Int J Mol Sci **20**(15).

Modrego, A., M. Amaranto, A. Godino, R. Mendoza, J. L. Barra and J. L. Corchero (2021). "Human alpha-Galactosidase A Mutants: Priceless Tools to Develop Novel Therapies for Fabry Disease." Int J Mol Sci **22**(12).

Monserrat, L., J. R. Gimeno-Blanes, F. Marin, M. Hermida-Prieto, A. Garcia-Honrubia, I. Perez, X. Fernandez, R. de Nicolas, G. de la Morena, E. Paya, J. Yague and J. Egido (2007). "Prevalence of fabry disease in a cohort of 508 unrelated patients with hypertrophic cardiomyopathy." J Am Coll Cardiol **50**(25): 2399-2403.

Moro, E., R. Tomanin, A. Friso, N. Modena, N. Tiso, M. Scarpa and F. Argenton (2010). "A novel functional role of iduronate-2-sulfatase in zebrafish early development." Matrix Biol **29**(1): 43-50.

Moura, A. P., T. Hammerschmidt, M. Deon, R. Giugliani and C. R. Vargas (2018). "Investigation of correlation of urinary globotriaosylceramide (Gb3) levels with markers of renal function in patients with Fabry disease." Clin Chim Acta **478**: 62-67.

Muller-Deile, J. and M. Schiffer (2016). "Podocyte directed therapy of nephrotic syndrome-can we bring the inside out?" Pediatr Nephrol **31**(3): 393-405.

Muto, R., Y. Suzuki, H. Shimizu, K. Yasuda, T. Ishimoto, S. Maruyama, Y. Ito and M. Mizuno (2022). "Recurrent Cerebrovascular Complications under Enzyme Replacement Therapy in a Patient with Fabry Disease on Peritoneal Dialysis." Intern Med.

Nagao, S., N. Satoh, S. Inaba and S. Iijima (1985). "Concentric lamellar spheres in urine from a female carrier of and patients with Fabry's disease--with special reference to polarization and electron microscopic comparison with nephrotic syndrome." J Dermatol **12**(1): 70-78.

Najafian, B., E. Svarstad, L. Bostad, M. C. Gubler, C. Tondel, C. Whitley and M. Mauer (2011). "Progressive podocyte injury and globotriaosylceramide (GL-3) accumulation in young patients with Fabry disease." Kidney Int **79**(6): 663-670.

Najafian, B., C. Tondel, E. Svarstad, M. C. Gubler, J. P. Oliveira and M. Mauer (2020). "Accumulation of Globotriaosylceramide in Podocytes in Fabry Nephropathy Is Associated with Progressive Podocyte Loss." J Am Soc Nephrol **31**(4): 865-875.

Nakagawa, T., H. Y. Lan, H. J. Zhu, D. H. Kang, G. F. Schreiner and R. J. Johnson (2004). "Differential regulation of VEGF by TGF-beta and hypoxia in rat proximal tubular cells." Am J Physiol Renal Physiol **287**(4): F658-664.

Nishibori, Y., K. Katayama, M. Parikka, A. Oddsson, M. Nukui, K. Hultenby, A. Wernerson, B. He, L. Ebarasi, E. Raschperger, J. Norlin, M. Uhlen, J. Patrakka, C. Betsholtz and K. Tryggvason (2011). "Glcci1 deficiency leads to proteinuria." J Am Soc Nephrol **22**(11): 2037-2046.

Nowak, A., F. Beuschlein, V. Sivasubramaniam, D. Kasper and D. G. Warnock (2022). "Lyso-Gb3 associates with adverse long-term outcome in patients with Fabry disease." J Med Genet **59**(3): 287-293.

Nowak, A., T. P. Mechtler, R. J. Desnick and D. C. Kasper (2017). "Plasma LysoGb3: A useful biomarker for the diagnosis and treatment of Fabry disease heterozygotes." Mol Genet Metab **120**(1-2): 57-61.

Ohshima, T., G. J. Murray, W. D. Swaim, G. Longenecker, J. M. Quirk, C. O. Cardarelli, Y. Sugimoto, I. Pastan, M. M. Gottesman, R. O. Brady and A. B. Kulkarni (1997). "alpha-Galactosidase A deficient mice: a model of Fabry disease." Proc Natl Acad Sci U S A **94**(6): 2540-2544.

Ortiz, A., D. P. Germain, R. J. Desnick, J. Politei, M. Mauer, A. Burlina, C. Eng, R. J. Hopkin, D. Laney, A. Linhart, S. Waldek, E. Wallace, F. Weidemann and W. R. Wilcox (2018). "Fabry disease revisited: Management and treatment recommendations for adult patients." Mol Genet Metab **123**(4): 416-427.

Ortiz, A., J. P. Oliveira, S. Waldek, D. G. Warnock, B. Cianciaruso, C. Wanner and R. Fabry (2008). "Nephropathy in males and females with Fabry disease: cross-sectional description of patients before treatment with enzyme replacement therapy." Nephrol Dial Transplant **23**(5): 1600-1607.

Ortiz, A., J. P. Oliveira, C. Wanner, B. M. Brenner, S. Waldek and D. G. Warnock (2008). "Recommendations and guidelines for the diagnosis and treatment of Fabry nephropathy in adults." Nat Clin Pract Nephrol **4**(6): 327-336.

Ortiz, A. and M. D. Sanchez-Nino (2018). "Enzyme replacement therapy dose and Fabry nephropathy." Nephrol Dial Transplant **33**(8): 1284-1289.

Outtandy, P., C. Russell, R. Kleta and D. Bockenhauer (2019). "Zebrafish as a model for kidney function and disease." Pediatr Nephrol **34**(5): 751-762.

Pan, X., Y. Ouyang, Z. Wang, H. Ren, P. Shen, W. Wang, Y. Xu, L. Ni, X. Yu, X. Chen, W. Zhang, L. Yang, X. Li, J. Xu and N. Chen (2016). "Genotype: A Crucial but Not Unique Factor Affecting the Clinical Phenotypes in Fabry Disease." PLoS One **11**(8): e0161330.

Parenti, G., D. L. Medina and A. Ballabio (2021). "The rapidly evolving view of lysosomal storage diseases." EMBO Mol Med **13**(2): e12836.

Park, E. S., J. O. Choi, J. W. Park, M. H. Lee, H. Y. Park and S. C. Jung (2009). "Expression of genes and their responses to enzyme replacement therapy in a Fabry disease mouse model." Int J Mol Med **24**(3): 401-407.

Paschke, E., G. Fauler, H. Winkler, A. Schlagenhauf, B. Plecko, W. Erwa, F. Breunig, W. Urban, B. Vujkovac, G. Sunder-Plassmann and P. Kotanko (2011). "Urinary total globotriaosylceramide and isoforms to identify women with Fabry disease: a diagnostic test study." Am J Kidney Dis **57**(5): 673-681.

Pattanayak, V., S. Lin, J. P. Guilinger, E. Ma, J. A. Doudna and D. R. Liu (2013). "High-throughput profiling of off-target DNA cleavage reveals RNA-programmed Cas9 nuclease specificity." Nat Biotechnol **31**(9): 839-843.

Pearce, E. L. and E. J. Pearce (2013). "Metabolic pathways in immune cell activation and quiescence." Immunity **38**(4): 633-643.

Pereira, E. M., A. Labilloy, M. L. Eshbach, A. Roy, A. R. Subramanya, S. Monte, G. Labilloy and O. A. Weisz (2016). "Characterization and phosphoproteomic analysis of a human immortalized podocyte model of Fabry disease generated using CRISPR/Cas9 technology." Am J Physiol Renal Physiol **311**(5): F1015-F1024.

Peterschmitt, M. J., N. P. S. Crawford, S. J. M. Gaemers, A. J. Ji, J. Sharma and T. T. Pham (2021). "Pharmacokinetics, Pharmacodynamics, Safety, and Tolerability of Oral Venglustat in Healthy Volunteers." Clin Pharmacol Drug Dev **10**(1): 86-98.

Petrey, A. C., H. Flanagan-Steet, S. Johnson, X. Fan, M. De la Rosa, M. E. Haskins, A. V. Nairn, K. W. Moremen and R. Steet (2012). "Excessive activity of cathepsin K is associated with cartilage defects in a zebrafish model of mucolipidosis II." Dis Model Mech **5**(2): 177-190.

Phillips, J. B. and M. Westerfield (2020). Chapter 47 - Zebrafish as a Model to Understand Human Genetic Diseases. The Zebrafish in Biomedical Research. S. C. Cartner, J. S. Eisen, S. C. Farmer et al., Academic Press**:** 619-626.

Picard, M., K. White and D. M. Turnbull (2013). "Mitochondrial morphology, topology, and membrane interactions in skeletal muscle: a quantitative three-dimensional electron microscopy study." J Appl Physiol (1985) **114**(2): 161-171.

Platt, F. M., B. Boland and A. C. van der Spoel (2012). "The cell biology of disease: lysosomal storage disorders: the cellular impact of lysosomal dysfunction." J Cell Biol **199**(5): 723-734.

Platt, F. M., A. d'Azzo, B. L. Davidson, E. F. Neufeld and C. J. Tifft (2018). "Lysosomal storage diseases." Nat Rev Dis Primers **4**(1): 27.

Pohlers, D., J. Brenmoehl, I. Loffler, C. K. Muller, C. Leipner, S. Schultze-Mosgau, A. Stallmach, R. W. Kinne and G. Wolf (2009). "TGF-beta and fibrosis in different organs - molecular pathway imprints." Biochim Biophys Acta **1792**(8): 746-756.

Pollman, M. J., L. Naumovski and G. H. Gibbons (1999). "Vascular cell apoptosis: cell type-specific modulation by transforming growth factor-beta1 in endothelial cells versus smooth muscle cells." Circulation **99**(15): 2019-2026.

Polo, G., A. P. Burlina, T. B. Kolamunnage, M. Zampieri, C. Dionisi-Vici, P. Strisciuglio, M. Zaninotto, M. Plebani and A. B. Burlina (2017). "Diagnosis of sphingolipidoses: a new simultaneous measurement of lysosphingolipids by LC-MS/MS." Clin Chem Lab Med **55**(3): 403-414.

Popli, S., D. J. Leehey, Z. V. Molnar, Z. M. Nawab and T. S. Ing (1990). "Demonstration of Fabry's disease deposits in placenta." Am J Obstet Gynecol **162**(2): 464-465.

Prabakaran, T., H. Birn, B. M. Bibby, A. Regeniter, S. S. Sorensen, U. Feldt-Rasmussen, R. Nielsen and E. I. Christensen (2014). "Long-term enzyme replacement therapy is associated with reduced proteinuria and preserved proximal tubular function in women with Fabry disease." Nephrol Dial Transplant **29**(3): 619-625.

Prabakaran, T., R. Nielsen, S. C. Satchell, P. W. Mathieson, U. Feldt-Rasmussen, S. S. Sorensen and E. I. Christensen (2012). "Mannose 6-phosphate receptor and sortilin mediated endocytosis of alpha-galactosidase A in kidney endothelial cells." PLoS One **7**(6): e39975.

Qian, Y., E. van Meel, H. Flanagan-Steet, A. Yox, R. Steet and S. Kornfeld (2015). "Analysis of mucolipidosis II/III GNPTAB missense mutations identifies domains of UDP-GlcNAc:lysosomal enzyme GlcNAc-1-phosphotransferase involved in catalytic function and lysosomal enzyme recognition." J Biol Chem **290**(5): 3045-3056.

Ramaswami, U., B. Najafian, A. Schieppati, M. Mauer and D. G. Bichet (2010). "Assessment of renal pathology and dysfunction in children with Fabry disease." Clin J Am Soc Nephrol **5**(2): 365-370.

Reboun, M., J. Sikora, M. Magner, H. Wiederlechnerova, A. Cerna, H. Poupetova, G. Storkanova, D. Musalkova, G. Dostalova, L. Golan, A. Linhart and L. Dvorakova (2022). "Pitfalls of X-chromosome inactivation testing in females with Fabry disease." Am J Med Genet A **188**(7): 1979-1989.

Reisin, R., A. Perrin and P. Garcia-Pavia (2017). "Time delays in the diagnosis and treatment of Fabry disease." Int J Clin Pract **71**(1).

Reynolds, T. M., K. L. Tylee, K. L. Booth, A. S. Wierzbicki and P. P. C. group (2021). "Identification of patients with Fabry disease using routine pathology results: PATHFINDER (eGFR) study." Int J Clin Pract **75**(2): e13672.

Riccio, E., M. Sabbatini, D. Bruzzese, L. Annicchiarico Petruzzelli, A. Pellegrino, L. Spinelli, R. Esposito, M. Imbriaco, S. Feriozzi, A. Pisani and A. G. on behalf of (2019). "Glomerular Hyperfiltration: An Early Marker of Nephropathy in Fabry Disease." Nephron **141**(1): 10-17.

Rider, S. A., F. A. Bruton, R. G. Collins, B. R. Conway and J. J. Mullins (2018). "The Efficacy of Puromycin and Adriamycin for Induction of Glomerular Failure in Larval Zebrafish Validated by an Assay of Glomerular Permeability Dynamics." Zebrafish **15**(3): 234-242.

Rombach, S. M., T. B. Twickler, J. M. Aerts, G. E. Linthorst, F. A. Wijburg and C. E. Hollak (2010). "Vasculopathy in patients with Fabry disease: current controversies and research directions." Mol Genet Metab **99**(2): 99-108.

Rossanti, R., K. Nozu, A. Fukunaga, C. Nagano, T. Horinouchi, T. Yamamura, N. Sakakibara, S. Minamikawa, S. Ishiko, Y. Aoto, E. Okada, T. Ninchoji, N. Kato, S. Maruyama, K. Kono, S. Nishi, K. Iijima and H. Fujii (2021). "X-chromosome inactivation patterns in females with Fabry disease examined by both ultra-deep RNA sequencing and methylation-dependent assay." Clin Exp Nephrol **25**(11): 1224-1230.

Roy, A., D. Xu, J. Poisson and Y. Zhang (2011). "A protocol for computer-based protein structure and function prediction." J Vis Exp(57): e3259.

Rozenfeld, P. A., M. de Los Angeles Bolla, P. Quieto, A. Pisani, S. Feriozzi, P. Neuman and C. Bondar (2020). "Pathogenesis of Fabry nephropathy: The pathways leading to fibrosis." Mol Genet Metab **129**(2): 132-141.

Ruderfer, I., A. Shulman, T. Kizhner, Y. Azulay, Y. Nataf, Y. Tekoah and Y. Shaaltiel (2018). "Development and Analytical Characterization of Pegunigalsidase Alfa, a Chemically Cross-Linked Plant Recombinant Human alpha-Galactosidase-A for Treatment of Fabry Disease." Bioconjug Chem **29**(5): 1630-1639.

Sachs, N. and A. Sonnenberg (2013). "Cell-matrix adhesion of podocytes in physiology and disease." Nat Rev Nephrol **9**(4): 200-210.

Sakuraba, H., M. Murata-Ohsawa, I. Kawashima, Y. Tajima, M. Kotani, T. Ohshima, Y. Chiba, M. Takashiba, Y. Jigami, T. Fukushige, T. Kanzaki and K. Itoh (2006). "Comparison of the effects of agalsidase alfa and agalsidase beta on cultured human Fabry fibroblasts and Fabry mice." J Hum Genet **51**(3): 180-188.

Sakuraba, H., T. Togawa, T. Tsukimura and H. Kato (2018). "Plasma lyso-Gb3: a biomarker for monitoring fabry patients during enzyme replacement therapy." Clin Exp Nephrol **22**(4): 843-849.

Sakuraba, H., T. Tsukimura, T. Togawa, T. Tanaka, T. Ohtsuka, A. Sato, T. Shiga, S. Saito and K. Ohno (2018). "Fabry disease in a Japanese population-molecular and biochemical characteristics." Mol Genet Metab Rep **17**: 73-79.

Salvi, S., E. Bandini, S. Carloni, V. Casadio, M. Battistelli, S. Salucci, I. Erani, E. Scarpi, R. Gunelli, G. Cicchetti, M. Guescini, M. Bonafe and F. Fabbri (2021). "Detection and Investigation of Extracellular Vesicles in Serum and Urine Supernatant of Prostate Cancer Patients." Diagnostics (Basel) **11**(3).

Samanta, R., C. Chan and V. S. Chauhan (2019). "Arrhythmias and Sudden Cardiac Death in End Stage Renal Disease: Epidemiology, Risk Factors, and Management." Can J Cardiol **35**(9): 1228-1240.

Sanchez-Nino, M. D., D. Carpio, A. B. Sanz, M. Ruiz-Ortega, S. Mezzano and A. Ortiz (2015). "Lyso-Gb3 activates Notch1 in human podocytes." Hum Mol Genet **24**(20): 5720-5732.

Sanchez-Nino, M. D., A. B. Sanz, S. Carrasco, M. A. Saleem, P. W. Mathieson, J. M. Valdivielso, M. Ruiz-Ortega, J. Egido and A. Ortiz (2011). "Globotriaosylsphingosine actions on human glomerular podocytes: implications for Fabry nephropathy." Nephrol Dial Transplant **26**(6): 1797-1802.

Sands, M. S. and B. L. Davidson (2006). "Gene therapy for lysosomal storage diseases." Mol Ther **13**(5): 839-849.

Schiffmann, R., D. G. Bichet, J. M. Aerts, N. Skuban and A. B. Mehta (2020). "Lyso−Gb3 is not a predictive biomarker of treatment response in migalastat-treated patients with migalastat-amenable variants." Molecular Genetics and Metabolism **129**(2): S144.

Schiffmann, R., M. Fuller, L. A. Clarke and J. M. Aerts (2016). "Is it Fabry disease?" Genet Med **18**(12): 1181-1185.

Schiffmann, R., O. Goker-Alpan, M. Holida, P. Giraldo, L. Barisoni, R. B. Colvin, C. J. Jennette, G. Maegawa, S. A. Boyadjiev, D. Gonzalez, K. Nicholls, A. Tuffaha, M. G. Atta, B. Rup, M. R. Charney, A. Paz, M. Szlaifer, S. Alon, E. Brill-Almon, R. Chertkoff and D. Hughes (2019). "Pegunigalsidase alfa, a novel PEGylated enzyme replacement therapy for Fabry disease, provides sustained plasma concentrations and favorable pharmacodynamics: A 1-year Phase 1/2 clinical trial." J Inherit Metab Dis **42**(3): 534-544.

Schiffmann, R., S. Waldek, A. Benigni and C. Auray-Blais (2010). "Biomarkers of Fabry disease nephropathy." Clin J Am Soc Nephrol **5**(2): 360-364.

Schiffmann, R., D. G. Warnock, M. Banikazemi, J. Bultas, G. E. Linthorst, S. Packman, S. A. Sorensen, W. R. Wilcox and R. J. Desnick (2009). "Fabry disease: progression of nephropathy, and prevalence of cardiac and cerebrovascular events before enzyme replacement therapy." Nephrol Dial Transplant **24**(7): 2102-2111.

Schindelin, J., I. Arganda-Carreras, E. Frise, V. Kaynig, M. Longair, T. Pietzsch, S. Preibisch, C. Rueden, S. Saalfeld, B. Schmid, J. Y. Tinevez, D. J. White, V. Hartenstein, K. Eliceiri, P. Tomancak and A. Cardona (2012). "Fiji: an open-source platform for biological-image analysis." Nat Methods **9**(7): 676-682.

Schneider, C. A., W. S. Rasband and K. W. Eliceiri (2012). "NIH Image to ImageJ: 25 years of image analysis." Nat Methods **9**(7): 671-675.

Schroder, J., R. Lullmann-Rauch, N. Himmerkus, I. Pleines, B. Nieswandt, Z. Orinska, F. Koch-Nolte, B. Schroder, M. Bleich and P. Saftig (2009). "Deficiency of the tetraspanin CD63 associated with kidney pathology but normal lysosomal function." Mol Cell Biol **29**(4): 1083-1094.

Schumann, A., K. Schaller, V. Belche, M. Cybulla, S. C. Grunert, N. Moers, J. O. Sass, A. Kaech, L. Hannibal and U. Spiekerkoetter (2021). "Defective lysosomal storage in Fabry disease modifies mitochondrial structure, metabolism and turnover in renal epithelial cells." J Inherit Metab Dis **44**(4): 1039-1050.

Schwartz, G. J., A. Munoz, M. F. Schneider, R. H. Mak, F. Kaskel, B. A. Warady and S. L. Furth (2009). "New equations to estimate GFR in children with CKD." J Am Soc Nephrol **20**(3): 629-637.

Schwend, T., E. J. Loucks, D. Snyder and S. C. Ahlgren (2011). "Requirement of Npc1 and availability of cholesterol for early embryonic cell movements in zebrafish." J Lipid Res **52**(7): 1328-1344.

Selvarajah, M., K. Nicholls, T. D. Hewitson and G. J. Becker (2011). "Targeted urine microscopy in Anderson-Fabry disease: a cheap, sensitive and specific diagnostic technique." Nephrol Dial Transplant **26**(10): 3195-3202.

Sessa, A., M. Meroni, G. Battini, M. Righetti, A. Maglio, A. Tosoni, M. Nebuloni, G. Vago and F. Giordano (2003). "Renal involvement in Anderson-Fabry disease." J Nephrol **16**(2): 310-313.

Sharma, S. and S. M. Black (2009). "Carnitine Homeostasis, Mitochondrial Function, and Cardiovascular Disease." Drug Discov Today Dis Mech **6**(1-4): e31-e39.

Shen, J. S., A. Busch, T. S. Day, X. L. Meng, C. I. Yu, P. Dabrowska-Schlepp, B. Fode, H. Niederkruger, S. Forni, S. Chen, R. Schiffmann, T. Frischmuth and A. Schaaf (2016). "Mannose receptor-mediated delivery of moss-made alpha-galactosidase A efficiently corrects enzyme deficiency in Fabry mice." J Inherit Metab Dis **39**(2): 293-303.

Shen, J. S., X. L. Meng, D. F. Moore, J. M. Quirk, J. A. Shayman, R. Schiffmann and C. R. Kaneski (2008). "Globotriaosylceramide induces oxidative stress and up-regulates cell adhesion molecule expression in Fabry disease endothelial cells." Mol Genet Metab **95**(3): 163-168.

Shiga, T., T. Tsukimura, Y. Namai, T. Togawa and H. Sakuraba (2021). "Comparative urinary globotriaosylceramide analysis by thin-layer chromatography-immunostaining and liquid chromatography-tandem mass spectrometry in patients with Fabry disease." Mol Genet Metab Rep **29**: 100804.

Shin, Y. J., Y. J. Jeon, N. Jung, J. W. Park, H. Y. Park and S. C. Jung (2015). "Substrate-specific gene expression profiles in different kidney cell types are associated with Fabry disease." Mol Med Rep **12**(4): 5049-5057.

Shiozuka, C., A. Taguchi, J. Matsuda, Y. Noguchi, T. Kunieda, K. Uchio-Yamada, H. Yoshioka, R. Hamanaka, S. Yano, S. Yokoyama, K. Mannen, A. B. Kulkarni, K. Furukawa and S. Ishii (2011). "Increased globotriaosylceramide levels in a transgenic mouse expressing human alpha1,4-galactosyltransferase and a mouse model for treating Fabry disease." J Biochem **149**(2): 161-170.

Shu, L., A. Vivekanandan-Giri, S. Pennathur, B. E. Smid, J. M. Aerts, C. E. Hollak and J. A. Shayman (2014). "Establishing 3-nitrotyrosine as a biomarker for the vasculopathy of Fabry disease." Kidney Int **86**(1): 58-66.

Silva, C. A. B., J. A. Moura-Neto, M. A. Dos Reis, O. M. Vieira Neto and F. C. Barreto (2021). "Renal Manifestations of Fabry Disease: A Narrative Review." Can J Kidney Health Dis **8**: 2054358120985627.

Simoncini, C., S. Torri, V. Montano, L. Chico, F. Gruosso, A. Tuttolomondo, A. Pinto, I. Simonetta, V. Cianci, A. Salviati, V. Vicenzi, G. Marchi, D. Girelli, D. Concolino, S. Sestito, M. Zedde, G. Siciliano and M. Mancuso (2020). "Oxidative stress biomarkers in Fabry disease: is there a room for them?" J Neurol **267**(12): 3741-3752.

Skrunes, R., C. Tondel, S. Leh, K. K. Larsen, G. Houge, E. S. Davidsen, C. Hollak, A. B. P. van Kuilenburg, F. M. Vaz and E. Svarstad (2017). "Long-Term Dose-Dependent Agalsidase Effects on Kidney Histology in Fabry Disease." Clin J Am Soc Nephrol **12**(9): 1470-1479.

Slaats, G. G., F. Braun, M. Hoehne, L. E. Frech, L. Blomberg, T. Benzing, B. Schermer, M. M. Rinschen and C. E. Kurschat (2018). "Urine-derived cells: a promising diagnostic tool in Fabry disease patients." Sci Rep **8**(1): 11042.

Smith, R. N., A. S. Agharkar and E. B. Gonzales (2014). "A review of creatine supplementation in age-related diseases: more than a supplement for athletes." F1000Res **3**: 222.

Song, H. Y., C. S. Chien, A. A. Yarmishyn, S. J. Chou, Y. P. Yang, M. L. Wang, C. Y. Wang, H. B. Leu, W. C. Yu, Y. L. Chang and S. H. Chiou (2019). "Generation of GLA-Knockout Human Embryonic Stem Cell Lines to Model Autophagic Dysfunction and Exosome Secretion in Fabry Disease-Associated Hypertrophic Cardiomyopathy." Cells **8**(4).

Spataro, R., M. Kousi, S. M. K. Farhan, J. R. Willer, J. P. Ross, P. A. Dion, G. A. Rouleau, M. J. Daly, B. M. Neale, V. La Bella and N. Katsanis (2019). "Mutations in ATP13A2 (PARK9) are associated with an amyotrophic lateral sclerosis-like phenotype, implicating this locus in further phenotypic expansion." Hum Genomics **13**(1): 19.

Speak, A. O., M. Salio, D. C. Neville, J. Fontaine, D. A. Priestman, N. Platt, T. Heare, T. D. Butters, R. A. Dwek, F. Trottein, M. A. Exley, V. Cerundolo and F. M. Platt (2007). "Implications for invariant natural killer T cell ligands due to the restricted presence of isoglobotrihexosylceramide in mammals." Proc Natl Acad Sci U S A **104**(14): 5971-5976.

Stadtman, E. R., H. Van Remmen, A. Richardson, N. B. Wehr and R. L. Levine (2005). "Methionine oxidation and aging." Biochim Biophys Acta **1703**(2): 135-140.

Stemple, D. L., L. Solnica-Krezel, F. Zwartkruis, S. C. Neuhauss, A. F. Schier, J. Malicki, D. Y. Stainier, S. Abdelilah, Z. Rangini, E. Mountcastle-Shah and W. Driever (1996). "Mutations affecting development of the notochord in zebrafish." Development **123**: 117-128.

Strauss, P., Ø. Eikrem, C. Tøndel, E. Svarstad, A. Scherer, S. Leh, A. Flatberg, N. Delaleu, E. Koch, V. Beisvag, L. Landolt and H. P. Marti (2019). Fabry Nephropathy: First mRNA-Seq Findings from Kidney Biopsies Before and After Enzyme Replacement Therapy (Abstract, 6th Update on Fabry Disease: Biomarkers, Progression and Treatment Opportunities). Nephron. 2019;142(3):169.

Sutariya, B., D. Jhonsa and M. N. Saraf (2016). "TGF-beta: the connecting link between nephropathy and fibrosis." Immunopharmacol Immunotoxicol **38**(1): 39-49.

Svara, T., M. Pogacnik and P. Juntes (2010). "Distribution and amount of cathepsin B in gentamicin-induced acute kidney injury in rats." Pol J Vet Sci **13**(1): 75-82.

Svarstad, E., B. M. Iversen and L. Bostad (2004). "Bedside stereomicroscopy of renal biopsies may lead to a rapid diagnosis of Fabry's disease." Nephrol Dial Transplant **19**(12): 3202-3203.

Svarstad, E., S. Leh, R. Skrunes, K. Kampevold Larsen, O. Eikrem and C. Tondel (2018). "Bedside Stereomicroscopy of Fabry Kidney Biopsies: An Easily Available Method for Diagnosis and Assessment of Sphingolipid Deposits." Nephron **138**(1): 13-21.

Svarstad, E. and H. P. Marti (2020). "The Changing Landscape of Fabry Disease." Clin J Am Soc Nephrol **15**(4): 569-576.

Svennerholm, L., G. Hakansson, J. E. Mansson and M. T. Vanier (1979). "The assay of sphingolipid hydrolases in white blood cells with labelled natural substrates." Clin Chim Acta **92**(1): 53-64.

Taguchi, A., H. Maruyama, M. Nameta, T. Yamamoto, J. Matsuda, A. B. Kulkarni, H. Yoshioka and S. Ishii (2013). "A symptomatic Fabry disease mouse model generated by inducing globotriaosylceramide synthesis." Biochem J **456**(3): 373-383.

Tang, D., X. Chen, R. Kang and G. Kroemer (2021). "Ferroptosis: molecular mechanisms and health implications." Cell Res **31**(2): 107-125.

Tang, W. H., Z. Wang, D. J. Kennedy, Y. Wu, J. A. Buffa, B. Agatisa-Boyle, X. S. Li, B. S. Levison and S. L. Hazen (2015). "Gut microbiota-dependent trimethylamine N-oxide (TMAO) pathway contributes to both development of renal insufficiency and mortality risk in chronic kidney disease." Circ Res **116**(3): 448-455.

Tebani, A., W. Mauhin, L. Abily-Donval, C. Lesueur, M. G. Berger, Y. Nadjar, J. Berger, O. Benveniste, F. Lamari, P. Laforet, E. Noel, S. Marret, O. Lidove and S. Bekri (2020). "A Proteomics-Based Analysis Reveals Predictive Biological Patterns in Fabry Disease." J Clin Med **9**(5).

Tobin, J. L. and P. L. Beales (2008). "Restoration of renal function in zebrafish models of ciliopathies." Pediatr Nephrol **23**(11): 2095-2099.

Todkar, K., H. S. Ilamathi and M. Germain (2017). "Mitochondria and Lysosomes: Discovering Bonds." Front Cell Dev Biol **5**: 106.

Togawa, T., I. Kawashima, T. Kodama, T. Tsukimura, T. Suzuki, T. Fukushige, T. Kanekura and H. Sakuraba (2010). "Tissue and plasma globotriaosylsphingosine could be a biomarker for assessing enzyme replacement therapy for Fabry disease." Biochem Biophys Res Commun **399**(4): 716-720.

Togawa, T., T. Kodama, T. Suzuki, K. Sugawara, T. Tsukimura, T. Ohashi, N. Ishige, K. Suzuki, T. Kitagawa and H. Sakuraba (2010). "Plasma globotriaosylsphingosine as a biomarker of Fabry disease." Mol Genet Metab **100**(3): 257-261.

Tondel, C., L. Bostad, A. Hirth and E. Svarstad (2008). "Renal biopsy findings in children and adolescents with Fabry disease and minimal albuminuria." Am J Kidney Dis **51**(5): 767-776.

Tondel, C., L. Bostad, L. M. Laegreid, G. Houge and E. Svarstad (2008). "Prominence of glomerular and vascular changes in renal biopsies in children and adolescents with Fabry disease and microalbuminuria." Clin Ther **30 Suppl B**: S42.

Tondel, C., L. Bostad, K. K. Larsen, A. Hirth, B. E. Vikse, G. Houge and E. Svarstad (2013). "Agalsidase benefits renal histology in young patients with Fabry disease." J Am Soc Nephrol **24**(1): 137-148.

Tondel, C., T. Kanai, K. K. Larsen, S. Ito, J. M. Politei, D. G. Warnock and E. Svarstad (2015). "Foot process effacement is an early marker of nephropathy in young classic Fabry patients without albuminuria." Nephron **129**(1): 16-21.

Tondel, C., U. Ramaswami, K. M. Aakre, F. Wijburg, M. Bouwman and E. Svarstad (2010). "Monitoring renal function in children with Fabry disease: comparisons of measured and creatinine-based estimated glomerular filtration rate." Nephrol Dial Transplant **25**(5): 1507-1513.

Torralba-Cabeza, M. A., S. Olivera, D. A. Hughes, G. M. Pastores, R. N. Mateo and J. I. Perez-Calvo (2011). "Cystatin C and NT-proBNP as prognostic biomarkers in Fabry disease." Mol Genet Metab **104**(3): 301-307.

Tousoulis, D., M. K. Georgakis, E. Oikonomou, N. Papageorgiou, M. Zaromitidou, G. Latsios, S. Papaioannou and G. Siasos (2015). "Asymmetric Dimethylarginine: Clinical Significance and Novel Therapeutic Approaches." Curr Med Chem **22**(24): 2871-2901.

Trimarchi, H., R. Canzonieri, A. Schiel, C. Costales-Collaguazo, J. Politei, A. Stern, M. Paulero, T. Rengel, J. Andrews, M. Forrester, M. Lombi, V. Pomeranz, R. Iriarte, A. Muryan, E. Zotta, M. D. Sanchez-Nino and A. Ortiz (2016). "Increased urinary CD80 excretion and podocyturia in Fabry disease." J Transl Med **14**(1): 289.

Trimarchi, H., R. Canzonieri, A. Schiel, J. Politei, C. Costales-Collaguazo, A. Stern, M. Paulero, T. Rengel, L. Valino-Rivas, M. Forrester, F. Lombi, V. Pomeranz, R. Iriarte, A. Muryan, A. Ortiz, M. D. Sanchez-Nino and E. Zotta (2017). "Expression of uPAR in Urinary Podocytes of Patients with Fabry Disease." Int J Nephrol **2017**: 1287289.

Trimarchi, H., R. Canzonieri, A. Schiel, J. Politei, A. Stern, J. Andrews, M. Paulero, T. Rengel, A. Araoz, M. Forrester, F. Lombi, V. Pomeranz, R. Iriarte, P. Young, A. Muryan and E. Zotta (2016). "Podocyturia is significantly elevated in untreated vs treated Fabry adult patients." J Nephrol **29**(6): 791-797.

Trimarchi, H., M. Forrester, F. Lombi, V. Pomeranz, M. S. Rana, A. Karl and J. Andrews (2014). "Amiloride as an Alternate Adjuvant Antiproteinuric Agent in Fabry Disease: The Potential Roles of Plasmin and uPAR." Case Rep Nephrol **2014**: 854521.

Trimarchi, H., A. Ortiz and M. D. Sanchez-Nino (2020). "Lyso-Gb3 Increases alphavbeta3 Integrin Gene Expression in Cultured Human Podocytes in Fabry Nephropathy." J Clin Med **9**(11).

Tseng, W. C., H. E. Loeb, W. Pei, C. H. Tsai-Morris, L. Xu, C. V. Cluzeau, C. A. Wassif, B. Feldman, S. M. Burgess, W. J. Pavan and F. D. Porter (2018). "Modeling Niemann-Pick disease type C1 in zebrafish: a robust platform for in vivo screening of candidate therapeutic compounds." Dis Model Mech **11**(9).

Tseng, W. L., S. J. Chou, H. C. Chiang, M. L. Wang, C. S. Chien, K. H. Chen, H. B. Leu, C. Y. Wang, Y. L. Chang, Y. Y. Liu, Y. J. Jong, S. Z. Lin, S. H. Chiou, S. J. Lin and W. C. Yu (2017). "Imbalanced Production of Reactive Oxygen Species and Mitochondrial Antioxidant SOD2 in Fabry Disease-Specific Human Induced Pluripotent Stem Cell-Differentiated Vascular Endothelial Cells." Cell Transplant **26**(3): 513-527.

Tsuboi, K. and H. Yamamoto (2017). "Efficacy and safety of enzyme-replacement-therapy with agalsidase alfa in 36 treatment-naive Fabry disease patients." BMC Pharmacol Toxicol **18**(1): 43.

Tsutsumi, O., M. Sato, K. Sato, K. Sato, M. Mizuno and S. Sakamoto (1985). "Early prenatal diagnosis of inborn error of metabolism: a case report of a fetus affected with Fabry's disease." Asia Oceania J Obstet Gynaecol **11**(1): 39-45.

Tyanova, S., T. Temu, P. Sinitcyn, A. Carlson, M. Y. Hein, T. Geiger, M. Mann and J. Cox (2016). "The Perseus computational platform for comprehensive analysis of (prote)omics data." Nat Methods **13**(9): 731-740.

Uceyler, N., J. Bottger, L. Henkel, M. Langjahr, C. Mayer, P. Nordbeck, C. Wanner and C. Sommer (2018). "Detection of blood Gb3 deposits as a new tool for diagnosis and therapy monitoring in patients with classic Fabry disease." J Intern Med **284**(4): 427-438.

Ueland, P. M. (2011). "Choline and betaine in health and disease." Journal of Inherited Metabolic Disease **34**(1): 3-15.

Ugur, B., H. Bao, M. Stawarski, L. R. Duraine, Z. Zuo, Y. Q. Lin, G. G. Neely, G. T. Macleod, E. R. Chapman and H. J. Bellen (2017). "The Krebs Cycle Enzyme Isocitrate Dehydrogenase 3A Couples Mitochondrial Metabolism to Synaptic Transmission." Cell Rep **21**(13): 3794-3806.

UniProt, C. (2021). "UniProt: the universal protein knowledgebase in 2021." Nucleic Acids Res **49**(D1): D480-D489.

Utsumi, K., K. Itoh, R. Kase, M. Shimmoto, N. Yamamoto, Y. Katagiri, K. Tanoue, M. Kotani, T. Ozawa, T. Oguchi and H. Sakuraba (1999). "Urinary excretion of the vitronectin receptor (integrin alpha V beta 3) in patients with Fabry disease." Clin Chim Acta **279**(1-2): 55-68.

Vallance, H. D., A. Koochin, J. Branov, A. Rosen-Heath, T. Bosdet, Z. Wang, S. L. Hazen and G. Horvath (2018). "Marked elevation in plasma trimethylamine-N-oxide (TMAO) in patients with mitochondrial disorders treated with oral l-carnitine." Mol Genet Metab Rep **15**: 130-133.

van den Berg, J. G., M. A. van den Bergh Weerman, K. J. Assmann, J. J. Weening and S. Florquin (2004). "Podocyte foot process effacement is not correlated with the level of proteinuria in human glomerulopathies." Kidney Int **66**(5): 1901-1906.

van der Tol, L., E. Svarstad, A. Ortiz, C. Tondel, J. P. Oliveira, L. Vogt, S. Waldek, D. A. Hughes, R. H. Lachmann, W. Terryn, C. E. Hollak, S. Florquin, M. A. van den Bergh Weerman, C. Wanner, M. L. West, M. Biegstraaten and G. E. Linthorst (2015). "Chronic kidney disease and an uncertain diagnosis of Fabry disease: approach to a correct diagnosis." Mol Genet Metab **114**(2): 242-247.

van der Veen, S. J., C. E. M. Hollak, A. B. P. van Kuilenburg and M. Langeveld (2020). "Developments in the treatment of Fabry disease." J Inherit Metab Dis **43**(5): 908-921.

van der Veen, S. J., S. Korver, A. Hirsch, C. E. M. Hollak, F. A. Wijburg, M. M. Brands, C. Tondel, A. B. P. van Kuilenburg and M. Langeveld (2022). "Early start of enzyme replacement therapy in pediatric male patients with classical Fabry disease is associated with attenuated disease progression." Mol Genet Metab **135**(2): 163-169.

Varela, P., G. Mastroianni Kirsztajn, H. Ferrer, C. Aranda, K. Wallbach, G. Ferreira da Mata, L. A. Moura, S. R. Moreira, C. Mendes, M. A. Curiati, A. M. Martins and J. Bosco Pesquero (2020). "Functional Characterization and Pharmacological Evaluation of a Novel GLA Missense Mutation Found in a Severely Affected Fabry Disease Family." Nephron **144**(3): 147-155.

Varshney, G. K., W. Pei, M. C. LaFave, J. Idol, L. Xu, V. Gallardo, B. Carrington, K. Bishop, M. Jones, M. Li, U. Harper, S. C. Huang, A. Prakash, W. Chen, R. Sood, J. Ledin and S. M. Burgess (2015). "High-throughput gene targeting and phenotyping in zebrafish using CRISPR/Cas9." Genome Res **25**(7): 1030-1042.

Vedder, A. C., G. E. Linthorst, M. J. van Breemen, J. E. Groener, F. J. Bemelman, A. Strijland, M. M. Mannens, J. M. Aerts and C. E. Hollak (2007). "The Dutch Fabry cohort: diversity of clinical manifestations and Gb3 levels." J Inherit Metab Dis **30**(1): 68-78.

Vedder, A. C., A. Strijland, M. A. vd Bergh Weerman, S. Florquin, J. M. Aerts and C. E. Hollak (2006). "Manifestations of Fabry disease in placental tissue." J Inherit Metab Dis **29**(1): 106-111.

Velasquez, M. T., A. Ramezani, A. Manal and D. S. Raj (2016). "Trimethylamine N-Oxide: The Good, the Bad and the Unknown." Toxins (Basel) **8**(11).

Virmani, M. A. and M. Cirulli (2022). "The Role of l-Carnitine in Mitochondria, Prevention of Metabolic Inflexibility and Disease Initiation." Int J Mol Sci **23**(5).

Vizcaino, J. A., E. W. Deutsch, R. Wang, A. Csordas, F. Reisinger, D. Rios, J. A. Dianes, Z. Sun, T. Farrah, N. Bandeira, P. A. Binz, I. Xenarios, M. Eisenacher, G. Mayer, L. Gatto, A. Campos, R. J. Chalkley, H. J. Kraus, J. P. Albar, S. Martinez-Bartolome, R. Apweiler, G. S. Omenn, L. Martens, A. R. Jones and H. Hermjakob (2014). "ProteomeXchange provides globally coordinated proteomics data submission and dissemination." Nat Biotechnol **32**(3): 223-226.

Vujkovac, B., I. Srebotnik Kirbis, T. Keber, A. Cokan Vujkovac, M. Tretjak and S. Rados Krnel (2022). "Podocyturia in Fabry disease: a 10-year follow-up." Clin Kidney J **15**(2): 269-277.

Wager, K., A. A. Zdebik, S. Fu, J. D. Cooper, R. J. Harvey and C. Russell (2016). "Neurodegeneration and Epilepsy in a Zebrafish Model of CLN3 Disease (Batten Disease)." PLoS One **11**(6): e0157365.

Waldek, S. and S. Feriozzi (2014). "Fabry nephropathy: a review - how can we optimize the management of Fabry nephropathy?" BMC Nephrol **15**: 72.

Wang, N., X. Bai, B. Jin, W. Han, X. Sun and X. Chen (2016). "The association of serum cathepsin B concentration with age-related cardiovascular-renal subclinical state in a healthy Chinese population." Arch Gerontol Geriatr **65**: 146-155.

Wang, S., R. Song, Z. Wang, Z. Jing, S. Wang and J. Ma (2018). "S100A8/A9 in Inflammation." Frontiers in Immunology **9**.

Wanner, N., B. Hartleben, N. Herbach, M. Goedel, N. Stickel, R. Zeiser, G. Walz, M. J. Moeller, F. Grahammer and T. B. Huber (2014). "Unraveling the role of podocyte turnover in glomerular aging and injury." J Am Soc Nephrol **25**(4): 707-716.

Warnock, D. G., D. G. Bichet, M. Holida, O. Goker-Alpan, K. Nicholls, M. Thomas, F. Eyskens, S. Shankar, M. Adera, S. Sitaraman, R. Khanna, J. J. Flanagan, B. A. Wustman, J. Barth, C. Barlow, K. J. Valenzano, D. J. Lockhart, P. Boudes and F. K. Johnson (2015). "Oral Migalastat HCl Leads to Greater Systemic Exposure and Tissue Levels of Active alpha-Galactosidase A in Fabry Patients when Co-Administered with Infused Agalsidase." PLoS One **10**(8): e0134341.

Warnock, D. G., A. Ortiz, M. Mauer, G. E. Linthorst, J. P. Oliveira, A. L. Serra, L. Marodi, R. Mignani, B. Vujkovac, D. Beitner-Johnson, R. Lemay, J. A. Cole, E. Svarstad, S. Waldek, D. P. Germain, C. Wanner and R. Fabry (2012). "Renal outcomes of agalsidase beta treatment for Fabry disease: role of proteinuria and timing of treatment initiation." Nephrol Dial Transplant **27**(3): 1042-1049.

Warnock, D. G., C. P. Thomas, B. Vujkovac, R. C. Campbell, J. Charrow, D. A. Laney, L. L. Jackson, W. R. Wilcox and C. Wanner (2015). "Antiproteinuric therapy and Fabry nephropathy: factors associated with preserved kidney function during agalsidase-beta therapy." J Med Genet **52**(12): 860-866.

Watanabe, M., M. E. Suliman, A. R. Qureshi, E. Garcia-Lopez, P. Barany, O. Heimburger, P. Stenvinkel and B. Lindholm (2008). "Consequences of low plasma histidine in chronic kidney disease patients: associations with inflammation, oxidative stress, and mortality." Am J Clin Nutr **87**(6): 1860-1866.

Watson, L., M. Keatinge, M. Gegg, Q. Bai, M. C. Sandulescu, A. Vardi, A. H. Futerman, A. H. V. Schapira, E. A. Burton and O. Bandmann (2019). "Ablation of the pro-inflammatory master regulator miR-155 does not mitigate neuroinflammation or neurodegeneration in a vertebrate model of Gaucher's disease." Neurobiol Dis **127**: 563-569.

Wei, C., C. C. Moller, M. M. Altintas, J. Li, K. Schwarz, S. Zacchigna, L. Xie, A. Henger, H. Schmid, M. P. Rastaldi, P. Cowan, M. Kretzler, R. Parrilla, M. Bendayan, V. Gupta, B. Nikolic, R. Kalluri, P. Carmeliet, P. Mundel and J. Reiser (2008). "Modification of kidney barrier function by the urokinase receptor." Nat Med **14**(1): 55-63.

Wei, Y., D. A. Waltz, N. Rao, R. J. Drummond, S. Rosenberg and H. A. Chapman (1994). "Identification of the urokinase receptor as an adhesion receptor for vitronectin." J Biol Chem **269**(51): 32380-32388.

Weidemann, F., M. D. Sanchez-Nino, J. Politei, J. P. Oliveira, C. Wanner, D. G. Warnock and A. Ortiz (2013). "Fibrosis: a key feature of Fabry disease with potential therapeutic implications." Orphanet J Rare Dis **8**: 116.

Wilcox, W. R., J. P. Oliveira, R. J. Hopkin, A. Ortiz, M. Banikazemi, U. Feldt-Rasmussen, K. Sims, S. Waldek, G. M. Pastores, P. Lee, C. M. Eng, L. Marodi, K. E. Stanford, F. Breunig, C. Wanner, D. G. Warnock, R. M. Lemay, D. P. Germain and R. Fabry (2008). "Females with Fabry disease frequently have major organ involvement: lessons from the Fabry Registry." Mol Genet Metab **93**(2): 112-128.

Wright, A. V., J. K. Nunez and J. A. Doudna (2016). "Biology and Applications of CRISPR Systems: Harnessing Nature's Toolbox for Genome Engineering." Cell **164**(1-2): 29-44.

Wu, J., Y. Yang, C. Sun, S. Sun, Q. Li, Y. Yao, F. Fei, L. Lu, Z. Chang, W. Zhang, X. Wang and F. Luo (2017). "Disruption of the gaa Gene in Zebrafish Fails to Generate the Phenotype of Classical Pompe Disease." DNA Cell Biol **36**(1): 10-17.

Xiao, K., D. Lu, J. Hoepfner, L. Santer, S. Gupta, A. Pfanne, S. Thum, M. Lenders, E. Brand, P. Nordbeck and T. Thum (2019). "Circulating microRNAs in Fabry Disease." Sci Rep **9**(1): 15277.

Xie, J., E. Farage, M. Sugimoto and B. Anand-Apte (2010). "A novel transgenic zebrafish model for blood-brain and blood-retinal barrier development." BMC Dev Biol **10**: 76.

Yadati, T., T. Houben, A. Bitorina and R. Shiri-Sverdlov (2020). "The Ins and Outs of Cathepsins: Physiological Function and Role in Disease Management." Cells **9**(7).

Yasuda, M., M. W. Huston, S. Pagant, L. Gan, S. St Martin, S. Sproul, D. Richards, S. Ballaron, K. Hettini, A. Ledeboer, L. Falese, L. Cao, Y. Lu, M. C. Holmes, K. Meyer, R. J. Desnick and T. Wechsler (2020). "AAV2/6 Gene Therapy in a Murine Model of Fabry Disease Results in Supraphysiological Enzyme Activity and Effective Substrate Reduction." Mol Ther Methods Clin Dev **18**: 607-619.

Yonishi, H., T. Namba-Hamano, T. Hamano, M. Hotta, J. Nakamura, S. Sakai, S. Minami, T. Yamamoto, A. Takahashi, W. Kobayashi, I. Maeda, Y. Hidaka, Y. Takabatake, N. Sakai and Y. Isaka (2021). "Urinary mulberry bodies as a potential biomarker for early diagnosis and efficacy assessment of enzyme replacement therapy in Fabry nephropathy." Nephrol Dial Transplant **37**(1): 53-62.

Zampetti, A., M. Gnarra, W. Borsini, F. Giurdanella, D. Antuzzi, A. Piras, C. Smaldone, M. Pieroni, C. Cadeddu, C. de Waure and C. Feliciani (2013). "Vascular endothelial growth factor (VEGF-a) in Fabry disease: association with cutaneous and systemic manifestations with vascular involvement." Cytokine **61**(3): 933-939.

Zancan, I., S. Bellesso, R. Costa, M. Salvalaio, M. Stroppiano, C. Hammond, F. Argenton, M. Filocamo and E. Moro (2015). "Glucocerebrosidase deficiency in zebrafish affects primary bone ossification through increased oxidative stress and reduced Wnt/beta-catenin signaling." Hum Mol Genet **24**(5): 1280-1294.

Zhang, H., W. Wen and J. Yan (2017). "Application of immunohistochemistry technique in hydrobiological studies." Aquaculture and Fisheries **2**(3): 140-144.

Zhang, T. and R. T. Peterson (2020). "Modeling Lysosomal Storage Diseases in the Zebrafish." Front Mol Biosci **7**: 82.

Zhang, T., S. A. Trauger, C. Vidoudez, K. P. Doane, B. R. Pluimer and R. T. Peterson (2019). "Parallel Reaction Monitoring reveals structure-specific ceramide alterations in the zebrafish." Sci Rep **9**(1): 19939.

Zhang, Z., P. Yue, T. Lu, Y. Wang, Y. Wei and X. Wei (2021). "Role of lysosomes in physiological activities, diseases, and therapy." J Hematol Oncol **14**(1): 79.

Zheng, W., H. Xu, S. H. Lam, H. Luo, R. K. Karuturi and Z. Gong (2013). "Transcriptomic analyses of sexual dimorphism of the zebrafish liver and the effect of sex hormones." PLoS One **8**(1): e53562.

Zhou, D. and Y. Liu (2016). "Renal fibrosis in 2015: Understanding the mechanisms of kidney fibrosis." Nat Rev Nephrol **12**(2): 68-70.

Zhou, J., M. Tawk, F. D. Tiziano, J. Veillet, M. Bayes, F. Nolent, V. Garcia, S. Servidei, E. Bertini, F. Castro-Giner, Y. Renda, S. Carpentier, N. Andrieu-Abadie, I. Gut, T. Levade, H. Topaloglu and J. Melki (2012). "Spinal muscular atrophy associated with progressive myoclonic epilepsy is caused by mutations in ASAH1." Am J Hum Genet **91**(1): 5-14.

Zhou, W. and F. Hildebrandt (2012). "Inducible podocyte injury and proteinuria in transgenic zebrafish." J Am Soc Nephrol **23**(6): 1039-1047.

Zizioli, D., M. Guarienti, C. Tobia, G. Gariano, G. Borsani, R. Bresciani, R. Ronca, E. Giacopuzzi, A. Preti, G. Gaudenzi, M. Belleri, E. Di Salle, G. Fabrias, J. Casas, D. Ribatti, E. Monti and M. Presta (2014). "Molecular cloning and knockdown of galactocerebrosidase in zebrafish: new insights into the pathogenesis of Krabbe's disease." Biochim Biophys Acta **1842**(4): 665-675.

Zon, L. I. and R. T. Peterson (2005). "In vivo drug discovery in the zebrafish." Nat Rev Drug Discov **4**(1): 35-44.

I

Molecular Genetics and Metabolism Reports 31 (2022) 100851

Contents lists available at ScienceDirect

Molecular Genetics and Metabolism Reports

journal homepage: www.elsevier.com/locate/ymgmr

Reduced α-galactosidase A activity in zebrafish (*Danio rerio)* mirrors distinct features of Fabry nephropathy phenotype

Hassan O.A. Elsaid [a,*], Jessica Furriol [a,b], Maria Blomqvist [c,d], Mette Diswall [c,d], Sabine Leh [a,e], Naouel Gharbi [f], Jan Haug Anonsen [f], Janka Babickova [a,g], Camilla Tøndel [a,h], Einar Svarstad [a], Hans-Peter Marti [a,b], Maximilian Krause [i,j]

[a] Department of Clinical Medicine, University of Bergen, Bergen, Norway
[b] Department of Medicine, Haukeland University Hospital, Bergen, Norway
[c] Department of Clinical Chemistry, Sahlgrenska University Hospital, Gothenburg, Sweden
[d] Department of Laboratory Medicine, Institute of Biomedicine, Sahlgrenska Academy, University of Gothenburg, Gothenburg, Sweden
[e] Department of Pathology, Haukeland University Hospital, Bergen, Norway
[f] Department of Climate & Environment, Industrial Biotechnology, NORCE, Bergen, Mekjarvik, Norway
[g] Institute of Molecular Biomedicine, Faculty of Medicine, Comenius University, Bratislava, Slovakia
[h] Department of Pediatrics, Haukeland University Hospital, Bergen, Norway
[i] Computational Biology Unit, Department of Informatics, University of Bergen, Bergen, Norway
[j] Sars Centre for Molecular Marine Biology, University of Bergen, Bergen, Norway

ARTICLE INFO

Keywords:
GLA
α-Galactosidase A
α-GAL activity
Zebrafish
Fabry disease

ABSTRACT

Fabry disease (FD) is a rare genetic lysosomal storage disorder, resulting from partial or complete lack of alpha-galactosidase A (α-GAL) enzyme, leading to systemic accumulation of substrate glycosphingolipids with a broad range of tissue damage. Current *in vivo* models are laborious, expensive, and fail to adequately mirror the complex FD physiopathology. To address these issues, we developed an innovative FD model in zebrafish.

Zebrafish *GLA* gene encoding α-GAL enzyme presents a high (>70%) homology with its human counterpart, and the corresponding protein has a similar tissue distribution, as evaluated by immunohistochemistry. Moreover, a similar enzymatic activity in different life stages could be demonstrated. By using CRISPR/Cas9 technology, we generated a mutant zebrafish with decreased *GLA* gene expression, and decreased expression of the specific gene product in the kidney. Mutant animals showed higher plasma creatinine levels and proteinuria. Transmission electron microscopy (TEM) studies documented an increased podocyte foot process width (FPW) in mutant, as compared to wild type zebrafish.

This zebrafish model reliably mirrors distinct features of human FD and could be advantageously used for the identification of novel biomarkers and for an effective screening of innovative therapeutic approaches.

1. Introduction

Fabry disease (FD) is a rare X-linked lysosomal storage disorder caused by a variety of mutations in the alpha-galactosidase gene (*GLA)* on *Xq21.3-q22*. The result of which is a wide spectrum of α-GAL enzyme activities, ranging from normal to complete deficiency [1], leading to different clinical phenotypes with both intra- and interfamilial clinical variabilities [2,3].

As α-GAL hydrolyzes glycosphingolipids and glycopeptides [4], its complete deficiency leads to multi-organ accumulation of the glycosphingolipid globotriaosylceramide (Gb3) [5], but mainly in the kidney, heart, and nervous system [6,7]. In the human kidney, the main clinical manifestations are due to Gb3 accumulation throughout the nephron and, predominantly, in renal epithelial cells [6]. Progressive Gb3 accumulation is associated with end-stage renal disease (ESRD) [8,9].

Although Gb3 and the deacetylated form lysoGb3 in plasma are currently used for FD diagnosis and to monitor treatment effectiveness [10,11], their ability to mirror all *GLA* gene mutations detected so far is debated [12–16].

Enzyme replacement therapy (ERT) has improved multiple aspects of FD. However, the associated complications *e.g.* allergies and variable efficiency that depend on the age and degree of nephropathy [17] as

* Corresponding author at: Department of Clinical Medicine, The Laboratory Building, Haukeland University Hospital, 5020 Bergen, P.O. Box 7804, Norway.
E-mail address: hassan.elsaid@uib.no (H.O.A. Elsaid).

https://doi.org/10.1016/j.ymgmr.2022.100851
Received 24 January 2022; Accepted 13 February 2022

well as the elevated mortality rates, contribute to considering ERT as a disease modifier rather than a cure [18]. Therefore, innovative new treatment options are still urgently needed. Nevertheless, the development of novel therapies for FD critically requires the availability of adequate experimental models [17–20].

In vitro studies using different cell lines may model the main FD hallmark, *e.g.* Gb3 accumulation [21–24], but fail to address the complexity of damaged organs [25]. Instead, murine FD models [26,27] recognized the role of ERT in decreasing Gb3 levels [28], and some of them succeeded in imitating the renal impairment of FD, however, hypertrophic cardiomyopathy was not reported in this FD model [29]. Fortunately, a study using FD model in rat have managed to recapitulate both renal and heart phenotypes [30], in addition, FD-related ocular manifestations was reported by the same research group [31]. However, knockout Fabry mice maintain a standard adult lifetime and their premature death was never attributed to the FD complication *i.e.* kidney or heart defects [29]. Others FD model appear clinically normal, and do not show obvious microscopic lesions in the kidney, liver, heart, spleen, lungs, and brain [32]. Therefore, current *in vitro* and *in vivo* models fail to fully elucidate FD physio-histopathology, and do not allow ERT optimization for personalized treatment. On top of that, murine studies can be laborious, and expensive, and it is challenging to follow the possible lack or reduction of α-GAL enzymatic activity early during intra-uterine gestation [25,32].

Thus, additional *in vivo* Fabry disease models are needed to explore glomerular filtration barrier integrity and to facilitate screening for potential drugs [25,32]. Moreover, inconsistency of Gb3 and lysoGb3 monitoring in kidney during treatment requires more out of the box thinking, including considering an animal model that is voided of Gb3/lysoGb3.

In this context, zebrafish is a good candidate since it lacks Gb3 synthase and, therefore, cannot produce Gb3 [33]. This could allow to investigate the substrate-independent role of *GLA* mutation and other low scale yet powerful markers that might be masked by the over-consideration of Gb3 and lysoGb3. Based on the unmistakable similarity of its kidney with the human one, zebrafish has extensively been used to study abnormalities in kidney development, inherited glomerulopathies, and ciliopathy-associated human cystic kidney diseases [34]. In the recent years, the use of zebrafish to study lysosomal storage disorders has grown tremendously [35], and with new advances in gene-editing technologies, researchers were able to produce zebrafish transgenic lines that facilitate the study of lysosomal storage disorders [36].

In addition to the similarities with human kidneys, zebrafish is valuable for other research-friendly characteristics such as ex-utero fertilization and development, rapid development from embryos to larvae in 5 days, and to full adult stage in 90 days, and high fecundity. Additionally, the transparency of embryos and larvae allow easy visualization of developmental processes or monitoring of the desired phenotype, [37]. Advantageously, the robust development of the pronephrone which is fully functioning at 4-day post-fertilization (dpf) identify zebrafish as an unavoidable organism in high throughput drug screening studies [34,38,39] and a useful bridge between *in vitro* cell- and *in vivo* rodent-based FD models [40].

On the basis of these considerations, we investigated the characteristics of α-GAL in wild-type zebrafish and evaluated the effects of the inhibition of *GLA* gene expression, to explore the possibility of using this valuable organism in FD studies.

2. Materials and methods

2.1. Ethical approval

The Norwegian Food Safety Authority (Mattilsynet) granted ethical approval for this study (FOTS ID 15256). All procedures were performed following standard protocols of the Zebrafish Facility, University of Bergen (UiB). We used the AB/Tübingen (AB/TU) strain of zebrafish for our experiments.

2.2. Zebrafish maintenance and sample collection

Eggs, embryos, larvae, juveniles, and adult fish were handled in compliance with applicable national and international standards, according to zebrafish facility regulation at the University of Bergen. Under normal laboratory conditions, an adult (90+ days post-fertilization dpf) wild-type zebrafish was held at 28 °C on a 14 h light/10 h dark period. Standard spawning protocol (www.zfin.org) was followed by egg harvesting. Eggs were stored in an E3 medium containing 0.01% methylene blue after harvesting. Embryos and larvae were incubated at 28 °C until 5 dpf. Current rules do not require permission for testing on zebrafish embryos before the free-feeding stage (5 dpf). According to the zebrafish facility rules, all invasive pain-causing interventions on stages older than 5 dpf were performed under anesthetic conditions.

2.3. Bioinformatics analysis and prediction of α-GAL structure in zebrafish

Using the BLAST algorithm with default parameters, we compared nucleotide and amino acid sequences to the non-redundant gene databases accessible at the National Centre for Biotechnology Information GenBank database (NCBI) http://blast.ncbi.nlm.nih.gov. NCBI BLAST (https://blast.ncbi.nlm.nih.gov/Blast.cgi) was used to evaluate sequence similarities against the Zebrafish May.2017 (GRCz11/danRer11) genome assembly. ClustalW was used to generate the multiple sequence alignment, which was then run on the Geneious software. The Ensembl db (http://www.ensembl.org) was used for comparative genomics analysis of *GLA* sequences in zebrafish and humans. The I-TASSER online modeling service was used to perform the homology modeling analysis [41]. The model was selected based on the confidence score (C-score), assessing the predictability of models. The significance of threading template alignments and the convergence parameters of structure assembly simulations are used to compute the C-Score. The standard C-score range is −5 to 2, with a higher C-score indicating a model with high confidence. The putative protein structure was selected based on the predicted 3D model with the highest C-score.

2.4. General CRISPR target design and generation of short guide RNA

Primers and single-guide RNA (sgRNA) sequences were designed by considering genomic variation and using the known genetic variation of the GRCz11 annotation (ENSDARG00000036155). Primers, single guide RNA (sgRNA), tracrRNA, and Cas9 Nuclease V3 were purchased from Integrated DNA Technologies BVBA (IDT, Leuven, Belgium). The CHOPCHOP web-tool [42] was used for both GN or NG as 5′ specifications. The Supplemental table displays primers and sgRNA sequences (Sup. 1).

2.5. Generation of mutant lines

Zebrafish *GLA* mutants were generated by CRISPR/Cas9-mediated gene tool. One-target region located within *GLA* exon five was chosen for sgRNA recognition. The corresponding sgRNA was injected into wild-type zebrafish embryos (n = 200) at the 1-cell stage together with cas9 protein. For mutation screening, sgRNA-injected embryos (Founder $0/F_0$) of 5 dpf were screened by PCR fragment analysis to confirm successful mutant generation. After validating the successful F_0 mosaic generation, larvae were raised to adulthood, screened individually, and positive mutants were out-crossed to TAB wild-type adults to obtain the first generation F_1 embryos with heterozygous genotype.

To obtain the $GLA^{-/-}$ mutant line, selected F_1 adult were in-crossed and produced the second generation F_2 in which the progeny was $GLA^{+/+}$, $GLA^{+/-}$ and $GLA^{-/-}$. Homozygous $GLA^{-/-}$ mutant individuals from

F_2 were genotyped, sequenced, and in-crossed to generate third generation F_3, 100% homozygous *GLA*$^{-/-}$ mutant. All work has been done on F_3 generation or its in-crossed progeny compared to the wild type of similar crossing batch Sup.2.

2.6. Genotyping and sequencing

Genotyping was performed using simplified PCR fragment analysis. To genotype *GLA* mutants, genomic DNA was extracted from either whole embryos/larvae or the tail fin of adults with the DNA crude extraction method. Briefly, samples were collected in 50 μL of 50 mM NaOH, samples were then heated at 95 °C for 20 min followed by quick cooling at 4 °C. Genomic DNA was used as template for genotyping PCR. The PCR was carried out at the following conditions: 95 °C for 5 min; 35 cycles of 94 °C for 30 s, 58 °C for 30 s, 72 °C for 30 s, and final elongation step of 72 °C for 5 min. PCR product was digested with restriction enzyme *Bsm*FI (R0572L), New England BioLabs, Ipswich, MA, USA) 65 °C for 1 h, following manufacturer instructions. Final digestion products were resolved on 2% agarose gels.

For sequencing, PCR products were cleaned up using ExoSAP-IT™ (Applied Biosystems™), following manufacturer instructions. Sequencing reactions were prepared following BigDye v.3.1 Protocol, Sequencing Facility, High Technology Center, UiB, with the following sequencing cycle: 96 °C for 5 min; 25 cycles of 96 °C for 10 s, 58 °C for 5 s, 60 °C for 4 min. Automated Sanger DNA Sequencing was performed using capillary based Applied Biosystem 3730XL Analyzer.

2.7. Alpha-galactosidase A activity assay and lysoGb3 measurement

To compare α-GAL activity levels at different developmental stages, samples were collected from 2dpf embryos (n = 7), 4dpf larvae (n = 8), and 30dpf juveniles (n = 4). For +90 dpf adults, kidney samples were pooled (3/sample, male n = 10, female n = 9). For a comparison between adult wild type and mutant, kidney lysates from each gender were sampled separately (n = 10). Samples were snap-frozen in liquid nitrogen immediately after collection and shipped in dry ice to Sahlgrenska University Hospital, Sweden, to measure α-GAL activity and lysoGb3 levels. Samples were stored at −80 °C upon arrival and before the analysis.

For α-GAL activity analysis, samples were kept on ice, diluted in 100–200 μL of deionized water, depending on tissue sample weight, and homogenized at 4 °C (glass/Teflon; 10–15 strokes). Protein concentration was determined by the BCA Protein Assay Reagent method (Pierce, Rockford, USA). Enzyme activity was assessed using the α-GAL standardized protocol used in clinical diagnostics [43,44]. Briefly, the activity of tissue homogenates was measured using a fluorometric assay utilizing 4-metylumbelliferyl (MU)-alpha-galactopyranoside (20 mM, Apollo Scientific) as substrate. Sodium acetate buffer (0.1 mM, pH 4.5) was used as substrate buffer. The substrate solution included *N*-acetyl-D-galactosamine (200 mM, Toronto Research Chemicals) as an inhibitor of alpha-*N*-acetyl-galactosamidase (previously named alpha-galactosidase B), as well as 2% delipidized bovine serum albumin. The enzyme reaction was performed at 37 °C, pH 4.5 for 30 min, and stopped with glycine buffer (0.25 M, pH 10.3, Merck). Fluorescence of samples, blanks, and standard solution (4-Methyl Umbelliferon 1 μM, diluted in Glycine buffer) was measured by spectrofluorometry (Jasco FP-6500, Jasco Inc., Easton, MD, USA) using an excitation wavelength of 360 nm and an emission wavelength of 448 nm. The activity of α-GAL was expressed as μkatal/kg protein.

Analysis of lysoGb3 was performed in tissue homogenates of zebrafish kidney by a modified method, as previously described [45]. Samples were prepared as described above, and 50 μL of the homogenate was used for analysis.

2.8. Customized polyclonal antibody synthesis

Alpha-galactosidase protein sequence was screened using Geneious prime software for potential antigenic regions using the default setting of the software. The minimum length of the antigenic region was set to 7 amino acids. The antigenic region prediction was powered by the EMBOSS6.5.7 tool plugin within Geneious prime software. The selected sequences were then investigated using BLAST against rabbit sequence for sequence similarities to avoid cross-reactivity. Moreover, GenScript® proprietary software evaluated their antigenicity. Accordingly, two antigenic sequences were selected for the rabbit-generated polyclonal antibody against zebrafish α-GAL protein. Both antigenic peptides were at the seventh exon of the protein. The two antigenic peptides of the carboxy-terminal amino acids 251–264 [(NH_2-) CKADSFELWERPLSG (-$CONH_2$)] and 271–284 [(NH_2-) CVVNRQEIGGPRRFT (-$CONH_2$)] were synthesized and coupled to KLH carrier *via* the cysteine residue (underlined). Antibodies were then produced by GenScript's standard protocol in New Zealand rabbits.

2.9. Plasma creatinine assessment

Zebrafish were euthanized by immersion in tricaine methanesulfonate MS-222300 mg/L, Sigma Chemical Co., St. Louis, Mo. (Cat. No. A-5040). Blood was immediately collected from the dorsal aorta, as described [46]. Briefly, a transverse cut was made just caudal to the dorsal fin. Blood spilling from this cut was rapidly collected by a heparin-coated micropipette tip and pooled to achieve the desired volume of 20 μL (n = 2/genotype).

Plasma concentrations of creatinine were measured by high-performance liquid chromatography/tandem mass spectrometry following [47] in collaboration with Bevital AS, Bergen, Norway.

2.10. Proteinuria assessment

In humans, albuminuria and proteinuria are standard clinical methods to evaluate kidney function. However, zebrafish does not produce albumin, therefore, albuminuria cannot be detected. We adopted a new method to qualitatively assess the pattern of proteinuria in zebrafish adults. For each measurement, one wild-type and one mutant fish were kept in 100 ml water for 24 h at 28.5 °C. Water samples (n = 5) were harvested after ensuring that the fish was alive, and blank was used as a negative control (only water). Protein was precipitated using Trichloroacetic acid (TCA): Chloroform method. Briefly, 100% TCA solution was added, mixed gently with the water sample and incubated at 4 °C for 30 min. Samples were then centrifuged at 13,000 rpm at 4 °C for 5 min and supernatants were discarded. Pellets were washed 2× with cold acetone, with each washing step followed by centrifugation at 13,000 rpm at 4 °C for 5 min. After drying the pellets, 20 μL of sample buffer was added and the mixture was incubated at 70 °C for 10 min. For SDS-PAGE, the samples were applied to NuPAGE 4–12% Bis-Tris Gels (Invitrogen). The gel was stained and destained with Coomassie Brilliant Blue R-250 Staining Solution kit, Cat#1610436, and imaged using ChemiDoc XRS+ system, BIO-RAD.

To identify protein/s in each gel, bands were excised using a clean blade under sterile conditions. Cut gel bands of similar sizes were placed into a sterile 70% ethanol-pre-cleaned 1.5 mL tube. Sufficient sterile water was added to cover excised gels. and samples were kept at —20C until being shipped to Department of Biosciences, University of Oslo, where they were analyzed using LC-MS/MS, detailed method below.

2.10.1. In-gel protein digest

Gel slices containing proteins were destained, reduced, alkylated, and digested with trypsin (Sigma) as previously described [37].

2.10.2. LC-MS/MS analysis of protein fractions

The generated peptide samples were analyzed using an Ultimate

3000 nano-UHPLC system (Dionex, Sunnyvale, CA, USA) connected to a QExactive mass spectrometer (ThermoElectron, Bremen, Germany) equipped with a nano electrospray ion source. For liquid chromatography separation, an Acclaim PepMap 100 column (C18, 3 μm beads, 100 Å, 75 μm inner diameter, 50 cm) (Dionex, Sunnyvale CA, USA) was used. A flow rate of 300 nL/min was employed with a solvent gradient of 3–55% B in 53 min, to 96% B in 2 min and retaining that for 5 min then back to 3% B in 3 min. Solvent A was 0.1% formic acid and solvent B was 0.1% formic acid/90% acetonitrile. The mass spectrometer was operated in the data-dependent mode to automatically switch between MS and MS/MS acquisition. Survey full scan MS spectra (from *m/z* 200 to 2000) were acquired with the resolution $R = 70{,}000$ at m/z 200, after accumulation to a target of 1e6. The maximum allowed ion accumulation times were 100 ms. The method used allowed sequential isolation of up to the ten most intense ions (intensity threshold 1.7e4), for fragmentation using higher-energy collision induced dissociation (HCD) at a target value of 10,000 charges and a resolution $R = 17{,}500$ with NCE 28. Target ions already selected for MS2 were dynamically excluded for 60 s. The isolation window was m/z = 2 without offset. The maximum allowed ion accumulation for the MS/MS spectrum was 60 ms. For accurate mass measurements, the lock mass option was enabled in MS mode for internal recalibration during the analysis.

2.10.3. Database search and label-free quantitation

Data were acquired using Xcalibur v2.5.5 and raw files were processed. Database searches were performed against the Zebrafish (*Danio Rerio*) (NCBI; taxon ID7955; 55,761 entries) and the PD common contaminants list, with the proteome discoverer v 2.4 software (ThermoScientific, Whaltham, Massachusetts, USA). The following parameters were used: digestion enzyme, trypsin; maximum missed cleavage, 2; minimum peptide length 4; parent ion error tolerance, 10.0 ppm; fragment ion mass error tolerance, 0.04 Da; and fixed modifications, carbamidomethylation of cysteines. Oxidation of methionine and acetylation of the N-terminus were specified as variable modifications and the maximum number of PTMs was set to 2. Peptide-spectrum matches was assessed with percolator with FDR target set at 0.01 (strict) and 0.05 (relaxed). Generated protein lists were manually curated, with low FDR proteins, proteins with single (low score) peptides, and contaminants removed. Functional annotation of proteins was done using the PD protein knowledge-database linked to GO: annotations.

2.11. Histology and immunohistochemistry

For standard histology and immunohistochemical staining, wild type (n = 6) and mutant (n = 3) adult (90 + dpf) zebrafish were euthanized in 300 mg/L tricaine methanesulfonate MS-222 Sigma (Cat. No. A-5040) and dissected open. Kidneys were exposed after discarding viscera under 1× PBS (Life Technologies, Cat. No. AM9625). Dissected fishes were fixed with 4% paraformaldehyde in 1× PBS for 48 h. Later, kidneys were removed, processed, and embedded in paraffin according to standard protocols of molecular imaging center MIC, UiB and Pathology Department, Haukeland University Hospital. Sections of 5 μM were acquired for histology (Hematoxylin and periodic acid Schiff stain) and immunohistochemical staining.

Immunohistochemistry was performed as previously described [48] with slight modifications. Antigen retrieval was skipped upon IHC protocol optimization. Staining with our customized rabbit polyclonal primary antibody (anti-α-GAL) was performed for one hour at room temperature at 1:600 concentration. For negative controls, the primary antibody was omitted. Slides were scanned with ScanScope XT® (Aperio) at x40 resulting in a resolution of 0.25 μm per Pixel. Digital slides were viewed in ImageScope 12.

Immunohistochemical positivity for anti-α-GAL was quantified using the color deconvolution algorithm version 9.1 (Aperio, CA, USA) after adjusting the default parameters to DAB staining. The total percentage of positive pixels was used as a visualization parameter and statistics was performed IBM SPSS V. 25.

For transmission electron microscopy (TEM), kidney samples of wild type (n = 9) and mutant (n = 8) were fixed overnight at 4 °C in 2.5%. Samples were washed 3 times in 0.1 M cacodylate buffer and then incubated for 1 h in 1% osmium tetraoxide and washed with cacodylate buffer. Samples were dehydrated in ascending ethanol concentrations and incubated in ethanol and propylene oxide (PO). Samples were then infiltrated with 25% Epon 812 resin and 75% PO for 35 min, followed by 50% Epon 812 resin and 50% PO for 1 h and exchanged with a new 50% Epon 812 resin and 50% PO for overnight incubation. Samples were exchanged with 75%: 25% (resin: PO), then pure epoxy resin for 3–4 h, then overnight. Finally, the resin exchanged completely with epoxy resin for 3 h, embedded in epoxy resin, and polymerized at 60 °C for 48 h.

Sections 500 nm to 1 μm thick were collected using a Leica ULTRACUT microtome. Thick sections were stained with 1% toluidine blue. 70–80 nm ultrathin sections were cut from this block, collected on 300-mesh copper grids, and stained with 2% uranyl acetate (aqueous) for 16 min and then with lead citrate for 12 min. Samples were imaged at MIC, Department of Biomedicine, UiB, on the Jeol JEM-1230 electron microscope at various magnifications.

2.11.1. Measurement of podocyte foot process width

Glomerular basement membrane GBM length was measured using Fiji (ImageJ) [49]. The number of podocyte foot processes along the GBM was counted manually. Any connected epithelial segment laying on GBM and separated by filtration slit was considered as a foot process. The arithmetic mean of the foot process width was calculated from the following equation:

$$\mathrm{FPW} = \frac{\pi}{4} \bullet \frac{\sum \mathrm{GBM\ length}}{\sum \mathrm{FP\ No.}}$$

Where ∑FP No. is the total number of foot processes counted in each picture, and ∑GBM length is the total GBM length measured in each picture. The hypothetical random variation in the angle of section relative to the long axis of the podocyte was corrected using the correction factor π/4. Mean width was calculated first for an individual sample, and then it was used to calculate the mean FPW for the two groups (wild type and mutant). 1–3 glomeruli were evaluated per fish (n = 9 wildtype, n = 8 mutant).

2.12. Statistical analyses

Statistical analysis was performed using IBM SPSS V 25 and GraphPad Prism V 9.2.0. Values are presented as violin plots (median/interquartile ranges) or as mean ± SD. The Kruskal–Wallis test with Dunn test for *post hoc* comparison or Mann-Whitney test were used to assess statistical significance. Differences were considered significant with p-values <0.05.

3. Results

3.1. Zebrafish GLA is the only orthologue for its human counterpart

To develop an innovative experimental model of potential relevance for the study of human FD, we first investigated the expression of *GLA* homologues in zebrafish.

We found only one previously annotated version of the human *GLA* gene counterpart in zebrafish (chromosome 14: NC_007125.7) in the National Centre for Biotechnology Information (NCBI) online databases, named galactosidase, alpha. This gene, similar to its human counterpart, is composed of seven exons, encoding a 1470 bp mRNA (NM_001006103). A polypeptide homologous to human α-GAL protein was also identified (NP_001006103.2).

To explore their exclusive homology to the human gene and protein

counterparts, we used the nucleotide (NC_000023.11) and the amino acid (NP_000160.1) sequences of human GLA gene and α-GAL protein as queries in non-redundant sequence databases from NCBI, against the Zebrafish May 2017 (GRCz11/danRer11). Indeed, zebrafish *GLA* gene mRNA is highly similar to its human counterpart (71% bp sequence identity). Moreover, a comparison between zebrafish and human proteins revealed a high degree of sequence similarity (65.53% amino acids identity). Most importantly, active, and substrate-binding sites are 100% conserved along with the primary structure of zebrafish protein.

Based on this background, we performed a homology modeling analysis on I-TASSER online modeling service, and we evaluated associated C-scores. After removing the first 20 amino acid residues comprising the signal sequence, the structure revealed was similar to its human counterpart, *e.g.* a homodimeric protein (Fig. 1 a1 and a2) with each monomer composed of two domains (Fig. 1 b1 and b2), first, a N-terminal $(\beta/\alpha)_8$ domain (residues 21 to 319), containing the active site, and second, a C-terminal domain (residues 320 to 409), containing antiparallel β8 strands packs against the first domain.

As expected from the high protein sequence similarity, the model fits well on the template when superimposed with Geneious prime software. The positions of the catalytic residues Nucleophile (159D) and Proton donor (220D) together with the substrate-binding site 192E are fully conserved (Fig. 1 C). Moreover, the position of the N-glycosylation site (N181), and the Ubiquitination sites (K116, 229, 297, 303, and 315), and the five-disulfide bond organization (C41–C83, C45–C52, C131–C161, C191– C212, and C367–C371) are similarly conserved. Among these, C131-C161 is the most important one, as it is directly involved in stabilizing the conformation of the active site. Also, amino acids, W36, D81, D82, Y123, K157, and R216 conferring substrate specificity for α-GAL are in topologically conserved positions (Fig. 1 C). The non-conserved residues between mammalian and zebrafish α-GAL enzymes are exposed on the surface of the predicted zebrafish α-GAL structure.

This data indicates that *GLA* is the only zebrafish orthologue for the human *GLA* gene and encodes a protein with high *in silico* similarity to its human counterpart.

3.2. Zebrafish-α-GAL tissue distribution and functional activity are similar to their human counterpart

The kidney is a major affected organ in classical FD in humans. To investigate the pattern of α-GAL enzyme distribution, as related to its human counterpart, immunohistochemical analysis of adult zebrafish kidneys was performed by using a customized polyclonal antibody. Worth mentioning here that only one antigenic peptide was able to produce an appropriate antibody against zebrafish α-GAL, that is amino acids 251–264 [(NH2-) CKADSFELWERPLSG (-CONH2)].

Distribution of the α-GAL enzyme immune-reactivity was limited to the cytoplasm of podocytes and proximal and distal tubule cells. However, while in the podocytes, the α-GAL signal was scarcely distributed in the cytoplasm, it was extensively present in the renal tubules (Fig. 2 A). Thus, immunohistochemical results indicate that the α-GAL distribution in the zebrafish's kidney is similar to that in the human kidney [50].

The sole presence of the protein does not necessarily reflect the same functional activity as in humans, where its deficiency is crucial in

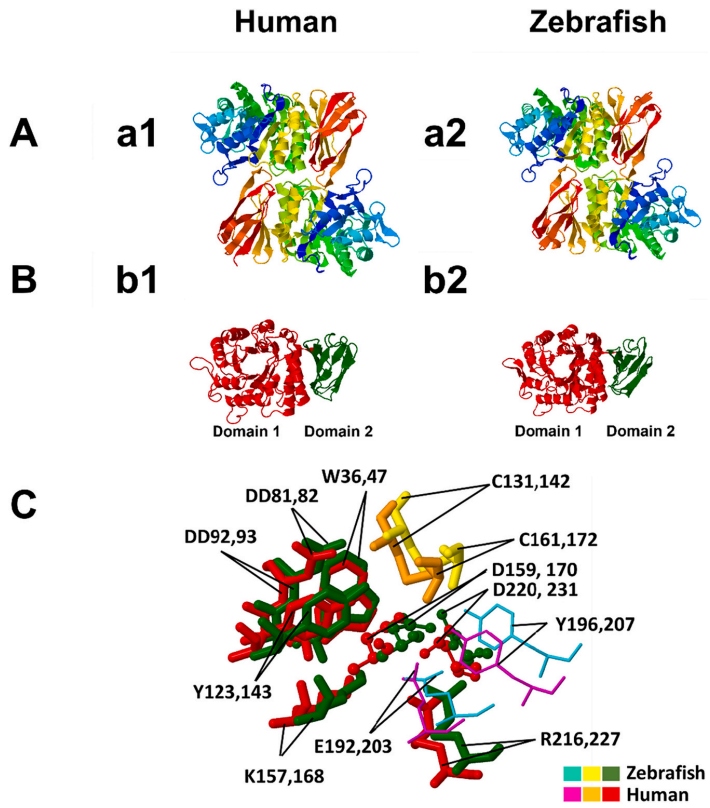

Fig. 1. Structure prediction of the zebrafish α-GAL. (a1) homodimer structure of human α-GAL; (a2) homodimer structure of zebrafish α-GAL. The dimers are colored from N-terminal (blue) to C-terminal (red). The structure prediction shows that the zebrafish α-GAL folds in a pattern highly similar to its human counterpart. (b1) is the monomer of a human α-GAL enzyme showing the two domains, while (b2) is the zebrafish α-GAL enzyme showing the same structure. Domain 1, (β/α)8 barrel, extends through residues 32–330 in human (red) and 21–319 in zebrafish (red), and contains the active site, while domain 2 extends through residues 331–429 in human (green) and 320–409 in zebrafish (green) and contains antiparallel β strands. C: the superimposed structure of the two enzymes active sites and substrate binding site, with substrate specificity residues W36, D81, D82, Y123, K157, R216 in zebrafish and W47, D92, D93, Y143, K168, R227 in human, are fully conserved between the two species. The active sites D159 and D220 in zebrafish, D170, and D231 in humans are also conserved. The residues C131 and C161 zebrafish and C142 and C172 human help to stabilize the conformation of the substrate-binding site through the formation of disulfide bonds. The substrate-binding site boundaries E192 and Y196 in zebrafish correspond to E203 and Y207 in humans. Color ligands for zebrafish and human are shown in plate C. (For interpretation of the references to color in this figure legend, the reader is referred to the web version of this article.)

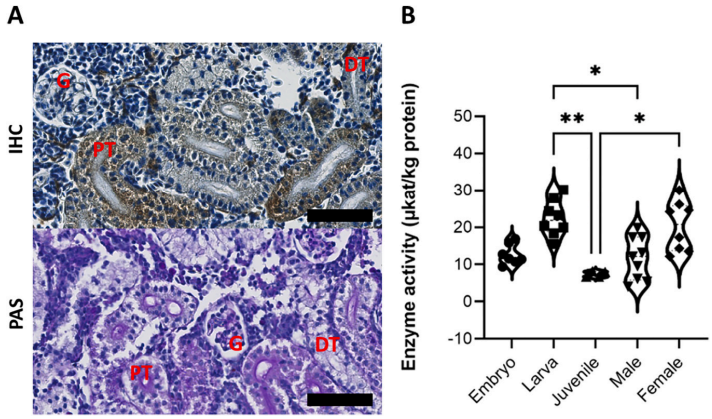

Fig. 2. Kidney tissue distribution and enzyme activity in wild type zebrafish. (A) Immunohistochemistry (IHC) staining for Zebrafish α-GAL in wild-type adult zebrafish kidney. The expression pattern is similar in both genders. The protein was abundantly detectable in the cytoplasm of renal tubule cells, and to a lower extent in the glomerulus. Hematoxylin was used as counterstain. The lower panel shows the three renal structures, as stained with Periodic Acid Schiff (PAS). Scale bar (in black) = 50um. (B) Wild-type zebrafish α-GAL activity as evaluated in the whole embryo, larvae, and juvenile whole body tissue lysates and in adult male and female kidney tissue lysates (Kruskal-Wallis, $P \leq 0.05$). Results of the Dunn *post hoc* test show a significant difference (*) between juvenile and larvae ($P < 0.05$) and juvenile and adult female specimens ($P < 0.05$). The violin plot represents these results within the 95th percentile. G = glomerulus, PT = proximal tubule, DT = distal tubule. Validation of the antibody is provided in Sup.4.

determining FD manifestations. We therefore evaluated the enzymatic activity of zebrafish α-GAL in the animal tissue lysates (embryo, larva, and juvenile) and in kidney lysates of adult males and females. A comparative analysis revealed a significant difference between larva and juvenile stages ($p = 0.006$), larva and adult male ($p = 0.03$), and between juvenile and adult female ($p = 0.048$) (Fig. 2 B).

These results not only demonstrate the presence of zebrafish α-GAL throughout different developmental stages, but also validate the functional similarity of zebrafish α-GAL and its human orthologue by utilizing the same chemical substrate. Thus, due to our in-depth bioinformatic analysis demonstrating high levels of identity on both sequence and structural levels coupled with our enzymatic *in-vitro* assay

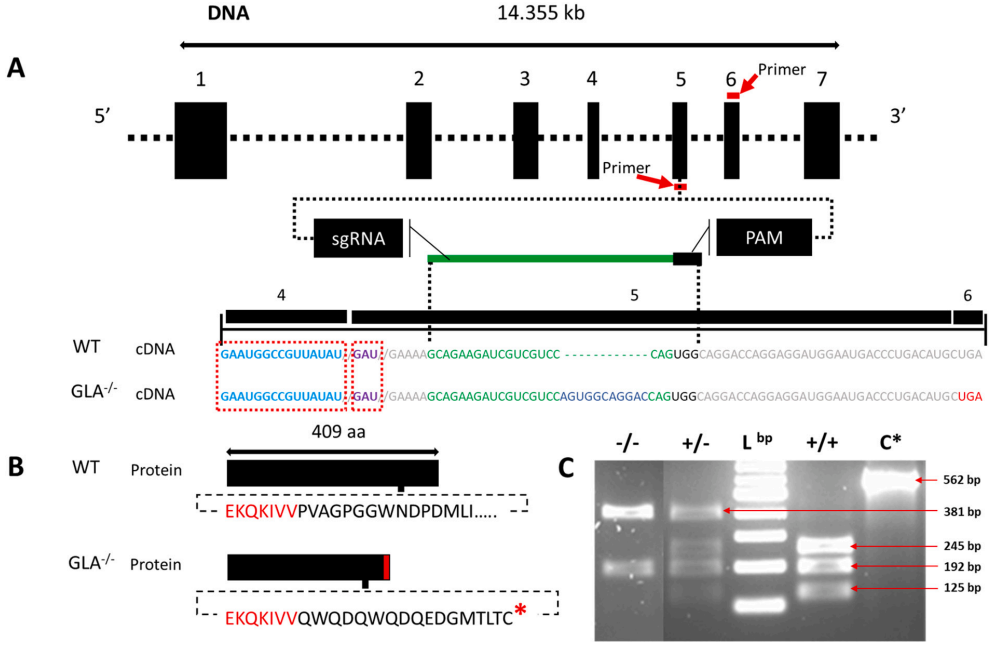

Fig. 3. Generation and verification of a GLA mutant line. (A) CRISPR/Cas9-based gene-editing tool used to generate mutant zebrafish. The targeted genomic sequence for the introduction of the insertion mutation in the exon 5 is illustrated. The eleven base pair insertion (shown in blue) is highlighted in the cDNA sequence. The putative stop codon after the insertion is highlighted in red. Guide RNA and PAM sequences are highlighted in green and black, respectively. Mutation occurred 45 bp from the proton donor catalytic site (in violet) and 120 bp from the substrate binding site (in light blue) that is in exon 4. Primers for genotyping and sequencing spanning exons 5 and 6 are indicated by the red bar (B) The insertion mutation leads to a frameshift with a premature stop codon (in red) 16 amino acid downstream the insertion region (the lower panel). (C) PCR screen shows that the insertion interrupts one of the two restriction enzyme digestion sites resulting in two PCR fragments in the mutant (−/−) instead of three in the wild type (+/+), L^{bp} = DNA ladder in base pairs (bp), C* = wild type undigested PCR product (the agarose gel image is edited for illustration, full image can be reviewed in sup.5). (For interpretation of the references to color in this figure legend, the reader is referred to the web version of this article.)

demonstrating functional similarity to human α-GAL we hereafter refer to NC_007125.7 as zebrafish α-GAL.

We additionally measured lysoGb3 in zebrafish kidney tissue lysate but obtained negative result Sup. 3. These results are in line with previous work [33] and supporting our *in-silico* observation that zebrafish lacks Gb3 synthase gene.

3.3. Generation and verification of the mutant line

To investigate "*in vivo*" the effects of reduced α-GAL enzyme production in zebrafish, we used CRISPR/Cas9 gene-engineering tool to edit the *GLA* gene. Sequencing of the edited line revealed a 11 bp insertion in exon 5 (the targeted region) at moderate proximity to the active site (Fig. 3). The mutation was 45 bp downstream from the proton donor catalytic site in exon 5 and 120 bp downstream from the substrate binding site, in exon 4 (Fig. 3). The insertion resulted in a frameshift started at position c.802, p244.P > Q, and a subsequent premature stop codon within exon 6 at c.842, p.261.I > *.

3.4. GLA indel mutation results in decreased enzymatic activity and expression of zebrafish α-GAL in renal tissues

DNA sequencing analysis indicates that the mutation introduced generated a frameshift in the resulting mRNA. To validate these results at the protein level, we measured the enzyme activity in the kidney tissue lysate of mutant animals and their wildtype counterpart. Our results revealed an approximately 65% decrease of enzyme activity in the mutant fish, as compared to the wild type ($p = 0.025$) (Table 1, Fig. 4).

Based on the enzyme activity data, we anticipated a reduced presence of the enzyme in the renal tissue. Therefore, we performed immunohistochemical analysis to quantify α-GAL protein expression in wild-type and mutant renal tissue. We observed that no or very weak α-GAL signal was detectable in mutant, as compared to wild type renal tissue ($p = 0.024$, Fig. 4). We also used periodic acid Schiff (PAS) stain to document glomerular changes and we observed dilated capillary loops and thinner Bowman's space (Fig. 4) in the mutant compared to the wild type kidneys.

3.5. Compromised renal function in GAL mutant zebrafish

Same as in humans, in zebrafish creatinine is freely filtered through the glomerulus. Therefore, plasma creatinine level mirrors the integrity of the glomerular barrier. We assessed the plasma creatinine of wild type and mutant zebrafish. We observed more than double volume plasma concentrations of creatinine in mutant compared to wild type animals (mean SD) in μmol/L: 10.08 ± 1.167 *vs.* 4.36 ± 0.4950 (Fig. 5 A), consistent with a severely compromised kidney function.

Accordingly, we were also interested in evaluating impaired filtration barrier integrity using zebrafish-adapted proteinuria assessment. Indeed, a high molecular weight protein leakage was detectable in mutant, compared to the wild type fish (Fig. 5 C). The main high molecular weights proteins crossing filtration barrier were detected at 80 kDa, 98 kDa and 150 kDa. These proteins were identified by mass spectrometry after individual bands were excised from polyacrylamide gels (Sup.6). Interestingly, the yolk-transport protein abundantly found in blood, vitellogenin, was also detectable in all three gel bands. This could be explained by non-specific protein fragmentation [51]. This protein is the zebrafish counterpart of human plasma albumin [52] and

Table 1
The α-GAL enzyme activity measurements in μkat/kg of protein in wild type and mutant. N:sample number; SD: standard deviation.

	N	Mean ± SD	Median	Mean Rank
Wild type	10	26.3 ± 15.4	28.60	13.45
Mutant	10	9.9 ± 1.9	9.700	7.55

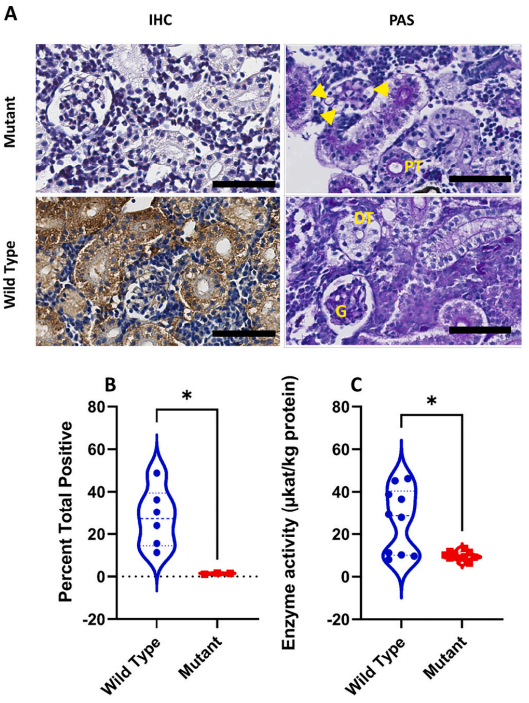

Fig. 4. Histological distribution and enzymatic activity of Zebrafish- α-GAL protein in the GLA mutant zebrafish. (A) Scanned digital images show α-GAL antibody and periodic acid Schiff staining. Note that PAS staining shows dilated capillary loops and thinner Bowman's space (yellow arrowheads) in mutant compared to wild type animals. (B) Quantification of immunohistochemical analysis of sections from wild-type and mutant kidneys. Signal intensity is significantly higher in wild type compared to mutant tissues (Mann-Whitney *U* test: $P < 0.05$). The violin plot represents these results within the 95th percentile, and the dash-line symbol inside the violin plot represents the median. Scale bar = 50um. (C) Comparison of α-GAL activity in wild type and mutant zebrafish kidney tissue lysate (Mann-Whitney Test, $P < 0.05$).

we therefore interpreted this as a valuable test to assess the integrity of the membrane-filtration barrier.

To further validate our results at the TEM level, we measured podocyte foot process width (FPW) (Fig. 5 B). In zebrafish, no reference or standard FPW is available. However, previous studies [53] suggest that in normal state, it is half-sized, compared to its human counterpart (508–827 nm) [54]. Accordingly, within GBM distances ranging between 21,000 and 207,000 nm (average total glomerular capillary circumference: 22157 nm), FPW ranged between 192 and 276 nm (235.5 ± 24.76 nm) in wild type but between 298 and 555 nm (383.4 ± 78.43 nm) in mutant animals ($P < 0.05$) (Fig. 5 B).

4. Discussion

Innovative supplemental therapeutic approaches for FD are urgently needed. However, *in vitro* and *in vivo* models currently used to test novel treatments, fail to adequately mirror FD pathobiology. Here, we have developed a zebrafish-based experimental model to allow a reliable and rapid *in vivo* assessment of the potential clinical relevance of new molecules and biologicals and to elucidate non Gb3-dependant pathophysiological disease mechanisms.

In-silico investigation demonstrated the presence of a single orthologue for human *GLA* gene in zebrafish. Furthermore, structure

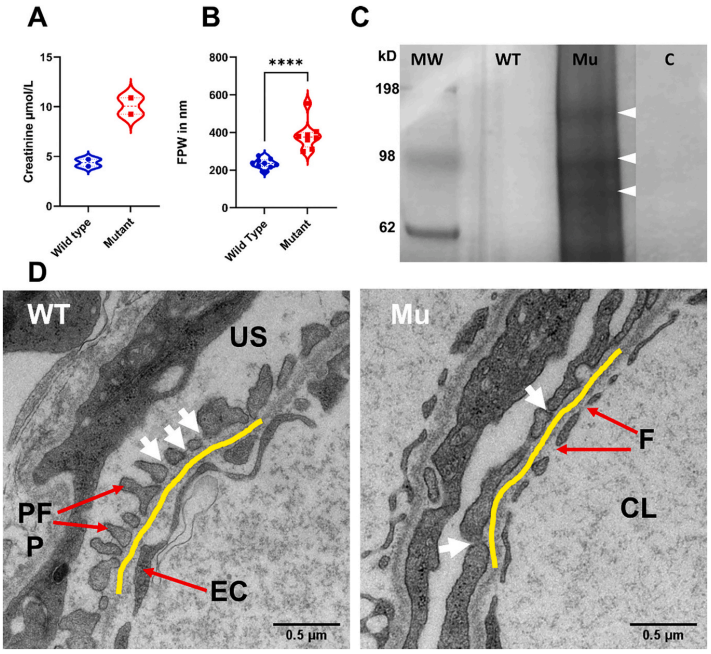

Fig. 5. GLA-mutant zebrafish show compromised filtration barrier function. (A) Renal impairment is documented by double plasma creatinine level in the mutant zebrafish. (B and D) FPW quantitation in adult zebrafish kidney on TEM images reveals wider foot processes (podocyte foot process effacement) in the mutant (Mann-Whitney Test, $P < 0.05$. Violin plots depict results within the 95th percentile. The yellow line highlights the GBM. White arrows point to the silt diaphragm between two adjacent foot processes. CL = capillary lumen, F = fenestrae, EC = endothelial cell, US = urinary space, PFP = podocyte foot process. (C) Renal function impairment is further validated by the leakage of high molecular weight proteins observed by SDS-PAGE electrophoresis. The illustrated protein bands in the fig. (80 kDa, 98 kDa and 150 kDa wight arrowheads) were identified by mass spectrometry analysis. MW = marker in kDa, WT = wild type, Mu = Mutant, C = control (water). The polyacrylamide gel image is edited for illustration, full gel image can be reviewed in Sup.7.

prediction revealed a high similarity between human and zebrafish α-GAL (Fig. 1), this is in agreement with previous report [55]. Importantly, by using a polyclonal antibody against zebrafish α-GAL we could show that the distribution of α-GAL in zebrafish kidneys closely resembles that of its human counterpart (Fig. 2 A). Most interestingly, the human α-GAL activity assays can effectively be used to measure zebrafish enzyme activity and we could therefore demonstrate that it is present in zebrafish as early as in 2 dpf embryo, 4 dpf larva, 30 dpf juvenile and adult fish tissues 90^{+} dpf (Fig. 2 B), and fluctuates similarly to humans [56]. We have noticed that enzyme activity in general is higher in adult wildtype female compared to adult male zebrafish, in agree with what have been described previously in Fabry mice [57] as well as in human [58]. For both Fabry mice and human this could be explained by the X-chromosome inactivation patterns [59], however, in zebrafish, as the *GLA* gene is not X-linked, we can attribute the enzyme activity difference to undetermined endogenous gender-related factors, *i.e.* gender-related expression pattern [52]. In fact, variable reports have indicated that individuals with FD disease are known for having normal values of the enzyme activity in response to variable mutations [60–62] while the lysoGb3 maintain elevating [63]. Apart from this, enzyme activity *in vitro* can differ from *in vivo* activity for many factors, *i.e.* the nature of the used substrate [64,65]. No difference was observed in the size or the weight between mutant and wildtype fish, however, we have observed higher mortality rates during the early embryonic stages, particularly when the crossing is made between younger mutant generations e. the 5th generation (F4) see Sup.8.

To provide a functional validation of our data, using CRISPR/Cas9 gene-editing tool, we introduced a hypomorphic mutation in exon 5 of *GLA* gene, resulting in decreased α-GAL activity. Sequence analysis indicates that the eleven base pair insertions at the end of the 5th exon and close to the active site (Fig. 3, Sup.9), resulted in a frameshift and introduced a premature stop codon at the beginning of the 6th exon. Notably, this mutation resembles a previously described rs869312402 c.785G > A-Trp262* mutation, which is pathogenic and leads to a classical FD phenotype in humans [66,67].

Most importantly, in animals bearing the engineered *GLA* gene, expression of the specific gene product in the kidneys was nearly undetectable by immunohistochemistry (Fig. 4 A and B), and enzyme activity was markedly reduced (Fig. 4 C).

During FD treatment, evaluation of proteinuria and serum/plasma creatinine is crucial to monitor disease progression and treatment outcome. Accordingly, we observed that plasma creatinine is higher in mutant, compared to wild type zebrafish. Moreover, proteinuria assessment unraveled a leak of high molecular weight proteins in the mutant fish. Combined, these observations support a glomerular filtration impairment. In agreement with this data, microscopic examination of kidney sections revealed increased glomerular size in mutant zebrafish characterized by dilated capillary loops, enlarged glomerular diameter, and thinner Bowman's space (Fig. 4 A). Similar findings have been reported in human Fabry nephropathy [68–71] but not in other FD model [29,72].

Increased podocyte and glomerular volumes have recently been described in classical FD patients by non-biased ultrastructural methods [73]. In accord with these reports, ultramicroscopic investigation revealed significant podocyte foot process effacement in the zebrafish mutant line.

Taken together, these results are consistent with the general assumption that damage of the kidney filtration barrier results in protein leakage and elevated plasma creatinine which are critical in defining glomerular filtration rate loss [74,75]. Most importantly, similarities with human FD phenotype not associated with Gb3 accumulation support the important role of substrate independent pathophysiologic mechanisms in Fabry nephropathy [76].

Limitations of the proposed model should be acknowledged. In particular, FD is characterized by a slow systematic accumulation of Gb3 [9,77,78] but zebrafish does not have Gb3 synthase gene, and hence no Gb3 accumulation can be expected. However, in FD, proteinuria represents an early clinical sign of kidney damage [79,80], even before Gb3 accumulation in the podocyte [79,81], and low range proteinuria may start as early as at 5 to 10 years of age [82,83]. Therefore, it is widely

recognized that apart from Gb3, in humans, multiple and not fully elucidated signal mechanisms do work in concert with histopathologic mechanisms [84]. Nevertheless, the possibility to insert Gb3 synthase gene or to transiently express it in zebrafish could be considered so that we can evaluate the effect of GLA inactivation on Gb3 *in vivo* and establish the hallmark of FD, Gb3 accumulation.

Notably, a residual enzyme activity was also detectable in mutant animals. It is worth mentioning that this residual activity could be due to α-*N*-acetylgalactosaminidase (α-galactosidase B) since the inhibitor (*N*-acetyl-D-galactosamine) concentration is optimized for human samples. Nevertheless, the low immunohistochemically detected signal of zebrafish α-GAL may compromise this assumption. Since α-GAL protein is remarkably undetectable by IHC in the mutant line, yet partially functioning, we speculate that the generated stop codon might be to some extent bypassed during protein translation, leading to structural deformation/protein misfolding with residual enzymatic activity.

On the other hand, the zebrafish model presents several advantages. Previously established Fabry mice, appear to be clinically normal, with no abnormality in blood and urine analyses and a normal lifetime. Kidney damage is only detectable by histological analysis in 20 weeks old mice (young adult) [32,85]. However, this could be achieved by day five post fertilization in zebrafish, thus in a considerably shorter time.

Besides the lack of the Henle loop, zebrafish and human kidneys are highly similar, sharing all fundamental functional units, and, especially, podocytes [22]. Moreover, expression pattern of zebrafish α-GAL is analogous to humans and enzyme activity can be easily and consistently measured throughout all developmental stages.

Another distinct advantage of zebrafish is represented by non-invasive drug administration protocols. Whether through an aqueous environment or oral gavage, this allows feasible drug delivery for both embryos and adult fish with reduced stress, thereby allowing more accurate observation of the histo- and physiopathology in the fish [86,87]. Additionally, progress in high-throughput drug screening in zebrafish has recently been documented [88].

Our results not only provide strong evidence for a structural and functional similarity of human and zebrafish α-GAL but indicate that the induction of mutations resulting in enzyme activity decrease efficiently models human FD, consistent with previous studies highlighting the use of zebrafish as a valuable kidney disease model.

Taken together, our data paves the way for a better molecular understanding of kidney phenotypes observed in FD patients and opens new avenues for the identification of novel biomarkers, and the performance of large-scale drug screenings.

Fund

This work was supported by an open project grant (number HV912233) to Hans-Peter Marti from the Western Norwegian Health Region (Helse vest).

Submission declaration and verification

This work described has not been published previously, and it is not under consideration for publication elsewhere. This work is approved by all authors and tacitly or explicitly by the responsible authorities where the work was carried out, and that, if accepted, it will not be published elsewhere in the same form, in English or any other language, including electronically without the written consent of the copyright holder.

Declaration of Competing Interest

Maria Blomqvist has given lectures in symposia and expert meetings sponsored by Sanofi Genzyme, Takeda Pharmaceutical Company and Biomarin Pharmaceutical. The authors declare no conflict of interest. Sabine Leh received speaker fees from Genzyme Sanofi. Einar Svarstad; speaker's fees and travel support from Amicus, Sanofi Genzyme, and Shire; advisory board honoraria from Amicus and Sanofi Genzyme. Camilla Tøndel; consultancy honoraria and/or research support from Amicus, Sanofi Genzyme, Chiesi, Protalix, Idorsia and Freeline.

Acknowledgements

We thank Professor Giulio C Spagnoli, National Research Council, Institute of Translational Pharmacology, Rome, Italy, for valuable improvement and discussions of the manuscript draft. We thank Dagny Ann Sandnes, Renal Research Group, UiB for assisting in IHC protocol optimization.

Appendix A. Supplementary data

Supplementary data to this article can be found online at https://doi.org/10.1016/j.ymgmr.2022.100851.

References

[1] J. Lukas, A.-K. Giese, A. Markoff, U. Grittner, E. Kolodny, H. Mascher, K.J. Lackner, W. Meyer, P. Wree, V. Saviouk, A. Rolfs, Functional characterisation of alpha-galactosidase a mutations as a basis for a new classification system in fabry disease, PLoS Genet. 9 (2013), e1003632, https://doi.org/10.1371/journal.pgen.1003632.

[2] V. Rickert, L. Wagenhäuser, P. Nordbeck, C. Wanner, C. Sommer, S. Rost, N. Üçeyler, Stratification of fabry mutations in clinical practice: a closer look at α-galactosidase A-3D structure, J. Intern. Med. 288 (2020) 593–604, https://doi.org/10.1111/joim.13125.

[3] A. Tuttolomondo, I. Simonetta, G. Duro, R. Pecoraro, S. Miceli, P. Colomba, C. Zizzo, A. Nucera, M. Daidone, T. Di Chiara, R. Scaglione, V. Della Corte, F. Corpora, D. Vogiatzis, A. Pinto, Inter-familial and intra-familial phenotypic variability in three sicilian families with Anderson-fabry disease, Oncotarget 8 (2017) 61415–61424, https://doi.org/10.18632/oncotarget.18250.

[4] T.F. Fitzmaurice, R.J. Desnick, D.F. Bishop, Human α-galactosidase a: high plasma activity expressed by the -30G→A allele, J. Inherit. Metab. Dis. 20 (1997) 643–657, https://doi.org/10.1023/A:1005366224351.

[5] A. Tuttolomondo, R. Pecoraro, I. Simonetta, S. Miceli, A. Pinto, G. Licata, Anderson-fabry disease: a multiorgan disease, Curr. Pharm. Des. 19 (2013) 5974–5996, https://doi.org/10.2174/13816128113199990352.

[6] J. Alroy, S. Sabnis, J.B. Kopp, Renal pathology in fabry disease, J. Am. Soc. Nephrol. 13 (2002) S134–S138, https://doi.org/10.1097/01.ASN.0000016684.07368.75.

[7] A. Tuttolomondo, R. Pecoraro, I. Simonetta, S. Miceli, V. Arnao, G. Licata, A. Pinto, Neurological complications of Anderson-fabry disease, Curr. Pharm. Des. 19 (2013) 6014–6030, https://doi.org/10.2174/13816128113199990387.

[8] D. Tapia, V. Kimonis, Stroke and chronic kidney disease in fabry disease, J. Stroke Cerebrovasc. Dis. (2020), 105423, https://doi.org/10.1016/j.jstrokecerebrovasdis.2020.105423.

[9] D.P. Germain, Fabry disease, Orphanet J. Rare Dis. 5 (2010) 30, https://doi.org/10.1186/1750-1172-5-30.

[10] T.M. Cox, Biomarkers in lysosomal storage diseases, in: A. Mehta, M. Beck, G. Sunder-Plassmann (Eds.), Fabry Dis. Perspect. from 5 Years FOS, Oxford PharmaGenesis, 2006.

[11] J.M. Aerts, J.E. Groener, S. Kuiper, W.E. Donker-Koopman, A. Strijland, R. Ottenhoff, C. van Roomen, M. Mirzaian, F.A. Wijburg, G.E. Linthorst, A. C. Vedder, S.M. Rombach, J. Cox-Brinkman, P. Somerharju, R.G. Boot, C.E. Hollak, R.O. Brady, B.J. Poorthuis, Elevated globotriaosylsphingosine is a hallmark of fabry disease, Proc. Natl. Acad. Sci. 105 (2008) 2812–2817, https://doi.org/10.1073/pnas.0712309105.

[12] H.-C. Liu, H.-Y. Lin, C.-F. Yang, H.-C. Liao, T.-R. Hsu, C.-W. Lo, F.-P. Chang, C.-K. Huang, Y.-H. Lu, S.-P. Lin, W.-C. Yu, D.-M. Niu, Globotriaosylsphingosine (lyso-Gb3) might not be a reliable marker for monitoring the long-term therapeutic outcomes of enzyme replacement therapy for late-onset fabry patients with the chinese hotspot mutation (IVS4+919G>A), Orphanet J. Rare Dis. 9 (2014) 111, https://doi.org/10.1186/s13023-014-0111-y.

[13] K. Kok, K.C. Zwiers, R.G. Boot, H.S. Overkleeft, J.M.F.G. Aerts, M. Artola, Fabry disease: molecular basisPathophysiology, Diagnostics and Potential Therapeutic Directions, Biomolecules 11 (2021) 271, https://doi.org/10.3390/biom11020271.

[14] M. Arends, C. Wanner, D. Hughes, A. Mehta, D. Oder, O.T. Watkinson, P.M. Elliott, G.E. Linthorst, F.A. Wijburg, M. Biegstraaten, C.E. Hollak, Characterization of classical and nonclassical fabry disease: a multicenter study, J. Am. Soc. Nephrol. 28 (2017) 1631–1641, https://doi.org/10.1681/ASN.2016090964.

[15] A. Nowak, F. Beuschlein, V. Sivasubramaniam, D. Kasper, D.G. Warnock, Lyso-Gb3 associates with adverse long-term outcome in patients with fabry disease, J. Med. Genet. (2021), https://doi.org/10.1136/jmedgenet-2020-107338 jmedgenet-2020-107338.

[16] T. Levstek, B. Vujkovac, K.Trebusak Podkrajsek, Biomarkers of Fabry nephropathy: review and future perspective, Genes (Basel) 11 (2020) 1091, https://doi.org/10.3390/genes11091091.

[17] A. Felis, M. Whitlow, A. Kraus, D.G. Warnock, E. Wallace, Current and investigational therapeutics for fabry disease, Kidney Int. Rep. 5 (2020) 407–413, https://doi.org/10.1016/j.ekir.2019.11.013.

[18] E. Svarstad, H.P. Marti, The changing landscape of fabry disease, Clin. J. Am. Soc. Nephrol. 000 (2020), https://doi.org/10.2215/CJN.09480819. CJN.09480819.

[19] O. Morand, J. Johnson, J. Walter, L. Atkinson, G. Kline, A. Frey, J. Politei, R. Schiffmann, Symptoms and quality of life in patients with fabry disease: results from an international patient survey, Adv. Ther. 36 (2019) 2866–2880, https://doi.org/10.1007/s12325-019-01061-x.

[20] T. Alegra, F. Vairo, M.V. de Souza, B.C. Krug, I.V.D. Schwartz, Enzyme replacement therapy for fabry disease: a systematic review and meta-analysis, Genet. Mol. Biol. 35 (2012) 947–954, https://doi.org/10.1590/S1415-47572012000600009.

[21] J.T.M. Neto, G.M. Kirsztajn, E.M. Pereira, H.M. Andrade, I.H.R. Oliveira, A. Labilloy, A.S. da Silva, Proteomic profiling of engineered human immortalized podocyte cell model of fabry disease, Mol. Genet. Metab. 126 (2019) S106–S107, https://doi.org/10.1016/j.ymgme.2018.12.269.

[22] M.C. Liebau, F. Braun, K. Höpker, C. Weitbrecht, V. Bartels, R.-U. Müller, S. Brodesser, M.A. Saleem, T. Benzing, B. Schermer, M. Cybulla, C.E. Kurschat, Dysregulated autophagy contributes to podocyte damage in Fabry's disease, PLoS One. 8 (2013), e63506, https://doi.org/10.1371/journal.pone.0063506.

[23] E.M. Pereira, A. Labilloy, M.L. Eshbach, A. Roy, A.R. Subramanya, S. Monte, G. Labilloy, O.A. Weisz, Characterization and phosphoproteomic analysis of a human immortalized podocyte model of fabry disease generated using CRISPR/Cas9 technology, Am. J. Physiol. Physiol. 311 (2016) F1015–F1024, https://doi.org/10.1152/ajprenal.00283.2016.

[24] H.-Y. Song, H.-C. Chiang, W.-L. Tseng, P. Wu, C.-S. Chien, H.-B. Leu, Y.-P. Yang, M.-L. Wang, Y.-J. Jong, C.-H. Chen, W.-C. Yu, S.-H. Chiou, Using CRISPR/Cas9-mediated GLA gene knockout as an in vitro drug screening model for fabry disease, Int. J. Mol. Sci. 17 (2016) 2089, https://doi.org/10.3390/ijms17122089.

[25] H. Hagmann, P.T. Brinkkoetter, Experimental models to study podocyte biology: stock-taking the toolbox of glomerular research, Front. Pediatr. 6 (2018) 193, https://doi.org/10.3389/fped.2018.00193.

[26] T. Ohshima, G.J. Murray, W.D. Swaim, G. Longenecker, J.M. Quirk, C. O. Cardarelli, Y. Sugimoto, I. Pastan, M.M. Gottesman, R.O. Brady, A.B. Kulkarni, α-galactosidase a deficient mice: a model of fabry disease, Proc. Natl. Acad. Sci. 94 (1997) 2540–2544, https://doi.org/10.1073/pnas.94.6.2540.

[27] M. Shimmoto, R. Kase, K. Itoh, K. Utsumi, S. Ishii, C. Taya, H. Yonekawa, H. Sakuraba, Generation and characterization of transgenic mice expressing a human mutant α-galactosidase with an R301Q substitution causing a variant form of fabry disease, FEBS Lett. 417 (1997) 89–91, https://doi.org/10.1016/S0014-5793(97)01263-5.

[28] K. Toyooka, Fabry disease, in: Handb. Clin. Neuro, 1st ed., Elsevier B.V, 2013, pp. 629–642, https://doi.org/10.1016/B978-0-444-52902-2.00037-0.

[29] A. Taguchi, H. Maruyama, M. Nameta, T. Yamamoto, J. Matsuda, A.B. Kulkarni, H. Yoshioka, S. Ishii, A symptomatic fabry disease mouse model generated by inducing globotriaosylceramide synthesis, Biochem. J. 456 (2013) 373–383, https://doi.org/10.1042/BJ20130825.

[30] J.J. Miller, K. Aoki, C.A. Mascari, A.K. Beltrame, O. Sokumbi, P.E. North, M. Tiemeyer, A.J. Kriegel, N.M. Dahms, α-galactosidase a-deficient rats accumulate glycosphingolipids and develop cardiorenal phenotypes of fabry disease, FASEB J. 33 (2019) 418–429, https://doi.org/10.1096/fj.201800771R.

[31] J.J. Miller, K. Aoki, C.A. Reid, M. Tiemeyer, N.M. Dahms, I.S. Kassem, Rats deficient in α-galactosidase a develop ocular manifestations of fabry disease, Sci. Rep. 9 (2019) 9392, https://doi.org/10.1038/s41598-019-45837-1.

[32] M.E. Haskins, U. Giger, D.F. Patterson, Animal Models of Lysosomal Storage Diseases: Their Development and Clinical Relevance, Oxford PharmaGenesis, 2006.

[33] K. Howe, M.D. Clark, C.F. Torroja, J. Torrance, C. Berthelot, M. Muffato, J. E. Collins, S. Humphray, K. McLaren, L. Matthews, S. McLaren, I. Sealy, M. Caccamo, C. Churcher, C. Scott, J.C. Barrett, R. Koch, G.-J. Rauch, S. White, W. Chow, B. Kilian, L.T. Quintais, J.A. Guerra-Assunção, Y. Zhou, Y. Gu, J. Yen, J.-H. Vogel, T. Eyre, S. Redmond, R. Banerjee, J. Chi, B. Fu, E. Langley, S.F. Maguire, G.K. Laird, D. Lloyd, E. Kenyon, S. Donaldson, H. Sehra, J. Almeida-King, J. Loveland, S. Trevanion, M. Jones, M. Quail, D. Willey, A. Hunt, J. Burton, S. Sims, K. McLay, B. Plumb, J. Davis, C. Clee, K. Oliver, R. Clark, C. Riddle, D. Elliott, G. Threadgold, G. Harden, D. Ware, S. Begum, B. Mortimore, G. Kerry, P. Heath, B. Phillimore, A. Tracey, N. Corby, M. Dunn, C. Johnson, J. Wood, S. Clark, S. Pelan, G. Griffiths, M. Smith, R. Glithero, P. Howden, N. Barker, C. Lloyd, C. Stevens, J. Harley, K. Holt, G. Panagiotidis, J. Lovell, H. Beasley, C. Henderson, D. Gordon, K. Auger, D. Wright, J. Collins, C. Raisen, L. Dyer, K. Leung, L. Robertson, K. Ambridge, D. Leongamornlert, S. McGuire, R. Gilderthorp, C. Griffiths, D. Manthravadi, S. Nichol, G. Barker, S. Whitehead, M. Kay, J. Brown, C. Murnane, E. Gray, M. Humphries, N. Sycamore, D. Barker, D. Saunders, J. Wallis, A. Babbage, S. Hammond, M. Mashreghi-Mohammadi, L. Barr, S. Martin, P. Wray, A. Ellington, N. Matthews, M. Ellwood, R. Woodmansey, G. Clark, J.D. Cooper, A. Tromans, D. Grafham, C. Skuce, R. Pandian, R. Andrews, E. Harrison, A. Kimberley, J. Garnett, N. Fosker, R. Hall, P. Garner, D. Kelly, C. Bird, S. Palmer, I. Gehring, A. Berger, C.M. Dooley, Z. Ersan-Ürün, C. Eser, H. Geiger, M. Geisler, L. Karotki, A. Kirn, J. Konantz, M. Konantz, M. Oberländer, S. Rudolph-Geiger, M. Teucke, C. Lanz, G. Raddatz, K. Osoegawa, B. Zhu, A. Rapp, S. Widaa, C. Langford, F. Yang, S.C. Schuster, N.P. Carter, J. Harrow, Z. Ning, J. Herrero, S.M.J. Searle, A. Enright, R. Geisler, R.H.A. Plasterk, C. Lee, M. Westerfield, P.J. de Jong, L.I. Zon, J.H. Postlethwait, C. Nüsslein-Volhard, T.J.P. Hubbard, H.R. Crollius, J. Rogers, D.L. Stemple, The zebrafish reference genome sequence and its relationship to the human genome, Nature 496 (2013) 498–503, https://doi.org/10.1038/nature12111.

[34] J. Gehrig, G. Pandey, J.H. Westhoff, Zebrafish as a model for drug screening in genetic kidney diseases, Front. Pediatr. 6 (2018) 183, https://doi.org/10.3389/fped.2018.00183.

[35] R. Santos, O. Amaral, Advances in sphingolipidoses: CRISPR-Cas9 editing as an option for modelling and therapy, Int. J. Mol. Sci. 20 (2019) 5897, https://doi.org/10.3390/ijms20235897.

[36] Z. Chen, A. Luciani, J.M. Mateos, G. Barmettler, R.H. Giles, S.C.F. Neuhauss, O. Devuyst, Transgenic zebrafish modeling low-molecular-weight proteinuria and lysosomal storage diseases, Kidney Int. 97 (2020) 1150–1163, https://doi.org/10.1016/j.kint.2019.11.016.

[37] I. Drummond, Kidney development and disease in the zebrafish, J. Am. Soc. Nephrol. 16 (2005) 299–304, https://doi.org/10.1681/ASN.2004090754.

[38] R.A. McKee, R.A. Wingert, Zebrafish renal pathology: emerging models of acute kidney injury, Curr. Pathobiol. Rep. 3 (2015) 171–181, https://doi.org/10.1007/s40139-015-0082-2.

[39] I.A. Drummond, A.J. Davidson, Zebrafish kidney development, in: Methods Cell Biol, Elsevier Ltd, 2016, pp. 391–429, https://doi.org/10.1016/bs.mcb.2016.03.041.

[40] S.A. Brittijn, S.J. Duivesteijn, M. Belmamoune, L.F.M. Bertens, W. Bitter, J. D. Debruijn, D.L. Champagne, E. Cuppen, G. Flik, C.M. Vandenbroucke-Grauls, R. A.J. Janssen, I.M.L. de Jong, E.R. de Kloet, A. Kros, A.H. Meijer, J.R. Metz, A. M. van der Sar, M.J.M. Schaaf, S. Schulte-Merker, H.P. Spaink, P.P. Tak, F. J. Verbeek, M.J. Vervoordeldonk, F.J. Vonk, F. Witte, H. Yuan, M.K. Richardson, Zebrafish development and regeneration: new tools for biomedical research, Int. J. Dev. Biol. 53 (2009) 835–850, https://doi.org/10.1387/ijdb.082615sb.

[41] A. Roy, D. Xu, J. Poisson, Y. Zhang, A protocol for computer-based protein structure and function prediction, J. Vis. Exp. (2011) 1–10, https://doi.org/10.3791/3259.

[42] K. Labun, T.G. Montague, M. Krause, Y.N. Torres Cleuren, H. Tjeldnes, E. Valen, CHOPCHOP v3: expanding the CRISPR web toolbox beyond genome editing, Nucleic Acids Res. 47 (2019) W171–W174, https://doi.org/10.1093/nar/gkz365.

[43] J.S. Mayes, J.B. Scheerer, R.N. Sifers, M.L. Donaldson, Differential assay for lysosomal alpha-galactosidases in human tissues and its application to Fabry's disease, Clin. Chim. Acta 112 (1981) 247–251, https://doi.org/10.1016/0009-8981(81)90384-3.

[44] L. Svennerholm, G. Håkansson, J.-E. Månsson, M., Thérèse vanier, the assay of sphingolipid hydrolases in white blood cells with labelled natural substrates, Clin. Chim. Acta. 92 (1979) 53–64, https://doi.org/10.1016/0009-8981(79)90396-6.

[45] G. Polo, A.P. Burlina, T.B. Kolamunnage, M. Zampieri, C. Dionisi-Vici, P. Strisciuglio, M. Zaninotto, M. Plebani, A.B. Burlina, Diagnosis of sphingolipidoses: a new simultaneous measurement of lysosphingolipids by LC-MS/MS, Clin. Chem. Lab. Med. 55 (2017) 403–414, https://doi.org/10.1515/cclm-2016-0340.

[46] P. Jagadeeswaran, J.P. Sheehan, F.E. Craig, D. Troyer, Identification and characterization of zebrafish thrombocytes, Br. J. Haematol. 107 (1999) 731–738, https://doi.org/10.1046/j.1365-2141.1999.01763.x.

[47] Ø. Midttun, G. Kvalheim, P.M. Ueland, High-throughput, low-volume, multianalyte quantification of plasma metabolites related to one-carbon metabolism using HPLC-MS/MS, Anal. Bioanal. Chem. 405 (2013) 2009–2017, https://doi.org/10.1007/s00216-012-6602-6.

[48] H. Zhang, W. Wen, J. Yan, Application of immunohistochemistry technique in hydrobiological studies, Aquac. Fish. 2 (2017) 140–144, https://doi.org/10.1016/j.aaf.2017.04.004.

[49] D.B. de Souza, B.M. Gregório, M. Benchimol, F.A.M. Nascimento, Evaluation of the glomerular filtration barrier by electron microscopy, in: Mod. Electron Microsc. Phys. Life Sci, InTech, 2016, pp. 1–15, https://doi.org/10.5772/61811.

[50] E.I. Christensen, Q. Zhou, S.S. Sørensen, Å.K. Rasmussen, C. Jacobsen, U. Feldt-Rasmussen, R. Nielsen, Distribution of α-galactosidase a in Normal human kidney and renal accumulation and distribution of recombinant α-galactosidase a in fabry mice, J. Am. Soc. Nephrol. 18 (2007) 698–706, https://doi.org/10.1681/ASN.2006080822.

[51] Y. Nishibori, K. Katayama, M. Parikka, Á. Oddsson, M. Nukui, K. Hultenby, A. Wernerson, B. He, L. Ebarasi, E. Raschperger, J. Norlin, M. Uhlén, J. Patrakka, C. Betsholtz, K. Tryggvason, Glcci1 deficiency leads to proteinuria, J. Am. Soc. Nephrol. 22 (2011) 2037–2046, https://doi.org/10.1681/ASN.2010111147.

[52] C. Li, X.F. Tan, T.K. Lim, Q. Lin, Z. Gong, Comprehensive and quantitative proteomic analyses of zebrafish plasma reveals conserved protein profiles between genders and between zebrafish and human, Sci. Rep. 6 (2016) 24329, https://doi.org/10.1038/srep24329.

[53] S.A. Rider, F.A. Bruton, R.G. Collins, B.R. Conway, J.J. Mullins, The efficacy of puromycin and adriamycin for induction of glomerular failure in larval zebrafish validated by an assay of glomerular permeability dynamics, Zebrafish 15 (2018) 234–242, https://doi.org/10.1089/zeb.2017.1527.

[54] J.K.J. Deegens, H.B.P.M. Dijkman, G.F. Borm, E.J. Steenbergen, J.G. van den Berg, J.J. Weening, J.F.M. Wetzels, Podocyte foot process effacement as a diagnostic tool in focal segmental glomerulosclerosis, Kidney Int. 74 (2008) 1568–1576, https://doi.org/10.1038/ki.2008.413.

[55] Y. Wu, H. Xia, J. Yuan, H. Xu, X. Deng, J. Liu, H. Zhang, H. Deng, Identification of a missense mutation in the α-galactosidase a gene in a chinese family with fabry disease, Curr. Genomics. 19 (2017) 70–75, https://doi.org/10.2174/1389202918666170915155033.

[56] G.S. Ribas, J.F. De Mari, G. Civallero, H.M. de Souza, M.G. Burin, C.R. Vargas, R. Giugliani, Validation of a multiplex tandem mass spectrometry method for the detection of selected lysosomal storage diseases in dried blood spots, J. Inborn Errors Metab. Screen. 5 (2017), https://doi.org/10.1177/2326409817692360, 232640981769236.

[57] B. Durant, S. Forni, L. Sweetman, N. Brignol, X.-L. Meng, E.R. Benjamin, R. Schiffmann, J.-S. Shen, Sex differences of urinary and kidney globotriaosylceramide and lyso-globotriaosylceramide in fabry mice, J. Lipid Res. 52 (2011) 1742–1746, https://doi.org/10.1194/jlr.M017178.
[58] R. Delarosa-Rodríguez, J.D. Santotoribio, H. Paula, A. González-Meneses, S. García-Morillo, P. Jiménez-Arriscado, J.M. Guerrero, H.C. Macher, Accuracy diagnosis improvement of fabry disease from dried blood spots: enzyme activity, lyso-Gb3 accumulation and GLA gene sequencing, Clin. Genet. 99 (2021) 761–771, https://doi.org/10.1111/cge.13936.
[59] R. Rossanti, K. Nozu, A. Fukunaga, C. Nagano, T. Horinouchi, T. Yamamura, N. Sakakibara, S. Minamikawa, S. Ishiko, Y. Aoto, E. Okada, T. Ninchoji, N. Kato, S. Maruyama, K. Kono, S. Nishi, K. Iijima, H. Fujii, X-chromosome inactivation patterns in females with fabry disease examined by both ultra-deep RNA sequencing and methylation-dependent assay, Clin. Exp. Nephrol. 25 (2021) 1224–1230, https://doi.org/10.1007/s10157-021-02099-4.
[60] M.A. Curiati, C.S. Aranda, S.O. Kyosen, P. Varela, V.G. Pereira, V. D'Almeida, J. B. Pesquero, A.M. Martins, The challenge of diagnosis and indication for treatment in fabry disease, J. Inborn Errors Metab. Screen. 5 (2017), https://doi.org/10.1177/2326409816685735, 232640981668573.
[61] Y. Kuramoto, A.T. Naito, H. Tojo, T. Sakai, M. Ito, M. Shibamoto, A. Nakagawa, T. Higo, K. Okada, T. Yamaguchi, J.-K. Lee, S. Miyagawa, Y. Sawa, Y. Sakata, I. Komuro, Generation of fabry cardiomyopathy model for drug screening using induced pluripotent stem cell-derived cardiomyocytes from a female fabry patient, J. Mol. Cell. Cardiol. 121 (2018) 256–265, https://doi.org/10.1016/j.yjmcc.2018.07.246.
[62] A. Mehta, M. Beck, F. Eyskens, C. Feliciani, I. Kantola, U. Ramaswami, A. Rolfs, A. Rivera, S. Waldek, D.P. Germain, Fabry disease: a review of current management strategies, QJM 103 (2010) 641–659, https://doi.org/10.1093/qjmed/hcq117.
[63] A. Nowak, T.P. Mechtler, R.J. Desnick, D.C. Kasper, Plasma LysoGb3: a useful biomarker for the diagnosis and treatment of fabry disease heterozygotes, Mol. Genet. Metab. 120 (2017) 57–61, https://doi.org/10.1016/j.ymgme.2016.10.006.
[64] Y. Ou, R.E. Wilson, S.G. Weber, Methods of measuring enzyme activity ex vivo and in vivo, Annu. Rev. Anal. Chem. 11 (2018) 509–533, https://doi.org/10.1146/annurev-anchem-061417-125619.
[65] A. Zotter, F. Bäuerle, D. Dey, V. Kiss, G. Schreiber, Quantifying enzyme activity in living cells, J. Biol. Chem. 292 (2017) 15838–15848, https://doi.org/10.1074/jbc.M117.792119.
[66] N.S.Rosa Neto, J.C.B. Bento, R.M.R. Pereira, Depression, sleep disturbances, pain, disability and quality of LIFE in Brazilian Fabry disease patients, Mol. Genet. Metab. Reports. 22 (2020) 100547, https://doi.org/10.1016/j.ymgmr.2019.100547.
[67] J. Shabbeer, M. Yasuda, S.D. Benson, R.J. Desnick, Fabry disease: identification of 50 novel α-galactosidase a mutations causing the classic phenotype and three-dimensional structural analysis of 29 missense mutations, Hum. Genomics. 2 (2006) 297–309, https://doi.org/10.1186/1479-7364-2-5-297.
[68] F. Weidemann, M.D. Sanchez-Niño, J. Politei, J.-P. Oliveira, C. Wanner, D. G. Warnock, A. Ortiz, Fibrosis: a key feature of fabry disease with potential therapeutic implications, Orphanet J. Rare Dis. 8 (2013) 116, https://doi.org/10.1186/1750-1172-8-116.
[69] Okamoto Hayashi, Kawano, iwasaki, development of organelle replacement therapy using a stearyl-polyhistidine peptide against lysosomal storage disease cells, Molecules 24 (2019) 2995, https://doi.org/10.3390/molecules24162995.
[70] M. Wani, I. Khan, R. Bhat, M. Ahmad, Fabry's disease: case series and review of literature, Ann. Med. Health Sci. Res. 6 (2016) 193, https://doi.org/10.4103/2141-9248.183935.
[71] F.A. Wijburg, B. Bénichou, D.G. Bichet, L.A. Clarke, G. Dostalova, A. Fainboim, A. Fellgiebel, C. Forcelini, K.A. Haack, R.J. Hopkin, M. Mauer, B. Najafian, C. R. Scott, S.P. Shankar, B.L. Thurberg, C. Tøndel, A. Tylki-Szymańska, U. Ramaswami, Characterization of early disease status in treatment-naive male paediatric patients with fabry disease enrolled in a randomized clinical trial, PLoS One. 10 (2015) 1–19, https://doi.org/10.1371/journal.pone.0124987.
[72] H. Trimarchi, The kidney in fabry disease, J. Inborn Errors Metab. Screen. 4 (2016), https://doi.org/10.1177/2326409816648169, 232640981664816.
[73] B. Najafian, C. Tøndel, E. Svarstad, M.C. Gubler, J.P. Oliveira, M. Mauer, Accumulation of globotriaosylceramide in podocytes in fabry nephropathy is associated with progressive podocyte loss, J. Am. Soc. Nephrol. 31 (2020) 865–875, https://doi.org/10.1681/ASN.2019050497.
[74] E. Svarstad, S. Leh, R. Skrunes, K.K. Larsen, Ø. Eikrem, C. Tøndel, K. Kampevold Larsen, Ø. Eikrem, C. Tøndel, Bedside stereomicroscopy of fabry kidney biopsies: an easily available method for diagnosis and assessment of sphingolipid deposits, Nephron 138 (2018) 13–21, https://doi.org/10.1159/000479751.
[75] D.P. Germain, J. Charrow, R.J. Desnick, N. Guffon, J. Kempf, R.H. Lachmann, R. Lemay, G.E. Linthorst, S. Packman, C.R. Scott, S. Waldek, D.G. Warnock, N. J. Weinreb, W.R. Wilcox, Ten-year outcome of enzyme replacement therapy with agalsidase beta in patients with fabry disease, J. Med. Genet. 52 (2015) 353–358, https://doi.org/10.1136/jmedgenet-2014-102797.
[76] F. Braun, L. Blomberg, S. Brodesser, M.C. Liebau, B. Schermer, T. Benzing, C. E. Kurschat, C.E. Kurschat, Enzyme replacement therapy clears Gb3 deposits from a podocyte cell culture model of fabry disease but fails to restore altered cellular signaling, Cell. Physiol. Biochem. 52 (2019) 1139–1150, https://doi.org/10.33594/000000077.
[77] C. Tøndel, L. Bostad, A. Hirth, E. Svarstad, Renal biopsy findings in children and adolescents with fabry disease and minimal albuminuria, Am. J. Kidney Dis. 51 (2008) 767–776, https://doi.org/10.1053/j.ajkd.2007.12.032.
[78] B. Najafian, E. Svarstad, L. Bostad, M.C. Gubler, C. Tøndel, C. Whitley, M. Mauer, Progressive podocyte injury and globotriaosylceramide (GL-3) accumulation in young patients with fabry disease, Kidney Int. 79 (2011) 663–670, https://doi.org/10.1038/ki.2010.484.
[79] A.L. Mena Rodríguez, M.V. Soto Abraham, M.Y. Valdespino Vázquez, B. de León Garza, Histopathological findings in renal biopsies in Anderson-fabry disease, Case Ser. Rev. Médica Del Hosp. Gen. México 81 (2018) 243–247, https://doi.org/10.1016/j.hgmx.2016.08.010.
[80] E. Riccio, M. Sabbatini, I. Capuano, A. Pisani, Early biomarkers of fabry nephropathy: a review of the literature, Nephron 143 (2019) 274–281, https://doi.org/10.1159/000502907.
[81] A.P. Moura, T. Hammerschmidt, M. Deon, R. Giugliani, C.R. Vargas, Investigation of correlation of urinary globotriaosylceramide (Gb3) levels with markers of renal function in patients with fabry disease, Clin. Chim. Acta 478 (2018) 62–67, https://doi.org/10.1016/j.cca.2017.12.033.
[82] F. Perretta, N. Antongiovanni, S. Jaurretche, Early renal involvement in a girl with classic fabry disease, Case Rep. Nephrol. 2017 (2017) 1–4, https://doi.org/10.1155/2017/9543079.
[83] B. Najafian, M. Mauer, R.J. Hopkin, E. Svarstad, Renal complications of fabry disease in children, Pediatr. Nephrol. 28 (2013) 679–687, https://doi.org/10.1007/s00467-012-2222-9.
[84] Ø. Eikrem, R. Skrunes, C. Tøndel, S. Leh, G. Houge, E. Svarstad, H.-P. Marti, Pathomechanisms of renal fabry disease, Cell Tissue Res. 369 (2017) 53–62, https://doi.org/10.1007/s00441-017-2609-9.
[85] K. Kimura, K. Takeuchi, Aging and longevity of the jel: ICR mouse, Okajimas Folia Anat. Jpn. 65 (1988) 35–42, https://doi.org/10.2535/ofaj1936.65.1_35.
[86] M. Dang, R.E. Henderson, L.A. Garraway, L.I. Zon, Long-term drug administration in the adult zebrafish using oral gavage for cancer preclinical studies, Dis. Model. Mech. 9 (2016) 811–820, https://doi.org/10.1242/dmm.024166.
[87] R.L. Vaz, T.F. Outeiro, J.J. Ferreira, Zebrafish as an animal model for drug discovery in Parkinson's disease and other movement disorders: a systematic review, Front. Neurol. 9 (2018), https://doi.org/10.3389/fneur.2018.00347.
[88] J. Gierten, C. Pylatiuk, O.T. Hammouda, C. Schock, J. Stegmaier, J. Wittbrodt, J. Gehrig, F. Loosli, Automated high-throughput heartbeat quantification in medaka and zebrafish embryos under physiological conditions, Sci. Rep. 10 (2020) 2046, https://doi.org/10.1038/s41598-020-58563-w.

III

International Journal of *Molecular Sciences*

MDPI

Type of the Paper (Article)

Gene expression analysis in *gla*-mutant zebrafish reveals enhanced Ca^{2+} signaling similar to Fabry disease

Hassan Osman Alhassan Elsaid[1,2], Håkon Tjeldnes[3], Mariell Rivedal[1], Camille Serre[1], Øystein Eikrem[2], Einar Svarstad[1], Camilla Tøndel[1,4], Hans-Peter Marti[1,2], Jessica Furriol[1,2,*,†] and Janka Babickova[1,5,†*]

[1] Department of Clinical Medicine, University of Bergen, Bergen, Norway
[2] Department of Medicine, Haukeland University Hospital, Bergen, Norway
[3] Computational Biology Unit, Department of Informatics, University of Bergen, Bergen, Norway
[4] Department of Pediatrics, Haukeland University Hospital, Bergen, Norway
[5] Institute of Molecular Biomedicine, Faculty of Medicine, Comenius University, Bratislava, Slovakia
* Correspondence: Jessica.Furriol@uib.no, Janka.Babickova@uib.no
† Equal contribution.

Abstract (200 words): Fabry disease (FD) is an X-linked inborn metabolic disorder due to partial or complete lysosomal α-galactosidase A deficiency. FD is characterized by progressive renal insufficiency and cardio- and cerebrovascular involvement. Restricted access on Gb3-independent tissue injury experimental models has limited the understanding of FD pathophysiology and delayed the development of new therapies. Accumulating glycosphingolipids, mainly Gb3 and lysoGb3, are Fabry specific markers used in clinical follow up. However, recent studies suggest there is a need for additional markers to monitor FD clinical course or response to treatment. We used a *gla*-knockout zebrafish (ZF) to investigate alternative biomarkers in Gb3-free-conditions. RNA sequencing was used to identify transcriptomic signatures in kidney tissues discriminating *gla*-mutant (M) from wild type (WT) ZF. Gene Ontology (GO) and KEGG pathways analysis showed upregulation of immune system activation and downregulation of oxidative phosphorylation pathways in kidneys from M ZF. In addition, upregulation of the Ca^{2+} signaling pathway was also detectable in M ZF kidneys. Importantly, disruption of mitochondrial and lysosome-related pathways observed in M ZF was validated by immunohistochemistry. Thus, this ZF model expands the pathophysiological understanding of FD, the Gb3-independent effects of *gla* mutations could be used to explore new therapeutic targets for FD.

Keywords: *gla*, Alpha-galactosidase A; zebrafish, cardiac involvement; Fabry disease; calcium signaling, oxidative stress)

Citation: Lastname, F.; Lastname, F.; Lastname, F. Title. *Int. J. Mol. Sci.* **2022**, *23*, x. https://doi.org/10.3390/xxxxx

Academic Editor: Firstname Lastname

Received: date
Accepted: date
Published: date

1. Introduction

Fabry disease (FD) is a rare lysosomal storage disorder affecting multiple organs. Organ dysfunction often correlated with accumulation of globotriaosylceramide (Gb3) in lysosomes in different cells [1]. Clinical symptoms are common in both gender and may appear in early childhood [2]. FD is classified into classical and non-classical phenotypes with a different degree of deficiency of α-GAL, the lysosomal enzyme responsible for Gb3 degradation [3]. While the classical form of the disease is characterized by null α-GAL activity, the non-classical phenotype is characterized by residual α-GAL activity and the absence of classical FD symptoms like acroparesthesia and low sweating ability. Cardiac and renal dysfunction is common in adult FD, with impaired quality of life and premature death [4, 5].

In early FD stages, renal involvement is clinically asymptomatic, as classically assessed and monitored by measuring albuminuria/proteinuria and glomerular filtration

rate (GFR) [6]. However, these tests have a low sensitivity for detecting early kidney damage, and aberrant readings frequently only represent late indicators of renal disease associated with irreparable structural damage [7] not benefiting from FD specific treatment like enzyme replacement therapy (ERT) [8]. Thus, they have limited sensitivity for early detection and monitoring of FD nephropathy, essential to preserving renal function [9, 10].

Accumulation of Gb3 and its deacylated form lysoGb3 is involved in various FD pathophysiological manifestations [11-13]. However, slowly progressive tissue deposition is insufficient to explain the gradual onset of organ dysfunction or adverse outcome [14-16]. For instance, plasma lysoGb3 levels fail to conclusively identify patients with milder phenotypes, particularly in females [17]. Other factors beyond Gb3 accumulation and lysoGb3 exposure may influence FD pathogenicity [18, 19]. We have recently shown that renal damage is evident in a Gb3-independent FD model [20].

Early biomarkers of FD nephropathy have been investigated in adult patients, with promising results. However, most studies were conducted by using proteomic or metabolomic technology [21], whereas RNA sequencing has more rarely been addressed [8].

More importantly, no studies have been conducted to explore genes encoding potential FD biomarkers associated with α-GAL deficiency in Gb3-free conditions. Such investigations might pave the way towards earlier detection of the disease prior to the development of the wide range of organ damage caused by Gb3 accumulation. To address this issue, we used a Gb3 synthase-free-*gla*- mutant zebrafish (ZF) as a FD model to investigate the Gb3-independent gene expression signature[20].

2. Results

2.1. RNA sequencing

First, we performed a quality control of the RNA-seq data obtained from zebrafish (ZF) kidney samples (n=16). Besides expected sex-related differences, this analysis showed a very high (r2>0.91) correlation among mutant (M, n= 8) and wild type (W, n=8) samples, consistent with high homogeneity and data reproducibility (Figure 1A). Most importantly, M and WT samples were indeed clustering better together than between each other, as shown by variance stabilized counts using both a clustering heatmap and a 2-dimensional principal component analysis (PCA) (Figure 1B-C), thereby suggesting that the expression of defined gene subset(s) clearly separated sample groups.

Gene expression changes in ZF kidney tissues were then comparatively analyzed in detail. In total, 22646 genes were successfully identified, and 4042 of them showing high FDR confidence (padj <0.05) were used for further analysis. A total of 2224 genes were differentially expressed (FDR ≤0.05, FC ≥0.5 and ≤-0.5) in mutant (M) compared to wildtype (WT) ZF with 1209 downregulated, and 1015 upregulated in MT vs. WT. Figure 1D reports the global differential expression pattern, showing that a higher number of downregulated genes displayed very high Log2 Fold Change.

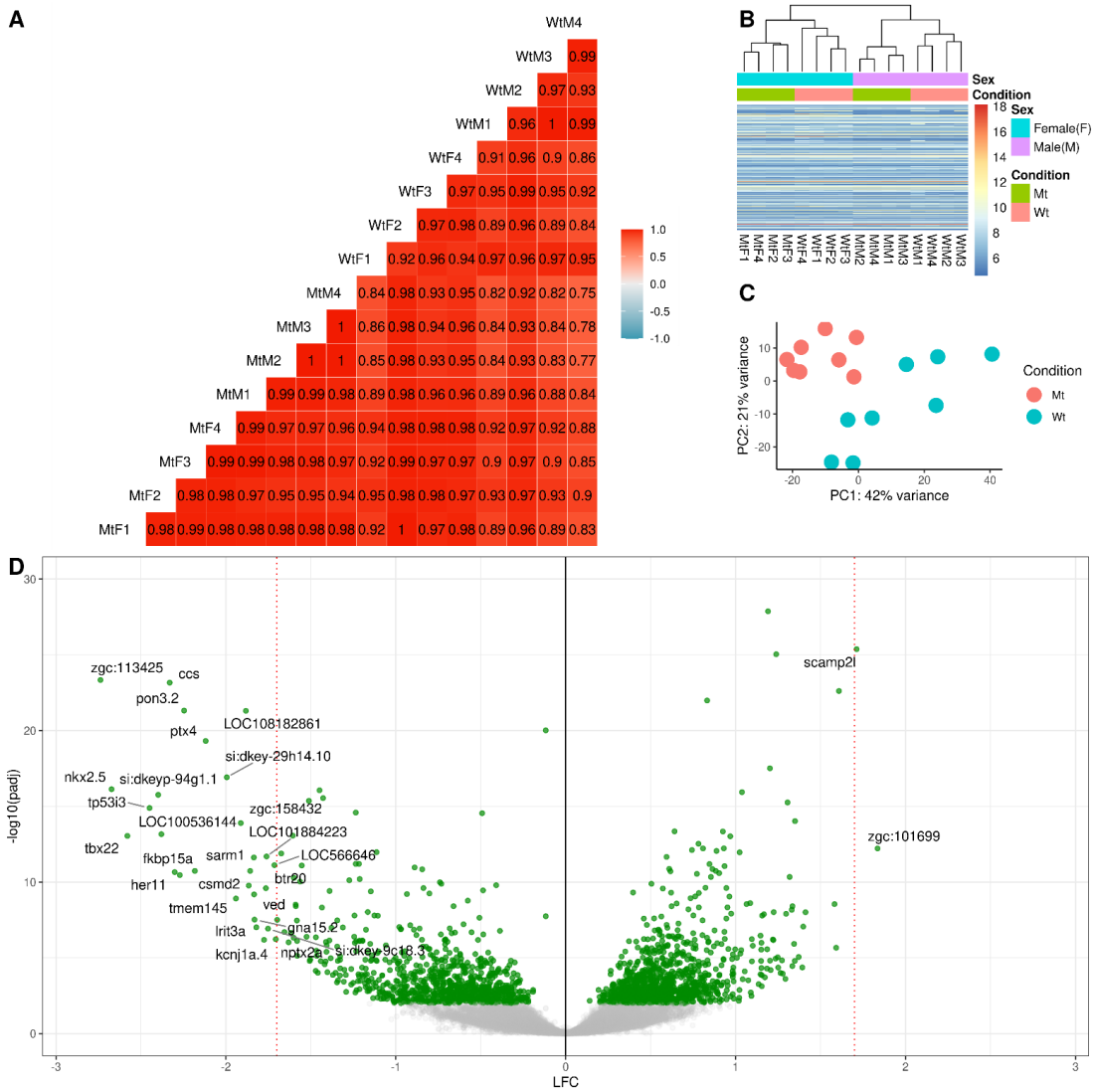

Figure 1. Quality Control and Fold Change. MtM: Mutant Male, MtF: Mutant Female, WtM: Wild type Male, WtF: Wild type Female. (A) Pearson Correlation for pairwise comparison of mRNA FPKM between samples, rounded to 2 decimals; (B) Heatmap clustering of variance stabilized counts for all genes binned into five hundred clusters, showing that both sex and condition are clustering together; (C) PCA analysis of variance stabilized counts for all genes, with batch correction for both Sex and Replicates; (D) Volcano plot of Log2 fold change (LFC) for all genes using DESeq2 differential expression analysis, with resulting -log10 adjusted p-values. (Negative LFC means LFC (Mutant Mt) < LFC (Wild type Wt). A high confidence set of genes are displayed with gene symbols (adjusted p-value < 0.000001 and absolute value of LFC > 1.7).

2.2. Differential gene expression analysis

Differentially expressed genes (DEGs) in M vs. WT ZF renal tissues were first analyzed by Gene Ontology (GO) term enrichment. A high number of genes markedly upregulated in M compared to WT samples were involved in different phases of the immune

response, including activation, regulation and effector functions, as indicated by GO terms of biological process (BP) analysis (Figure 2A). On the other hand, downregulated genes were relevant to energy production and consumption, aerobic respiration and oxidative phosphorylation (Figure 2B).

In cell compartment (CC) terms, genes upregulated in M vs. WT specimens mostly encoded proteins expressed on the external sides of cell membranes, in the cytoskeleton and cytoplasmic vesicles (Figure 2C). In contrast, downregulated genes mainly encoded proteins associated with the mitochondrial compartment, including mitochondrial inner membranes and involved in the respiratory chain (Figure 2D).

Finally, molecular function (MF) term analysis showed that genes upregulated in M samples encoded proteins widely involved in cytokine and chemokine binding and signaling, and antigen binding, in addition to different transporter activities (Figure 2E). On the other hand, downregulated genes mainly encoded proteins involved in oxidoreductase activity, electron transfer activity, NAD(P)H dehydrogenase activity, and pyruvate transmembrane transporter activity (Figure 2F).

KEGG analysis revealed that 1129 genes upregulated and 782 downregulated in M, compared to WT kidney samples, were associated with various molecular pathways. Upregulated genes were relevant to endocytosis, cell cycle, phagosome functions, ferroptosis, ECM-receptor interaction, cellular senescence, focal adhesion, glutathione metabolism, and calcium signaling pathways (Figure 3A-B). In contrast, downregulated genes were mainly involved in oxidative phosphorylation, in defined metabolic pathways, including carbon and fatty acid metabolism, and peroxisome functions (Figure 3C-D).

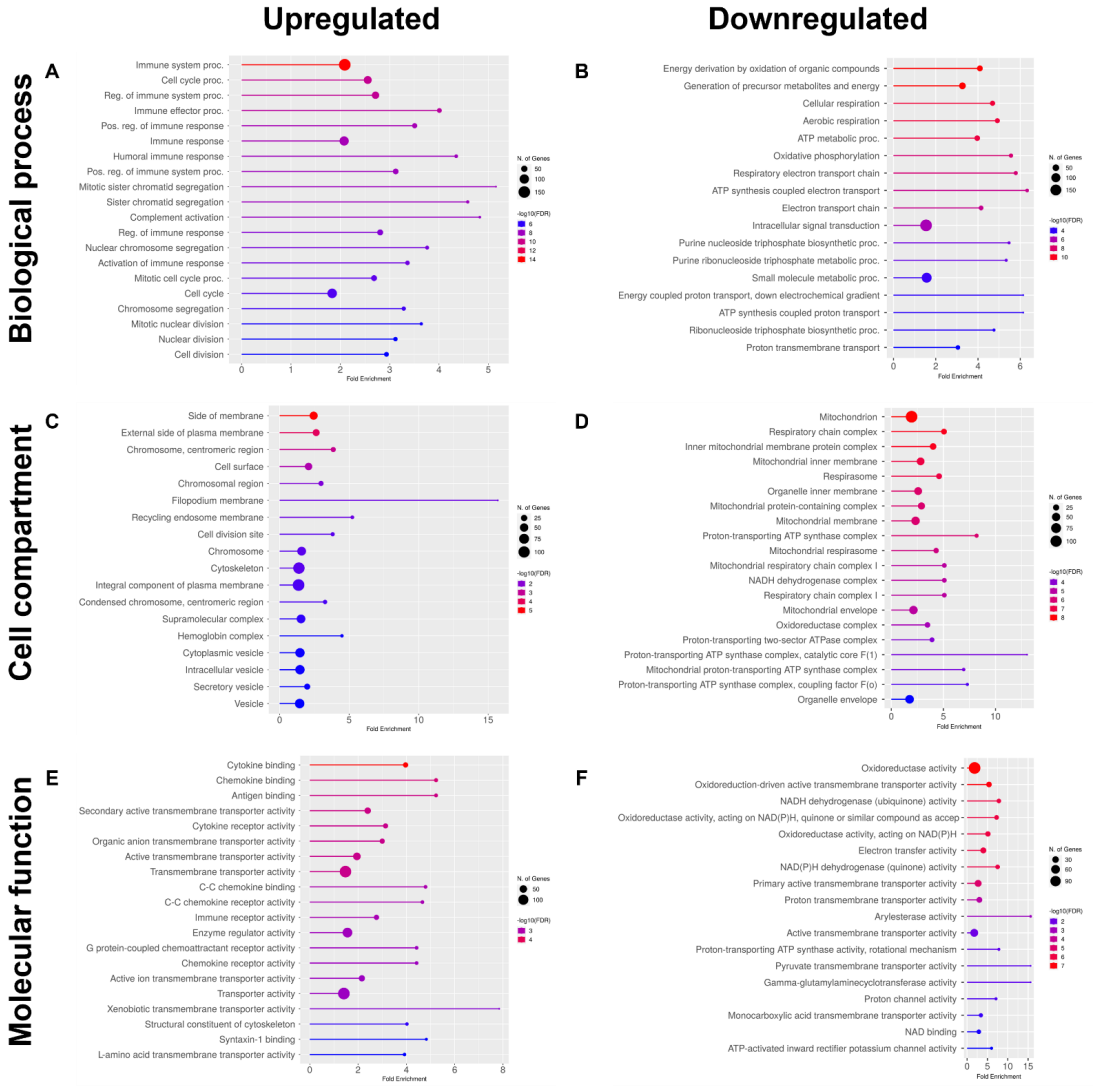

Figure 2. Gene ontology (GO) enrichment analysis of pathways upregulated and downregulated in renal tissues from the mutant, compared to wildtype ZF. Data refers to GO Biological Process (BP: A and B, respectively), Cellular component (CC, C and D, respectively) and Molecular function (MF: E and F, respectively). In all cases, the twenty most enriched pathways are reported. FDR ≤0.05.

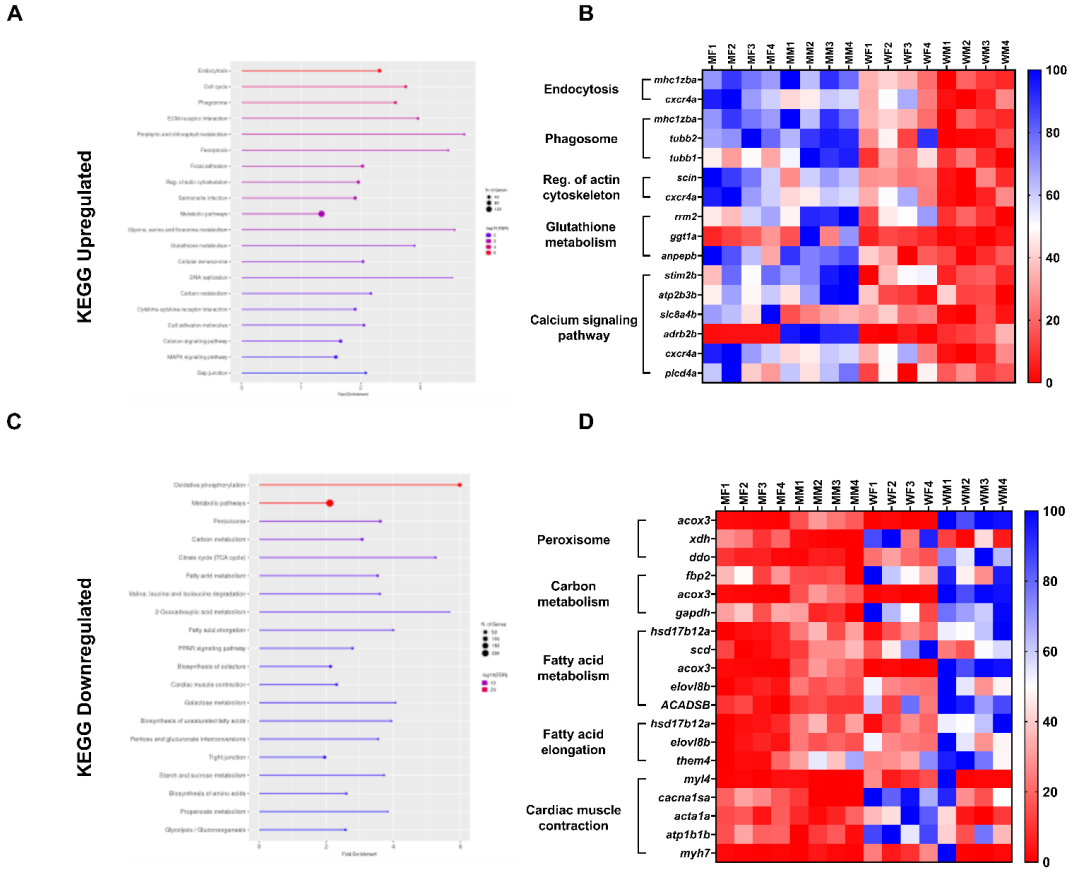

Figure 3. KEGG pathway enrichment analysis in mutant compared to wildtype ZF. (A) KEGG pathways associated with the upregulated genes; (B) Heat map of the upregulated genes corresponding to the highlighted pathway, only showing protein-encoding genes with FC >0.8 (percentage row normalized, where dark blue is the maximum per row); (C) KEGG pathway associated with the downregulated genes; (D) Heatmap of the downregulated genes corresponding to the highlighted pathway, only showing protein-encoding genes with FC < -0.8. The twenty most enriched pathways are reported. Enrichment FDR ≤0.05. MF1-4 (mutant female), MM1-4 (mutant male), WF1-4 (wild type female), WM1-4 (wild type male).

2.3. Validation by IHC

To validate gene expression data, we tested by immunohistochemistry (IHC) the expression of proteins encoded by genes differentially expressed in renal tissues from M and WT ZF. The selection of proteins was based on the extent of the dysregulation of encoding genes and the availability of commercially validated ZF antibodies. Two proteins, isocitrate dehydrogenase subunit alpha (Idh3a), expressed in mitochondria, and cathepsin B (Ctsb), expressed in lysosomes, met these criteria (Figure 4A). A semiquantitative immunohistochemical analysis demonstrated reduced average signals in kidneys from M compared to their WT counterparts (Figure 4B), consistent with expression patterns of the corresponding genes (Figure 4C).

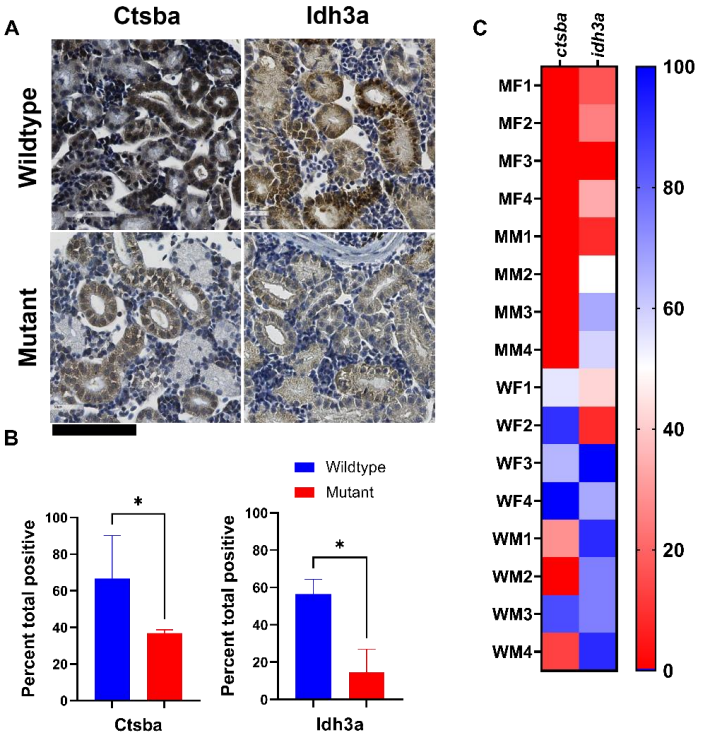

Figure 4. Immunohistochemical detection of selected proteins in kidneys from WT and M ZF reveals protein expression disturbances in mitochondria and lysosomes. (A) Representative IHC staining specific for mitochondrial marker isocitrate dehydrogenase (NAD(+))3 alpha (Idh3a) and lysosomal marker cathepsin B (Ctsb) in kidney tissue sections from WT and M ZF (upper right and upper left panels, and lower right and lower left panels, respectively; (B) Quantification of immunohistochemical staining of sections from WT and M ZF kidneys. Signal intensity is significantly higher in WT than in M for both proteins. (Mann Whitney test U $P<0.05$). Wildtype (WT), mutant (M). Scale bar (bottom left corner, in black) = 100μm; (C) Count (FPKM) heatmap (percentage column normalized, where dark blue is the maximum per column) showing the expression of the selected downregulated genes *ctsba* and *idh3a*.

3. Discussion

In our previous study, we developed an innovative model of FD in ZF [20], amenable to investigations addressing pathogenetic mechanisms and identifying potential drug targets. Here we further expand the pathophysiological understanding of FD and show that a thorough analysis of gene expression in kidneys from *gla*-mutant and WT ZF reveals specific patterns of potential clinical relevance.

Gene ontology (GO) data document that genes associated with different aspects of the immune response are highly significantly upregulated in M ZF. This data is supported by the analysis of molecular function (MF), showing upregulation of genes associated with chemokine and cytokine activity, and response to antigens.

Similarly to other lysosomal storage disorders, previous studies have repeatedly suggested an important role of immune response in FD pathogenesis [22, 23]. However, immune system activation was generally attributed to Gb3 accumulation [24, 25], leading to

invariant natural killer T cells (iNKT) activation. In this respect, our data provide important new information. Indeed, while both innate and adaptive immune systems are functional in ZF [26, 27], mutant *gla* knock-out ZF does not produce Gb3 [20]. Therefore, our results indicate that immune system activation closely resembling that observed in FD patients [28, 29] takes actually place in the absence of Gb3 as well, and set the stage for the identification of novel "immunostimulatory" compounds [30] of potential clinical relevance in FD. Accordingly, *zgc:101699* gene, the second most upregulated gene in kidneys from M ZF, encodes a phospholipase, belonging to a protein family highly overexpressed upon inflammation in different animal classes.

Our group's transcriptomics analysis from kidney biopsy revealed differences between FD patients at three time points (baseline, five years post-ERT, and 8-10 years post ERT) and healthy controls [31-33]. Gene Set Enrichment Analysis in the glomerular compartment demonstrated enriched gene sets of extracellular matrix, EMT, fibrosis, and immune response. The early ERT intervention seemed to return the upregulated pathways to normal, similar to the control samples [31]. However, these enriched pathways remained high in the long-term, e.g., 10 years of ERT [32, 33]. Our results are in line with these investigations. Furthermore, we have also identified that complement component 1, q subcomponent, C chain gene (*c1qc*) is significantly upregulated in the mutant fish compared to the wild type, which has already been shown by Strauss et al., [32] and Heo et al., [34]. While Eikrem et al. and Strauss et al. [31-33] have shown these results in humans in the presence of Gb3, we have shown that similar results can also be achieved in its absence. Our results indicate that other pathways might be responsible for triggering and maintaining such pathways independently of Gb3, which is supported by previous research [35].

Interestingly, we have observed upregulation of Mannose-6-Phosphate Receptors (*m6pr*) at the gene expression level (this study) accompanied by downregulation of M6pr protein abundance (our previous work paper 2) in the mutant fish kidney compared to the wildtype, similar to the recent finding of Frustaci et al. in endomyocardial biopsy [36]. The contrasted regulation can be attributed to the post-translation degradation. M6PR is the lysosomal receptor for α-GAL [37, 38]; therefore, its downregulation can negatively impact the efficacy of the ERT. Our results give the first wet lab evidence on the previously suggested Gb3 independent effects and strongly suggest that Gb3 independent effects should be extensively investigated.

Most notably, GO analysis of genes downregulated in M ZF indicates that, among others, genes involved in "Cellular respiration", "Aerobic respiration and "Oxidative phosphorylation" are markedly affected. This data suggests a prevailingly anaerobic, glycolytic metabolism, representing an inefficient, emergency energy production pathway, in M ZF kidneys, consistent with an ongoing immune system activation [39].

KEGG analysis further supports these findings, since pathways associated with inflammation, such as phagosome activation, endocytosis and ferroptosis are upregulated in kidneys from M ZF. Possibly as a consequence of immune stimulation, calcium signaling pathway is also upregulated in M ZF. Remarkably, previous studies using *GLA* mutant human inducible pluripotent stem cells (iPSC) in a kidney organoid template, have shown an increased calcium influx into the cytoplasm in response to oxidative stress [40]. Additionally, in Fabry knockout murine tissues, expression of S100 calcium-binding proteins A8 and A9 (also known as MRP8 and MRP14), was markedly elevated at the gene and protein levels [41]. Importantly, S100A8/A9, Ca^{2+} sensors involved in cytoskeleton remodeling and arachidonic acid metabolism, are expressed constitutively by neutrophils and monocytes and are actively produced during inflammation, promoting leukocyte recruitment and cytokine production [42].

In line with GO data, KEGG analysis confirms that metabolic pathways, and, in particular oxidative phosphorylation, are downregulated in kidneys from M ZF. In addition, the expression of a variety of cytochrome genes, typically detectable in mitochondria, but collectively included in the "cardiac muscle contraction" pathway in the KEGG analysis,

is also markedly downregulated in kidneys from M ZF. Taken together these observations delineate a mitochondrial stress scenario, possibly associated with Ca^{2+} signaling dysregulation, in line with our previous findings, and with previous reports in FD [40, 43, 44], and in other heart and muscle disorders [45].

Based on transcriptome data and on the availability of ZF-specific reagents, we tested the expression of selected proteins in kidneys from M and WT ZF to validate our findings at the protein level.

Isocitrate dehydrogenase catalytic subunit alpha (Idh3a) is a mitochondrial protein encoded by a gene downregulated in kidneys from M compared to WT ZF. Idh3a promotes ATP production by catalyzing oxidative decarboxylation of isocitrate to 2-oxoglutarate. Downregulation of this enzyme is also known to affect neurotransmission [46]. Consistent with gene expression data, Idh3a protein expression was also decreased in M, as compared to WT ZF kidney sections.

The lysosomal/cytoplasmic vessel cysteine protease cathepsin Ba (*ctsba*), an orthologous to human *CTSB* gene was also downregulated at both the gene and protein level. CTSB is a key player in lysosomal homeostasis and its dysregulation has been attributed to variable lysosomal abnormalities [47-49]. CTSB downregulation results in autophagosome accumulation due to compromised lysosomal clearance [50]. In general terms, dysregulation of cathepsins (CTSs) expression and/or activity, impairing cellular homeostasis, leads to a variety of human diseases, including, among others, cardiovascular diseases, neurodegenerative disorders, and kidney dysfunctions [47]. However, CTSB expression has not been associated with FD so far. In Niemann-Pick type C (NPC) disorder, a rare neurodegenerative disorder, inhibition of this protease results in lysosomal dysfunction [51]. In fact, CTSB resides not only in the lysosome, but also in the cytosol and the extracellular space, where it participates in many functions, e.g., inflammasome triggering, apoptosis, and extracellular matrix degradation [49]. The CTSB can be a potential biomarker as it can be measured in urine and plasma [52, 53], and previous studies have shown its downregulation is associated with the state of renal tubular injury [53-57], even at an early stage in life [52].

Limitations of our study should be acknowledged. In particular, in ZF, kidney is also a major hematopoietic organ [58-61], and, as such, it physiologically includes myeloid cells at different maturation stages. However, genes encoding cytokines and chemokines are highly upregulated in kidneys from M, as compared to WT ZF, thereby ruling out the possibility that the mere nature of the experimental model accounts for our results. Moreover, admittedly, our study exclusively focuses on gene expression in ZF kidneys, whereas other organs are also affected in FD. However, alterations of kidney functions do represent some of the most common FD symptoms. On the other hand, the scarce availability of ZF-specific antibodies has limited the validation, at the protein level, of our gene expression data.

Nonetheless, our findings show that even in the absence of Gb3 and lysoGb3, specific alterations of gene and protein expression may be detected in M ZF. While validating this model as an important tool to explore FD pathogenesis and to identify new drug targets, our data paves the way for studies investigating novel, clinically relevant FD markers.

In conclusion, for the first time we have demonstrated a Gb3-free impact equivalent to FD in humans in our gla-mutant zebrafish. Independent of Gb3, calcium ion flux disruption and altered mitochondrial and lysosomal pathways can be established and maintained. Our findings therefore support the hypothesis that additional mechanisms are involved in the onset and maintenance of these processes in FD.

4. Materials and Methods

Ethical approval

FOTS ID 15256 was granted by the Norwegian Food Safety Authority (Mattilsynet) for this study. All procedures were performed following the Zebrafish Facility protocol at the University of Bergen (UiB), by using the AB/Tübingen (AB/TU) strain of ZF.

Zebrafish maintenance and sample collection

Eggs, embryos, larvae, juveniles, and adult fish were handled in compliance with applicable national and international standards, according to ZF facility regulation at the University of Bergen. Under normal laboratory conditions, an adult (90+ days post-fertilization dpf) wild-type ZF was held at 28°C on a 14 h light/10 h dark period. Standard spawning protocol (www.zfin.org) was followed by egg harvesting. Eggs were stored in an E3 medium containing 0.01 % methylene blue after harvesting. Embryos and larvae were incubated at 28 °C until 5 dpf. Current regulation does not require permission for testing on ZF embryos before the free-feeding stage (5 dpf). Instead, according to the ZF facility rules, all invasive pain-causing interventions on stages older than 5 dpf was performed under anesthetic conditions. For sample collection, adult ZF were humanely euthanized in 300 mg/L tricaine methanesulfonate MS222 Sigma (Cat. No. A-5040), and then dissected open. Kidneys were exposed after discarding the viscera under cold 1X PBS Life Technologies (Cat. No. AM9625), removed and placed into clean RNAse-free tube prefilled with RNAlater™ Stabilization Solution (AM7021). Three kidneys were pooled per sample. Samples were kept overnight at 4°C and stored at -80°C until further RNA extraction take place.

RNA extraction and sequencing

Total RNA was extracted from whole kidneys (N= 8/group) using RNeasy Mini Kit (74104) following the manufacturer's protocol. Quantification of RNA concentration and purity was determined using NanoDrop 2000. The integrity of the RNA, cDNA library construction and Illumina sequencing were performed by NovoGene as described previously [62].

RNA sequences analysis

Raw data (FASTQ format) was processed using the STAR aligner and resulting files were processed with R/Bioconductor packages (R version 4.2). After initial QC checks in fastp, read mapping was done with STAR (version 2.7.4a). STAR used the indexed version of Danio rerio: GRCz11 Ensembl patch 101. The whole process was wrapped up using the RNA-seq pipeline in ORFik [63-66]. Number of reads per gene for each sample were counted using count Overlaps (a hit is >1 nucleotide of read overlapping any gene exon on the same strand). In the pairwise comparison (M vs. WT), DEGs were identified by using the DESeq2 R package (version 1.36.0) and selected using a Wald's test with filter criterion of FDR <0.05 and FC >0.5 [67]. FC values were shrunk using a Normal prior, with remaining options for DESeq2 set to default values. Processing script found at: *https://github.com/Roleren/fabry_article_code*. RNA-seq data is available at ENA project id number: PRJEB55250.

Gene ontology (GO) and KEGG pathway analyses were performed using ShinyGO 0.76 [68]. Genes/pathways with adjusted p-value < 0.05 were considered as significantly differentially enriched. Heatmap for Count (FPKM) was produced using GraphPad Prism V 9.2.0. We used FC of ±0.8 as produced FC using DESeq2 more realistic [69, 70] as it focuses on analysis strength, not the expression [67].

IHC

Kidney samples of adult ZF (90+dpf) were used. N=12 (6/genotype, 3 males, 3 females). IHC was performed as previously described [71] with slight modifications for each antibody. Heat-induced antigen retrieval was performed for 3 min in Dako Target Retrieval Solution, pH 6 (CTSB) and pH 9 (IDH3a). Staining was performed by one hour incubation at room temperature. Antibodies used were IDH3a GTX124431 (1:200) from GeneTex and CTSB M1506-1 (1:1000) from HUABIO. For negative controls, the primary

antibody was omitted. Slides were scanned with ScanScope XT® (Aperio) at x40 resulting in a resolution of 0.25 micrometer per Pixel. Digital slides were viewed in ImageScope 12.

IHC positivity for each antibody was quantified using the color deconvolution algorithm version 9.1 (Aperio, CA, USA) after adjusting the default parameters to DAB staining. Total percentage of positive pixels was used as a visualization parameter and statistics was performed using GraphPad Prism V 9.2.0. Values are presented as mean ±SD and Mann-Whitney test was used to assess statistical significance. Differences were considered significant with p-values <0.05.

Supplementary Materials: Not applicable.

Author Contributions: Conceptualization, M.HP., F.J., and E.H; methodology, F.J., E.H; software, E.H., T.H.; validation, E.H., T.H., and R.M.; formal analysis, E.H., and T.H.; investigation, E.H., F.J., and R.M.; resources, E.H., F.J., and T.H.; data curation, E.H., T.H; writing—original draft preparation, E.H.; writing—review and editing, E.H., T.H., E.O., R.M., S.C., S.E., T.C., M.HP., F.J., B.J.; visualization, E.H., and T.H.; supervision, F.J., B.J., and M.HP.; project administration, M.HP.; funding acquisition, M.HP. All authors have read and agreed to the published version of the manuscript.

Funding: This research was funded by an open project grant from the Western Norway Health Region (Helse Vest) to Hans-Peter Marti; project number: F-11546, 912233 (HV912233), and European Union's Horizon 2020 research and innovation programme under the Marie Skłodowska-Curie grant agreement; project number: 842619-DIE_CKD to Janka Babickova.

Institutional Review Board Statement: This study is approved by the Norwegian Food Safety Authority (Mattilsynet). FOTS ID 15256.

Informed Consent Statement: Not applicable.

Data Availability Statement:

- RNA-seq raw data project id: PRJEB55250
- Data processing scripts: https://github.com/Roleren/fabry_article_code

Acknowledgments: We thank Professor Giulio C Spagnoli, National Research Council, Institute of Translational Pharmacology, Rome, Italy, for valuable improvement and discussions of the manuscript draft. We thank Dagny Ann Sandnes, Renal Research Group, UiB for assisting in IHC protocol optimization.

Conflicts of Interest: Einar Svarstad; speaker's fees and travel support from Amicus, Sanofi Genzyme, and Shire; advisory board honoraria from Amicus and Sanofi Genzyme. Camilla Tøndel; consultancy honoraria and/or research support from Amicus, Sanofi Genzyme, Chiesi/Protalix, Idorsia, Acelink and Freeline.

References

1. Germain, D. P., Fabry disease. *Orphanet J Rare Dis* **2010,** 5, 30.
2. Tondel, C.; Bostad, L.; Hirth, A.; Svarstad, E., Renal biopsy findings in children and adolescents with Fabry disease and minimal albuminuria. *Am J Kidney Dis* **2008,** 51, (5), 767-76.
3. Smid, B. E.; van der Tol, L.; Cecchi, F.; Elliott, P. M.; Hughes, D. A.; Linthorst, G. E.; Timmermans, J.; Weidemann, F.; West, M. L.; Biegstraaten, M.; Lekanne Deprez, R. H.; Florquin, S.; Postema, P. G.; Tomberli, B.; van der Wal, A. C.; van den Bergh Weerman, M. A.; Hollak, C. E., Uncertain diagnosis of Fabry disease: consensus recommendation on diagnosis in adults with left ventricular hypertrophy and genetic variants of unknown significance. *Int J Cardiol* **2014,** 177, (2), 400-8.
4. Carnicer-Caceres, C.; Arranz-Amo, J. A.; Cea-Arestin, C.; Camprodon-Gomez, M.; Moreno-Martinez, D.; Lucas-Del-Pozo, S.; Molto-Abad, M.; Tigri-Santina, A.; Agraz-Pamplona, I.; Rodriguez-Palomares, J. F.; Hernandez-Vara, J.; Armengol-Bellapart, M.; Del-Toro-Riera, M.; Pintos-Morell, G., Biomarkers in Fabry Disease. Implications for Clinical Diagnosis and Follow-up. *J Clin Med* **2021,** 10, (8).
5. Rubino, M.; Monda, E.; Lioncino, M.; Caiazza, M.; Palmiero, G.; Dongiglio, F.; Fusco, A.; Cirillo, A.; Cesaro, A.; Capodicasa, L.; Mazzella, M.; Chiosi, F.; Orabona, P.; Bossone, E.; Calabro, P.; Pisani, A.; Germain, D. P.; Biagini, E.; Pieroni, M.; Limongelli, G., Diagnosis and Management of Cardiovascular Involvement in Fabry Disease. *Heart Fail Clin* **2022,** 18, (1), 39-49.
6. Najafian, B.; Tondel, C.; Svarstad, E.; Gubler, M. C.; Oliveira, J. P.; Mauer, M., Accumulation of Globotriaosylceramide in Podocytes in Fabry Nephropathy Is Associated with Progressive Podocyte Loss. *J Am Soc Nephrol* **2020,** 31, (4), 865-875.
7. Silva, C. A. B.; Moura-Neto, J. A.; Dos Reis, M. A.; Vieira Neto, O. M.; Barreto, F. C., Renal Manifestations of Fabry Disease: A Narrative Review. *Can J Kidney Health Dis* **2021,** 8, 2054358120985627.
8. Svarstad, E.; Marti, H. P., The Changing Landscape of Fabry Disease. *Clin J Am Soc Nephrol* **2020,** 15, (4), 569-576.
9. Tondel, C.; Bostad, L.; Larsen, K. K.; Hirth, A.; Vikse, B. E.; Houge, G.; Svarstad, E., Agalsidase benefits renal histology in young patients with Fabry disease. *J Am Soc Nephrol* **2013,** 24, (1), 137-48.
10. van der Veen, S. J.; Korver, S.; Hirsch, A.; Hollak, C. E. M.; Wijburg, F. A.; Brands, M. M.; Tondel, C.; van Kuilenburg, A. B. P.; Langeveld, M., Early start of enzyme replacement therapy in pediatric male patients with classical Fabry disease is associated with attenuated disease progression. *Mol Genet Metab* **2022,** 135, (2), 163-169.
11. Nowak, A.; Beuschlein, F.; Sivasubramaniam, V.; Kasper, D.; Warnock, D. G., Lyso-Gb3 associates with adverse long-term outcome in patients with Fabry disease. *J Med Genet* **2022,** 59, (3), 287-293.
12. Sanchez-Nino, M. D.; Carpio, D.; Sanz, A. B.; Ruiz-Ortega, M.; Mezzano, S.; Ortiz, A., Lyso-Gb3 activates Notch1 in human podocytes. *Hum Mol Genet* **2015,** 24, (20), 5720-32.

13. Effraimidis, G.; Feldt-Rasmussen, U.; Rasmussen, A. K.; Lavoie, P.; Abaoui, M.; Boutin, M.; Auray-Blais, C., Globotriaosylsphingosine (lyso-Gb3) and analogues in plasma and urine of patients with Fabry disease and correlations with long-term treatment and genotypes in a nationwide female Danish cohort. *J Med Genet* **2021,** 58, (10), 692-700.
14. Azevedo, O.; Cordeiro, F.; Gago, M. F.; Miltenberger-Miltenyi, G.; Ferreira, C.; Sousa, N.; Cunha, D., Fabry Disease and the Heart: A Comprehensive Review. *Int J Mol Sci* **2021,** 22, (9).
15. Bichet, D. G.; Aerts, J. M.; Auray-Blais, C.; Maruyama, H.; Mehta, A. B.; Skuban, N.; Krusinska, E.; Schiffmann, R., Assessment of plasma lyso-Gb3 for clinical monitoring of treatment response in migalastat-treated patients with Fabry disease. *Genet Med* **2021,** 23, (1), 192-201.
16. Liu, H. C.; Lin, H. Y.; Yang, C. F.; Liao, H. C.; Hsu, T. R.; Lo, C. W.; Chang, F. P.; Huang, C. K.; Lu, Y. H.; Lin, S. P.; Yu, W. C.; Niu, D. M., Globotriaosylsphingosine (lyso-Gb3) might not be a reliable marker for monitoring the long-term therapeutic outcomes of enzyme replacement therapy for late-onset Fabry patients with the Chinese hotspot mutation (IVS4+919G>A). *Orphanet J Rare Dis* **2014,** 9, 111.
17. Smid, B. E.; van der Tol, L.; Biegstraaten, M.; Linthorst, G. E.; Hollak, C. E.; Poorthuis, B. J., Plasma globotriaosylsphingosine in relation to phenotypes of Fabry disease. *J Med Genet* **2015,** 52, (4), 262-8.
18. Shen, J. S.; Meng, X. L.; Moore, D. F.; Quirk, J. M.; Shayman, J. A.; Schiffmann, R.; Kaneski, C. R., Globotriaosylceramide induces oxidative stress and up-regulates cell adhesion molecule expression in Fabry disease endothelial cells. *Mol Genet Metab* **2008,** 95, (3), 163-8.
19. Liebau, M. C.; Braun, F.; Hopker, K.; Weitbrecht, C.; Bartels, V.; Muller, R. U.; Brodesser, S.; Saleem, M. A.; Benzing, T.; Schermer, B.; Cybulla, M.; Kurschat, C. E., Dysregulated autophagy contributes to podocyte damage in Fabry's disease. *PLoS One* **2013,** 8, (5), e63506.
20. Elsaid, H. O. A.; Furriol, J.; Blomqvist, M.; Diswall, M.; Leh, S.; Gharbi, N.; Anonsen, J. H.; Babickova, J.; Tondel, C.; Svarstad, E.; Marti, H. P.; Krause, M., Reduced alpha-galactosidase A activity in zebrafish (Danio rerio) mirrors distinct features of Fabry nephropathy phenotype. *Mol Genet Metab Rep* **2022,** 31, 100851.
21. Levstek, T.; Vujkovac, B.; Trebusak Podkrajsek, K., Biomarkers of Fabry Nephropathy: Review and Future Perspective. *Genes (Basel)* **2020,** 11, (9).
22. Mauhin, W.; Lidove, O.; Masat, E.; Mingozzi, F.; Mariampillai, K.; Ziza, J. M.; Benveniste, O., Innate and Adaptive Immune Response in Fabry Disease. *JIMD Rep* **2015,** 22, 1-10.
23. Rigante, D.; Cipolla, C.; Basile, U.; Gulli, F.; Savastano, M. C., Overview of immune abnormalities in lysosomal storage disorders. *Immunol Lett* **2017,** 188, 79-85.
24. De Francesco, P. N.; Mucci, J. M.; Ceci, R.; Fossati, C. A.; Rozenfeld, P. A., Fabry disease peripheral blood immune cells release inflammatory cytokines: role of globotriaosylceramide. *Mol Genet Metab* **2013,** 109, (1), 93-9.
25. Pereira, C. S.; Pérez-Cabezas, B.; Ribeiro, H.; Maia, M. L.; Cardoso, M. T.; Dias, A. F.; Azevedo, O.; Ferreira, M. F.; Garcia, P.; Rodrigues, E.; Castro-Chaves, P.; Martins, E.; Aguiar, P.; Pineda, M.; Amraoui, Y.; Fecarotta, S.; Leão-Teles, E.; Deng, S.; Savage, P. B.; Macedo, M. F., Lipid Antigen Presentation by CD1b and CD1d in Lysosomal Storage Disease Patients. *Frontiers in Immunology* **2019,** 10.
26. Langenau, D. M.; Zon, L. I., The zebrafish: a new model of T-cell and thymic development. *Nat Rev Immunol* **2005,** 5, (4), 307-17.
27. Lewis, K. L.; Del Cid, N.; Traver, D., Perspectives on antigen presenting cells in zebrafish. *Dev Comp Immunol* **2014,** 46, (1), 63-73.
28. Matafora, V.; Cuccurullo, M.; Beneduci, A.; Petrazzuolo, O.; Simeone, A.; Anastasio, P.; Mignani, R.; Feriozzi, S.; Pisani, A.; Comotti, C.; Bachi, A.; Capasso, G., Early markers of Fabry disease revealed by proteomics. *Mol Biosyst* **2015,** 11, (6), 1543-51.

29. Rozenfeld, P.; Feriozzi, S., Contribution of inflammatory pathways to Fabry disease pathogenesis. *Mol Genet Metab* **2017,** 122, (3), 19-27.
30. van Eijk, M.; Ferraz, M. J.; Boot, R. G.; Aerts, J., Lyso-glycosphingolipids: presence and consequences. *Essays Biochem* **2020,** 64, (3), 565-578.
31. Eikrem, O.; Delaleu, N.; Strauss, P.; Sekulic, M.; Tøndel, C.; Leh, S.; Svarstad, E.; Skrunes, R.; Nowak, A.; Rusu, E. E.; Osman, T. A.; Marti, H. P., Systems Analyses of Renal Fabry Transcriptome and Response to Enzyme Replacement Therapy (ERT) Identifies a Cross-Validated and Druggable ERT-Resistant Module (Abstract, ASN, Kidney Week). J Am Soc Nephrol 31, 2020: 510. In.
32. Strauss, P.; Eikrem, Ø.; Tøndel, C.; Svarstad, E.; Scherer, A.; Leh, S.; Flatberg, A.; Delaleu, N.; Koch, E.; Beisvag, V.; Landolt, L.; Marti, H. P., Fabry Nephropathy: First mRNA-Seq Findings from Kidney Biopsies Before and After Enzyme Replacement Therapy (Abstract, 6th Update on Fabry Disease: Biomarkers, Progression and Treatment Opportunities). Nephron. 2019;142(3):169. In.
33. Eikrem, O.; Strauss, P.; Sekulic, M.; Tøndel, C.; Flatberg, A.; Skrunes, R.; Landolt, L.; Babickova, J.; Leh, S.; Scherer, A.; Svarstad, E.; Marti, H. P., Fabry Nephropathy: Transcriptome Sequencing of Microdissected Renal Compartments from Archival Kidney Biopsies at Baseline, and After 5 and 10 Years of Enzyme Replacement Therapy (Abstract, ASN, Kidney Week). J Am Soc Nephrol 29, 2018: 310. In.
34. Heo, S. H.; Kang, E.; Kim, Y. M.; Go, H.; Kim, K. Y.; Jung, J. Y.; Kang, M.; Kim, G. H.; Kim, J. M.; Choi, I. H.; Choi, J. H.; Jung, S. C.; Desnick, R. J.; Yoo, H. W.; Lee, B. H., Fabry disease: characterisation of the plasma proteome pre- and post-enzyme replacement therapy. *J Med Genet* **2017,** 54, (11), 771-780.
35. Braun, F.; Blomberg, L.; Brodesser, S.; Liebau, M. C.; Schermer, B.; Benzing, T.; Kurschat, C. E., Enzyme Replacement Therapy Clears Gb3 Deposits from a Podocyte Cell Culture Model of Fabry Disease but Fails to Restore Altered Cellular Signaling. *Cell Physiol Biochem* **2019,** 52, (5), 1139-1150.
36. Frustaci, A.; Verardo, R.; Scialla, R.; Bagnato, G.; Verardo, M.; Alfarano, M.; Russo, M. A., Downregulation of Mannose-6-Phosphate Receptors in Fabry Disease Cardiomyopathy: A Potential Target for Enzyme Therapy Enhancement. *J Clin Med* **2022,** 11, (18).
37. Sands, M. S.; Davidson, B. L., Gene therapy for lysosomal storage diseases. *Mol Ther* **2006,** 13, (5), 839-49.
38. Prabakaran, T.; Nielsen, R.; Satchell, S. C.; Mathieson, P. W.; Feldt-Rasmussen, U.; Sorensen, S. S.; Christensen, E. I., Mannose 6-phosphate receptor and sortilin mediated endocytosis of alpha-galactosidase A in kidney endothelial cells. *PLoS One* **2012,** 7, (6), e39975.
39. Pearce, E. L.; Pearce, E. J., Metabolic pathways in immune cell activation and quiescence. *Immunity* **2013,** 38, (4), 633-43.
40. Kim, J. W.; Kim, H. W.; Nam, S. A.; Lee, J. Y.; Cho, H. J.; Kim, T. M.; Kim, Y. K., Human kidney organoids reveal the role of glutathione in Fabry disease. *Exp Mol Med* **2021,** 53, (10), 1580-1591.
41. Park, E. S.; Choi, J. O.; Park, J. W.; Lee, M. H.; Park, H. Y.; Jung, S. C., Expression of genes and their responses to enzyme replacement therapy in a Fabry disease mouse model. *Int J Mol Med* **2009,** 24, (3), 401-7.
42. Wang, S.; Song, R.; Wang, Z.; Jing, Z.; Wang, S.; Ma, J., S100A8/A9 in Inflammation. *Frontiers in Immunology* **2018,** 9.
43. Schumann, A.; Schaller, K.; Belche, V.; Cybulla, M.; Grunert, S. C.; Moers, N.; Sass, J. O.; Kaech, A.; Hannibal, L.; Spiekerkoetter, U., Defective lysosomal storage in Fabry disease modifies mitochondrial structure, metabolism and turnover in renal epithelial cells. *J Inherit Metab Dis* **2021,** 44, (4), 1039-1050.
44. Biancini, G. B.; Vanzin, C. S.; Rodrigues, D. B.; Deon, M.; Ribas, G. S.; Barschak, A. G.; Manfredini, V.; Netto, C. B.; Jardim, L. B.; Giugliani, R.; Vargas, C. R., Globotriaosylceramide is correlated with oxidative stress and inflammation in Fabry patients treated with enzyme replacement therapy. *Biochim Biophys Acta* **2012,** 1822, (2), 226-32.

45. Rossi, A.; Pizzo, P.; Filadi, R., Calcium, mitochondria and cell metabolism: A functional triangle in bioenergetics. *Biochim Biophys Acta Mol Cell Res* **2019,** 1866, (7), 1068-1078.
46. Ugur, B.; Bao, H.; Stawarski, M.; Duraine, L. R.; Zuo, Z.; Lin, Y. Q.; Neely, G. G.; Macleod, G. T.; Chapman, E. R.; Bellen, H. J., The Krebs Cycle Enzyme Isocitrate Dehydrogenase 3A Couples Mitochondrial Metabolism to Synaptic Transmission. *Cell Rep* **2017,** 21, (13), 3794-3806.
47. De Pasquale, V.; Moles, A.; Pavone, L. M., Cathepsins in the Pathophysiology of Mucopolysaccharidoses: New Perspectives for Therapy. *Cells* **2020,** 9, (4).
48. Man, S. M.; Kanneganti, T. D., Regulation of lysosomal dynamics and autophagy by CTSB/cathepsin B. *Autophagy* **2016,** 12, (12), 2504-2505.
49. Yadati, T.; Houben, T.; Bitorina, A.; Shiri-Sverdlov, R., The Ins and Outs of Cathepsins: Physiological Function and Role in Disease Management. *Cells* **2020,** 9, (7).
50. Mizunoe, Y.; Kobayashi, M.; Tagawa, R.; Nakagawa, Y.; Shimano, H.; Higami, Y., Association between Lysosomal Dysfunction and Obesity-Related Pathology: A Key Knowledge to Prevent Metabolic Syndrome. *Int J Mol Sci* **2019,** 20, (15).
51. Cermak, S.; Kosicek, M.; Mladenovic-Djordjevic, A.; Smiljanic, K.; Kanazir, S.; Hecimovic, S., Loss of Cathepsin B and L Leads to Lysosomal Dysfunction, NPC-Like Cholesterol Sequestration and Accumulation of the Key Alzheimer's Proteins. *PLoS One* **2016,** 11, (11), e0167428.
52. Aisa, M. C.; Cappuccini, B.; Barbati, A.; Orlacchio, A.; Baglioni, M.; Di Renzo, G. C., Biochemical parameters of renal impairment/injury and surrogate markers of nephron number in intrauterine growth-restricted and preterm neonates at 30-40 days of postnatal corrected age. *Pediatr Nephrol* **2016,** 31, (12), 2277-2287.
53. Wang, N.; Bai, X.; Jin, B.; Han, W.; Sun, X.; Chen, X., The association of serum cathepsin B concentration with age-related cardiovascular-renal subclinical state in a healthy Chinese population. *Arch Gerontol Geriatr* **2016,** 65, 146-55.
54. Svara, T.; Pogacnik, M.; Juntes, P., Distribution and amount of cathepsin B in gentamicin-induced acute kidney injury in rats. *Pol J Vet Sci* **2010,** 13, (1), 75-82.
55. Herzog, C.; Yang, C.; Holmes, A.; Kaushal, G. P., zVAD-fmk prevents cisplatin-induced cleavage of autophagy proteins but impairs autophagic flux and worsens renal function. *Am J Physiol Renal Physiol* **2012,** 303, (8), F1239-50.
56. Liu, W. J.; Shen, T. T.; Chen, R. H.; Wu, H. L.; Wang, Y. J.; Deng, J. K.; Chen, Q. H.; Pan, Q.; Huang Fu, C. M.; Tao, J. L.; Liang, D.; Liu, H. F., Autophagy-Lysosome Pathway in Renal Tubular Epithelial Cells Is Disrupted by Advanced Glycation End Products in Diabetic Nephropathy. *J Biol Chem* **2015,** 290, (33), 20499-510.
57. Goncalves, I.; Hultman, K.; Duner, P.; Edsfeldt, A.; Hedblad, B.; Fredrikson, G. N.; Bjorkbacka, H.; Nilsson, J.; Bengtsson, E., High levels of cathepsin D and cystatin B are associated with increased risk of coronary events. *Open Heart* **2016,** 3, (1), e000353.
58. Traver, D., Cellular Dissection of Zebrafish Hematopoiesis. In *Methods in Cell Biology*, Academic Press: 2004; Vol. 76, pp 127-149.
59. Bailone, R. L.; Fukushima, H. C. S.; Ventura Fernandes, B. H.; De Aguiar, L. K.; Correa, T.; Janke, H.; Grejo Setti, P.; Roca, R. O.; Borra, R. C., Zebrafish as an alternative animal model in human and animal vaccination research. *Lab Anim Res* **2020,** 36, 13.
60. Povoa, V.; Rebelo de Almeida, C.; Maia-Gil, M.; Sobral, D.; Domingues, M.; Martinez-Lopez, M.; de Almeida Fuzeta, M.; Silva, C.; Grosso, A. R.; Fior, R., Innate immune evasion revealed in a colorectal zebrafish xenograft model. *Nat Commun* **2021,** 12, (1), 1156.
61. Trede, N. S.; Langenau, D. M.; Traver, D.; Look, A. T.; Zon, L. I., The Use of Zebrafish to Understand Immunity. *Immunity* **2004,** 20, (4), 367-379.

62. Zhang, X.; Zhou, Q.; Zou, W.; Hu, X., Molecular Mechanisms of Developmental Toxicity Induced by Graphene Oxide at Predicted Environmental Concentrations. *Environ Sci Technol* **2017,** 51, (14), 7861-7871.
63. Tjeldnes, H.; Labun, K.; Torres Cleuren, Y.; Chyzynska, K.; Swirski, M.; Valen, E., ORFik: a comprehensive R toolkit for the analysis of translation. *BMC Bioinformatics* **2021,** 22, (1), 336.
64. Chen, S.; Zhou, Y.; Chen, Y.; Gu, J., fastp: an ultra-fast all-in-one FASTQ preprocessor. *Bioinformatics* **2018,** 34, (17), i884-i890.
65. Dobin, A.; Davis, C. A.; Schlesinger, F.; Drenkow, J.; Zaleski, C.; Jha, S.; Batut, P.; Chaisson, M.; Gingeras, T. R., STAR: ultrafast universal RNA-seq aligner. *Bioinformatics* **2013,** 29, (1), 15-21.
66. Gentleman, R. C.; Carey, V. J.; Bates, D. M.; Bolstad, B.; Dettling, M.; Dudoit, S.; Ellis, B.; Gautier, L.; Ge, Y.; Gentry, J.; Hornik, K.; Hothorn, T.; Huber, W.; Iacus, S.; Irizarry, R.; Leisch, F.; Li, C.; Maechler, M.; Rossini, A. J.; Sawitzki, G.; Smith, C.; Smyth, G.; Tierney, L.; Yang, J. Y.; Zhang, J., Bioconductor: open software development for computational biology and bioinformatics. *Genome Biol* **2004,** 5, (10), R80.
67. Love, M. I.; Huber, W.; Anders, S., Moderated estimation of fold change and dispersion for RNA-seq data with DESeq2. *Genome Biol* **2014,** 15, (12), 550.
68. Ge, S. X.; Jung, D.; Yao, R., ShinyGO: a graphical gene-set enrichment tool for animals and plants. *Bioinformatics* **2020,** 36, (8), 2628-2629.
69. Thawng, C. N.; Smith, G. B., A transcriptome software comparison for the analyses of treatments expected to give subtle gene expression responses. *BMC Genomics* **2022,** 23, (1), 452.
70. Seyednasrollah, F.; Laiho, A.; Elo, L. L., Comparison of software packages for detecting differential expression in RNA-seq studies. *Brief Bioinform* **2015,** 16, (1), 59-70.
71. Zhang, H.; Wen, W.; Yan, J., Application of immunohistochemistry technique in hydrobiological studies. *Aquaculture and Fisheries* **2017,** 2, (3), 140-144.

Graphic design: Communication Division, UiB / Print: Skipnes Kommunikasjon AS

uib.no

ISBN: 9788230860342 (print)
9788230854716 (PDF)